THE THERMAL DECOMPOSITION OF MERCURIC OXALATE AND INORGANIC AZIDES.

by

D.J. MOORE B.Sc. (Hons.),(Rhodes).

A thesis submitted in fulfilment of the requirements for the Degree of Doctor of Philosophy of Rhodes University.

Department of Chemistry,
Rhodes University,
Grahamstown,
South Africa.

JANUARY, 1966.

ACKNOWLEDGEMENTS.

The author wishes to express his sincere thanks to Prof. E.G. Prout, M.Sc., Ph.D.(S.A.) of Rhodes University for his invaluable advice, direction and criticisms throughout the period of this research project.

Thanks are also due to Mr. S.G. Harris, Mr. G. Ranftelschofer and Mr. A.W. Sonemann for assistance in the technical aspects of the work, and to the typist, Mrs. M. Booth.

The author is also indebted to Messrs. African Explosives and Chemical Industries and the Ernest Oppenheimer Memorial Trust for scholarships held at different stages of the work.

CONTENTS.

Page

Page

Page

Page

Page

Page

Page

Page

1. INTRODUCTION.

1.1. The Thermal Decomposition of Solids.

The chemical reactivity of a solid is influenced to a marked degree by the presence of imperfections or defects in the solid. Bond strengths are considerably weaker at points of imperfection than elsewhere in the solid, and hence the initiation of reaction is favoured at these sites due to the relative ease of bond rupture. Line defects, such as edge or screw dislocations, jogs, Smekal cracks etc, are of prime importance in such changes. The surface of a solid or in intergranular boundaries, where a state of strain exists, are also favourable places for the initiation of a reaction. Point defects e.g. vacancies or interstitial ions or atoms also play important roles in chemical change, often in conjuction with line defects.

A characteristic feature of the thermal decomposition of a solid is the initiation and propagation of the reaction from a number of preferred centres, termed nuclei. As indicated above, nuclei are generally formed at imperfections in the lattice. Certainty as to the nature of nuclei does not always exist but it is generally accepted that they are composed of solid reactant product. For example, nuclei of metallic barium are found in the thermal decomposition of barium azide.[1]

Differences in physical properties, such as molecular volume, between the product and parent phases usually results in strain in the original lattice and this will favour the spread of the reaction from the original nucleus.

Nuclei can be classified into two main groups, viz. compact nuclei and diffuse nuclei. The latter are spread uniformly throughout the solid. They form in large numbers but are not directly observable since they do not grow to a visible size. An example of this occurs in the thermal decomposition of/.....

position of mercury fulminate[2]. Similar activation energies for nuclear formation and growth favours their formation.

Usually the activation energy for nucleus growth is less than that for nucleus formation. This favours the formation of compact nuclei. These nuclei are directly observable. They grow in a variety of shapes dependent on the physical properties of the solid e.g. spherical nuclei have been observed in the thermal decomposition of barium azide[3], and horn-shaped nuclei in the dehydration of copper sulphate pentahydrate[4].

The number of potential nucleus forming sites (and hence nuclei) can be increased by a number of means. Grinding or crushing of whole crystals usually achieves this. In some reactions, such as in the dehydration of hydrates[5], scratching of the surface facilitates nucleus formation. Preirradiation of the solid can also result in a large increase in the number of nuclei. Several instances have been recorded where preirradiation with ultra-violet light[6], X-rays[7], γ-rays[8], electrons[9] or neutrons[10] has had this effect. An increase in the concentration of defects of one form or another can usually be associated with any of the above treatments.

The majority of the thermal decompositions which have been studied are of the type

$$A_{(solid)} \rightarrow B_{(solid)} + C_{(gas)}$$

A convenient means of following the course of these reactions is to measure the pressure of the gas(es) evolved and then to plot rate/time, pressure/time or α/time curves (where α is the fractional decomposition). Mathematical analyses of these plots often yield much information as to the nature of nucleation processes and the shape and mode of growth of the nuclei. However, the applicability of a particular mathematical analysis is not conclusive proof for a particular mechanism and further evidence is usually desired.

Visual observations/.....

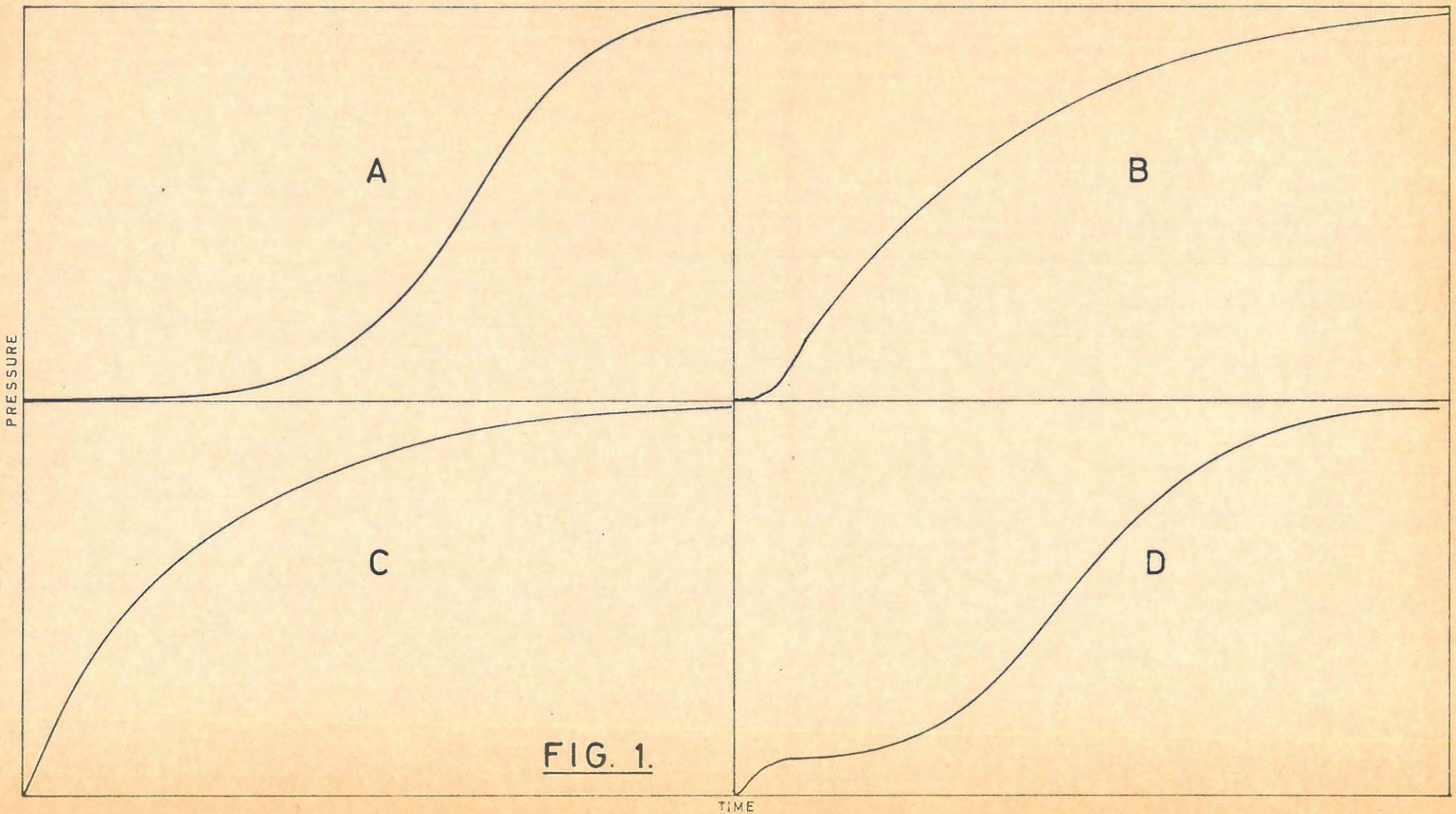

FIG. 1.

Visual observations of the decomposing solid and consideration of its chemical and physical properties, such as crystal structure, conductivity and general chemical reactivity are also of considerable importance in deducing the mode of thermal decomposition of the solid.

Four main types of thermal decompositions of a solid can be classified according to the shape of the pressure/time plots These are shown in FIGURE 1. Those in group (a) are sigmoid curves with a marked induction period with little or no evolution of gas, followed by periods of acceleration and decay of the reaction. The permanganates[11] show plots which are typically of this type. In group (b) there is a very pronounced decay period and only a short acceleratory period. The thermal decomposition of mercuric oxalate[12] and lead styphnate[13] follow this type of decomposition. In group (c) there is virtually no induction period and the reaction rate is a maximum near the beginning of the decomposition. An example of this is the decomposition of lead azide[14]. The fourth class of decompositions, (d), show a rapid initial burst of gas followed by a period of slow gas evolution which leads into an acceleratory and then into a decay period. This class is in fact a combination of (a) and (c). The thermal decomposition of potassium azide[15], and lithium aluminium hydride[16], are examples of this.

In general, the pressure/time curves for the thermal decomposition of a solid will possess all or some of the following features:

(i) An induction period which may or may not be preceeded by an initial burst of gas,

(ii) a period of acceleration of the reaction and,

(iii) a decay period or period of deceleration.

The induction period is considered to be the time during which nuclei are forming. Nuclear growth predominates during

the acceleratory/.....

the acceleratory period, although formation can still occur. The decay period corresponds to that period where overlap of the growing nuclei has occurred and reaction proceeds from a shrinking reactant/product interface.

As is evident from the above the mechanism of a particular decomposition and the kinetic equation which will describe the acceleration of the reaction will be dependent upon two factors viz., the rate of nucleus formation, and secondly the rate and mode of growth of the nuclei.

Nuclear Formation.

The nature of the reactions associated with the formation of nuclei were not fully understood until the work of Mott and Gurney[17] on the photolysis of silver halides helped clarify the situation. Nevertheless, the laws of nucleation and some of those governing nucleus growth had been derived at a fairly early stage. The laws of nucleation can be divided into two sections, viz:

(i) Nucleation involving a single step, and

(ii) Nucleation involving multiple steps.

In (i) it is assumed that the decomposition of a single molecule will lead to the formation of a nucleus. If there are N_o potential nucleus forming sites, the rate of nucleus formation will be given by

$$dN/dt = k_1(N_o - N) \quad \ldots\ldots(1.1)$$

where N is the number of nuclei at time t. If the loss of possible sites by ingestion is ignored at this stage then on integration the equation becomes

$$N = N_o (1 - e^{-k_1 t}) \quad \ldots\ldots(1.2)$$

and hence from 1.1

$$dN/dt = k_1 N_o e^{-k_1 t} \quad \ldots\ldots(1.3)$$

Equation (1.3) is known as the exponential law of nucleus formation./.....

formation. In the early stages of the reaction, and especially if the activation energy of nucleus formation is large (i.e. k_1 small) then the approximate relationship

$$dN/dt = k_1 N_o \quad \ldots\ldots\ldots\ldots\ldots\ldots\ldots\ldots\ldots\ldots (1.4)$$

is obtained, i.e. the number of nuclei increases linearly with time. This has been found to be valid in the dehydration of copper sulphate pentahydrate[4] and chrome alum[18].

If k_1 is very large then $N \rightarrow N_o$ i.e. instantaneous nucleation occurs and the reaction proceeds from a fixed number of centres.

When nucleation involves multiple steps, the rate of nucleus formation increases as powers of t greater than unity. This can be accounted for in two ways. Firstly several successive decompositions may be required to form a stable nucleus, or alternatively, a stable nucleus may result from a bimolecular process involving the combination of two active intermediares, each of which is formed at a constant rate. Bagdassarian[19] has shown that both these possibilities will lead to nucleation according to the same power law, the number of nuclei, N, at time t being given by

$$N = Dt^B \quad \ldots\ldots\ldots\ldots\ldots\ldots\ldots\ldots\ldots\ldots (1.5)$$

or the rate of nucleation

$$dN/dt = DBt^{B-1} \quad \ldots\ldots\ldots\ldots\ldots\ldots\ldots\ldots\ldots\ldots (1.6)$$

where D = a constant

B = the number of successive decompositions required

or B - 1 = the number of separate entities required to form a stable nucleus.

Examples where the number of nuclei have been observed to increase as a power of time are the dehydration of nickel sulphate pentahydrate[20] and the thermal decomposition of single crystals of barium azide[3].

To summarize/.....

To summarize, the rate of nucleus formation could be instantaneous, as a linear or exponential function of time, or as a power of the time.

Nuclear growth and the acceleratory period:

The acceleratory period of a thermal decomposition is a time where nucleus growth predominates. The main laws of nucleus growth can be divided into five groups. They are:

(i) The power law;

(ii) The exponential law,

(iii) The Prout-Tompkins equation;

(iv) The modified Prout-Tompkins equation;

(v) The Avrami-Erofeyev equation.

(i) The Power Law.

If nucleation proceeds according to a power law, then assuming a constant rate of nucleus growth, and ignoring overlap and ingestion of nuclei, it can be shown[21] that the fraction, α, decomposed at any time t is given by

$$\alpha = C' t^n \quad \ldots\ldots\ldots\ldots\ldots\ldots\ldots\ldots\ldots\ldots\ldots\ldots (1.7)$$

where C' = a constant

n = an integer.

Since $\alpha = p/p_f$ where p is the pressure at time t and p_f is the final pressure, equation 1.7 can be rewritten in the form

$$p = C t^n \quad \ldots\ldots\ldots\ldots\ldots\ldots\ldots\ldots\ldots\ldots\ldots\ldots (1.8)$$

where $n = B + \lambda$ with B having the same value as before and $\lambda = 1$, 2 or 3 depending on whether the nuclei grow 1, 2 or 3-dimensionally, i.e. are linear, plate-like or spherical.

Equation 1.8 is known as the Power Law. It has been successfully applied to the decomposition of a number of compounds. In the decomposition of barium styphnate monohydrate[22] a value of $n = 2$ was obtained, where there was two-dimensional growth from a fixed number of nuclei. Aged mercury fulminate[23]

obeys the/.....

obeys the power law with n = 3. This could correspond to three-dimensional growth from a fixed number of nuclei, or two-dimensional growth of nuclei whose numbers are increasing linearly with time. A value of n = 4, corresponding to spherical nuclei increasing linearly with time, has been obtained for the ammonium chromates[24], while Wischin[3] deduced a value of n = 6 corresponding to spherical nuclei increasing in number as the cube of the time, in the thermal decomposition of single crystals of barium azide.

(ii) The Exponential Law.

Among the earlier work the kinetics of the thermal decomposition of freshly prepared whole crystals of mercury fulminate[25] could not be explained on the basis of the power law theory. Garner and Hailes[25] derived the concept of linear branching chains to account for the decomposition mechanism. Assuming that the rate of nucleus formation is constant, and that there is a constant branching coefficient, k_2, then the nett rate of nucleus production is given by,

$$dN/dt = k'N + k_2N \quad \ldots\ldots\ldots\ldots\ldots\ldots\ldots\ldots\ldots\ldots (1.9)$$

from which it can be shown that

$$p = C'e^{k_2t} \quad \ldots\ldots\ldots\ldots\ldots\ldots\ldots\ldots\ldots\ldots (1.10)$$

Equation 1.10 is known as the Exponential Law. However, although it described the pressure/time plots in a number of cases, an objection to the theory was that linear branching chains would tend to separate the crystal into mosaic blocks which would then decompose slowly. This original idea has thus been extended by the concept of branching plate-like nuclei, firstly suggested by McDonald[26], a mechanism which would also be described by equation 1.10. This idea has been applied to the thermal decomposition of silver oxalate[27], where it is suggested that the reaction proceeds along grain boundaries and dislocations, and branches at intersections of any of these in the crystal.

(iii) The Prout-Tompkins/....

(iii) The Prout-Tompkins Equation.

It was pointed out by Prout and Tompkins[28], when investigating the thermal decomposition of potassium permanganate, that a weakness in the chain theory was that it did not allow for interference between branching nuclei. Their proposed mechanism for the decomposition of potassium permanganate took this into account. It was assumed that there were N_o nuclei originally present and concentrated mainly at surface imperfections. The production of product molecules would give rise to lateral strains on the surface resulting in the formation of cracks in the surface. These would be regions of strain favouring decomposition and reaction would proceed along them. In this manner surface coverage would be obtained. This would produce more cracking perpendicular to the inner surface of product followed by decomposition along these planes. Thus the reaction would proceed by a branching mechanism.

Now if there are N_o original nuclei and if k_3 is the probability of branching and k_4 the probability of termination of nuclei by interference, then by anlogy with equation (1.9) the overall rate of nucleation will be given by

$$dN/dt = k_1N_o + (k_3-k_4)\ N \qquad \ldots\ldots\ldots\ldots\ldots\ldots\ldots\ldots (1.11)$$

The initial N_o potential nucleus forming sites are soon exhausted and the equation thus becomes

$$dN/dt = (k_3-k_4)\ N \qquad \ldots\ldots\ldots\ldots\ldots\ldots\ldots\ldots\ldots\ldots (1.12)$$

Assuming the rate of decomposition $d\alpha/dt$ to be proportional to the number of nuclei present then

$$d\alpha/dt = k'N \qquad \ldots\ldots\ldots\ldots\ldots\ldots\ldots\ldots\ldots\ldots (1.13)$$

Equations (1.12) and (1.13) cannot be integrated unless the fractional dependence of k_3 and k_4 on α is known. Now the pressure/time plot for potassium permanganate is symmetrical and at the inflexion point $\alpha = 0.5$. Certain boundary conditions can thus be applied viz,

At t = o/.....

At $t = o \quad \alpha = o \quad \therefore \quad k_4 = o$

At $t = t_i \quad \alpha = \alpha_i = {}^1/_2$ $d\alpha/dt$ is at a maximum and $k_3 = k_4$ since dN/dt changes sign. The boundary condition is thus

$$k_4 = k_3 \frac{\alpha}{\alpha_i} \qquad \text{.....(1.14)}$$

Substituting this into equation (1.12) we get

$$dN/dt = k_3 \left(1 - \frac{\alpha}{\alpha_i}\right)N \qquad \text{.....(1.15)}$$

or from equation 1.13

$$dN/d\alpha = k \left(1 - \frac{\alpha}{\alpha_i}\right) \qquad \text{.....(1.16)}$$

where $k = k_3/k'$

on integration this yields

$$N = k \left(\alpha - \frac{\alpha^2}{2\alpha_i}\right) \qquad \text{.....(1.17)}$$

which on substitution into equation 1.13 becomes

$$d\alpha/dt = k_3\alpha(1-\alpha) \qquad \text{.....(1.18)}$$

when $\alpha = {}^1/_2$. Further integration now yields

$$\log (\alpha/1-\alpha) = k_3 t + c_3 \qquad \text{.....(1.19)}$$

or since $\alpha = p/p_f$

$$\log (p/p_f - p) = k_3 t + c_3 \qquad \text{.....(1.20)}$$

Equation 1.20 is known as the Prout-Tompkins Equation. It has successfully been applied to the thermal decomposition of irradiated and unirradiated permanganates[11], and several other compounds including lead oxalate[29], nickel formate[30], and lanthanum oxalate[31].

(iv) <u>The Modified Prout-Tompkins Equation</u>.

In a study of the thermal decomposition of silver permanganate[32] Prout and Tompkins found it necessary to modify their equation. In this case it was assumed that the branching coefficient, k_3, was not constant, but varied inversely with the time so that it now became

$$k_3 = k_3'/t \qquad \text{.....(1.21)}$$

The final/.....

The final equation then becomes

$$\log (p/p_f - p) = k_3' \log t + c_3' \quad \ldots\ldots\ldots\ldots\ldots\ldots (1.22)$$

which is the Modified Prout-Tompkins Equation.

The nature of the chains postulated in the exponential law and Prout-Tompkins equations has been subjected to a certain amount of criticism, particularly by McDonald[33] and Hill[34]. The latter suggested that the chains were more likely to be diffusion chains, consisting of a few ions or atoms of the product wandering through the dislocation network of the crystal until they reach a nucleus forming site which they could "fertilize" and turn into a nucleus. No details of what the "fertilization" process involved were given.

(v) The Avrami-Erofeyev Equation.

The effects of ingestion of potential nucleus forming sites by growing nuclei or the over-lapping of such nuclei is not allowed for in (i) - (iv). Avrami[35], in a mathematical study of the kinetics of phase changes, analysed reaction/time curves using the concept of a random nucleation process at potential nucleus forming sites, followed by nuclear growth. The potential nucleus forming sites were termed "germ nuclei" and those which became active and started growing were termed "grains" or "growth nuclei". Sites which were ingested by growing nuclei, and hence never became active, were called "phantom nuclei".

Suppose N_o is the total number of germ nuclei at time $t = 0$. This number will decrease with time, and at time $t = t$ their number will be $N'(t)$, since $N(t)$ become active growth nuclei and $N''(t)$ are ingested by the growth of $N(t)$ nuclei. Thus for any time dt the decrease in the number of germ nuclei is equal to the sum of the numbers of growth and phantom nuclei formed, i.e.

$$-dN' = dN + dN'' \quad \ldots\ldots\ldots\ldots\ldots\ldots\ldots\ldots (1.23)$$

where dN/.....

where $dN = k_1' N' dt$ .....(1.24)

and $dN'' = N'/1-\alpha . dt$ .....(1.25)

Previously ingestion i.e. dN" had been assumed negligible and thus

$$-dN' = k_1' N' dt \quad \text{.....(1.26)}$$

or $N = N_o e^{-k_1' t}$ .....(1.27)

On allowing for ingestion then from equations 1.23, 1.24 and 1.25 we get

$$dN'/dt + k_1' N' + N'/1-\alpha . d\alpha/dt = 0 \quad \text{.....(1.28)}$$

which on rearranging and integrating yields

$$N' = N_o e^{-k_1' t} . (1-\alpha) \quad \text{.....(1.29)}$$

and thus $dN/dt = k_1' N_o e^{-k_1' t} . (1-\alpha)$ .....(1.30)

Thus for small α values nucleation obeys the exponential law

$$N(t) = k_1' N_o \int_o^t e^{-k_1' y} \left[1-\alpha(y)\right] dy \quad \text{.....(1.31)}$$

If the nuclei grow three-dimensionally then

$$\alpha = \frac{s k_1' N_o k_2'^3}{V_o} \int_o^t e^{-k_1' y} (t-y)^3 \left[1-\alpha(y)\right] dy \quad \text{..(1.32)}$$

where s is a shape factor, and V_o is the volume of product obtained from the complete decomposition of w_o g. of reactant.

As the nuclei grow larger they will eventually impinge on one another and growth will cease at the point where they touch. The fraction α decomposed at a time t will thus be less than the value calculated from equation 1.32 where impingement is neglected. The problem is best overcome by introducing the concept of the "extended fractional decomposition α_{ex}", which is the total fraction of reactant which would have decomposed in time t, including the contributions of phantom nuclei and ignoring overlap. It is best obtained by calculating the total or "extended" volume V_{ex} occupied by these nuclei. Thus

$$\alpha_{ex} = 1/V_o/ \ldots\ldots$$

$$\alpha_{ex} = 1/V_o \cdot \int_o^t V(ty)\left[dN'/dt\right]_{t=y} dy \quad \ldots\ldots\ldots\ldots\ldots (1.33)$$

where V(ty) is the volume at time t of a nucleus formed at t = y.

$$V(ty) = s\left[k_2' (t-y)\right]^3 \quad \ldots\ldots\ldots\ldots\ldots\ldots\ldots\ldots (1.34)$$

where k_2' is the linear rate of isotropic growth. Hence

$$\alpha_{ex} = \frac{s k_2'^3 k_1' N_o}{V_o} \int_o^t e^{-k_1' y} (t-y)^3 dy = V_{ex}/V_o \ldots (1.35)$$

Since the integral in equation 1.35 is readily evaluated the problem is thus to relate the extended volume, V_{ex}, to the actual volume, V, of the product. Avrami has shown that this can be done in a quite general way but the final formula are rather intractable. However, he has also shown that where the distribution of the nuclei is uniform or even locally random then

$$dV_{(t)}/d\, V_{ex}(t) = 1 - V_{(t)} \quad \ldots\ldots\ldots\ldots\ldots\ldots\ldots (1.36)$$

or on integration and rearranging

$$V_{(t)} = 1 - e^{-V_{ex}(t)} \quad \ldots\ldots\ldots\ldots\ldots\ldots\ldots (1.37)$$

Since V is proportional to α thus

$$d\alpha/d\alpha_{ex} = 1-\alpha \quad \ldots\ldots\ldots\ldots\ldots\ldots\ldots\ldots (1.38)$$

This satisfies the boundary condition since at $\alpha = 0$ $d\alpha/dt = d\alpha_{ex}/dt$ and at $\alpha = 1$ $d\alpha/dt = 0$ but $d\alpha_{ex}/dt$ is finite.

Thus from equations 1.35 and 1.38

$$\alpha_{ex} = \int_o^{\infty} d\alpha/1-\alpha = \frac{s k_2'^3 k_1' N_o}{V_o} \int_o^t e^{-k_1' t} (t-y)^3 dy \ldots (1.39)$$

$$\text{or } -\log(1-\alpha) = \frac{6\, s\, N_o\, k_2'^3}{V_o\, k_1'^3} \left[e^{-k_1' t} - 1 + k_1' t - (k_1' t)^2/2 + (k_1' t)^3/3\right] \quad \ldots\ldots\ldots\ldots\ldots (1.40)$$

This is the most general solution to the problem of random nucleation followed by three-dimensional growth. If α is very small and hence overlap and ingestion are negligible then

$$\alpha = \alpha_{ex}/\ldots\ldots\ldots\ldots\ldots$$

$\alpha = \alpha_{ex}$ and hence

$$\alpha = \frac{6s\ N_o\ k_2'^3}{V_o\ k_1'^3}\left[e^{-k_1't} - 1 + k_1't - (k_1't)^2/2 + (k_1't)^3/3\right] \quad \ldots\ldots(1.41)$$

From this it is seen that if $k_1't$ is very small then

$$\alpha = ct^4 \quad \ldots\ldots(1.42)$$

or for plate-like nuclei or instantaneous nucleation followed by three-dimensional growth

$$\alpha = c't^3 \quad \ldots\ldots(1.43)$$

or for linear growth

$$\alpha = c''t^2 \quad \ldots\ldots(1.44)$$

When $k_1't$ is very large equation 1.40 reduces to

$$-\log(1-\alpha) = sN_o\ k_2'^3/V_o.\ t^3 = k_5t^3 \quad \ldots\ldots(1.45)$$

Using a different approach Erofeyev[36] derived a similar equation to this. Without making any special assumptions regarding the properties of the reacting system he first derived the general kinetic equation

$$\alpha = 1 - \exp\left(-\int_o^t p\,dt\right) \quad \ldots\ldots(1.46)$$

or

$$-\ln(1-\alpha) = \int_o^t p\,dy \quad \ldots\ldots(1.47)$$

where p is the probability of the reaction of an individual molecule in a time interval dt. This general equation was then applied to the formation and growth of reaction nuclei in a solid.

If the rate of formation of nuclei is given by dV/dt, then for a constant rate of nucleation we get

$$dV/dt = \text{const} \quad \ldots\ldots(1.48)$$

or of the rate is a power of time then

$$dV/dt = \text{const}\ t^z \quad \ldots\ldots(1.49)$$

where z is/.....

where z is the number of electrons required to set up a stable nucleus. In both cases, for three dimensional nuclei, the probability pdt is proportional to the total volume of the spherical layers traced, at the constant t, around the nuclear centres that have arisen at the instant t^x. Theradii of the spheres limiting the layers are

$$r = u\,(t-t^x) \text{ and } r + dr = u\,(t + dt - t^x)$$

Accordingly we have

$$pdt = dt \int_0^t 4\pi u^3\,(t-t^x)^2\, dV/dt.\, dt \qquad \ldots\ldots\ldots\ldots (1.50)$$

Now if nucleation proceeds as a power of time, then from equations 1.49 and 1.50 we get

$$pdt = \text{const}\ t^{z+3}\, dt \qquad \ldots\ldots\ldots\ldots\ldots\ldots\ldots\ldots (1.51)$$

and from this and equation 1.46 we get

$$\alpha = 1-\exp(-kt^{z+4}) \qquad \ldots\ldots\ldots\ldots\ldots\ldots\ldots\ldots (1.52)$$

e.g. if the rate of nucleation is as the square of time then

$$\alpha = 1-\exp(-kt^6) \qquad \ldots\ldots\ldots\ldots\ldots\ldots\ldots\ldots (1.53)$$

which for small values of t reduces to

$$\alpha = \text{const}\ t^6 \qquad \ldots\ldots\ldots\ldots\ldots\ldots\ldots\ldots (1.54)$$

which is the power law equation postulated by Wischin[3] for barium azide.

For a constant rate of nucleation equations 1.48 and 1.50 combine to give

$$pdt = \text{const}\ t^3 dt \qquad \ldots\ldots\ldots\ldots\ldots\ldots\ldots\ldots (1.55)$$

and this from equation 1.46 yields

$$\alpha = 1-\exp(-kt^4) \qquad \ldots\ldots\ldots\ldots\ldots\ldots\ldots\ldots (1.56)$$

i.e. this would correspond to three-dimensional nuclei increasing in number at a constant rate.

For cylindrical nuclei

$$\alpha = 1-\exp(-kt^3) \qquad \ldots\ldots\ldots\ldots\ldots\ldots\ldots\ldots (1.57)$$

and for flat/.....

and for flat nuclei

$$\alpha = 1-\exp(-kt^2) \quad \ldots\ldots\ldots\ldots\ldots\ldots\ldots\ldots\ldots\ldots (1.58)$$

Thus in general according to the shape of the nuclei and their rate of increase

$$\alpha = 1-\exp(-k_5 t^n) \quad \ldots\ldots\ldots\ldots\ldots\ldots\ldots\ldots\ldots\ldots (1.59)$$

or $$-\log(1-\alpha) = k_5 t^n \quad \ldots\ldots\ldots\ldots\ldots\ldots\ldots\ldots\ldots\ldots (1.60)$$

which is of the same form as equation 1.45 derived by Avrami.

In cases where there is considerable overlap and ingestion of nuclei which form and grow according to a power law, equations 1.59 and 1.60 are most commonly used to describe the course of the reaction. The expressions are known as the Avrami-Erofeyev Equations.

In virtually all of the thermal decompositions which have been studied the acceleratory period can be accounted for topographically in terms of a reaction mechanism described by one of the above five groups of equations.

The Decay Reaction.

The decay period corresponds to that period where extensive overlap of the growing nuclei has occurred and reaction thus proceeds from a shrinking reactant/product interface. If the interface remains intact the Avrami-Erofeyev equation may still hold i.e.

$$\alpha = 1-\exp(-k_5 t^3) \quad \ldots\ldots\ldots\ldots\ldots\ldots\ldots\ldots\ldots\ldots (1.61)$$

with the value of n = 3, since ingestion of potential nucleus forming sites will be virtually complete. However, this is seldom the case since the strain produced by differences in the molecular volumes of parent and product phases usually results in the collapse of the interface. This could leave isolated blocks of reactant containing no nuclei in which the rate of reaction is proportional to the amount of substance undecomposed. Hence

$$d\alpha/dt \ldots\ldots\ldots\ldots$$

$$d\alpha/dt = k_7 (1-\alpha) \quad \ldots\ldots\ldots\ldots\ldots\ldots\ldots\ldots\ldots\ldots (1.62)$$

and thus $-\log (1-\alpha) = k_7 t$ ..... (1.63)

or $\log (p_f/p_f-p) = k_7 t$ ..... (1.64)

Equations 1.62, 1.63 and 1.64 are different forms of the Unimolecular Decay Law.

Prout and Tompkins[28], in their study on the thermal decomposition of potassium permanganate, suggested that the rate of reaction in the decay was proportional to the number of unreacted molecules, which is proportional to (p_f-p). Also, for decomposition to be favoured, an unreacted molecule should be adjacent to a product molecule because contiguity facilitates decomposition. Thus the rate reaction is

$$dp/dt = k_8 (p_f-p) P \quad \ldots\ldots\ldots\ldots\ldots\ldots\ldots\ldots\ldots\ldots (1.65)$$

where P is the probability of the favoured situation and is determined by α, i.e. by p/p_f. Therefore

$$dp/dt = k_8 (p_f-p) p/p_f \quad \ldots\ldots\ldots\ldots\ldots\ldots\ldots\ldots\ldots\ldots (1.66)$$

On integration between limits this reduces to

$$\log (p/p_f-p) = k_8 t + c_8 \quad \ldots\ldots\ldots\ldots\ldots\ldots\ldots\ldots\ldots\ldots (1.67)$$

which is the Prout-Tompkins Equation (1.20) only with the rate constant, k_8, different from that for the acceleratory period.

Frequently, in cases where there is rapid and efficient surface nucleation of particles, the surfaces of the particles become coated with a layer of product at an early stage of the reaction, (e.g. curves b and c, FIGURE 1). The rate determining step could then be the rate of penetration of this interface into the particle. If the particles are spherical and of initial radius r, then the fraction decomposed at time t is given by

$$\alpha = {}^4/_3 \pi a^3 - {}^4/_3 \pi (a - k't)^3 / {}^4/_3 \pi a^3 \quad \ldots\ldots\ldots\ldots (1.68)$$

$$= 1 - \left(\frac{1-k't}{a}\right)^3 \quad \ldots\ldots\ldots\ldots\ldots\ldots\ldots\ldots\ldots\ldots (1.69)$$

$$= 1 - (1-k_9 t)^3 \quad \ldots\ldots\ldots\ldots\ldots\ldots\ldots\ldots\ldots\ldots (1.70)$$

or $1-(1-\alpha)/$.....

or $1-(1-\alpha)^{1/3} = k_9 t$ .....(1.71)

Equation 1.71 is known as the Contracting Sphere Equation.

It is also possible to get other shapes of contracting interfaces, e.g. a contracting parallelopiped, or rectangle, or circle depending on the geometry of both the particles and the interface. These can be treated in a similar manner to the contracting sphere example.

In most of the thermal decompositions studied the decay reaction can be described in terms of one of the equations, 1.61, 1.64, 1.67 or 1.71.

Mathematical analyses of the pressure/time plots can thus yield much information on the reaction mechanisms of thermal decompositions. However, as stated earlier, a particular analysis is not conclusive proof of any one mechanism and further evidence must be sought. In this regard the effects of preirradiation on the subsequent thermal decomposition has proved to be a powerful tool. Initially, such studies were confined to the effects of preirradiation with ultra-violet light, but this has since been extended to include the effects of high energy radiation such as γ-rays. The study of the effects of such preirradiations has often been invaluable in elucidating the nature of the irradiation damage.

1.2. Effects of Ultra-Violet Light on Solids.

1.2.1. The Interaction of Light with Matter.

The effects of ultra-violet light on solids, can generally be accounted for in terms of electronic processes, with the production of various types of point defects. Ionic solids are insulators, excepting for possible ionic conduction, since each energy state in the first electron band contains its maximum number of 2 electrons i.e. it is a "full band". An electron in the full band may aquire sufficient energy to be raised

into the next/.....

into the next band when the solid is irradiated with light of a wavelength characteristic of the particular solid. There is an abundance of empty states in this band. The excited electron is thus mobile and can move through the crystal. This second band is termed the "conduction band". The positive hole created by the loss of the electron from the full band is also mobile. The photoconductivity of insulators can thus be explained in terms of mobile electrons and mobile positive holes.

Inorganic salts exhibit regions of absorption of light of characteristic wavelengths. The absorption spectra consist of a short series of broad peaks, usually one to three in numbers, with no resolvable fine structure. The absorption spectra of the alkali halides have been extensively studied. The effects given below were obtained from these halides but can be fairly generally applied to other ionic solids. Each absorption peak corresponds to the elevation of electrons to a particular excited state. Fergusson[37] has shown that photoconductance is not observed in sodium chloride at wavelengths above that corresponding to the peak for the second absorption band. The first peak must thus represent a mode of excitement below the conduction band and the second peak the series limit, as was suggested by Mott.[38] The first peak is considered to correspond to an excited electron which is still bound to its positive hole. The excited electron and positive hole can move through the crystal as a single entity which is termed an exciton.[39]

The primary effect of irradiation with ultra-violet light is thus to elevate electrons into excited states, resulting in the formation of excitons or free electrons and their conjugate positive holes. In disposing of the extra energy which an excited crystal has obtained a number of secondary effects can result. Fluorescence and phosphorescence have often been observed due to free electrons returning to the ground state accompanied by the re-emission of the absorbed energy. Re-

emission of/.....

emission of absorbed radiation from the first band (excitons) has never been observed, and it is considered that excitons dissipate their energy by scattering or transferring energy to imperfections.[40]

Since the conduction electrons are mobile, it is possible for them to move through the lattic and be trapped at sites where this is energetically possible. On exposure to ultra-violet light or electron bombardment the alkali halides aquire a deep colour which gradually fades. Since only a single peak is observable it was concluded that the colour was due to a single transition. The centres responsible for this absorption were termed F-centres by Pohl.[41] De Boer[42] suggested that F-centres were formed by an electron being trapped by an anion vacancy, a view which has subsequently been confirmed.

It is also possible for the positive holes formed to react with vacant lattice sites. The existence of V-centres has been demonstrated,[43] and identified with the interaction of positive holes and cation vacancies.

Further interaction of these point defects with electrons, or under suitable conditions, amongst themselves, can give rise to a large variety of other centres. For example an F-centre may trap a second electron to give rise to an F'-centre. Combination of an F-centre with an anion vacancy would produce an R_1-centre, and with a second F-centre an R_2-centre (or double F-centre). M-centres result from the combination of F-centres with cation/anion vacancy pairs. Analogues of these centres are also obtained by corresponding interactions of V-centres.

The production of point defects under the action of ultra-violet light is of fundamental importance to the theories of the photolysis of solids, and the effects of such preirradiation on the thermal decomposition of solids.

1.2.2. Photolysis, and the Effects of Preirradiation with Ultra-Violet Light on the Thermal Decomposition of Solids.

In the case/.....

In the case of the alkali halides the effects described in the previous section are all reversible under suitable conditions of temperature and illumination. In other cases, especially in the silver halides and many metallic azides, and, to a lesser extent, in oxalates, styphnates and fulminates, definite chemical changes do occur on irradiation. One of the most important of the earlier papers on photolysis was that by Mott and Gurney[17] on the photolytic decomposition of silver bromide. The value of this work was that the authors were able to reconcile two apparently contradictory facts, namely, that while irradiation was done uniformly over the whole surface, reaction took place at discrete nuclei. It was found possible to transfer their ideas to the formation and growth of nuclei in thermal decompositions. It had previously been established that irradiation with light, above the first absorption edge, produced a new band in the visible spectrum[44] accompanied by photoconductance.[45] Gurney and Mott thus concluded that free electrons were produced on irradiation. The positive holes so formed could then react with bromine ions forming neutral bromine atoms. These then combined to give bromine gas which easily escaped since the process was a surface one. The mobile electrons could be trapped at metastable positions and also by interstitial silver ions from Frenkel defects, yielding silver atoms. The silver atoms then trapped a further electron forming an Ag^- ion, a process favoured by a high concentration of conduction electrons. A migrating interstitial Ag^+ ion, neutralized the charge on the Ag^- ion and repitition of this process eventually produced a speck of silver. The metallic speck then catalysed the reaction since the lowest vacant energy levels in metallic silver were lower than the energy levels of the conduction band of the crystal. Electron capture was thus favoured, and the reverse process became unlikely. Hence the result was a <u>growing</u> nucleus accompanied by escape

of the bromine/.....

of the bromine formed.

Sheppard[46,47] had shown that traces of certain impurities (mainly thioureas) could greatly increase the sensitivity of silver halides to light because of the formation of sensitivity specks of silver sulphide. Gurney and Motts theory could explain this since the conduction levels of Ag_2S are lower than those for Ag Br. Electrons were thus localised in the conduction bands of the specks which could then attract Ag^+ ions and normal growth could proceed.

Anastasevich and Frenkel[48] considered that silver bromide contained Schottky defects and that photolysis occurred by the capture of photoelectrons at vacant anion sites to give F-centres. Migration of F-centres took place by successive displacements of adjacent anion sites. These F-centres thus flocked together to form colloidal silver particles from which growth took place.

Mitchell[49] discussed the results obtained by Stasiw and Teltow[50-54] on the photodecomposition of silver bromide containing traces of sulphide. In contrast to Gurney and Mott he concluded that the Ag_2S went into solid solution forming singly charged S^- ions and F-centres. The F-centres aggregated and formed colloidal silver particles which acted as electron traps. These, he concluded, were the sensitivity specks. On illumination electrons could leave the F-centres and be transferred to the aggregates which then increased in size by a process of ionic migration, as in the Mott theory. Movement of F-centres was considered to be by a slowly moving vacant anion site coming to within a few lattice spaces of the F-centre, when the electron jumped across by the tunnel effect. The original site then diffused away.

In a discussion of the photographic process Mitchell[55] proposed a modification of Mott's theory to explain the growth of nuclei in non-sensitized crystals of silver bromide. He

suggested that/.....

suggested that the free electrons could be trapped by silver ions in the sub-boundaries of the crystal to give silver atoms. Since diffusion of silver atoms along sub-boundaries and surfaces was possible, a silver atom could associate itself with a drifting silver ion to form a positively charged pair (Ag_2^+) which could then combine with a further electron. Nuclei grew by repitition of this process. In support of this type of mechanism, Grimly and Mott[56] have shown, on theoretical grounds, that massive silver in contact with silver bromide, and in thermodynamic equilibrium with the defects of the ionic lattice, should aquire a positive charge due to attachment of interstitial Ag^+ ions. A group of three silver atoms was estimated as being the lower limit of size that could aquire a positive charge.

Garner and Maggs[6] showed that ultra-violet light could produce photolysis in barium azide. The reaction occurred at the interface between the product and the reactant and nitrogen was evolved at a constant rate. Preirradiation also shortened the induction period and increased the reaction rate in the thermal decomposition of barium and strontium azides. An enormous increase in the number of nuclei was observed.

Mott[57] examined the photolysis of barium azide and concluded that exactly the same theory as proposed by Mott and Gurney[17] for the photodecomposition of silver bromide could be applied in this case. He further concluded that the mechanism for the thermal decomposition was the same as that for photolysis.

The Mott theory required that barium azide should show photoconductance. Thomas and Tompkins[58,59] have shown that this is not the case. They also concluded that the rate of nucleus growth could not be accounted for by any mechanism involving both cation and anion migration. Instead they postulated a theory involving the production and trapping of excitons.

Irradiation with ultra-violet light produced excitons which were mobile and could migrate. These were subsequently trapped at some imperfections the most likely being cation vacancies although any imperfections could act as traps. It was considered that at cation vacancies the decomposition of two excitons occurred with zero activation energy. At other trapping centres a small energy of activation was needed to overcome steric hindrance. The excitons only existed for a short time before reverting to the ground state, but if two were trapped in adjacent positions before this then reaction occurred. This reaction resulted in the liberation of nitrogen and the formation of two anion vacancies and two electrons, the original trap being regenerated. Nucleus growth then took place by the transformation of lattice Ba^{++} ions to barium atoms with the atoms occupying the lattice position of the salt. On further growth this recrystallized to the metal lattice. The nitrogen could then escape through the cracks formed in the crystal by this process.

Thomas and Tompkins[60] also reported a decrease in the duration of the induction period and an increase in the rate of the thermal decomposition after irradiation with ultra-violet light. These effects were accounted for in terms of the large number of anion vacancies formed by irradiation. These facilitated nucleus formation. The acceleratory period was analysed by the power law in the form $p = C\,(t-y)^n$ where y is a slow growth correction for small nuclei. The value of n was normally 6 but after heavy doses decreased to 3, due to nucleus formation during irradiation.

The photolysis of solid potassium azide was studied by Jacobs and Tompkins.[61] The salt turned blue on irradiation. The production of excitons was again considered to be the main mode of excitement. The results were the same as those for barium azide. The quantum yield was low and the rate of evolution of nitrogen at constant temperature and intensity was

constant./.....

constant. The rate varied as the square of the intensity and at constant intensity could be expressed by a similar function of temperature as found in barium azide. It was thus concluded that the mechanism of photolysis was as in barium azide, but with one modification. It was reasoned that all the trapping centres were cation vacancies and that exciton pairs trapped at such points had a small but finite activation energy for decomposition. However, as the complex aquired thermal energy from the lattice so the steric factor decreased, and zero activation energies became more likely. It was also shown[62] that preirradiation had no effect on the thermal decomposition of potassium azide. However, the blue colour obtained on irradiation could be more fully explained. On warming the colour rapidly faded. In addition to vacancies and positive holes, irradiation also produced F-centres, formed by electrons from excitons tunneling to anion vacancies. The complex of the F-centre and the positive hole formed in the process constituted a colour centre. On heating the reverse process rapidly occurred with bleaching of the colour. Hence electrons were never elevated into the conduction band which was consistent with the absence of photoconductance.

In a subsequent investigation, using both low and high pressure mercury lamps, Jacobs, Tompkins and Young[63] concluded that the photolytic decomposition of barium azide was more complex than originally proposed. A number of mechanisms which were dependent on the wavelength of the radiation were considered possible. The primary act of the low pressure arc was the production of mobile excitons which were trapped and then decomposed according to the original mechanism. The radiation from the high pressure arc had a longer wavelength with insufficient energy to produce excitons in the bulk of the lattice. However, at special positions near dislocations where the selection rules were relaxed, absorption of radiation could produce positive holes and electrons. These were localized for a time/.....

lized for a time with a high probability for the reverse reaction. The positive hole could, however, react with a second azide ion to give nitrogen, the barium produced being deposited along the plane of the mosaic boundary containing the active sites. Filamentary metal was thus formed in the dislocation network comprising the grain boundaries. The metal could trap positive holes and thus catalyse further decomposition. Once macroscopic specks of metal had been formed photolysis could be induced by radiation of longer wavelength (>3,300Å). At the metal there was transfer of electrons from adjacent azide ions to the metal to give positive holes trapped next to negatively charged metal specks. There was a finite possibility that during its like-time a positive hole would react with an adjacent azide ion to yield nitrogen, and the metal speck would thus grow in size.

Further mechanisms for the photodecomposition of barium azide were postulated by Jacobs, Tompkins and Verneker[64]. At least two mechanisms were considered to be operative. The first action of the radiation was the production and trapping of excitons as before,[63] only the number of traps decreased with time due to the crystal assuming different properties in these regions. Once barium atoms were formed they could lose electrons to the conduction band to yield Ba^+ ions. These were neutralized by the transfer of electrons from adjacent azide ions. The positive holes formed could then react with each other or with excitons to yield nitrogen. Since this also resulted in the formation of more barium atoms the process was accelerated. These mechanisms could explain the initial decrease and subsequent increase in the rate obtained experimentally. At high concentrations of positive holes the rate determining step was the rate of production of excitons. This gave a constant rate of photolysis.

Dodds[65] has shown that the photolysis of sodium azide can be explained by an exciton mechanism similar to that proposed

by Thomas and Tompkins/.....

by Thomas and Tompkins[54,55] for barium azide.

Garner and Reeves[66] found that the acceleratory period in the thermal decomposition of calcium and strontium azides obeyed the equation

$$p^{1/3} = m^{1/3} k (t-t_o)$$

where m is the mass decomposed. Irradiation with ultra-violet light improved the extent of fit, shortened the induction period and caused a threefold increase in the acceleratory rate constant. They considered that after irradiation there were more nuclei which were also more uniform in size.

Finch, Jacobs and Tompkins[27] transferred the exciton theory to the photolysis and thermal decomposition of irradiated silver oxalate. Little modification was needed. The main difference was that a single oxalate exciton could decompose whereas two azide excitons were necessary. It was proposed that on irradiation an exciton was formed which could be trapped at an anion vacancy. Further excitation of the complex by light could result in the vacancy capturing a second electron giving an oxalate radical associated with an anion vacancy containing two electrons. This radical could then decompose according to the equation

$$[Ox]^{2-} \rightarrow 2\,CO_2 + [2e^-]$$

where $[2e^-]$ = 2 anion vacancies and 2 electrons.

Preirradiation increased the rate of the thermal decomposition. Thermal nuclei were assumed to form at anion vacancies by the same mechanism as photolytic nuclei. The increased number of anion vacancies resulting from preirradiation facilitated this and hence increased the rate.

Prout and Tompkins[12] found higher initial rates in the thermal decomposition of mercuric oxalate on preirradiation with ultra-violet light or electron bombardment. They concluded that the effect was a surface one, an electron being ejected

from a surface/.....

from a surface oxalate group and then being recaptured by a mercury ion in the second molecular layer. This electron transfer was then followed by an intramolecular change in which "mercurous oxalate" was formed. Decomposition of this gave the higher initial rate.

The results of electron bombardment can usually be explained by mechanisms similar to those used in a study of ultra-violet light effects. Groocock and Tompkins[9] investigated the decomposition of azides by electron bombardment and found this to be the case. However, two differences were found in the case of barium azide. In the equation $p = C(t-y)^n$, C increased as the square of the electron flux but linearly with the light intensity, and secondly, in the thermal decomposition the value of n remained at 6 throughout but with prolonged irradiation by ultra-violet light dropped to 3. The high concentration of electrons resulted in all the anion vacancies capturing electrons to form F-centres. These were immobile due to the absence of vacancies and hence no nuclei formed during bombardment.

Meiler and Noyes[67] decomposed potassium chlorate with ultra-violet light of wavelengths below 280 $m\mu$ and also with 22 volt electrons. No mechanisms were postulated.

Miller and Brous[68] studied the decomposition of sodium azide by electron bombardment and ultra-violet light. A reproducible threshold value for decomposition was found, but otherwise the results were inconclusive, being affected by several factors.

Jacobs[69,70] bombarded films of potassium chloride on nickel with electrons, and found that the electrons trapped in the salt could be released by electrons of a critical energy which approximated to the photoenergy required to free electrons trapped at F-centres in potassium chloride.

The interpretations of photolytic mechanisms has been of great value in achieving a better understanding of the nature

of thermal/.....

of thermal decompositions, since the photo- and thermal processes can frequently be equated. This has been expecially the case for the processes of nucleation and nuclear growth.

1.3. Effects of High Energy Radiation on Solids.

1.3.1. The Interaction of High Energy Radiation with Matter.

The term "high energy radiation" includes the effects of particles, such as protons, neutrons and relativistic electrons, and γ-rays, and X-rays of very short wavelengths. In this energy range direct changes which could be produced by irradiation are, (i) actual displacements of atoms or ions from lattice sites into interstitial positions, (ii) ionisation and electronic excitation, (iii) radiolysis of the reactant resulting in the production of foreign "inclusions" in the original lattice, and (iv) nuclear transmutations. Secondary effects are, further excitation and disruption of the structure by atoms and electrons which have been knocked on, and trapping of excited electrons to produce electronic point defects.

The effect of neutron bombardment is influenced by the velocity of the neutrons. The energy of neutrons varies from about 2 MeV for fast neutrons to 0.025 eV for thermal neutrons. Seitz and Koehler[71] have estimated the minimum energy (E_d) for displacement of atoms into interstitial positions to be of the order of 25 eV. Values approximating to this have been obtained for graphite[72] and copper[73] although detailed theoretical calculations on copper[74] and germanium[75] indicate that the value is also affected by the lattice type and the direction of displacement. Thus fast neutrons will produce damage mainly by collision processes when target atoms are knocked out of place. When a fast neutron "collides" with an atomic nucleus it transfers energy to the nucleus and if this is above the threshold value a primary knock-on is formed which ploughs a

track through/.....

track through the material. The further interaction of such a knock-on has been analysed by Kinchin and Pease[76] and several other.[77-80] The primary knock-on can "collide" with several other atomic nuclei in turn, producing further knock-ons and each time losing energy until it comes to rest. The secondary can also produce further knock-ons and henoe several atoms can be displaced by a cascade process resulting from a single neutron. By making certain assumptions Kinchin and Pease were able to calculate the number of displaced atoms in such a system.

A drawback to this is that atoms are usually affected in large groups, not singly. An approach has thus been developed where the excitation is considered to be of the form of a spreading and dying of heat conduction, the regions affected being termed spikes. Theories of thermal and displacement spikes have been proposed by Seitz[81] and Brinkman,[82,83] respectively. Where the excitation is small and few or no atoms leave their sites , the disturbance is called a thermal spike. Where considerable displacement occurs due to a large number of atoms being brought rather violently to the molten state with considerable turbulent flow the disturbed area is termed a displacement spike.

With thermal neutrons, neutron capture by atomic nuclei can occur if materials of suitable cross-section are irradiated. If the transmutation product is unstable then the process is tantamount to the introduction of impurity atoms. The γ-rays of capture and decay may have considerable energy and cause further damage by ionisation processes. In addition the atom involved in the neutron capture process may be given sufficient recoil energy to displace it into an interstitial position. The transmutations in Li^6 and B^{10} can result in radiation effects with local damage.[84,85]

A recent development has been the use of computer methods to calculate the effect of a large number of atoms in a lattice

interacting with/.....

interacting with realistic forces. This technique was intiated by Vineyard et al and a number of results have been published for face-centred and body-centred cubic lattices.[86-90] The results obtained from these studies support the predictions of the cascade theories.

Both Coulombic interactions and elastic collisions can occur with heavy charged particles. At high initial particle velocities electronic excitation predominates but as the particle slows down collisions with lattice atoms become more frequent. The energies of the primary knock-ons formed are, however, considerably less than those from neutron bombardment.

Only relativistic electrons have sufficient energy to produce displacements. Displacement cross-sections are very small for electron energies in excess of the threshold value, and since electron/target-atom collisions are heavily biased towards small energy transfer the knock-ons produced seldom have sufficient energy to produce secondaries. Thus damage due to high energy electrons consists mainly of isolated pairs of vacancies and interstitials.

Irradiation of matter with γ-rays and short X-rays has the primary effect of producing ionisation in all solids, which can result in the production of Compton and photoelectrons. Dugdale[91] has pointed out that γ-rays may have sufficient energy for the Compton and photoelectrons generated by them to exceed the threshold for displacement. He showed that disordering could be produced in Cu_3Au by means of γ-rays from Co^{60}. Displacements in Ge by γ-ray irradiation have been reported by Cleland et al.[92]

γ-ray irradiation is thus, in effect, an internal bombardment of the solid by electrons varying in speed from very fast to very slow. It therefore produces the simplest type of damage. The energies of the electrons are close enough to threshold so that only isolated vacancy-interstitial pairs are produced. These are distributed uniformly thoughout the

specimen since/.....

specimen since the absorption of γ-rays is small enough to ensure this. Kinchin and Pease[76] state that for light elements ($Z < 50$) the predominant interaction is the Compton effect while for heavy elements there may be direct displacements of atoms by recoil from the photoelectric effect.

Apart from these effects already mentioned two other possible interactions of γ-rays with matter have been suggested.

Seitz[93] proposed his exciton theory whereby excitons are produced by radiation and travel through the crystal until they encounter a lattice irregularity. Jogs in dislocation lines are likely sites. At these points the energy is discharged into the lattice producing a local "hotspot". Temporary heating of the lattice jogs can induce dislocation climb, i.e. vacancies can be boiled off. The energies involved ($\sim$ 10eV) are sufficient to produce such an effect. Also migration of point defects away from their points of origin may be caused by further absorption of excitons on the defects. The theory offers an attractive explanation for the production of colour centres in ionic crystals.

Varley[94,95 96] suggested a mode of interaction of γ-rays with matter which applies only to substances with highly ionic bonding. He stated that on γ-ray irradiation some negative ions could become temporarily positively charged by the stripping of two or more electrons. The electrons will diffuse away and the positive ion will be left in a very unstable electronic position. This instability could lead to ejection of the ion to an interstitial site where it would ultimately aquire electrons to become partially neutralized. The vacant lattice site could also capture an electron and so become an F-centre.

A combined mechanism with the Varley process occurring near dislocations followed by the interstitials joining the dislocation core and hence producing climb has been suggested by Mitchell et al.[97]

One further/.....

One further suggestion which has been made is that double ionisation could occur by an Auger-type process.[98-102] The ejection of an electron from the K-shell would result in an L-shell electron replacing it. The energy emitted during this process could eject a second electron from the L-shell by an internal conversion process.

1.3.2. The Thermal Decomposition of Preirradiated Solids.

Preirradiation of solids with high energy radiation can often result in marked changes in the subsequent thermaldecomposition of many compounds. Prior to 1954 this field of research had received comparitively little attention, but in the last decade considerably greater interest has been taken in such studies.

The earliest work was that of Garner and Moon[103] and Muraour[104] in 1933. The latter bombarded ∝-lead azide and silver acetylide with high energy electrons. The salts darkened and a slow decomposition occurred at room temperature analogous to that on heating the compounds. However, no study was made of the high temperature decomposition of the irradiated salts.

Garner and Moon studied the effects produced by the emission from radium on the thermal decomposition of crystals of barium azide. No effect was found when the irradiations were done at room temperature. When the radium needle (1 mg. in a glass tube) was placed next to the sample at the temperature of decomposition a fourfold increase in the rate was observed. The main effect of the emission was not in nucleus formation, as expected, but appeared to be an increase in the rate of nuclear growth. The nuclei were very similar in character for both the thermal and accelerated processes, but those on the crystal face nearest the radium needle were much larger than the others.

A similar acceleration of the reaction was found by Maggs[105]

for strontium/.....

for strontium azides using the same radium needle.

Following these early papers the effects of high energy preirradiation remained a dormant field until 1954. Interest was then revived in an indirect way when Bowden and Singh[106] attempted to initiate the detonation of explosives by irradiation. The basis of the attempts was the possibility that there would be a high concentration of energy in a small portion of the lattice on exposure to high energy and ionising radiation. Irradiation was done with electrons, neutrons, fission products, and X-rays, on several detonators and high explosives. However, detonation of the solid was not achieved excepting when using an intense electron beam. The latter effect was shown to be a thermal effect due to bulk heating of the crystals. As an incidental study the thermal decomposition of the preirradiated azides were examined. It was found that lithium azide decomposed with a greatly reduced induction period and a considerably accelerated rate after preirradiation with thermal neutrons (approximate dose 2.5×10^{11} nvt). Lead and cadmium azides were only slightly affected and no effect was found for silver azide.

Flanagan[107] investigated the effect of neutron bombardment on the subsequent thermal decomposition of lead styphnate monohydrate, in what was the first detailed study of the effect of high energy radiation on explosives. He had previously shown[108] that preirradiation with γ-rays had virtually no effect on the thermal stability of the compound. For neutron irradiation only comparitively large doses affected the decomposition. No aging effect was found, and the effect was independent of the neutron flux, the total neutron dose being the important quantity. The pressure/time plots were of the type (d) in FIGURE 1. A greater initial burst of gas was found and the activation energy for the process decreased from 31 kcal. $mole^{-1}$ to 10 kcal. $mole^{-1}$ after irradiation.

The primary effect of irradiation was considered to be the

nuclear reaction

$$N^{14} + n \rightarrow C^{14} + p$$

and also direct atomic displacements resulting from knock-ons. The recoil energy of the C^{14} atom is 45,000 eV. The recoil would thus immediately rupture the C-N bond and would subsequently damage the lattice by elastic collisions once sufficient energy had been lost by the inelastic processes. Similarly the proton with a recoil energy of 0.56 MeV would produce atomic displacements. These regions of damage were believed to be homogeneously distributed throughout the material forming "irradiation nuclei". Dehydration did not remove any of the damage, i.e. the "radiation nuclei" remained intact. This suggested that the significant form of the radiation damage was the irreversible alteration of the styphnate units rather than displaced ions or vacancies. The low activation energy of 10 kcal.mole^{-1} for the initial decomposition was considered to represent the decomposition of these altered groups. The altered groups appeared to be stabilized in the lattice in some manner because of the stability of the radiation damage (no age effects after 3 years) and the very small quantities of gas evolved during the irradiation.

The thermal decompositon of preirradiated ∝-lead azide has been studied by Groocock[109] and Jach.[10]

Groocock found that heavy doses of pile-irradiation or high energy X-rays increased the decomposition rates and shortened the explosion time. There was also a progressive fall in the activation energies of the decomposition processes. No definite conclusion as to the nature of the damage were reached.

Jach investigated the thermal decomposition of pile-irradiated colloidal ∝-lead azide. The dose given was 35 hours at a flux of 7-8 x 10^{12} neutrons cm^{-2} sec^{-1}. Irradiation virtually eliminated both the induction and acceleratory periods. The maximum rate which normally occurred at about

$\alpha = 0.40$ took place at almost $\alpha = 0$, and the pressure/time plots consisted almost entirely of a decay reaction. Activation energies calculated from the maximum velocity and decay rate constant were of the order of 10 kcal.mole^{-1} less than the corresponding ones for the unirradiated salt.

For the unirradiated salt it was considered that the reaction initially occurred preferentially at surfaces, cracks, dislocations etc. The acceleratory period represented 2 and 3-dimensional growth of these nuclei and the decay region was the 3-dimensional penetration of the interface after coalescence of the nuclei. The changes in the kinetics after irradiation were attributed to the formation of a large number of nuclei which grew very rapidly at the decomposition temperature. This gave rapid surface coverage followed by 3-dimensional penetration of the interface.

The nature of the radiation damage was considered to be analogous to that in the nitrates.[110-113] Initially nitrogen would be produced at all surfaces, internal and external, and at imperfections such as dislocation etc. Further irradiation would then probably cause decomposition at normal lattice sites with the build up of gaseous nitrogen internally which then diffused and accumulated in pockets of high pressure gas which caused rupture and further decomposition at the newly formed surfaces. Vacancies and/or clusters of vacancies would then be left behind where lead would accumulate. Most of the damage would be permanent.

The decrease in the activation energies was associated a change in the excitation energy of the electrons resulting from the excessive local strain induced by a radiolysis of 20% prior to thermal decomposition.

Erofeyev and Sviridov[114] obtained complex results for the thermal decomposition of barium azide preirradiated with X-rays. The Avrami-Erofeyev equation

$\alpha = 1-\exp/\ldots\ldots\ldots\ldots$

$$\alpha = 1-\exp(-k_5 t^n) \quad \ldots\ldots(1.59)$$

was used to analyse the pressure/time plots. Large variations in the value of n, depending on the dose and temperature, were found. The presence of moisture introduced further complications. On increasing the dose the induction period shortened. The acceleratory rate constant increased at first but decreased again at high doses. No theoretical analysis was given.

Boldyrev and Skorik[71] found that a larger irradiation effect with X-rays on barium azide was obtained if preirradiation was done at the threshold temperature for decomposition than at room temperature. They suggested that stable irradiation nuclei could form at the threshold temperature, but at room temperature any nuclei formed were unstable. The greater preirradiation effect was thus due to a larger number of initial nuclei when irradiation was done at the threshold temperature for decomposition.

Prout and Brown[115,116] have shown that the thermal decomposition of calcium azide is extremely sensitive to preirradiation by γ-rays and X-rays. The induction period was sharply decreased and the acceleratory and decay rate constants were greatly increased after irradiation. The pressure/time plots for both the unirradiated and irradiated decompositions were described, over the acceleratory period, by the power law with n = 3. The contracting sphere formula described the decay period. No change in the activation energies was observed. The irradiation effects were associated with a large increase in the number of point defects, especially anion vacancies, in the material.

The substances dealt with so far are all primary or secondary explosives, or closely related compounds. Preirradiation effects on several non-explosive solids have also been studied.

In an initial study, Freeman and Anderson[117] found that preirradiation with X-rays significantly affect the thermal

decomposition of ammonium perchlorate. The reaction was studied by differential thermal analysis. This effect and the effects of γ-ray preirradiation were later investigated more fully by Freeman, Anderson and Campisi.[118] The thermal decomposition of ammonium perchlorate was shown to be a multistage reaction which was profoundly affected by preirradiation with X-rays or γ-rays. The low temperature stages were those most markedly affected. The number of stages was unchanged but the decomposition temperature for each stage was lowered on irradiation.

Three posible interpretations were considered in explaining the results. These were (i) the presence of new chemical species formed during irradiation induced decomposition, (ii) lattice defects which acted as reaction nuclei, caused by radiation induced decomposition and (iii) the presence of electronic lattice defects.

Further experimental work with samples doped with possible radiolysis products, and also X-ray powder photographs indicated that (i) and (ii) were not operative and it was concluded that (iii) was the mechanism responsible for the irradiation effects. These electronic defects were considered to be positive holes created in the electronic structure of the perchlorate ions by the X- or γ-rays. Transfer of electrons from the ClO_4^- ions to interstitial NH_4^+ ions was considered to occur. The less stable ClO_4 radicals could then be expected to decompose at a lower temperature than the ClO_4^- ions. Confirmation of these views was obtained by studying the irradiation effects on ammonium perchlorate doped with Ag^+ or Cu^{++} ions. These could act as electron traps and also as bridges in the electron transfer process, e.g.

$$Cu^{++} + ClO_4^- \rightarrow Cu^+ + ClO_4$$

$$Cu^+ + NH_4^+ \rightarrow Cu^{++} + NH_4$$

It was predicted that the doped samples would show greater

sensitivity to/.....

sensitivity to preirradiation than the pure samples. Experimental evidence proved this to be so.

Freeman et al[119-124] have extended this work considerably using several different techniques, and the whole problem has subsequently been reviewed by Freeman and Anderson.[124] The greater sensitivity of samples doped with Ag^+ ions was confirmed and it has been shown that the unirradiated sample is unaffected by this doping.[119] Electrical conductivity measurements[120] have supported the electron transfer mechanism.

The presence of NH_3^+, ClO_3 and the ClO_3^- ion have been shown from ESR[121] and EPR[122] studies. The two ions were considered to be formed by breakdown of the NH_4^+ and ClO_4^- ions followed by electron transfer reactions. The ClO_3^- ion was apparently formed by annealing of the ClO_3 radical. Evidence indicated that the NH_3^+ ion could also anneal.

Samples doped with ClO_3^- ions behaved in a similar manner to irradiated material,[119] indicating that nuclei originated at sites of radiation induced reaction. The chlorate ions being relatively unstable could decompose to oxygen and chloride, resulting in the formation of vacancies and strain in the solid. The importance of lattice imperfections was also indicated by the high reactivity of the NH_4ClO_4 sublimate, which exhibited marked X-ray broadening but has been shown[122] not to contain chlorate ions.

The effects of preirradiation on the thermal decomposition of a number of oxalates has been studied. Prout and Brown[125] investigated the thermal decomposition of nickel oxalate, preirradiated with γ-rays (1.1 MeV) and found the results to resemble those for lead styphnate in many ways. The decomposition of unirradiated material showed an initial burst of gas obeying the contracting area equation. This corresponded to surface coverage of the particles. It was followed by accelerator and decay periods which followed the Prout-Tompkins mechanism. Preirradiation resulted in a higher rate for the

initial and/.....

initial and acceleratory reactions. The salt darkened on irradiation. The amount of gas evolved in the initial reaction increased with dose but the duration of this reaction was constant. The activation energies of the acceleratory and decay periods were unchanged, but that for the initial reaction decreased from 33.0 kcal.mole^{-1} to 15.7 kcal.mole^{-1} on irradiation. The initial reaction was described by the unimolecular decay law after irradiation. A different reaction was thus considered to occur in this phase of decomposition, and it was in this initial stage, that the explanations to the preirradiation effects were sought.

No drop in the final pressure was observed on irradiation. The colour of the irradiated salt indicated the production of Ni by the γ-rays. The primary act of preirradiation was considered to be the freeing of electrons from the oxalate ions. Subsequently the electrons were trapped by Ni^{++} ions to produce Ni and an unstable intermediate arising from the oxalate radical. The nature of this intermediate was uncertain, but it was produced in amounts proportional to the γ-ray dose. The initial reaction was considered to be the decomposition of the intermediate. The damage was considered to occur mainly on the surface, in sub-grain boundaries, and at imperfections and dislocations. At the end of the initial decomposition there was thus once again a surface coverage of the particles by Ni, and the Prout-Tompkins mechanism could then operate. The increased rate in the acceleratory period was assumed to be due to additional vacancies formed by the decomposition of the intermediate.

Jach[126] obtained similar results for nickel oxalate preirradiated with neutrons. However, he did not study the initial decomposition in any detail, which is the period of real significance, as was shown by Prout and Brown.

Herley and Prout[127] have reported on increase in the rate of thermal decomposition of preirradiated (γ-rays) lead oxalate.

The effect of/.....

The effect of reactor irradiation on the thermal decomposition of silver oxalate has been studied by Haynes and Young.[128] The pressure/time plots for the unirradiated salt did not show an induction period. The acceleratory period obeyed the exponential law and the decay period the contracting sphere equation. The rate of decomposition over the acceleratory period was increased by preirradiation and the third power law fitted the irradiated plots. The decay rate was unchanged as was the analytical equation. No detailed mechanism to account for the irradiation effect was presented. It was suggested that electron traps were created by γ-rays, and that "germ nuclei" were formed by fast neutrons. These nuclei grew three-dimensionally and poisoned the branching mechanism.

The sensitivity of silver oxalate to γ-rays was also investigated by Boldyrev et al.[129] Addition of impurities such as cadmium decreased the rate of both the irradiated and unirradiated decompositions. Irradiation was considered to produce breaking of bonds followed by electronic excitement.[130] Trapping of electrons at favourable sites would then occur. The cadmium was considered to be able to trap positive holes.

Young[131] has shown that the thermal decomposition of uranyl oxalate is affected by thermal neutrons. It was considered that in the irradiated material the sub-grains were traversed by a fixed number of linear imperfections which corresponded to the recoil paths of the fission fragments. Nucleation was favoured along these lines. Thus the reaction followed the kinetics of an expanding cylinder in the acceleratory period. In heavily dosed material irradiation affected the initial reaction more than the maximum rate due to early overlap of a large number of cylindrical zones.

The thermal decomposition of unirradiated and preirradiated (γ-rays) potassium bromate was studied by Jach[132] in the temperature range 342°-412°C. At low temperature (<367°C) the unirradiated decomposition consisted virtually of a unimolecular

decay only/.....

decay only. The reaction was a true solid state one and the bromide ions formed were considered to catalize the reaction. Considerable splintering of the crystal was observed. At higher temperatures a distinct acceleratory period preceded the decay. Considerable melting on the crystal surface was observed. This was thought to be due to the formation of a eutectic mixture of reactant and product. Preirradiation resulted in pressure/time plots similar to the low temperature runs over the whole temperature range, and an increase in the reaction rate was obtained. There was a decrease in the activation energy after heavy γ-ray doses. Melting occurred at all temperatures, but to a lesser extent. Previous investigators[133] had shown that radiolysis occurred at room temperature to an extent of 0.7% decomposition at the dose used in this study (9.5×10^7 rad). It was considered that the irradiation products produced shattering of the crystals resulting in an increase in the number of irregularities, which facilitated an increased rate.

The thermal decomposition of preirradiated permanganates has been systematically and extensivoly examined. This work was initiated when Prout[8] discovered the preirradiation of potassium permanganate by reactor irradiation, Co^{60} γ-rays, and 145 MeV protons, drastically altered the subsequent thermal decomposition. There was a progressive shortening of the induction period and an acceleration of the rate with increasing dose. Splintering was observed in unirradiated crystals, and became more marked after irradiation. After heavy doses violent fracturing was observed at the start of the acceleratory period. No radiolysis was detected from the final pressure measurements.

The nature of the radiation damage was considered to be the displacement of potassium ions into interstitial positions by recoil Compton electrons, some of which would have had energy

above the/.....

above the threshold for displacement. The damage was considered to consist of randomly distributed vacancy/interstitial pairs. On heating, at the decomposition temperature, recombination of the vacancies and interstitials occurred with the associated release of Wigner energy which was of sufficient magnitude to produce fracturing of bonds, resulting in a centre of decomposed material where decomposition was then favoured, and hence a decomposition "spike" would be formed. Further annealing of the damage, during the induction period, produced an increase in the size and number of spikes. After heavy doses the large number of spikes at the end of the induction period produced severe strains on the crystal lattice causing violent fracturing. The activation energy for changes occurring during the induction period was 1.31 eV. By analogy with cold worked copper[134] and molybdenum[91] it was assumed that recombination of defects took place through vacancy migration.

Prout et al then made a systematic study of the effects of γ-rays on the thermal decomposition of the permanganates of lithium[135], sodium[135], rubidium[136] and caesium[135]. The decomposition of irradiated silver[137] and barium[138] permanganates was also investigated. Lithium and barium showed only small irradiation effects. No systematic variation of the irradiation effect with increasing atomic weight was found, e.g. in the alkali metals the effects for Cs and Na were comparable. Dienes and Vineyard[139] have shown that for γ-rays of 1 MeV or less the number of displaced atoms is a maximum for light elements and decreases rapidly with increasing atomic number, becoming zero at an atomic weight of 125. Consequently, the absence of a systematic decrease in the irradiation effect, and the pronounced effect found for $CsMnO_4$, precluded the possibility of the effect being due to the formation of displaced cations by interaction with Compton electrons. A modification of the Varley displacement mechanism was thus proposed[135] to account for the irradiation effects. Irradiation was thought to produce multiple ionisation/.....

tiple ionisation of the permanganate ions causing them to become temporarily positively charged. There would then be strong Coulombic repulsion between the stripped ions and the cations. Examination of the crystal structure of $KMnO_4$ indicated that spatially the cations have a greater freedom of movement than the anions. Consequently, it was considered that the Coulombic repulsive forces ejected the cations into interstitial positions, producing a high density of defects (vacancy/interstitial pairs) as before. This mechanism would account for the experimental results more adequately, since the identity of the cation was relatively unimportant.

Boldyrev et al[140-142] did not agree with Prout's theory. The effect of preirradiation with 200 keV X-rays on the thermal decomposition of the permanganates increased in the order Li, K, Rb, Cs and Ag. They proposed[141,142] that the main effect of irradiation resulted in the appearance in the crystal lattice of various defects and inclusions of radiolysis products which catalysed the decomposition. Lattice deformation at the radiolysis product interface and favouring of the electronic and ionic stages at these points would accelerate the reaction. However, no details as to the nature of the radiolysis products, or the mechanisms of the radiolysis and catalysis were given. It was considered that displacement effects could play a secondary role.

Further investigations of the irradiation damage have been made by Prout et al using X-ray photographic methods. In treating the problem of a monatomic lattice containing a random distribution of distortion centres Huang[143] found three effects viz:

(i) a reduction in intensity of the Bragg reflections by an artificial temperature factor,

(ii) a slowly varying background scatter,

(iii) a characteristic diffuse scattering in the neighbourhood

of the Bragg/.....

of the Bragg directions.

The effects of reactor irradiation on boron carbide was interpretated by Senio and Tucker[144] using this analysis. In addition, electron density profiles drawn through carbon atoms showed a 46% displacement of the central atom in the linear chain of three carbon atoms.

Prout and Woods[145] attempted to detect interstitial atoms in γ-ray irradiated silver permanganate in a similar way. No artificial temperature factor was observed and no displacement of the silver or manganese atoms was detected from Fourier projections. However, Laue photographs taken at the end of the induction period showed marked asterism indicating very high stresses. This was not found in unirradiated crystals. The oxygen atoms could not be resolved due to the heavy silver atoms, and the possibility of rupture of the Mn-O bonds could not be discounted.

Consequently Prout and Brown[146,147] made a similar study of heavily irradiated (500 Mrad) potassium permanganate. A small lattice expansion was observed. Pronounced diffuse reflections independent of temperature were found. The diffuse maxima around the reciprocal lattice points were ellipsoidal in form. Konazaki[148] has shown from calculations on cubic crystals that isolated defects (vacancies or interstitials) would show lemniscate type maxima, and pairs of defects would show ellipsoidal maxima. He also predicted a lattice expansion. Thus pairs of defects appear to have been created in $KMnO_4$. Fourier projections and difference syntheses of irradiated and unirradiated $KMnO_4$ crystals showed no change, after irradiation, in the heights of the peaks due to O, Mn and K atoms. However, this did not discount the formation of interstitial oxygen atoms and their associated vacancies since, as indicated by Ozaroff,[149] counter techniques are essential for the measurement of intensites if changes in the electron density distribution due to the lighter oxygen atoms are to be detected. Blaunshtein and

Starodubtsev[150]/.....

Starodubtsev[150] have reported the presence of gaseous oxygen in $KMnO_4$ crystals after massive irradiation with Co^{60} γ-rays.

In view of these investigations, Prout[151] now considers that preirradiation causes rupture of the Mn-O bonds with the production of interstitial oxygen atoms and vacancies. On heating the unstable residue of the MnO_4 group decomposes to give more oxygen and possibly MnO_2. The diffusion of this oxygen, and that already present before heating occurs, produces pockets of gas at very high pressure. The stresses thus caused produce fracture at the end of the induction period with the formation of small fragments, the surfaces of which are highly nucleated. Thereafter decomposition on the damaged fragments is rapid and a considerable acceleration of the reaction occurs.

The thermal decomposition of all solids is not necessarily affected by preirradiation e.g. silver oxide[152]. It would be highly desirable to be able to predict whether the decomposition of a solid would be affected by preirradiation. In 1959, on the limited amount of work available at the time, Prout[153] tentatively suggested that those compounds which decomposed according to a branching chain (e.g. Prout-Tompkins) mechanism would be the ones affected by preirradiation. However, subsequent work did not confirm this. An examination of the substances affected might lead to the conclusion that a polyatomic anion is a prerequisite for an irradiation effect. However, ammonium dichromate[154,155] is unaffected by γ-rays. Consequently, any useful criteria are still obscure. It has, however, been observed by Prout[151] that the irradiation effects do appear to be able to take two forms. Firstly, there is the production of unstable compounds, decomposition of which affects the normal pyrolysis. Examples of this are found with nickel oxalate[125] and lead styphnate.[107] Secondly there is the production of electronic point defects by irradiation which determine the nature of the subsequent thermal decomposition. This has

been found/.....

been found, for example, in lead azide[10] and ammonium perchlorate.[118]

1.3.3. Radiolysis of Solids.

The radiolysis of solids is of importance to thermal decompositions in so far as the radiolysis products might affect the subsequent thermal decomposition. Several papers concerned solely with radiolytic reactions, and the mechanisms of these reactions, have been published, some of which are discussed below. As in photolysis, the mechanisms are often similar to those for thermal decompositions, but this is not necessarily always so.

The decomposition of sodium azide under the action of X-rays has been examined by Heal,[156] and can be explained on a basis similar to the photolytic decomposition. Radiation is considered to produce positive holes (N_3) and conduction electrons, or excitons which would then be thermally excited to form positive holes. The holes are then trapped at lattice imperfections where they react with an azide ion to yield nitrogen, i.e.

$$N_3 + N_3^- \rightarrow 3N_2 + e^-$$

Boldyrev et al[157] have reported that during the γ-radiolysis of alkali metal azides the initial yield of product is proportional to the free space in the lattice. There is no correspondence between the relative radiation and thermal stabilities of the metal azides.

The radiation induced decomposition of inorganic nitrates has been extensively studied. A general review of the subject has been given by Johnson.[158] The primary reaction on irradiation is generally accepted to be

$$NO_3^- \rightarrow NO_2^- + O$$

although for barium nitrate[159] consideration has also been given to the reactions

$$NO_3^- \rightarrow /.....$$

$$NO_3^- \rightarrow NO_3 + e'$$

$$NO_3 + e^- \rightarrow NO_2^- + O$$

A great deal of uncertainty exists as to the nature of the radiolysis, and the factors affecting it. Doigan and Davis[160] attributed the different yields (G-values) to the field strength exerted by the cation. The yields decreased through the series Cs, K, Ba, Pb, Ag, Sr, Na and Li nitrates. Hennig et al[161] considered that the difference in the free space was the influencing factor.

An extensive study by Cunningham and Heal[113] supported this latter idea since the radiolytic yield plotted against the free space yielded a smooth curve. It was considered that the oxygen atoms from the reaction combined at favourable lattice sites to give molecular oxygen.

Hochanadel and Davis[162] obtained similar variations in G-values as did Doigan and Davis. They proposed that the decomposition mechanism was,

$$NO_3^- \rightarrow NO_2^- + O$$

$$NO_3^- + O \rightarrow NO_2^- + O_2$$

$$NO_2^- + O \rightarrow NO_3^-$$

The extent of the last reaction was considered to be negligible.

Cunningham[111], using isotopes of oxygen, found a pronounced isotopic effect for the radiolysis of potassium nitrate at very low fractional decompositions. Attempts were made to explain this by the Franck-Rabinowitch cage effect and the jump frequency of the oxygen atom.

Measurements of the heats of solution[163] of irradiated nitrates established that the strain energy was greatest in the more tightly packed lattices and that more than one maximum in the heat of solution/dose curves occurred. These facts supported the belief that the oxygen liberated was present in

the lattice as molecules and not atoms.

The nitrates of Pb, Li and Ag have been shown to yield the oxides of the metal as well as NO_2^- and O_2, while ESR studies have revealed the presence of the species NO_3, $NO_3^=$, NO_2 and O_2^-, although some have only been detected at temperatures of 77°K or less.

Chen and Johnson[164] considered that the mechanism proposed by Hochanadel and Davis[162] was valid except that the reverse reaction i.e. $NO_2^- + O \rightarrow NO_3^-$ occurred to a significant extent. On this basis they obtained good agreement with the experimental results. The relative yields for different cations were considered to be due to the differences in the relative importance of the last two reactions.

As indicated, some attempts to account for the relative ease of decomposition of nitrates in terms of the concept of free space have been made. This concept has subsequently been applied to several other salts. In the alkali and alkaline earth perchlorates[165] and the alkali metal bromates[166] such correlations have been claimed. However, in surveying the evidence thus far accumulated, Johnson[158] concluded that each compound should be considered as a unique system, and that broad generalisations regarding relative yields are invalid.

Boyd et al[166] found an exponential dependance of the radiolytic yield (G) on the free space in the alkali bromates. Radiolysis was considered to occur at random in the crystal lattice, or possibly in the vicinity of defects, i.e. the break up of excited or ionised bromate ions occurred at widely separated lattice sites. This was in contrast to the thermal decomposition reactions, which were surface ones followed by an interface reaction. The primary step of radiolysis was considered to be the excitation or ionisation of bromate ions i.e.

$$BrO_3^- \rightarrow BrO_3^{-*} \quad \text{or} \quad BrO_3 + e^-$$

Direct or stepwise decomposition to the bromide and oxygen then occurred./.....

then occurred. The decomposition reactions for the exciton would be,

$$BrO_3^{-*} \rightarrow BrO_2^- + O \text{ or } BrO_2 + O^-$$
$$BrO_3^{-*} \rightarrow BrO^- + O_2$$
$$BrO_3^{-*} \rightarrow Br^- + O + O_2$$

Heal[167] found that potassium perchlorate decomposed under X-ray irradiation to give potassium chloride and potassium chlorate in the molar ration of 1:4. Irradiation appeared to produce excitons which would then be trapped at imperfections. Simultaneous trapping of two excitons led to decomposition according to the equation

$$2\ ClO_4^- \rightarrow 2\ ClO_3^- + O_2$$

Alternatively a single trapped exciton could decompose to yield a chloride ion and oxygen

$$ClO_4^- \rightarrow Cl^- + 2O_2$$

Logan and Moore[168] have indicated that the important factors affecting radiolytic yields (G-values) are the relative ease of transferring energy to the lattice vibrational modes, and the density of vibrational states as well as to their average energies.

The foregoing survey of radiolytic reactions is of value in the study of the thermal decomposition of solids in that it will perhaps assist in determining the nature of defects produced during the preirradiation, and the radiolytic products which may be produced as inclusions, with particular emphasis on thermally unstable radiolytic products.

2. PREVIOUS WORK ON THE THERMAL DECOMPOSITION OF MERCURIC OXALATE AND THE ALKALINE EARTH AZIDES.

2.1. Mercuric Oxalate.

Prout and Tompkins[12] studied the thermal decomposition of unirradiated mercuric oxalate and the effects of preirradiation by ultra-violet light, cathode rays, and a high density electron beam, on the decomposition. The acceleratory period of the decomposition for the unirradiated salt obeyed the equation,

$$\frac{dp}{dt} = k_{10}t + c_{10} \quad \ldots\ldots\ldots\ldots\ldots\ldots\ldots\ldots\ldots\ldots (2.1)$$

and the decay period was described by the expression

$$(dp/dt)^{1/2} = k_{11}t + c_{11} \quad \ldots\ldots\ldots\ldots\ldots\ldots\ldots\ldots\ldots\ldots (2.2)$$

They proposed that the acceleratory reaction was a surface one proceeding by the two-dimensional growth of a fixed number of nuclei. After surface coverage the reaction rate was controlled by the rate of linear propagation of the reactant interface inwards.

Preirradiation by ultra-violet light or cathode rays increased the initial rate of decomposition, but did not affect the decay stage. The salt darkened on irradiation. It was suggested that the effect was a surface one and that irradiation produced mercurous oxalate by a mechanism of electron transfer. This salt decomposed faster than the parent material producing the higher initial rate.

A high density electron beam did not affect the decomposition but resulted in considerable loss of weight of the salt accompanied by evolution of gas.

2.2. Barium Azide.

Harvey[1] investigated the thermal decomposition of single crystals of barium azide. He obtained p/t plots which possessed marked induction periods where there was a slow linear evolution of gas. This was followed by an acceleratory period where the

power law/.....

power law with n = 10 (from plots of log p vs log t) approximately fitted the p/t plot. Up to $\alpha = 0.10$ the exponential law described the acceleration. It was used in the form,

$$\log \left(\frac{dp}{dt} - a\right) = k_{12}t + c_{12} \quad \ldots\ldots\ldots\ldots\ldots\ldots (2.3)$$

where a = rate of evolution of gas over the induction period.

The last 20% of the decomposition obeyed the unimolecular decay law.

It was also established that the reaction proceeded from nuclei of metallic barium. These were concentrated on the surface but also appeared in the interior of the crystal. Their numbers increased with time but an expression for the rate of increase could not be obtained. He was unable to give a theoretical explanation of the results.

Garner, Gomm and Hailes[169] explained the fit of the exponential law up to $\alpha = 0.10$ in terms of the reaction spreading uniformly from nuclei only within individual grains composing the crystal. At bounding grain surfaces reaction is retarded and spreads from grain to grain only at a few favoured points giving a branching mechanism.

Wischin[3] was able to perform visual observations and measurements on the barium nuclei and also study the p/t plots. Single crystal were used. The following expressions were obtained:

(i) the radius of the nuclei, r, increased linearly with time, i.e.

$$r = k_{13}t \quad \ldots\ldots\ldots\ldots\ldots\ldots\ldots\ldots\ldots\ldots (2.4)$$

(ii) the number of nuclei, N, increased as the third power of time,

$$N = k_{14}t^3 \quad \ldots\ldots\ldots\ldots\ldots\ldots\ldots\ldots\ldots\ldots (2.5)$$

(iii) the pressure of nitrogen evolved increased as the 6th to 8th power of time

$$p = Ct^{(6-8)} \quad \ldots\ldots\ldots\ldots\ldots\ldots\ldots\ldots\ldots\ldots (2.6)$$

The activation energies for the above processes were 23.5

74.0 and 166.0 kcal. $mole^{-1}$, respectively.

It was thought that the nuclei started growing from the time of commencement of heating.

From (i) and (ii) above, it was suggested that the correct theoretical value for the pressure increase was as the 6th power of time. The most probably mechanism for nucleus formation was thought to be that proposed by Mott.[57] It was considered that a slow surface evaporation of nitrogen occurred, the barium atom left behind being mobile. When two atoms met a nucleus was formed. This would agree with the experimentally found bimolecular rate of formation of nuclei.

Thomas and Tompkins[60] suggested that the departure from the value of n = 6 for the evolution of nitrogen was due to the slow growth of small nuclei. Below a critical size a nucleus was envisaged as growing more slowly than a large one. They stated that the power law should be used in the form,

$$p = C (t - y) \quad \ldots\ldots\ldots\ldots\ldots\ldots\ldots\ldots\ldots (2.7)$$

where y is a slow growth correction, or the time taken for a nucleus to grow to the critical size for normal growth. The slow growth was explained by the fact that the activation energy for the process was 29 kcal.$mole^{-1}$ compared to 23.5 kcal. $mole^{-1}$ for normal growth. The activation energy for pressure evolution was given as 145 kcal.$mole^{-1}$.

It was proposed that the mechanism for nucleus formation involved the loss of an electron from an azide ion into the conduction band of the crystal thus forming a positive hole. This could react with an excited azide ion (exciton) forming nitrogen and an F-centre and anion vacancy complex. This then dissociated to form a free F-centre and vacancy. The F-centres could then aggregate forming double F-centres which were regarded as nuclei. Nucleus growth took place by the ejection of the electron of an azide ion into the conduction band of the metal forming a positive hole which could react with an exciton or an azide

ion whenever/.....

ion whenever enough energy was available, liberating nitrogen. The F-centre complex thus formed is bound to the nucleus.

A decrease in the induction period and an increase in the reaction rate on preirradiation with ultra-violet light was found. Prolonged irradiation reduced the value of n in the power law to 3. The irradiation effect was attributed to the production of anion vacancies which facilitated the movement of F-centres and hence of nucleus formation.

Bartlett, Tompkins and Young[170] reported the results of the visual observation of the slow growth of nuclei in large, relatively perfect crystals.

Garner and Moon[103] found that a radium needle placed next to a crystal of barium azide increased the rate of thermal decomposition. They concluded that this was due to an increase in the rate of growth of nuclei and not of number.

The effect of ultra-violet light on the thermal decomposition was initially investigated by Garner and Maggs.[6] They found an increase in the reaction rate, a decrease in the induction period, and an increase in the value of n in the power law from 6 to 8 as the dose was increased. A plot of log γ (dose) vs t_i gave a linear plot. Visual observations showed an enormous increase in the number of nuclei. The threshold wave length for photochemical action corresponded approximately to that for the ultra-violet absorption edge of the N_3^- ion in the solid state and in solution.

They proposed that the increase in the power from 6 to 8 was due to the number of barium atoms required to form a nucleus increasing from 2 to 3 or 4 after irradiation. The effect of irradiation was to produce a "latent image" which developed into nuclei on heating. This latent image was associated with holes produced by the ultra-violet light at which points nuclei could form. On prolonged irradiation photolysis took place.

In a publication on the decomposition of the alkaline earth

azides, Garner /.....

azides, Garner and Reeves[66] confirmed the sixth power law. They proposed that nucleation took place at points of emergence of edge dislocations. The long induction periods were thought to be due to time taken for F-centres to aggregate and form nuclei. Irradiation with ultra-violet light produced sites which normally did not develop into nuclei. It was also suggested that the reaction for the decomposition of barium azide was,

$$N_3^- + N_3^- \rightarrow 3N_2 + 2e^-$$

since no nitride was formed.

Groocock and Tompkins[9] investigated the effect of electron bombardment on the thermal decomposition of barium azide. Similar results to those obtained with ultra-violet light irradiation were obtained. However, the exponent n in the power law remained at 6 even at high doses.

Osinovik[171] also reported a large increase in the maximum rate after irradiation with fast electrons. He also stated that there was a remarkable shortening of the induction period after several days exposure of the salt to gamma-rays.

Erofeyev and Sviridov[114] examined the effects of preirradiation by X-rays on the kinetics of the thermal decomposition of barium azide. Complex results were obtained. Analysis of the acceleratory period was performed using the Avrami-Erofeyev equation,

$$-\ln(1-\alpha) = (k_5 t^n) \quad \ldots\ldots\ldots\ldots\ldots\ldots\ldots\ldots (2.8)$$

Values of n were determined from the plots of log $[-\log(1-\alpha)]$ vs log t. The value of n varied from 7.9 to 12 as the temperature of decomposition increased.

Preirradiation by X-rays produced a steady decrease in the duration of the induction period. The acceleratory rate constant increased at first but after long times of exposure a deceleration was found. A decrease in the inflexion point was also observed. Complex p/t plots were obtained at high doses, e.g. at an irradiation time of 3 hours the p/t plot had two

points of maximum/.....

points of maximum velocity. The salt developed a grey colour after long exposures. Moist samples of barium azide decomposed more slowly and were characterized by a smaller effect of preirradiation than the dry salt. No ageing of the irradiation effect was found. An effect similar to the irradiation effect was obtained by heating the unirradiated salt for a short time at the temperature of decomposition. Preirradiation caused involved variations on the value of n in the Avrami-Erofeyev equation. As the irradiation time increased n diminished from 8 to 6, then increased to 12-15 and finally decreased again to 3. For the same dose and different temperatures n increased from 3 at 114°C to 7 at 126° and 132°C and dropped to 5 at 138°C. Activation energies could not be calculated in the conventional manner because of the variation of n with temperature. Using the temperature dependance of the time for 25% decomposition to be reached it was found that preirradiation produced a decrease in the total activation energy for the thermal decomposition.

Thomas and Tompkins[60] had reported a decrease in the reaction rate with time. In contradiction to this Erofeyev and Sviridov found a slight increase in the rate of decomposition of the unirradiated salt after prolonged storage.

Boldyriev and Skorik[7] found that barium azide irradiated with X-rays at the threshold decomposition temperature showed a greater preirradiation effect than that preirradiated at room temperature. It was suggested that the nuclei, which were aggregates of atoms or F-centres, formed and grew by trapping electrons followed by neutralisation of the charge by migrating interstitial cation or anion vacancies. Nuclei were only stable above a critical size. The concentration of free electrons increased under X-ray irradiation. At room temperature the interstitial vacancies possessed low mobility and hence few stable nuclei could be formed. However, for irradiation at the threshold temperature their mobility had increased; thus

a large number/.....

a large number of stable nuclei could form and hence a higher rate of decomposition took place.

2.3. Strontium Azide.

Maggs[105] made the first study of the thermal decomposition of strontium azide. He obtained p/t plots with a marked induction period followed by a period of rapid acceleration. The early stages of the acceleratory period were obeyed by the exponential law viz,

$$\log p = k_2 t + c_2 \quad \ldots\ldots\ldots\ldots\ldots\ldots\ldots\ldots (2.9)$$

the activation energy for acceleration was calculated to be 20 kcals.mole^{-1}.

A radium needle placed next to the salt reduced the induction period and resulted in a large increase in k. The activation energy, however, remained the same. It was also stated that ultra-violet light increased the reaction rate. Maggs suggested that the action of the radiation was either to increase the rate of growth of the nuclei or to increase their rate of formation.

Garner and Maggs[6] studied the effect of ultra-violet light on the thermal decomposition of strontium azide and made a similar study on barium azide. The results were similar, with a decrease in the induction period and an increase in the reaction rate. The exponent n in the power law increased from 6-8 with increasing dose. The same theoretical explanation was considered valid for both compounds. (Cf BaN_6).

Garner and Reeves[66] found that the acceleratory period of the p/t plots obeyed the power law with n = 3, i.e.

$$p^{1/3} = Ct + c_1$$

The equation was only valid over the latter stages of the acceleratory period. Preirradiation with ultra-violet light decreased the inflexion point, improved the extent of fit of the power law and increased the acceleratory rate constant. It

was considered/.....

was considered that the improved extent of fit of the power law was due to equalisation of sizes of nuclei before the end of the induction period, by the ultra-violet radiation. The increased rates were due to greater numbers of nuclei produced at sites caused by irradiation.

Sviridov[172] found that preirradiation in air at room temperature by X-rays resulted in a faster decomposition at 126°C. In 20 minutes 30% decomposition occurred, whereas with the unirradiated salt the first sign of decomposition occurred only after 3 hours.

2.4. Calcium Azide.

Andreev[173] did an initial investigation into the thermal decomposition of calcium azide and showed that there was a marked induction period followed by an acceleratory period which obeyed the equation

$$(dp/dt) = k_{15}p^n \quad \ldots\ldots\ldots\ldots\ldots\ldots\ldots\ldots\ldots\ldots (2.10)$$

where n varied from 0.66 at 100°C to 0.80 at high temperatures. Activation energies were determined by split run techniques and the following values obtained in the acceleratory period:

(i) 20.8 kcal. mole^{-1} from 61° to 81°C

(ii) 22.1 kcal . mole^{-1} from 80° to 100°C

(iii) 27 kcal . mole^{-1} from 93° to 106°C

Marke[174] confirmed this analysis. He concluded that the mode of decomposition was in general agreement with the chain theory but that the nuclei were not as diffuse as would be expected.

The decay reaction obeyed the unimolecular decay law

$$\log (p_f - p) = k_7 t + c_7 \quad \ldots\ldots\ldots\ldots\ldots\ldots\ldots (2.11)$$

The activation energies for the acceleratory and decay periods were 13 kcals.mole^{-1} and 19 kcal . mole^{-1}, respectively. The activation energy plots, however, were not good due to poor reproducibility of the results.

Garner and Reeves/.....

Garner and Reeves[66] found that the acceleratory period followed the power law with n = 3 i.e.

$$p^{1/3} = Ct + c_1$$

The results were not very reproducible. Grinding produced a fourfold increase in C. The activation energy for the acceleratory period, from split runs, was in agreement with that obtained by Marke. Preirradiation with ultra-violet light shortened the induction period, increased the acceleratory rate constant, and improved the extent of fit of the power law. The interpretation of the results was considered to be the same as that for strontium and barium azides (Cf 2.2 and 2.3).

Tompkins and Young[175,176] examined the kinetics of the decomposition of calcium azide and concluded that the power law (n=3) was valid. However, they obtained anomalous results for the activation energy of the acceleratory period, which appeared to be influenced by the temperature range of the determination, the method employed, and on whether fresh or aged material was used. At temperatures below 97°C the activation energy for the acceleratory period, as determined on freshly prepared material, by split run techniques, was 18 kcal.mole^{-1}. This was also true for temperatures above 112°C. Between these two temperatures anomalous rate constants were obtained and the Arrhenius plots were not linear. When individual runs were used the activation energy obtained was 35 kcal.mole^{-1}. Using aged or annealed samples a value of 18 kcal.mole^{-1} was obtained irrespective of the method employed.

These results were associated with an excess of vacancies in freshly prepared material. On heating these formed clusters at the surface and became nuclei on electron capture. The number of clusters was temperature dependent and increased with temperature. Thus the fixed number of nuclei growing three-dimensionally during the acceleratory period varied as the temperature of decomposition of indivudual runs was altered.

This caused/.....

This caused the pre-exponential factor in the Arrhenius expression to be temperature dependent and an erroneous activation energy was determined. In split runs with only one temperature during the induction period, this fixed the number of nuclei and hence a true activation energy was obtained. Above 97°C bulk nuclei started to form in addition to the surface ones giving rise to the anomalous rate constants. This process was complete at 112°C.

On ageing or annealing the excess vacancies were eliminated by aggregation or diffusion to boundary sinks. The equilibrium concentration was thus reached and cluster formation was complete. Thus a constant number of nuclei were always formed at all temperatures and the true activation energy of 18 kcal.mole^{-1} was obtained.

With aged or fresh material below 97°C preirradiation with ultra-violet light decreased the induction period and increased the reaction rate. It was proposed that this was due to formation and growth of nuclei on irradiation. The extent of fit of the power law also improved. With fresh salt above 97°C the validity of the power law was reduced virtually to zero. These effects were again associated with excess vacancies and the procution of bulk nuclei at higher temperatures.

An extensive study of the thermal decomposition of unirradiated and preirradiated (γ-rays, X-rays and ultra-violet light) calcium azide was completed by Prout and Brown[115,116] shortly before the publication of Tompkins and Young. Their results for the unirradiated salt were in contradiction to those of Tompkins and Young with regard to the activation energy for the acceleratory period. The power law (n = 3) described the acceleratory period and the contracting sphere equation fitted the decay reaction. A value of 27 kcal.mole^{-1} was obtained for the activation energy of the acceleratory period, as determined from individual runs, in the temperature range 105°-130°C. This disagreed with both values obtained by Tompkins and Young.

The activation/.....

The activation energies for the decay and induction periods were 18.8 and 18.2 kcal.mole^{-1} respectively. A large increase in the reaction rate and a marked shortening of the induction period was found on preirradiation with γ-rays, X-rays or ultraviolet light. However, the kinetic expressions remained the same throughout, as did the activation energies.

It was considered that the decomposition of the unirradiated salt comprised a slow surface decomposition of azide ions during the induction period, with the formation of nitrogen and calcium atoms. These calcium atoms were at the lattice spacing of the calcium ions in the salt. At the end of the induction period recrystallization of the atoms occurred with the formation of metallic specks which were the nuclei. During the acceleratory period growth of these nuclei occurred. Nuclear growth occurred by the elevation of an electron from an azide ion into the lowest vacant energy level in the metal speck. The azide radical (positive hole) reacted with a second azide ion to yield nitrogen, the calcium formed adding on to the nucleus. The decay reaction took place at a contracting spherical metal interface. From the activation energy value it was considered that the reaction was the decomposition of strained azide ions. These were produced either by the compressive forces exerted by the metal sheath, or more probably, the high pressures exerted by trapped nitrogen.

Preirradiation produced a large increase in the concentration of vacancies. On heating these aggregated at the surface producing regions of strain where decomposition was favoured. The induction period was thus shortened and the increased number of nuclei resulted in high decomposition rate constants.

3. OBJECTS OF THE RESEARCH.

3.1. The Thermal Decomposition of Irradiated Mercuric Oxalate.

Irradiation of a solid with γ-rays may create the following types of damage:

(i) radiolysis with the production of an intermediate which is thermally unstable at the normal decomposition temperature of the solid,

(ii) electronic defects, e.g. vacancies, positive holes, F-centres.

The thermal decomposition of nickel oxalate[125] is accelerated if the salt is exposed to γ-rays before heating. The change in kinetics is explained by suggesting that (i) above occurs during irradiation. It was of interest to determine whether the thermal decomposition of mercuric oxalate would be similarly affected by preirradiation and if so whether the changes could be explained by (i) or (ii) above. The radiation change might be different, since mercuric oxalate differs from nickel oxalate in that it is sensitive to ultra-violet light whereas the latter is not. It was considered that a parallel investigation of the other commonly used radiations i.e. X-rays and ultra-violet light might assist in elucidating any effects found with γ-rays.

3.2. The Thermal Decomposition of Irradiated Alkaline Earth Azides.

The work of Garner[103] and Maggs[105] on the decomposition of irradiated (Ra needle) barium azide and calcium azide respectively, indicates that the decomposition of the alkaline earth azides might be affected by γ-rays. The effects of ultra-violet light on the subsequent thermal decomposition of barium azide has been explained by assuming that irradiation produces changes of type (ii). Thus, if an irradiation effect is found with γ-rays it would be of interest to determine whether the

effective irradiation/.....

effective irradiation change is (i) or (ii) or both. Here, too, it was considered that the study would be more complete if the effect of other radiations was studied. Consequently the decomposition of barium and strontium azides was investigated. A similar study of the decomposition of calcium azide was commenced by Mr. M.E. Brown of this department. However, on the completion of the studies by Brown it was felt necessary, for the completeness of this work, to extend his research by a few additional experiments with ultra-violet light.

The publication by Tompkins and Young[176] appeared after the completion of Brown's studies, and it was felt necessary to attempt to resolve the discrepancy between the findings of Brown, and Tompkins and Young with regard to the activation energy for the reaction during the acceleratory period of the thermal decomposition of calcium azide.

FIG. 2.

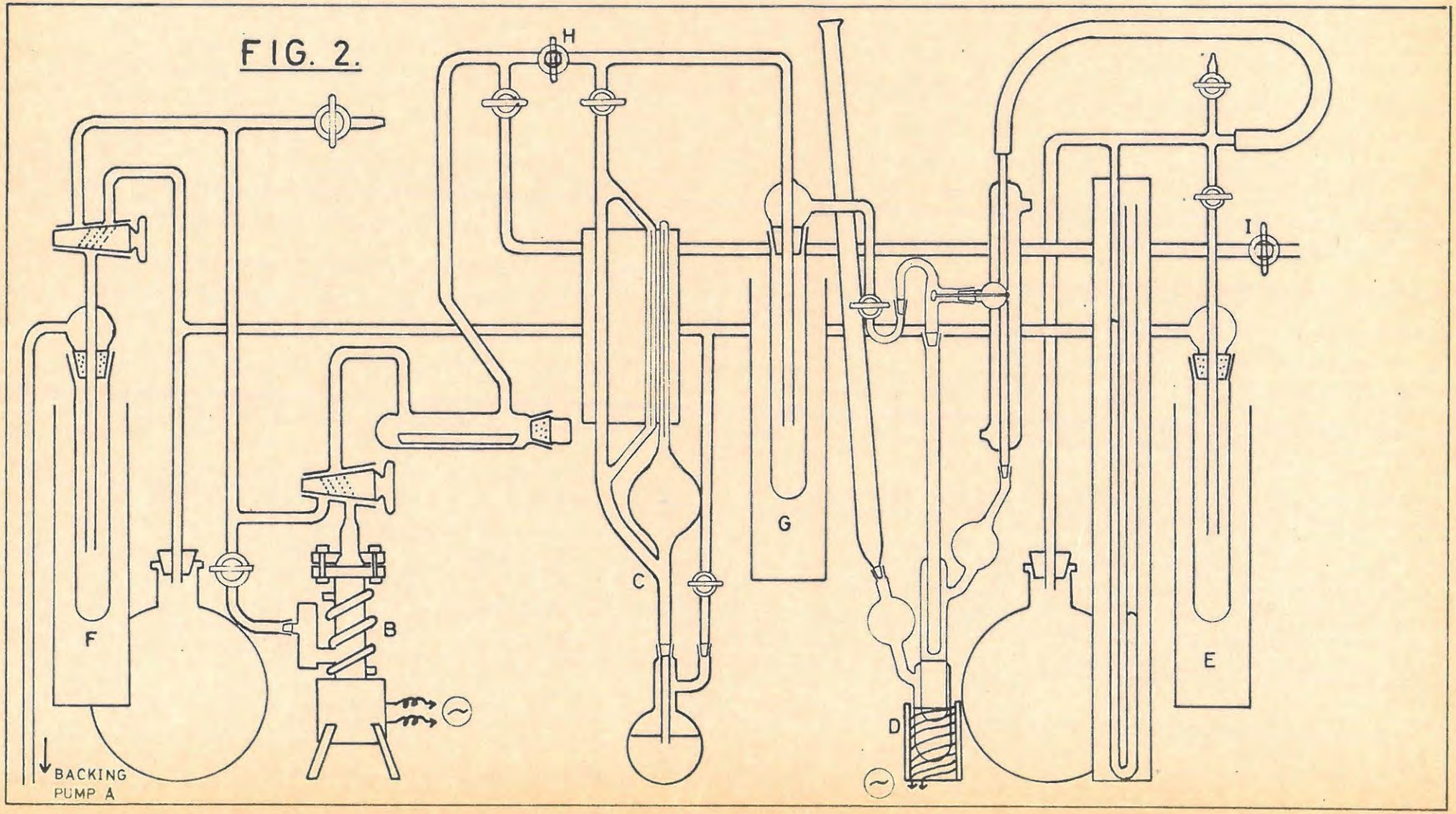

4. APPARATUS AND EXPERIMENTAL PROCEDURES.

4.1. Apparatus.

4.1.1. The High Vacuum Line.

The course of all the thermal decompositions was followed in a high vacuum line. This is shown diagrammatically in FIGURE 2. It has been described in detail by Herley.[177] The main features are the pumping system, the pressure gauge and the decomposition chamber.

The pumping system comprised a three-stage Edwards "Speedivac" oil diffusion pump (B), model 203B which was backed by an Edwards "Speedivac" gas ballast rotary high vacuum pump (A) model 2SC20A. This system enabled pressures down to 1×10^{-6} cm.Hg. to be obtained.

A calibrated McLeod gauge (C) was used to measure pressures. The volume of the McLeod bulb was 123.1 ml. at 25°C.

Decompositions were performed in the decomposition chamber (D). This has been described in detail by Prout and Herley.[178] The temperature control was approximately 0.03°C in the temperature range at which the work was carried out. Silicone oil was used in the outer jacket. Liquids used in the inner jacket at various temperatures were; tetrachloroethylene (80°-120°C), acetylene tetrachloride (120°-145°C) and ethyl salicylate (180°-230°C).

Cold traps (E,F and G) surrounded by liquid air were strategically placed to condense water vapour or any other condensable gases. These were positioned, (i) between the decomposition chamber and the McLeod gauge to protect the former from mercury vapour and water vapour (G), (ii) just before the oil diffusion pump (F) and (iii) in the back line (E). In the work on mercuric oxalate a P_2O_5 trap replaced the cold trap between the McLeod gauge and the decomposition chamber.

The volume of that section of the line used in a decomposi-

tion (i.e. excluding/.....

tion (i.e. excluding the pumping system) was determined before the work was commenced, and found to be 785.1 ml. at 25°C.

4.1.2. Preirradiation Equipment.

(a) γ-rays. The majority of these preirradiations were carried out in the spent fuel facility at Harwell. The average γ-ray energy was ~1 Mev and the dose rate 4 Mrad. hour^{-1}. In cases where the required dose was too low for accurate dosage at Harwell (1,000-100,000 rad), the Co^{60} source at Wantage was used. Here the dose rate was 3,400 rad min^{-1}. However, in any one particular series, all irradiations were performed in the same source for comparitive purposes.

(b) X-rays. A Philips PW 1009 X-ray generator, employing a sealed X-ray tube, Cu, was used. The X-ray tube was mounted horizontally in order to obtain a vertical beam which was directed onto the sample. For mercuric oxalate the tube was operated at an applied voltage of 40kV and a tube current of 20mA. In the work on the azides the voltage was 10 kV and the current 5 mA. White radiation was used throughout.

(c) Ultra-violet light. The mercuric oxalate irradiations were performed in sunlight as no ultra-violet lamp was available at that stage. Irradiations on the azides were carried out using a Hanovia low intensity ultra-violet lamp.

4.2. Experimental Procedures.

The samples were decomposed in a small pyrex bucket. Before each run the bucket was carefully cleaned in hot nitric acid, rinsed with pure water, dried by heating to a dull red heat in a flame and then allowed to cool. The required weight of sample was weighed into the bucket which was then placed in the high vacuum line. The line was pumped hard for several hours before commencing a decomposition. (Preliminary tests showed that a satisfactory vacuum could be maintained for at least 48 hours). The decomposition system was then isolated

from the pumping/.....

from the pumping system, by closing tap H, and the bucket lowered into the decomposition chamber, the temperature having been previously adjusted to the required value. The stopwatch was started and the pressure measured at various times. The level of the liquid air surrounding the cold trap in the decomposition system was kept constant throughout the duration of a run. The final pressure p_a was read half an hour after the apparent end of a run.

Preirradiations by γ-rays were done in darkened sealed evacuated pyrex ampoules. Each ampoule was approximately the same size as the glass bucket and contained sufficient sample for one run only. When the ampoules returned from irradiation they were opened under argon and immediately placed into the vacuum line, the ampoule taking the place of the pyrex bucket for the decomposition.

Preirradiations with X-rays or ultra-violet light were performed by spreading the sample out in a thin layer on a flat bottomed porcelain dish and placing it directly beneath the radiation source. The same procedure was adopted for irradiations in sunlight. In this case all irradiations were done between 11 a.m. and 1 p.m. as the U.V. intensity of sunlight remains fairly constant over this time. In any one series irradiations were done simultaneously for comparitive purposes. The X-ray and ultra-violet light irradiations were all done in air.

A few more specialised procedures require explanation. These are given below.

(i) Water interruptions.

Valuable information on the azide decompositions was obtained from a series of runs where the decomposition was interrupted and water vapour admitted onto the salt. These are termed "water interruptions". The following procedure was adopted. The cold trap (G) in the decomposition system was

thoroughly cleaned/.....

thoroughly cleaned and a small amount (1 cc) of degassed water placed in the bottom. The water was then solidified by the liquid air surrounding the trap which also ensured complete elimination of any water vapour. The sample was then placed in the line and the normal decomposition procedure followed. When the reaction had reached the selected point of interruption the sample was lifted out of the decomposition chamber and allowed to cool for ten minutes during which time the line was pumped hard. The decomposition system was then isolated from the pumping system again and the liquid air removed from around the cold trap which was then warmed to 20°C. This melted the ice and the resulting water vapour was allowed to expand onto the sample and remain in contact with it for 10 minutes. The liquid air Dewar was then replaced around the trap and the line pumped hard for one hour after which the decomposition was allowed to continue.

(ii) Interruption followed by irradiation.

These experiments were also concerned only with the azides. It was desired to irradiate the samples at various stages in the decomposition. As the reaction products included the free metal (Ba, Sr or Ca) which was very reactive in air, special precautions were necessary to prevent the sample from coming into contact with water vapour or oxygen while irradiating after interruption of the run. In the case of X-ray irradiation, a special pyrex ampoule was made which was considerably longer than the normal one and which had a ground glass socket at the top with a corresponding stopper. The decompositions were done in the normal manner up to the point where irradiation was desired. The ampoule was then lifted out of the decomposition chamber and allowed to cool for 10 minutes during which time the line was pumped hard. High purity nitrogen was then bled into the line at tap I until atmospheric pressure was reached, any trace of water vapour being eliminated by the cold trap. The ampoule was then removed from the line and

the stopper/.....

the stopper immediately inserted into the socket. The ampoule was then placed in the X-ray beam and the irradiation thus done in an atmosphere of dry nitrogen. The decomposition system was flushed out again with high purity nitrogen before reloading the sample into the line, which was then pumped hard for two hours before continuing with the run.

Interruptions followed by irradiations with ultra-violet light were done in the same manner excepting that a quartz ampoule, transparent to this radiation, was used.

For interruptions followed by γ-ray irradiations the pyrex ampoules used were baked in an oven for several days at 300^{o}C before use. At the point of interruption the ampoule was cooled and high purity nitrogen allowed in as before. The ampoule was then removed from the line, immediately re-evacuated, sealed and sent off for irradiation. However, despite these precautions, it was discovered that it was impossible to prevent water vapour from coming out of the walls of the ampoules. This reacted with the free metal forming the metal hydroxide. Irradiations were thus carried out on a mixture of the azide and the metal hydroxide. Experimental evidence of this was obtained (Cf BaN_6 6) and no solution to the problem could be found.

5. THE THERMAL DECOMPOSITION OF MERCURIC OXALATE.

THROUGHOUT THESE RESULTS, AND THOSE FOR THE ALKALINE EARTH AZIDES, THE RATE CONSTANTS (k) ARE NUMBERED SO THAT THOSE FOR THE ACCELERATORY PERIODS CARRY A LOWER NUMBER THAN THOSE FOR THE DECAY PERIODS. THESE CONSTANTS ARE NOT EQUIVALENT TO ANY CORRESPONDINGLY NUMBERED ONES IN THE INTRODUCTION. THE NUMBERING OF THE MATHEMATICAL EQUATIONS IN ALL THE RESULTS DOES NOT CORRESPOND TO THAT IN THE INTRODUCTION, BUT IS CONSISTENT THROUGHOUT THE RESULTS.

5.1. RESULTS.

Unless otherwise stated, (i) all pressures are recorded in units of 10^{-3} cm mercury, (ii) in any one series the results are all normalised to a common final pressure, p_f, for comparitive purposes. The final pressure actually recorded before normalisation is p_a. Time is recorded in minutes.

5.1.1. Preparation.

Mercuric oxalate was prepared by the method of Prout and Tompkins.[12] Equal volumes (250 ml) of $M/10$ mercuric acetate and $M/10$ oxalic acid were added dropwise at equal rates to 100 ml of distilled water at 25°C with vigorous mechanical stirring. The resulting precipitate of mercuric oxalate was filtered off, washed thoroughly with distilled water, and dried and stored in vacuo over P_2O_5 in a darkened dessicator. The above operations were performed in a dark room using red light as the salt is light sensitive.

5.1.2. Unirradiated Mercuric Oxalate.

(i) Reproducibility.

5.0 mg were used in each run. The decomposition temperature was 206°C. Three consecutive runs were done. The results are given in TABLE 1.

TABLE 1/.....

TABLE 1.

206°C	Run 1.				5.0 mg.
t	p	t	p	t	p
1	0.11	20	46.14	110	111.91
2	0.19	25	54.21	120	115.22
3	0.39	30	60.33	130	116.89
4	1.30	35	66.28	140	118.58
5	3.01	40	71.87	150	120.27
6	5.57	45	76.74	160	121.43
7	8.41	50	80.94	180	123.16
8	12.25	55	84.24	200	124.31
9	16.17	60	87.12	220	125.47
10	20.35	70	94.03	240	126.62
12	27.43	80	100.16	p_f	127.20
14	33.42	90	104.36	p_a	126.67
16	38.40	100	108.09		

206°C	Run 2.				5.0 mg.
t	p	t	p	t	p
1	0.06	20	46.02	110	109.20
2	0.11	25	53.82	120	111.85
3	0.23	30	60.65	130	113.99
4	1.01	35	65.83	140	116.30
5	2.50	40	71.23	150	117.78
6	4.67	45	75.12	160	118.84
7	7.64	50	79.08	180	121.61
8	11.50	55	82.69	200	123.80
9	15.16	60	85.92	220	124.39
10	19.32	70	92.08	240	126.61
12	26.75	80	97.46	p_f	127.20
14	33.09	90	101.47	p_a	129.36
16	38.49	100	105.56		

206°C	Run 3.				4.9 mg.
t	p	t	p	t	p
1	0.08	20	45.94	110	114.56
2	0.22	25	54.46	120	116.80
3	0.46	30	61.22	130	119.07
4	1.32	35	67.08	140	120.80
5	2.98	40	72.34	150	121.94
6	5.30	45	77.30	160	123.10

TABLE 1 Cont./.....

TABLE 1 cont.

t	p	t	p	t	p
7	7.98	50	81.99	180	124.28
8	11.05	55	86.31	200	125.46
9	14.20	60	90.23	220	126.03
10	17.97	70	96.81	240	126.64
12	24.72	80	102.04	p_f	127.20
14	31.36	90	106.31	p_a	124.37
16	36.87	100	110.67		

Reproducibility was satisfactory. The acceleratory period rate constants, k_1 (equation 1) obtained were 1.812, 1.832 and 1.800 x 10^{-2} cm $^{1/2}$Hg min^{-1} respectively, and in the decay period the rate constant k_7 (equation 2) gave values of 3.80, 3.45 and 4.00 x 10^{-3} min^{-1} respectively.

(ii) Effect of varying the temperature of decomposition.

The activation energies were determined by evaluating the rate constants at various temperatures. Results are given in TABLE 2. The rate constants, k_1 and k_7, appear in TABLE 3.

TABLE 2.

200°C	Run 1				5.2 mg.
t	p	t	p	t	p
1	0.30	25	29.03	200	99.07
2	0.60	30	33.09	220	103.66
3	0.75	35	36.87	250	109.80
4	1.30	40	40.27	280	114.14
5	2.55	50	46.28	300	116.60
6	4.12	60	51.69	320	119.07
7	5.85	70	56.75	340	121.07
8	7.50	80	62.02	360	123.09
9	9.08	90	66.05	380	124.11
10	10.81	100	69.04	400	125.12
12	14.02	120	76.04	420	126.15
14	16.88	140	83.38	p_f	127.20
16	19.21	160	88.89	p_a	130.80
20	23.88	180	93.69		

TABLE 2, cont/.....

TABLE 2 cont.

206°C	Run 2.				5.4 mg.
t	p	t	p	t	p
1	0.22	25	52.47	130	108.68
2	0.32	30	58.63	140	110.91
3	0.45	35	63.90	150	112.49
4	1.42	40	67.68	160	114.71
5	3.09	45	71.13	170	116.37
6	5.66	50	74.21	180	118.06
7	8.85	55	77.36	200	120.31
8	12.38	60	80.12	220	122.66
9	16.22	70	85.77	250	124.91
10	19.80	80	90.42	260	125.47
12	26.77	90	94.61	280	126.09
14	32.98	100	98.67	p_f	127.20
16	37.91	110	102.85	p_a	127.18
20	45.24	120	106.25		

220°C	Run 3				5.0 mg.
t	p	t	p	t	p
1	0.46	9	51.90	35	119.05
2	0.95	10	60.56	40	122.21
3	1.73	12	73.46	45	124.15
4	4.21	14	82.73	50	125.45
5	9.30	16	88.59	55	126.03
6	17.70	20	98.77	60	126.63
7	29.62	25	107.84	p_f	127.20
8	41.15	30	114.50	p_a	123.21

230°C	Run 4.				5.1 mg.
t	p	t	p	t	p
1	0.43	9	61.32	30	119.98
2	1.07	10	66.16	35	123.72
3	6.70	12	75.04	40	125.86
4	17.14	14	82.99	45	126.67
5	30.53	16	90.10	p_f	127.70
6	41.78	18	96.39	p_a	126.68
7	50.08	20	101.94		
8	56.11	25	112.78		

TABLE 2, cont/.....

TABLE 2 cont.

246°C	Run 5.				4.8 mg.
t	p	t	p	t	p
1	0.20	5	93.12	p_f	127.20
2	0.38	6	119.31	p_a	120.78
3	3.59	7	124.54		
4	22.43	8	126.52		

TABLE 3.

RATE CONSTANTS		
Temperature °C	k_1 $cm^{1/2}$ min^{-1}	k_7 min^{-1}
200	1.309×10^{-2}	1.72×10^{-3}
206	1.963×10^{-2}	2.77×10^{-3}
220	3.403×10^{-2}	1.24×10^{-2}
230	4.908×10^{-2}	1.995×10^{-2}
246	1.063×10^{-1}	1.05×10^{-1}

(iii) Measurement of particle size.

The particles were approximately spherical. The average radius determined by direct measurement under high magnification was 2.0×10^{-5} cm.

(iv) Analysis of gas(es) evolved on decomposition.

Carbon dioxide and carbon monoxide have been named as the gases liberated during a decomposition.[12] A decomposition was done at 206°C with a liquid air trap in the line. After four hours the decomposition chamber was isolated from the cold trap and McLeod gauge and the liquid air Dewar was removed from around the trap. The results listed in TABLE 4 show that the gas evolved is almost completely condensable in the trap. Analysis of the condensed gas showed that it was carbon dioxide only.

TABLE 4/.....

TABLE 4.

206°C	Run 1.				5.3 mg.
t	p	t	p	t	p
1	0.04	30	3.18	246	117.92
2	0.07	40	3.47	247	122.52
3	0.10	50	3.77	248	138.08
4	0.17	60	4.18	249	133.20
5	0.22	80	4.29	250	130.78
6	0.30	100	4.40	251	129.59
7	0.34	120	4.52	252	128.40
8	0.53	140	4.63	253	127.80
9	0.79	160	4.74	254	127.42
10	1.00	180	4.85	p_f	127.20
12	1.33	200	4.97	p_a	123.79
15	2.01	240	4.79		
20	2.47	Dewar	Removed		
25	2.82	245	5.09		

(v) Percentage decomposition.

In view of the results of (iv) above, the chemical equation for the thermal decomposition is considered to be;

$$4HgC_2O_4 \rightarrow 2Hg + 2HgO + C + 7CO_2$$

The percentages calculated in terms of this equation are given in TABLE 5. The average percentage decomposition obtained from these values is 102% of that calculated theoretically

TABLE 5.

Temperature °C	Weight used	% decomposition.
206°C	10.4 mg.	114.10
206°C	10.0 mg.	91.40
206°C	10.4 mg.	103.35
206°C	5.0 mg.	95.80
220°C	5.0 mg.	104.95
200°C	5.0 mg.	103.10

(vi) Mathematical analysis of the results.

A typical plot for the thermal decomposition of mercuric oxalate is shown in FIGURE 3. There is a brief period of acceleration and a prolonged decay reaction.

The power law/.....

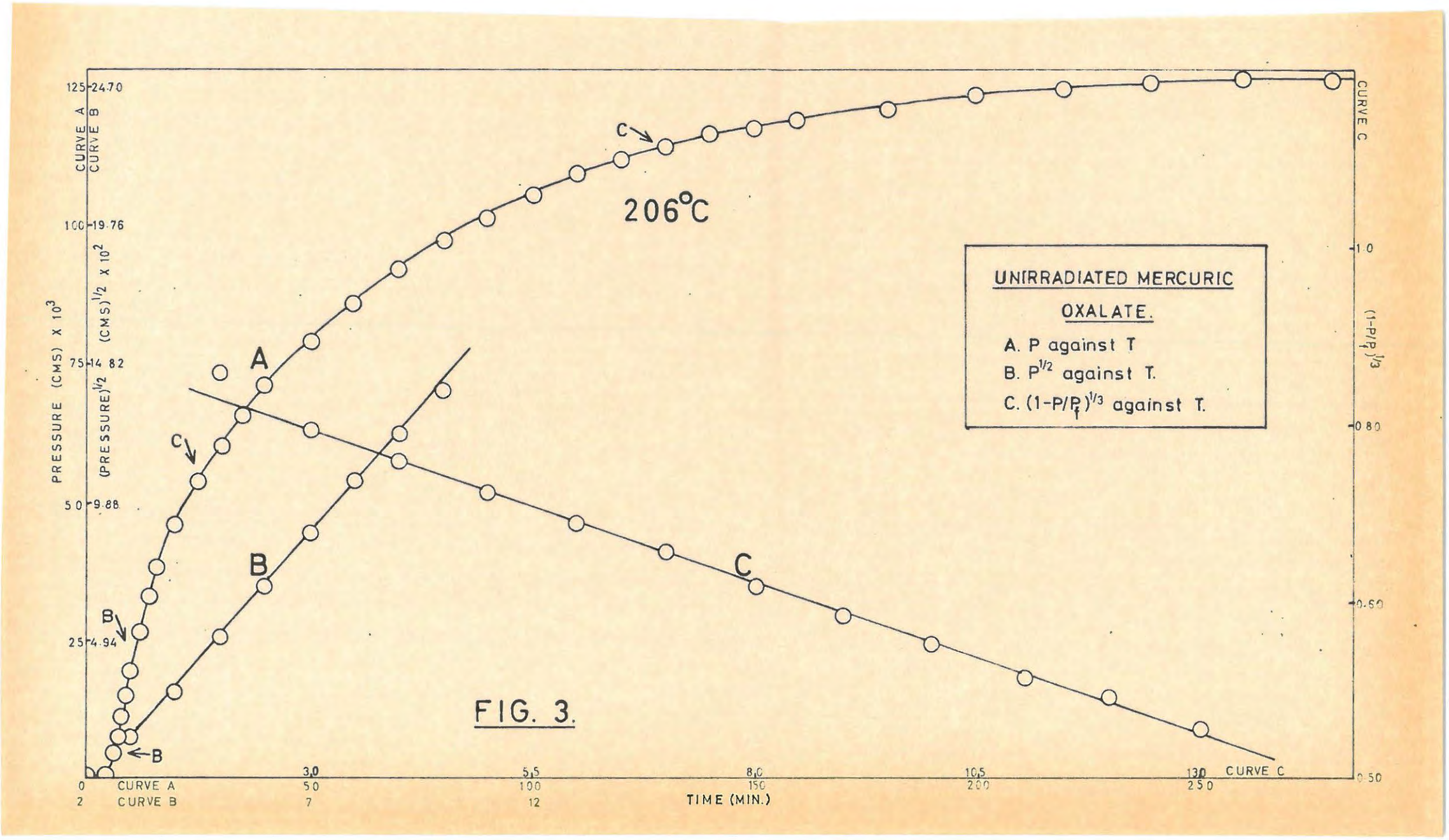
206°C
UNIRRADIATED MERCURIC OXALATE.
A. P against T
B. $P^{1/2}$ against T.
C. $(1-P/P_f)^{1/3}$ against T.
A
B
C
PRESSURE (CMS) X 10^3
$(PRESSURE)^{1/2}$ $(CMS)^{1/2}$ X 10^2
$(1-P/P_f)^{1/3}$
CURVE A
CURVE B
CURVE C
TIME (MIN.)
125 24.70
100 19.76
75 14.82
50 9.88
25 4.94
0
2
3.0
50
7
5.5
100
12
8.0
150
10.5
200
13.0
250
1.0
0.80
0.50
0.50

FIG. 3.

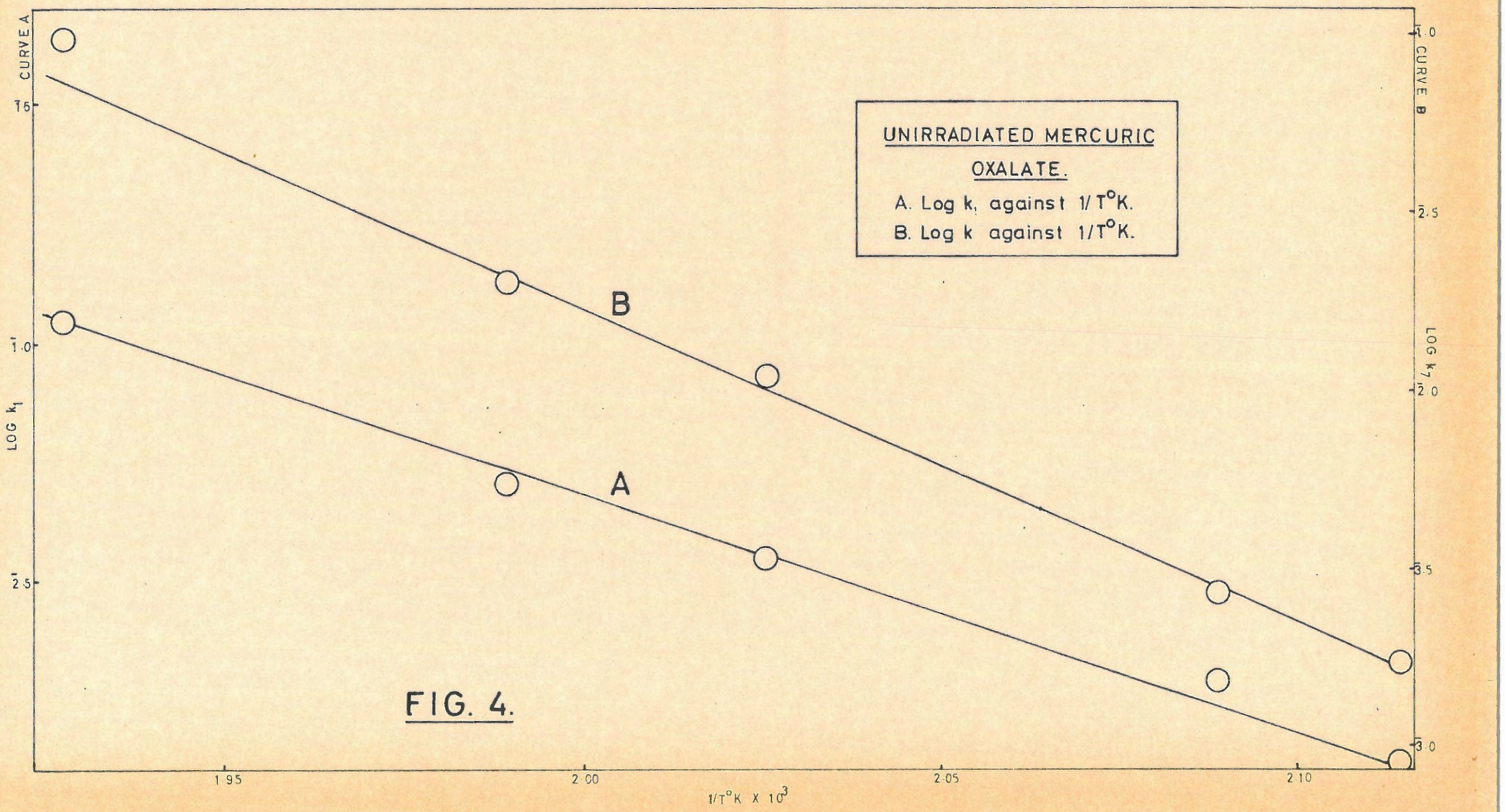
UNIRRADIATED MERCURIC
OXALATE.
A. Log k, against 1/T°K.
B. Log k against 1/T°K.
CURVE A
CURVE B
LOG k1
LOG k2
1/T°K X 10³
1·95
2·00
2·05
2·10
B
A

FIG. 4.

The power law with n = 2 i.e.

$$p^{1/2} = k_1 t + c_1 \quad \ldots\ldots\ldots\ldots\ldots\ldots\ldots\ldots (1)$$

describe the acceleratory reaction. The plot of $p^{1/2}$ vs t is shown in FIGURE 3.

The decay reaction follows the contracting sphere formula, viz.,

$$(1 - {}^{p}/_{p_f})^{1/3} = k_7 t + c_7 \quad \ldots\ldots\ldots\ldots\ldots\ldots\ldots\ldots (2)$$

The plot of $(1 - {}^{p}/_{p_f})^{1/3}$ vs t is also shown in FIGURE 3.

The critical increments were evaluated using the Arrhenius expression,

$$2.303 \log_{10} k = \frac{-E}{RT} + K$$

where E = the activation energy

k = the rate constant

T = the decomposition temperature in degrees Kelvin

K = a constant

R = 1.987 calories $\text{degree}^{-1} \text{mole}^{-1}$.

Plots of log k_1 and log k_7 vs. $^{1}/_{T}$ are shown in FIGURE 4. The activation energies obtained were

(a) Acceleratory period 25.6 kcals.mole^{-1}.

(b) Decay period 40.3 kcals.mole^{-1}.

Prout and Tompkins obtained the following values

(a) Acceleratory period 25.6 kcals.mole^{-1}.

(b) Decay period 40.3 kcals.mole^{-1}.

The results are thus in agreement with the earlier work done by Prout and Tompkins

5.1.3. Preirradiated (sunlight) Mercuric Oxalate.

(i) Preliminary investigation.

The method employed for irradiation has been described. A sample of mercuric oxalate was preirradiated for 45 minutes and subsequently decomposed at 206°C. The results are shown in FIGURE 5 and tabulated in TABLE 6.

TABLE 6/.....

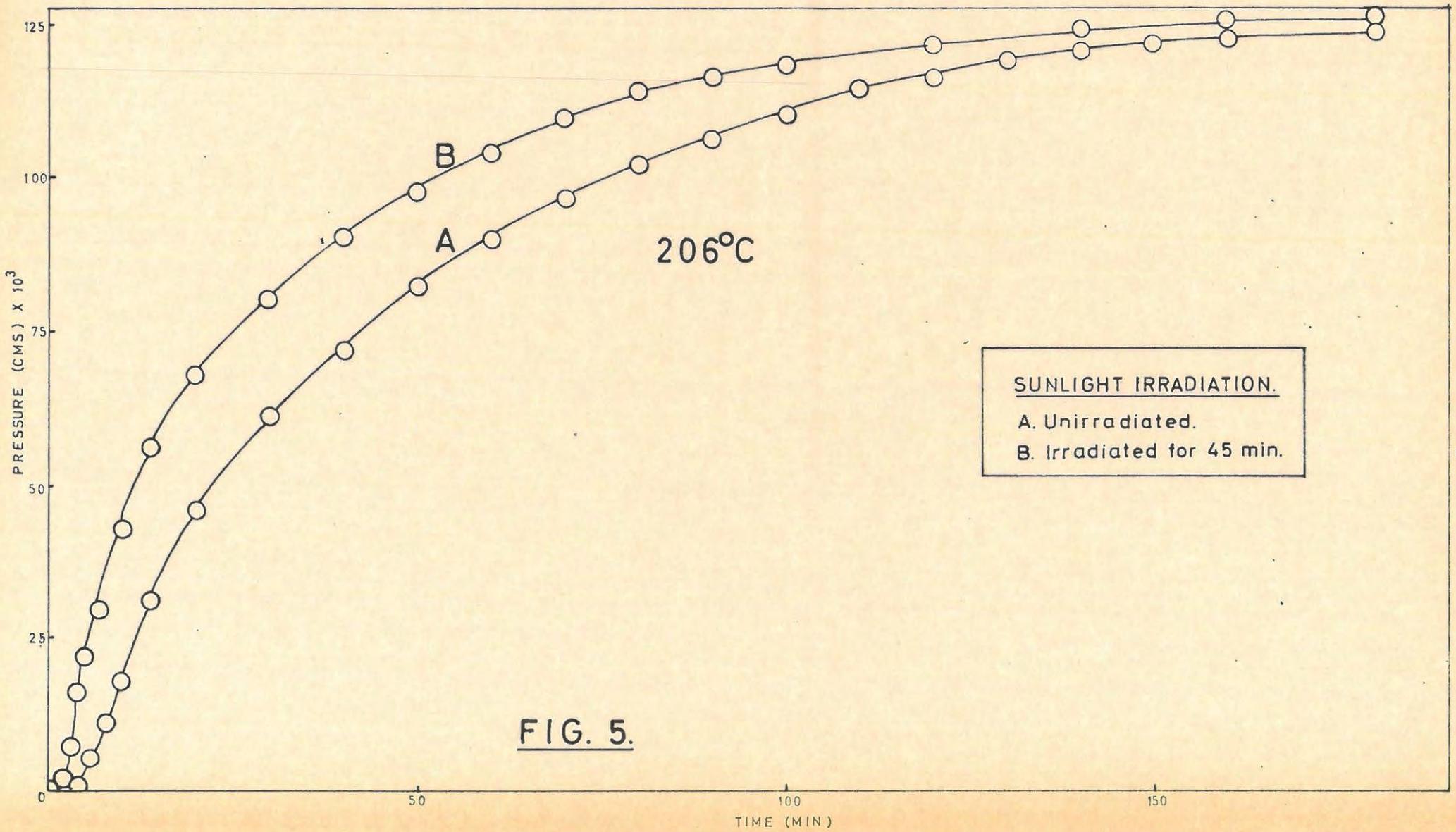
125
100
75
50
25
0
PRESSURE (CMS) X 10^3
B
A
206°C
SUNLIGHT IRRADIATION.
A. Unirradiated.
B. Irradiated for 45 min.
50
100
150
TIME (MIN)

FIG. 5.

TABLE 6.

206°C 45 min. sunlight. Run 1.					4.8 mg.
t	p	t	p	t	p
1	0.08	14	56.26	70	109.55
2	2.46	16	61.40	80	114.28
3	7.37	20	68.17	90	116.10
4	16.24	25	74.31	100	117.92
5	21.06	30	80.20	120	122.21
6	25.66	35	85.30	140	124.68
7	30.09	40	90.53	160	126.56
8	34.59	45	94.29	p_f	127.20
9	38.59	50	97.59	p_a	122.64
10	42.89	55	101.50		
12	50.53	60	104.25		

206°C Unirradiated blank. Run 2.					4.9 mg.
t	p	t	p	t	p
1	0.08	20	45.94	110	114.56
2	0.22	25	54.46	120	116.80
3	0.46	30	61.22	130	119.07
4	1.32	35	67.08	140	120.80
5	2.98	40	72.34	150	121.94
6	5.30	45	77.30	160	123.10
7	7.98	50	81.99	180	124.28
8	11.05	55	86.31	200	125.46
9	14.20	60	90.23	220	126.03
10	17.97	70	96.81	240	126.64
12	24.72	80	102.04	p_f	127.20
14	31.36	90	106.31	p_a	124.37
16	36.87	100	110.67		

At this temperature the main effect is seen to be an increase in the acceleratory rate constant. The decay period is relatively unaffected except that it is displaced to shorter times.

(ii) Study of the initial phase of decomposition with preirradiated salt.

The initial reaction was more closely studied than by Prout and Tompkins by decomposing a larger amount

of salt/.....

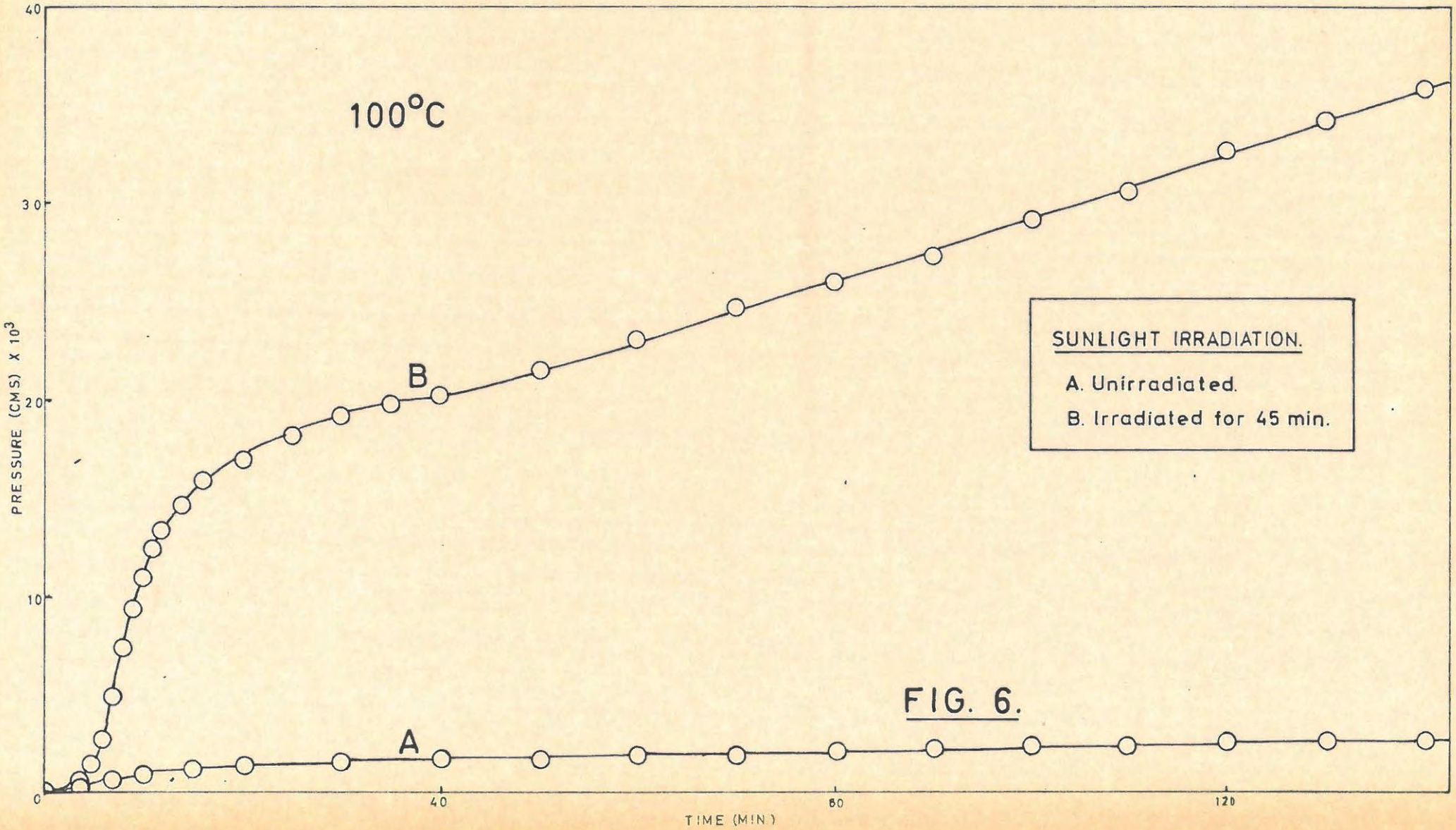
100°C
SUNLIGHT IRRADIATION.
A. Unirradiated.
B. Irradiated for 45 min.
B
A
PRESSURE (CMS) X 10³
TIME (MIN.)
0
10
20
30
40
40
80
120

FIG. 6.

of salt (35 mg) at a lower temperature. The real nature of the preirradiation effect by sunlight on the thermal decomposition is shown in FIGURE 6 and TABLE 7 where the decomposition temperature is 100°C. Pressures are not normalised.

TABLE 7.

100°C 45 min sunlight Run 1.					35 mg.
t	p	t	p	t	p
1	0.10	12	13.31	80	25.99
2	0.24	14	14.66	90	27.32
3	0.45	16	15.88	100	29.24
4	0.69	20	16.92	110	30.66
5	1.24	25	18.23	120	32.70
6	2.66	30	19.12	130	34.20
7	4.84	35	19.81	140	35.72
8	7.38	40	20.27	150	37.92
9	9.32	50	21.69	160	39.86
10	10.97	60	23.16	170	41.84
11	12.38	70	24.68	180	43.18

100°C Unirradiated blank Run 2.					35 mg.
t	p	t	p	t	p
1	0.02	8	0.77	60	1.74
2	0.10	10	0.92	80	1.91
3	0.19	12	1.02	100	2.10
4	0.35	15	1.07	120	2.25
5	0.41	20	1.24	150	2.65
6	0.56	30	1.40	180	2.92
7	0.69	40	1.61		

The initial reaction of preirradiated mercuric oxalate comprises a well defined acceleratory period followed by a "decay" period as compared to practically no decomposition of the unirradiated oxalate. The "decay" passes into a slow, almost linear evolution of gas.

(iii) Effect of/.....

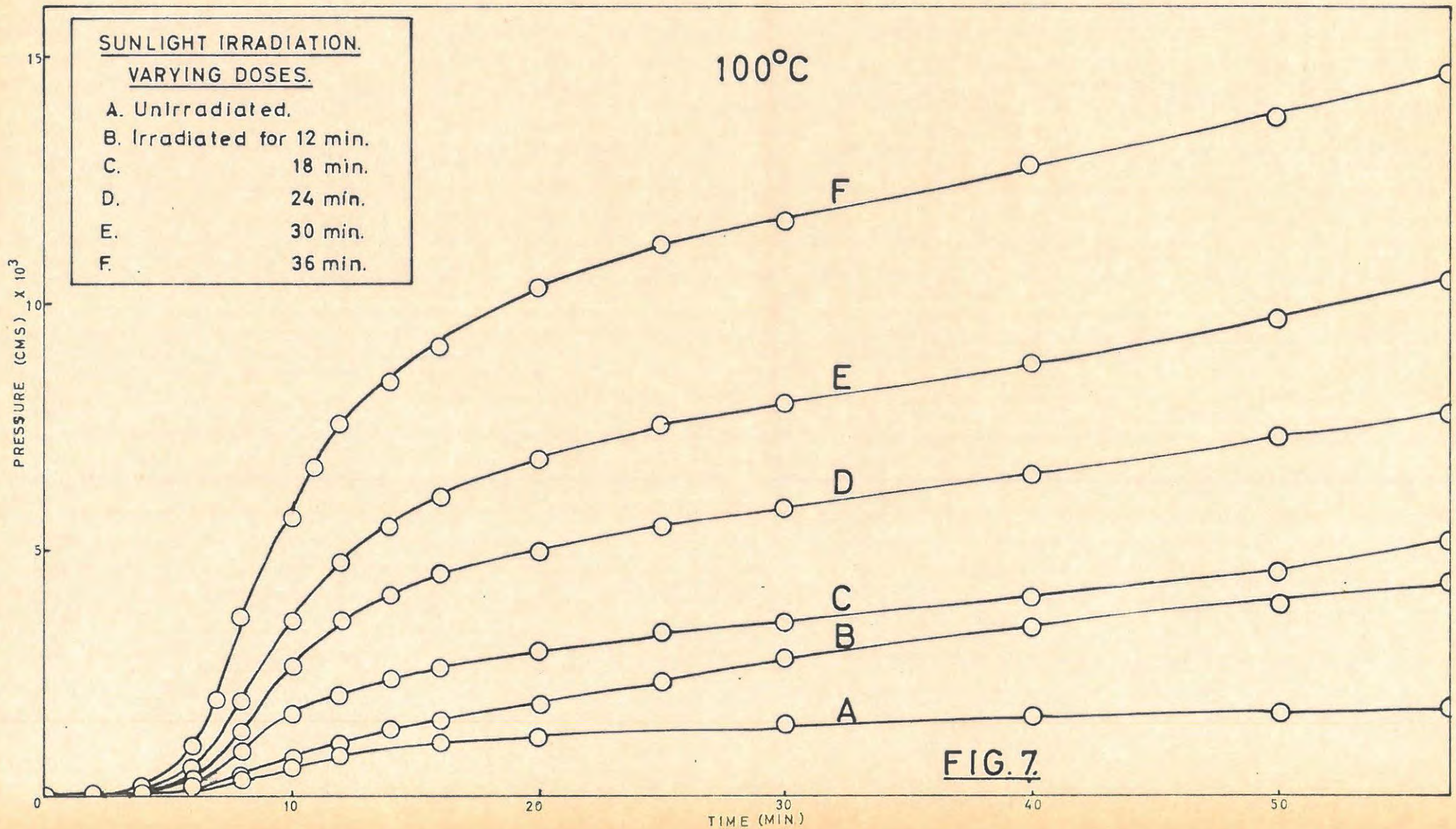
SUNLIGHT IRRADIATION.
VARYING DOSES.
A. Unirradiated.
B. Irradiated for 12 min.
C. 18 min.
D. 24 min.
E. 30 min.
F. 36 min.
100°C
PRESSURE (CMS) X 10³
TIME (MIN.)
0
5
10
15
10
20
30
40
50
A
B
C
D
E
F

FIG. 7.

(iii) Effect of varying sunlight dose on the initial reaction.

The effect on the initial reaction of varying the preirradiation dose was fully investigated. The decomposition temperature was 100°C. The irradiation times increased from 0 min. to 42 min. The effect on the subsequent thermal decomposition is shown in TABLE 8 and FIGURE 7. Pressures are not normalised.

TABLE 8.

100°C 6 min. sunlight. Run 1.					36.1 mg
t	p	t	p	t	p
1	0.07	9	0.21	30	0.86
2	0.08	10	0.26	40	1.01
3	0.08	11	0.32	50	1.41
4	0.08	12	0.39	60	1.67
5	0.08	14	0.49	80	2.74
6	0.13	16	0.60	100	4.24
7	0.17	20	0.64	120	5.67
8	0.18	25	0.77		

100°C 12 min. sunlight. Run 2.					36.2 mg.
t	p	t	p	t	p
1	0.05	10	0.72	35	3.16
2	0.07	11	0.92	40	3.37
3	0.08	12	1.07	50	3.87
4	0.10	13	1.18	60	4.50
5	0.11	14	1.30	80	5.91
6	0.15	16	1.48	100	8.10
7	0.22	20	1.81	120	10.29
8	0.39	25	2.25		
9	0.56	30	2.74		

100°C 18 min. sunlight. Run 3.					35.1 mg.
t	p	t	p	t	p
1	0.01	9	1.36	30	3.47
2	0.02	10	1.61	40	3.98
3	0.11	11	1.81	50	4.50
4	0.19	12	2.02	60	5.18

TABLE 8 cont/.....

TABLE 8 cont.

t	p	t	p	t	p
5	0.22	14	2.33	80	5.84
6	0.35	16	2.57	100	6.54
7	0.60	20	2.91	120	7.20
8	0.91	25	3.28		

100°C 24 min. sunlight Run 4.					36.2 mg.
t	p	t	p	t	p
1	0.02	9	2.10	30	5.79
2	0.04	10	2.66	40	6.56
3	0.04	11	3.10	50	7.24
4	0.04	12	3.57	60	7.81
5	0.10	14	4.07	80	9.64
6	0.27	16	4.50	100	12.38
7	0.69	20	4.95	120	15.06
8	1.30	25	5.42		

100°C 30 min. sunlight. Run 5.					36.2 mg.
t	p	t	p	t	p
1	0.03	9	2.92	30	7.95
2	0.07	10	3.57	40	8.70
3	0.08	11	4.28	50	9.64
4	0.11	12	4.72	60	10.63
5	0.22	14	5.42	80	13.12
6	0.52	16	6.04	100	15.88
7	1.12	20	6.83	120	19.12
8	1.95	25	7.52		

100°C 36 min. sunlight Run 6.					36.4 mg.
t	p	t	p	t	p
1	0.02	9	4.50	30	11.66
2	0.04	10	5.67	40	12.75
3	0.11	11	6.70	50	13.88
4	0.24	12	7.52	60	15.06
5	0.45	14	8.40	80	17.57
6	1.00	16	9.16	100	20.50
7	1.95	20	10.29	120	23.64
8	3.64	25	11.14		

TABLE 8 cont/.....

TABLE 8 cont.

100°C 42 min. sunlight Run 7.					36.4 mg.
t	p	t	p	t	p
1	0.02	9	3.19	30	9.32
2	0.03	10	4.18	40	10.29
3	0.05	11	4.95	50	11.31
4	0.08	12	5.67	60	12.38
5	0.13	14	6.78	80	14.86
6	0.39	16	7.24	100	17.57
7	1.02	20	8.24	120	20.74
8	2.02	25	9.01		

The rate constants (k_1) for this initial reaction and the corresponding doses are given in TABLE 9.

TABLE 9.

Dose min.	k_1 cm$^{1/2}$min.$^{-1}$
6	1.636×10^{-3}
12	3.681×10^{-3}
18	5.849×10^{-3}
24	9.571×10^{-3}
30	1.096×10^{-2}
36	1.252×10^{-2}

The pressure (p_f') at which the slow evolution of gas begins is related to the time of irradiation, T, by the expression:

$$p_f' = k'T + C \quad \text{.....(3)}$$

The plot of p_f' vs T is shown in FIGURE 8.

TABLE 10 shows the complete decomposition at 180°C of 5 mg mercuric oxalate preirradiated for 0 min. 18 min. and 36 min. respectively. Very little information could be obtained from these runs. The decay period is extremely slow at this temperature, and once 50 - 60% decomposition had been reached the reaction was allowed to go to completion overnight.

TABLE 10/.....

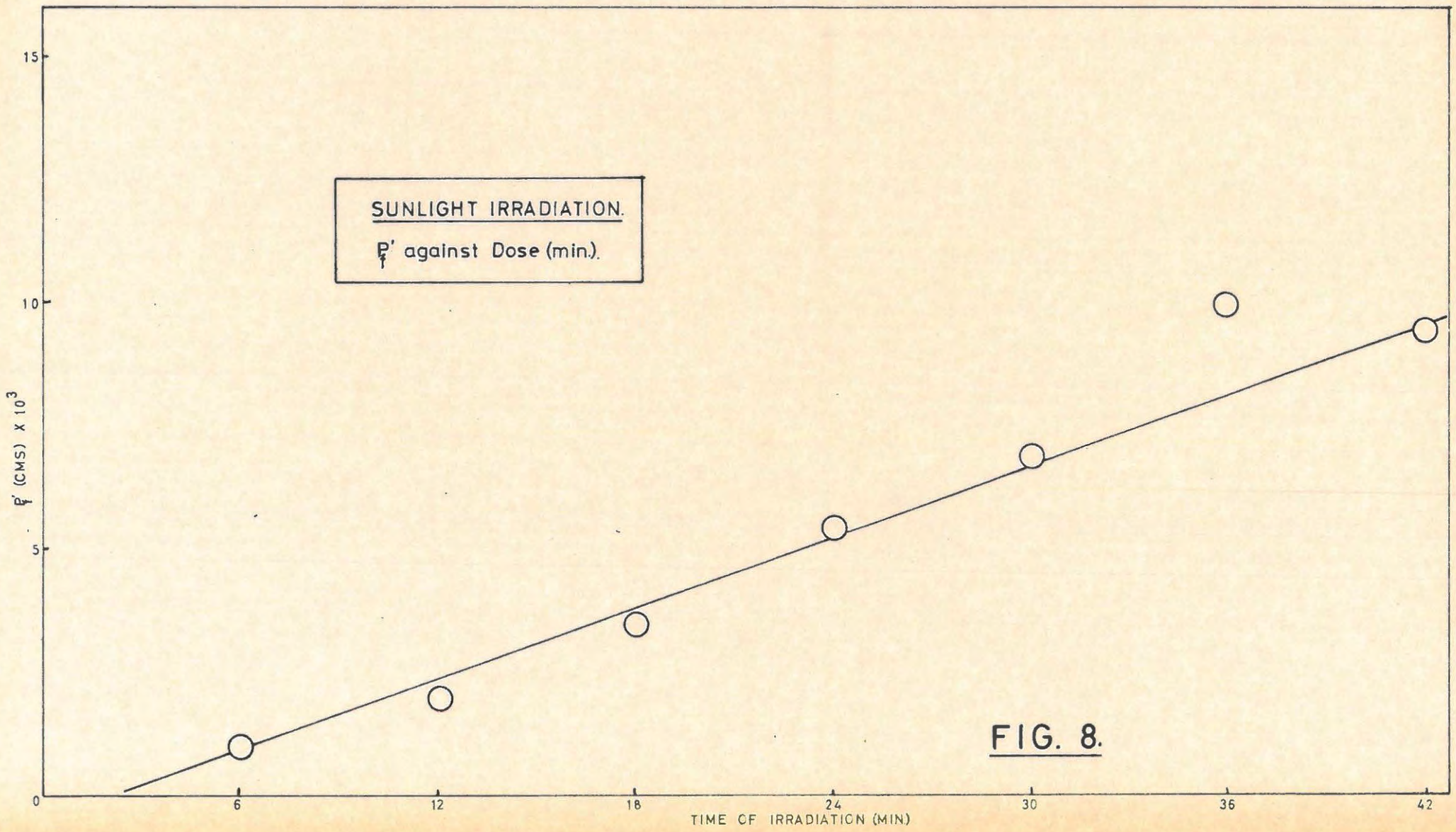
SUNLIGHT IRRADIATION.
P_f' against Dose (min.).
P_f' (CMS) X 10^3
15
10
5
0
6
12
18
24
30
36
42
TIME OF IRRADIATION (MIN)

FIG. 8.

TABLE 10.

180°C Unirradiated blank Run 1.					5.0 mg.
t	p	t	p	t	p
1	0.61	25	10.24	270	47.00
2	0.94	30	11.99	300	49.98
3	0.99	35	13.48	330	51.88
4	1.27	40	14.67	360	53.91
5	2.00	50	16.96	390	55.76
6	2.64	60	18.96	420	56.77
7	3.37	80	22.29	450	58.02
8	4.07	100	25.89	480	59.31
9	4.63	120	28.63	510	60.42
10	5.09	150	31.80	540	61.56
12	5.82	180	35.76	p_f	127.21
15	7.02	210	39.52	p_a	118.10
20	8.48	240	43.46		

180°C 18 min. sunlight. Run 2.					5.1 mg.
t	p	t	p	t	p
1	0.08	20	22.56	180	50.15
2	0.22	25	24.58	210	53.55
3	0.89	30	26.16	240	57.07
4	3.77	35	27.52	280	61.10
5	8.94	40	28.63	310	64.00
6	11.99	50	31.51	340	66.97
7	14.07	60	33.30	370	69.14
8	15.48	80	36.71	400	72.22
9	16.32	100	38.97	p_f	127.20
10	17.18	120	41.64	p_a	123.79
12	18.73	140	45.09		
15	20.35	160	47.59		

180°C 36 min. sunlight. Run 3.					4.8 mg.
t	p	t	p	t	p
1	0.06	20	24.01	180	56.42
2	0.34	25	25.88	210	59.71
3	1.65	30	27.54	240	62.47
4	5.18	35	29.20	280	66.05
5	10.49	40	31.02	320	69.35
6	13.65	50	33.45	360	72.10
7	15.28	60	35.67	400	74.57

TABLE 10 cont/.....

TABLE 10 cont.

t	p	t	p	t	p
8	16.56	80	40.61	p_f	127.20
9	17.67	100	44.81	p_a	129.14
10	18.35	120	47.74		
12	19.99	140	50.91		
15	21.70	160	53.67		

(iv) Effect on the initial reaction of varying the temperature of decomposition.

The initial decomposition of salt preirradiated for 40 min. was studied in the temperature range 80°C - 105°C. From these runs the rate constants for the acceleratory and decay periods were evoluated. The p/t values and the rate constants, k_1 and k_8 (equations 1 and 4) are listed in TABLES 11 and 13 respectively.

The slopes k_1 of the almost linear reaction after the initial "decay" reaction was determined at various temperatures in the range 110° - 136°C. These and the p/t values are given in TABLES 13 and 12 respectively.

Pressures are not normalised.

TABLE 11

80°C 40 min. sunlight. Run 1.					36.1 mg.
t	p	t	p	t	p
1	0.04	10	0.92	22	4.61
2	0.05	11	1.30	25	4.95
3	0.06	12	1.74	30	5.42
4	0.08	13	2.10	40	6.43
5	0.10	14	2.57	50	7.24
6	0.13	15	3.00	60	7.81
7	0.22	16	3.28	70	8.55
8	0.35	18	3.77	80	9.16
9	0.60	20	4.28		

TABLE 11 cont/.....

TABLE 11 cont.

84°C 40 min. sunlight. Run 2.					35.1 mg.
t	p	t	p	t	p
1	0.30	11	4.95	25	9.48
2	0.86	12	5.42	30	10.29
3	1.07	13	5.78	35	11.00
4	1.07	14	6.30	40	11.31
5	1.18	15	6.83	50	12.02
6	1.42	16	7.24	60	12.75
7	1.88	17	7.52	70	13.12
8	2.49	18	7.81	80	13.50
9	3.28	20	8.55	100	14.27
10	4.07	22	9.01	120	15.47

94°C 40 min. sunlight. Run 3.					35.6 mg.
t	p	t	p	t	p
1	0.02	11	5.07	40	11.00
2	0.04	12	5.92	50	11.48
3	0.06	13	6.43	60	12.02
4	0.08	14	6.96	70	12.38
5	0.17	16	7.81	80	12.75
6	0.45	18	8.40	100	13.50
7	1.02	20	8.85	120	14.47
8	1.95	25	9.64		
9	3.00	30	10.29		
10	4.18	35	10.63		

100°C 40 min. sunlight. Run 4.					35.4 mg.
t	p	t	p	t	p
1	0.07	9	6.30	22	11.49
2	0.13	10	7.38	25	11.84
3	0.29	11	8.25	30	12.20
4	0.42	12	8.85	40	12.75
5	0.82	14	9.80	50	13.45
6	1.81	16	10.46	60	14.08
7	3.28	18	10.80	70	14.66
8	4.95	20	11.14	80	15.12

TABLE 11 cont/.....

TABLE 11 cont.

105°C 40 min. sunlight. Run 5.					35.2 mg.
t	p	t	p	t	p
1	0.06	10	10.13	50	18.90
2	0.15	12	11.31	55	20.01
3	0.27	15	12.38	60	21.21
4	0.52	20	13.50	65	22.18
5	1.54	25	14.47	70	23.16
6	3.47	30	15.26	80	25.72
7	5.67	35	15.88	90	28.41
8	7.81	40	16.98	100	30.95
9	9.16	45	17.79	120	35.42

TABLE 12.

110°C 40 min. sunlight. Run 1.					16.4 mg.
t	p	t	p	t	p
1	0.07	12	5.42	35	9.01
2	0.17	14	5.81	40	9.64
3	0.32	16	6.17	45	10.49
4	0.56	18	6.49	50	11.31
5	1.07	20	6.83	55	12.21
6	2.02	22	7.13	60	13.12
7	3.00	24	7.52	65	13.96
8	3.87	26	7.81	70	14.66
9	4.50	28	8.10		
10	4.84	30	8.48		

115°C 40 min. sunlight. Run 2.					16.3 mg.
t	p	t	p	t	p
1	0.07	12	5.76	32	10.46
2	0.13	13	5.92	34	11.04
3	0.21	14	6.12	36	11.67
4	0.52	16	6.48	38	12.38
5	1.48	18	6.86	40	13.12
6	2.74	20	7.24	42	13.88
7	3.87	22	7.75	44	14.50
8	4.50	24	8.22	46	14.90
9	4.93	26	8.70	48	15.47
10	5.30	28	9.26	50	15.87
11	5.42	30	9.90	60	18.21

TABLE 12 Cont/.....

TABLE 12 cont.

120°C 40 min. sunlight. Run 3.					16.5 mg.
t	p	t	p	t	p
1	0.04	13	6.38	25	12.00
2	0.07	14	6.70	26	12.57
3	0.17	15	7.02	27	13.12
4	0.52	16	7.52	28	13.65
5	1.67	17	8.04	29	14.19
6	3.10	18	8.46	30	14.66
7	4.07	19	8.85	31	15.06
8	4.84	20	9.32	32	15.47
9	5.18	21	9.96	35	17.14
10	5.42	22	10.42	40	18.89
11	5.67	23	10.97	50	22.67
12	6.01	24	11.59	60	25.46

125°C 40 min. sunlight. Run 4.					16.2 mg.
t	p	t	p	t	p
1	0.10	11	8.40	21	16.29
2	0.27	12	9.01	22	17.13
3	0.52	13	9.64	24	18.67
4	1.67	14	10.46	26	20.04
5	3.67	15	11.31	28	21.21
6	5.54	16	12.20	30	22.18
7	6.17	17	13.12	40	26.78
8	6.70	18	14.07	50	30.09
9	7.25	19	15.06	60	32.40
10	7.81	20	15.78		

130°C 40 min. sunlight. Run 5.					16.3 mg.
t	p	t	p	t	p
1	0.60	11	10.97	24	25.20
2	0.81	12	12.38	26	26.78
3	1.07	13	13.69	28	27.84
4	3.37	14	15.47	30	28.69
5	5.42	15	16.66	35	30.66
6	6.70	16	18.01	40	32.40
7	7.52	17	18.90	50	35.42
8	8.10	18	20.04	60	37.29
9	8.70	20	21.93		
10	9.64	22	23.67		

TABLE 12 cont/.....

TABLE 12 cont.

136°C 40 min. sunlight. Run 6.					16.4 mg.
t	p	t	p	t	p
1	0.03	11	10.97	24	26.51
2	0.04	12	12.93	27	28.41
3	0.13	13	14.86	30	29.81
4	1.18	14	16.92	35	31.53
5	3.10	15	18.45	40	33.00
6	4.28	16	19.58	45	34.32
7	5.18	17	20.74	50	35.42
8	5.79	18	21.93	60	37.49
9	6.97	20	23.66		
10	8.85	22	24.94		

TABLE 13.

Temperature °C	k_1 cm$^{1/2}$min.$^{-1}$	k_8 min.$^{-1}$	k cm min.$^{-1}$
80	5.644×10^{-3}		
84	6.609×10^{-3}	3.70×10^{-2}	
94	1.099×10^{-2}	5.20×10^{-2}	
100	1.350×10^{-2}	8.60×10^{-2}	
105	1.734×10^{-2}	1.15×10^{-1}	
110			1.492×10^{-4}
115			3.173×10^{-4}
120			4.820×10^{-4}
125			8.034×10^{-4}
130			1.339×10^{-3}
136			1.902×10^{-3}

(v) Visual Observations.

Irradiation by sunlight produced a darkening of the salt. Unirradiated mercuric oxalate is white in colour. After ten minutes irradiation it is a very light grey. A distinct darkening of the colour is observable after approximately 20 min. At a dose of 40 min. the salt is a dark grey.

(vi) Mathematical analysis of the results and evaluation of activation energies.

FIGURE 9 shows the p/t plot for the initial reaction

of preirradiated/.....

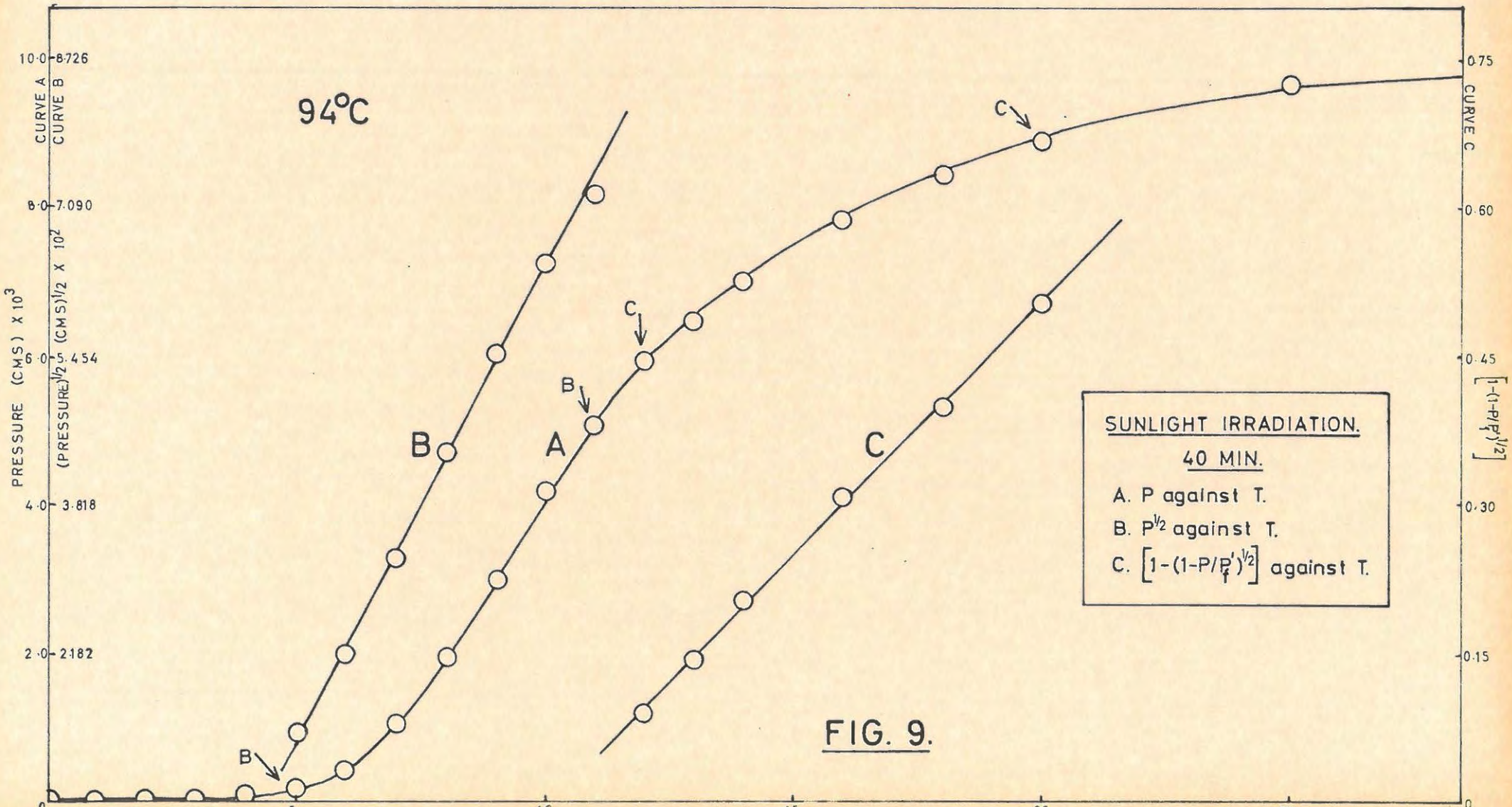
94°C
CURVE A
CURVE B
CURVE C
PRESSURE (CMS) X 10³
(PRESSURE)½ (CMS)½ X 10²
[1-(1-P/P'i)½]
TIME (MIN.)
10·0
8·0
6·0
4·0
2·0
0
8·726
7·090
5·454
3·818
2·182
0·75
0·60
0·45
0·30
0·15
0
5
10
15
20
25
A
B
C
SUNLIGHT IRRADIATION.
40 MIN.
A. P against T.
B. P½ against T.
C. [1-(1-P/P'i)½] against T.

FIG. 9.

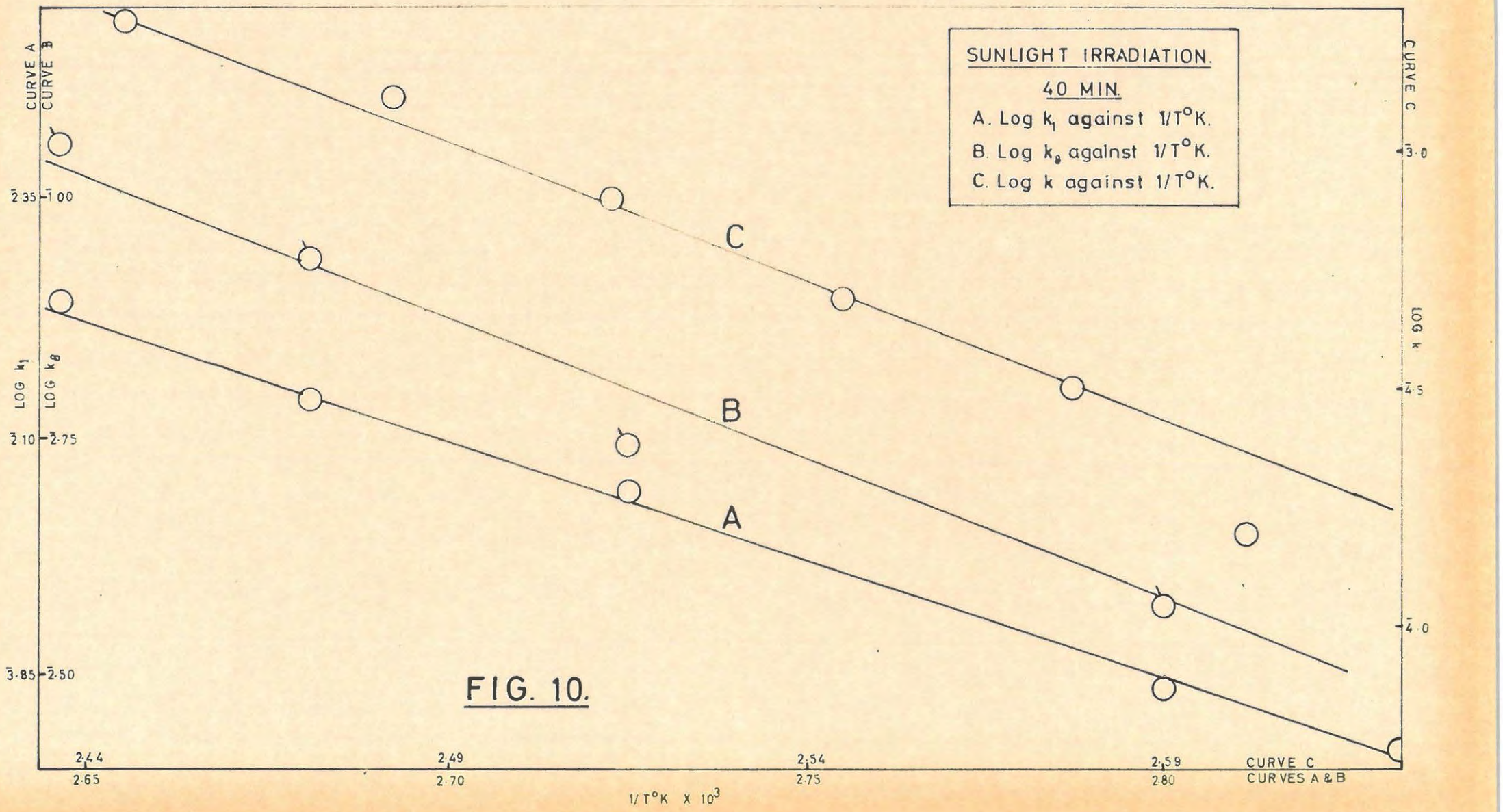
SUNLIGHT IRRADIATION.
40 MIN.
A. Log k_1 against $1/T^{\circ}K$.
B. Log k_θ against $1/T^{\circ}K$.
C. Log k against $1/T^{\circ}K$.
CURVE A
CURVE B
CURVE C
LOG k_1
LOG k_θ
LOG k
$\bar{2}\cdot35$
$\bar{1}\cdot00$
$\bar{2}\cdot10$
$\bar{2}\cdot75$
$\bar{3}\cdot85$
$\bar{2}\cdot50$
$\bar{3}\cdot0$
$\bar{2}\cdot5$
$\bar{4}\cdot0$
C
B
A
2·44
2·65
2·49
2·70
2·54
2·75
2·59
2·80
$1/T^{\circ}K \times 10^3$
CURVE C
CURVES A & B

FIG. 10.

of preirradiated mercuric oxalate. The irradiation time was 40 min. and the decomposition temperature 94°C.

The acceleratory period obeyed the power law with n = 2 i.e.

$$p^{1/2} = k_1 t + c_1 \quad \ldots\ldots\ldots\ldots\ldots\ldots\ldots\ldots (1)$$

The "decay" reaction obeys the equation for a reaction interface contracting two dimensionally, i.e. the contracting area formula. This equation can be written in the form

$$\left[1-(1- {}^{p}/_{p_f'})^{1/2}\right] = k_8 t + c_8 \ldots\ldots\ldots\ldots\ldots\ldots (4)$$

where p_f' is taken as the pressure at the commencement of the linear portion of the p/t plot.

The evolution of gas after the "decay" period was almost linear with time and consequently the velocity constant for this phase of the decomposition was evaluated using the expression

$$p = kt + c \ldots\ldots\ldots\ldots\ldots\ldots\ldots\ldots\ldots\ldots (5)$$

Plots of $p^{1/2}$ vs t and $\left[1-(1- {}^{p}/_{p_f'})^{1/2}\right]$ vs t for the acceleratory and "decay" periods respectively are also shown in FIGURE 9.

Plots of log k_1, log k_8 and log k vs $^{1}/_{T}$ gave the following activation energies.

(i) Acceleratory period : 11.3 kcals.mole^{-1}.

(ii) "Decay" period: 12.7 kcals.mole^{-1}.

(iii) Linear period: 26.1 kcals.mole^{-1}.

FIGURE 10 shows the graphical plots for the determination of these energies.

(vii) Percentage decomposition.

No change in the percentage decomposition after preirradiation with sunlight was observable.

5.1.4. Preirradiated/.....

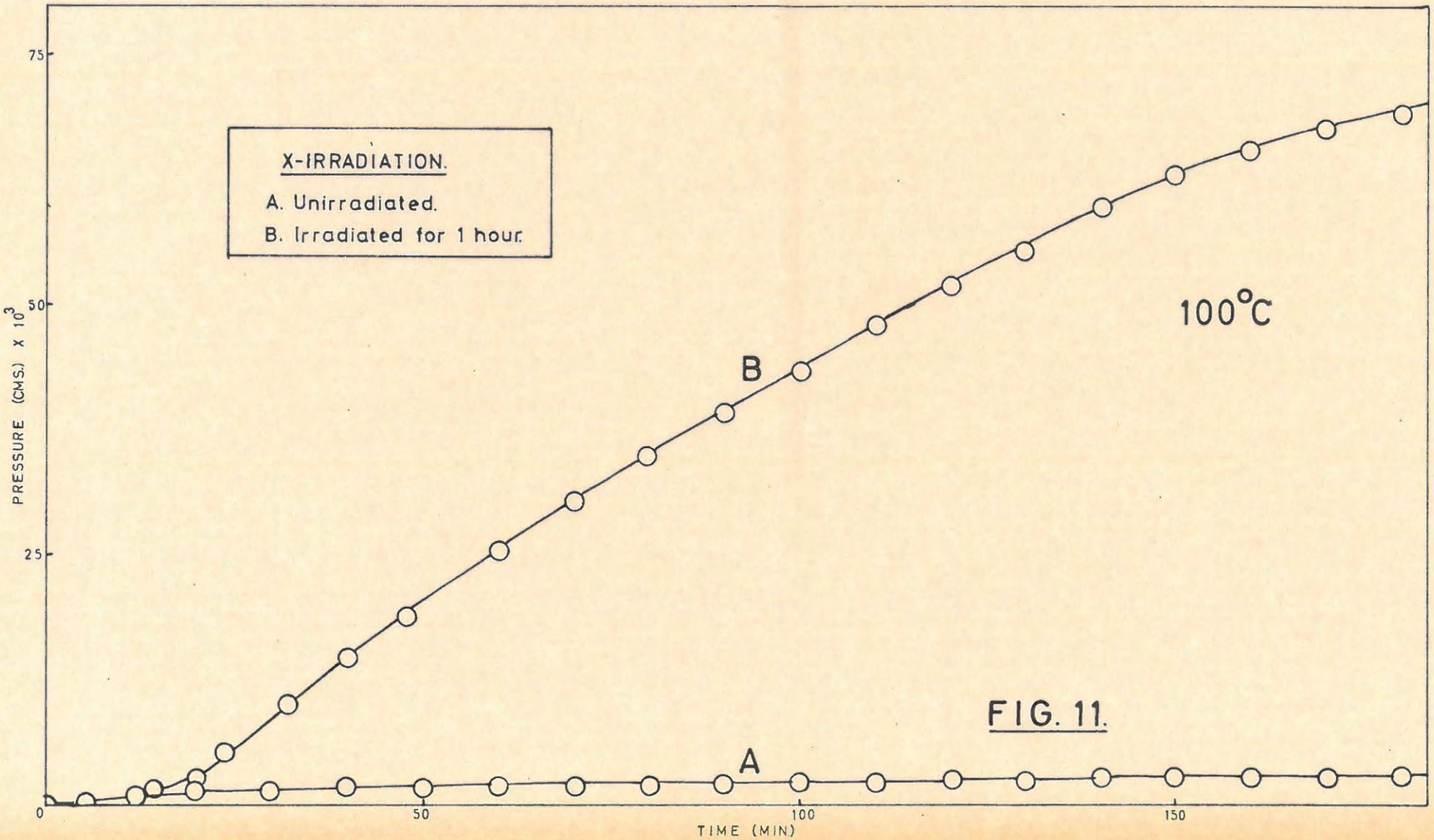
X-IRRADIATION.
A. Unirradiated.
B. Irradiated for 1 hour.
100°C
B
A
PRESSURE (CMS.) X 10^3
TIME (MIN)
0
25
50
75
50
100
150

FIG. 11.

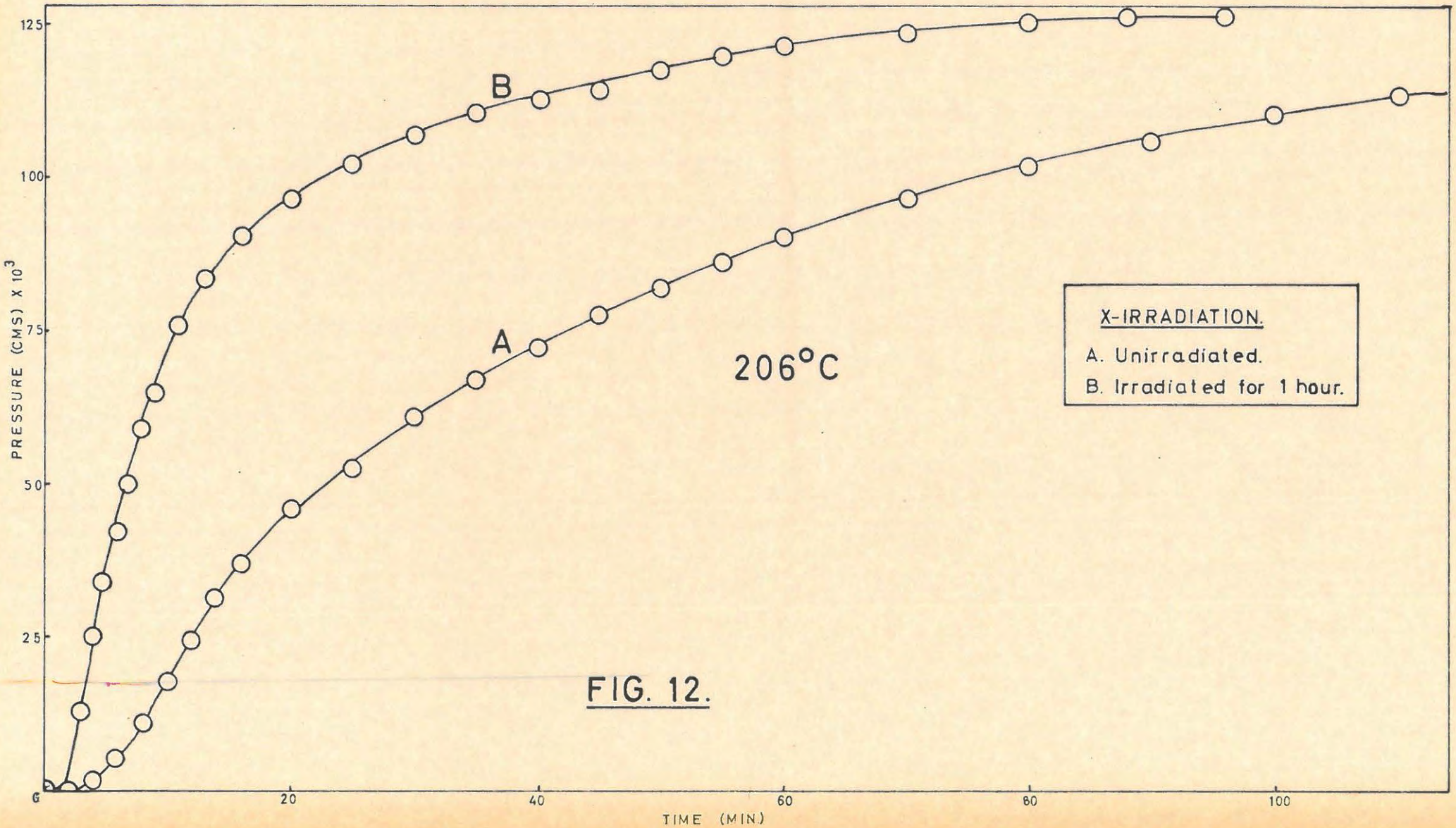
125
100
75
50
25
0
PRESSURE (CMS) X 10^3
B
A
206°C
X-IRRADIATION.
A. Unirradiated.
B. Irradiated for 1 hour.
20
40
60
80
100
TIME (MIN.)

FIG. 12.

5.1.4. Preirradiated (X-rays) Mercuric Oxalate.

(i) Preliminary investigation.

The apparatus and techniques involved in X-ray irradiations have been described. The X-ray tube was operated at an applied voltage of 40 kV and a tube current of 20 mA. All irradiations was done in air.

A preirradiation dose of one hour was chosen for the preliminary work. The initial reaction was studied at 100°C and the complete decomposition at 206°C. The results are tabulated in TABLE 14 and shown graphically in FIGURES 11 and 12. Pressures are not normalised on the initial reaction.

TABLE 14.

206°C 1 hr. X-rays. Run 1.					5.3 mg.
t	p	t	p	t	p
1	1.14	12	79.86	45	114.35
2	1.37	13	83.08	50	117.64
3	13.07	14	86.36	55	120.42
4	25.16	15	88.27	60	122.10
5	34.29	16	90.19	65	122.36
6	42.48	18	94.66	70	124.36
7	50.82	20	96.59	80	126.64
8	59.12	25	102.69	90	126.98
9	65.55	30	106.84	p_f	127.20
10	70.59	35	110.04	p_a	131.22
11	75.82	40	112.18		

100°C 1 hr. X-ray. Run 2.					38.1 mg.
t	p	t	p	t	p
1	0.02	30	8.75	90	39.34
2	0.09	32	9.91	95	41.29
3	0.26	34	11.16	100	43.28
4	0.44	36	12.38	105	45.75
5	0.58	38	13.48	110	47.75
6	0.76	40	14.62	115	49.52
7	0.80	42	15.82	120	51.70
8	0.89	44	16.85	125	53.17

TABLE 14 Cont/.....

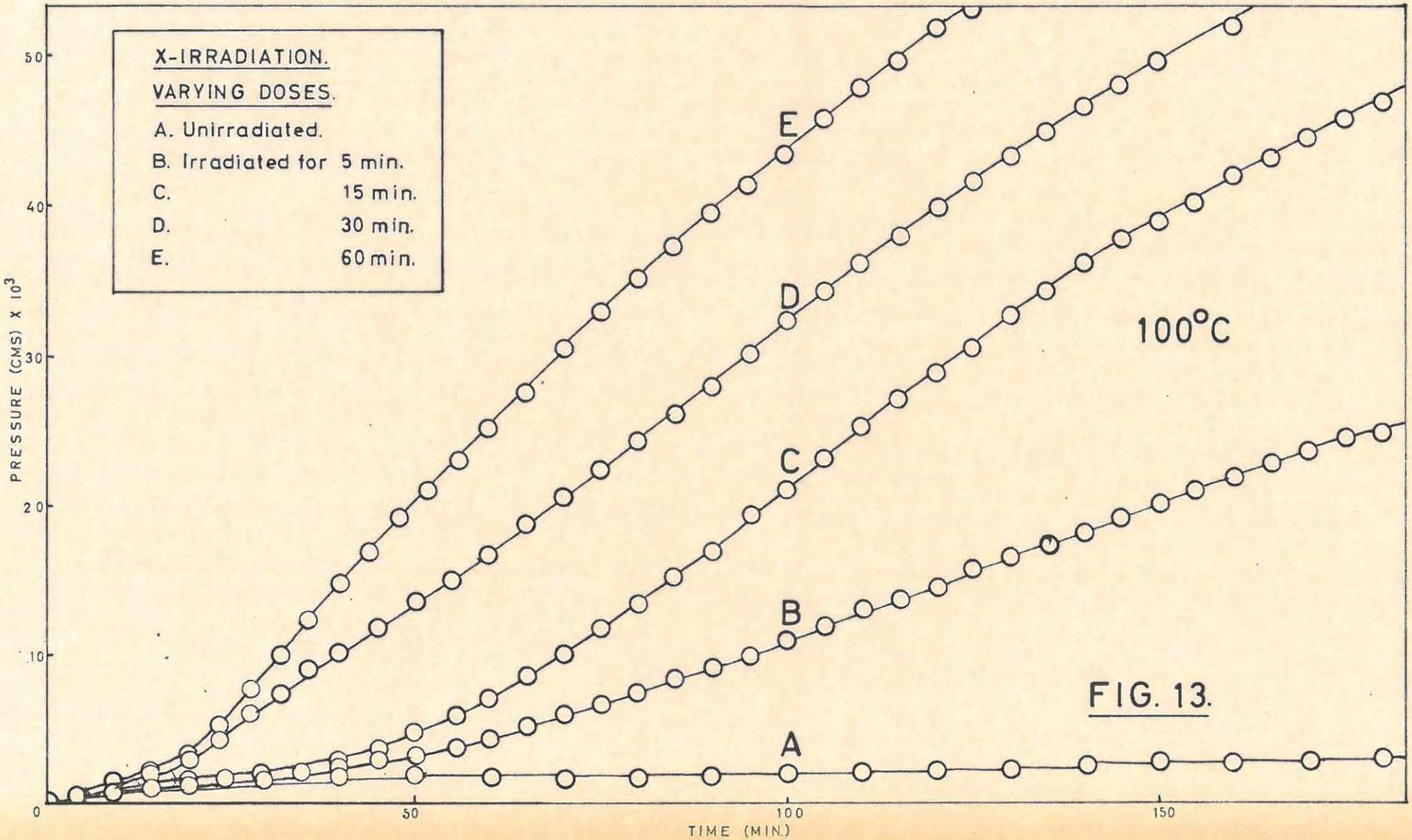
X-IRRADIATION.
VARYING DOSES.
A. Unirradiated.
B. Irradiated for 5 min.
C. 15 min.
D. 30 min.
E. 60 min.
100°C
A
B
C
D
E
PRESSURE (CMS) X 10³
TIME (MIN.)
0
10
20
30
40
50
50
100
150

FIG. 13.

TABLE 14 cont.

t	p	t	p	t	p
9	1.04	46	17.91	130	55.43
10	1.20	48	19.01	135	57.74
11	1.26	50	20.14	140	59.69
12	1.37	52	21.07	145	61.28
14	1.56	54	22.01	150	62.88
16	1.82	56	22.98	155	64.10
18	2.34	60	25.23	160	65.33
20	3.09	65	27.59	165	66.58
22	4.05	70	30.33	170	67.41
24	5.15	75	32.62	175	68.25
26	6.24	80	34.99	180	69.09
28	7.44	85	37.14		

(ii) Effect of varying doses of X-rays.

Here again both the initial reaction and the complete decomposition were studied. Irradiation times varied from 0 to 2 hrs. The results are contained in TABLES 15 and 16 while FIGURES 13 and 14 illustrate them graphically. The acceleratory rate constants, k_1, for the initial reaction are given in TABLE 17. The acceleratory period in the complete decomposition is too rapid for accurate evaluation of the rate constant. The rate constants increase as the dose increases. The inflexion point in the p/t plots for the initial reaction falls as the time of irradiation increases. Pressures are not normalised.

TABLE 15.

100°C 5 min. X-rays. Run 1.					38.2 mg.
t	p	t	p	t	p
2	0.03	45	2.74	115	13.50
4	0.07	50	3.10	120	14.47
6	0.22	55	3.57	125	15.57
8	0.27	60	4.18	130	16.30
10	0.39	65	5.07	135	17.14
12	0.60	70	5.79	140	18.01
14	0.77	75	6.56	145	18.90

TABLE 15 Cont/.....

TABLE 15 cont.

t	p	t	p	t	p
16	0.87	80	7.38	150	19.81
18	0.97	85	8.10	155	20.74
20	1.07	90	9.01	160	21.69
25	1.36	95	9.80	165	22.76
30	1.61	100	10.80	170	23.41
35	1.95	105	11.67	175	24.17
40	2.33	110	12.75	180	24.68

100°C 15 min. X-rays. Run 2.					38.2 mg.
t	p	t	p	t	p
2	0.04	45	3.67	115	27.05
4	0.07	50	4.61	120	28.69
6	0.13	55	5.67	125	30.37
8	0.22	60	6.97	130	32.40
10	0.32	65	8.40	135	34.20
12	0.52	70	9.96	140	36.04
14	0.73	75	11.66	145	37.60
16	0.87	80	13.31	150	38.88
18	1.02	85	15.06	155	40.19
20	1.18	90	16.71	160	41.84
25	1.48	95	18.90	165	43.19
30	1.81	100	20.97	170	44.56
35	2.33	105	23.16	175	45.96
40	2.92	110	25.20	180	47.01

100°C 30 min. X-rays. Run 3.					38.0 mg.
t	p	t	p	t	p
2	0.01	32	7.38	95	30.09
4	0.32	34	8.10	100	32.11
6	0.56	36	8.73	105	34.20
8	0.87	38	9.32	110	36.02
10	1.30	40	9.96	115	37.92
12	1.47	45	11.56	120	39.86
14	1.67	50	13.31	125	41.51
16	1.95	55	14.86	130	43.19
18	2.41	60	16.50	135	44.91
20	2.92	65	18.45	140	46.66
22	3.67	70	20.27	145	48.09

TABLE 15 cont/.....

TABLE 15 cont.

t	p	t	p	t	p
24	4.39	75	22.18	150	49.53
26	5.18	80	24.17	160	51.95
28	5.92	85	25.98	170	55.15
30	6.70	90	27.86	180	56.69

100°C 60 min X-rays Run 4.					38.1 mg.
t	p	t	p	t	p
1	0.02	30	8.75	90	39.34
2	0.09	32	9.91	95	41.29
3	0.26	34	11.16	100	43.28
4	0.44	36	12.38	105	45.75
5	0.58	38	13.48	110	47.75
6	0.74	40	14.62	115	49.52
7	0.80	42	15.82	120	51.70
8	0.89	44	16.85	125	53.17
9	1.04	46	17.91	130	55.43
10	1.20	48	19.01	135	57.74
11	1.25	50	20.14	140	59.69
12	1.37	52	21.07	145	61.28
14	1.56	54	22.01	150	62.88
16	1.82	56	22.98	155	64.10
18	2.34	60	25.23	160	65.33
20	3.09	65	27.59	165	66.58
22	4.05	70	30.33	170	67.41
24	5.15	75	32.62	175	68.25
26	6.24	80	34.99	180	69.09
28	7.44	85	37.14		

100°C 120 min. X-rays. Run 5.					38.0 mg.
t	p	t	p	t	p
1	0.16	32	10.85	105	46.30
2	0.84	34	11.94	110	48.53
3	0.94	36	12.89	115	50.81
4	0.99	38	13.88	120	52.76
6	1.16	40	14.91	125	53.94
8	1.35	45	17.51	130	55.94
10	1.54	50	20.09	135	57.98
12	1.75	55	22.58	140	59.63
14	2.05	60	24.95	145	61.32

TABLE 15 cont/.....

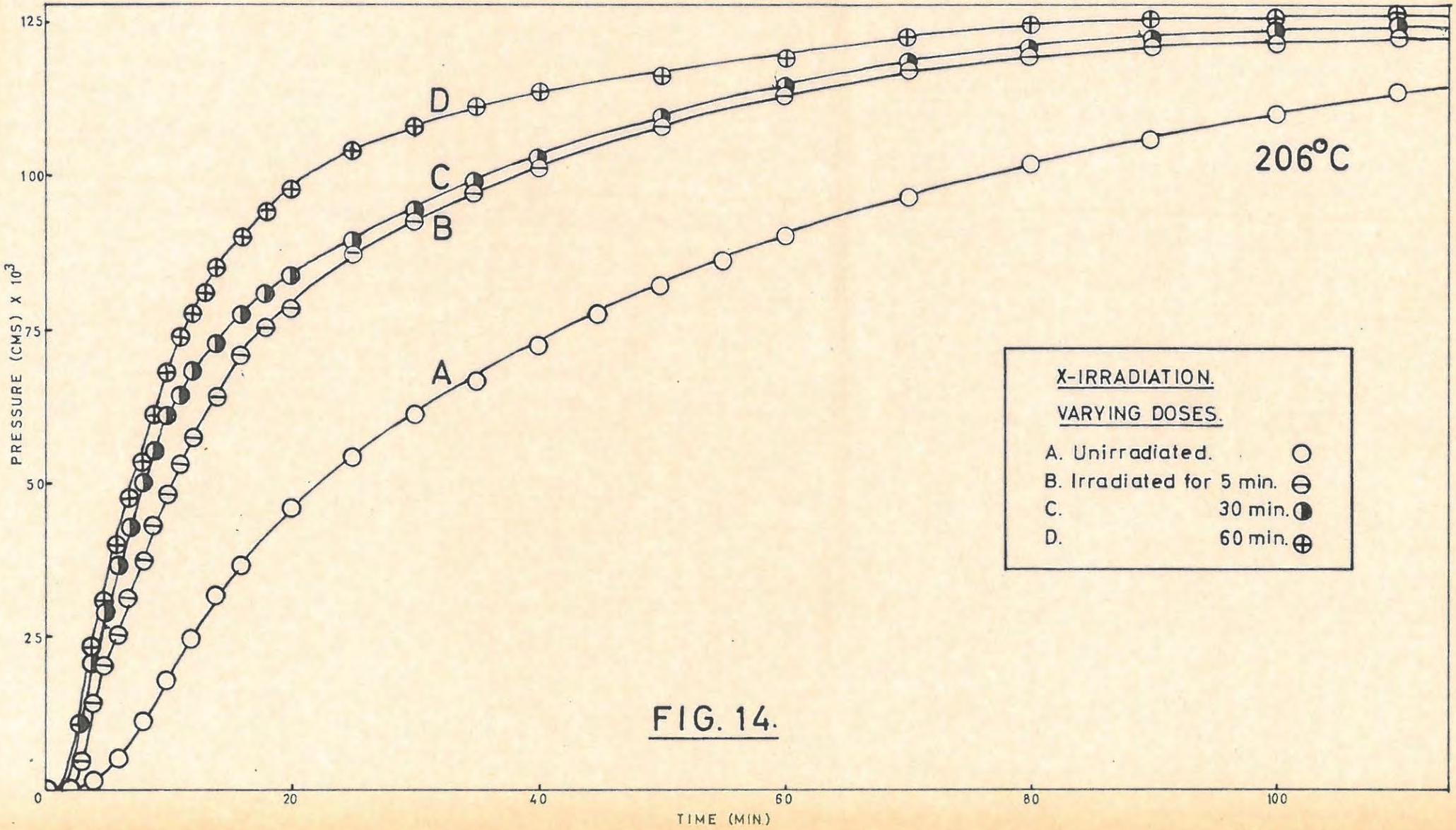
125
100
75
50
25
0
20
40
60
80
100
PRESSURE (CMS) X 10^3
TIME (MIN.)
D
C
B
A
206°C
X-IRRADIATION.
VARYING DOSES.
A. Unirradiated.
B. Irradiated for 5 min.
C. 30 min.
D. 60 min.

FIG. 14.

TABLE 15 cont.

t	p	t	p	t	p
16	2.62	65	27.45	150	63.02
18	3.37	70	29.45	155	65.18
20	4.32	75	32.46	160	66.49
22	5.39	80	34.96	165	67.82
24	6.44	85	37.24	170	69.27
26	7.58	90	39.58	175	70.06
28	8.66	95	41.99	180	70.97
30	9.64	100	44.12		

TABLE 16

206°C 5 min. X-rays Run 1.					5.1 mg.
t	p	t	p	t	p
1	0.03	12	57.32	60	113.97
2	0.14	13	61.09	70	117.49
3	4.80	14	64.55	80	119.86
4	14.74	16	71.28	90	121.66
5	20.44	18	75.00	120	124.07
6	25.66	20	78.82	140	125.29
7	31.47	25	87.65	160	125.90
8	37.21	30	92.95	180	126.51
9	43.08	35	97.20	p_f	127.20
10	48.23	40	101.54	p_a	118.64
11	53.27	50	108.23		

206°C 15 min. X-rays. Run 2.					5.1 mg.
t	p	t	p	t	p
1	0.08	11	63.22	40	104.17
2	0.15	12	66.85	50	110.01
3	6.15	13	70.11	60	114.79
4	17.88	14	72.98	80	119.67
5	25.19	16	77.88	100	123.40
6	32.43	18	81.40	120	124.66
7	39.89	20	84.48	140	125.29
8	46.55	25	90.82	160	125.92
9	52.91	30	96.27	p_f	127.20
10	57.94	35	100.75	p_a	112.48

TABLE 16 cont/.....

TABLE 16 cont.

206°C 30 min. X-rays. Run 3.					5.1 mg.
t	p	t	p	t	p
1	0.21	11	64.72	40	102.31
2	0.77	12	68.01	50	109.22
3	11.66	13	71.12	60	114.70
4	20.96	14	72.87	70	118.05
5	28.94	16	76.90	80	120.87
6	36.64	18	80.11	100	124.31
7	43.51	20	83.39	120	126.05
8	50.24	25	89.15	140	126.63
9	55.89	30	94.61	p_f	127.20
10	61.03	35	98.68	p_a	129.08

206°C 60 min. X-rays. Run 4.					5.0 mg.
t	p	t	p	t	p
1	0.45	11	73.03	40	113.53
2	0.89	12	77.72	50	116.74
3	12.74	13	81.58	60	119.96
4	23.17	14	85.04	70	123.33
5	31.64	16	90.61	80	125.35
6	39.70	18	94.64	90	126.10
7	47.18	20	97.97	100	126.56
8	54.90	25	104.49	p_f	127.20
9	61.93	30	108.97	p_a	119.90
10	68.48	35	111.81		

206°C 120 min. X-rays. Run 5.					5.0 mg.
t	p	t	p	t	p
1	0.03	12	79.84	45	117.39
2	0.77	13	83.37	50	119.20
3	5.77	14	86.98	60	121.64
4	19.96	15	89.61	80	125.38
5	27.56	16	92.13	100	126.01
6	36.38	18	96.61	120	126.63
7	44.91	20	98.82	140	126.80
8	53.52	25	105.59	p_f	127.20
9	61.13	30	109.07	p_a	113.28
10	68.78	35	112.00		
11	74.45	40	114.97		

TABLE 17/.....

TABLE 17.

Temp. °C.	Irradiation time min.	k_1 cm.$^{1/2}$ min.$^{-1}$	Inflexion Point.
100°C	5	1.06×10^{-3}	20.74
100°C	15	1.513×10^{-3}	15.06
100°C	30	2.781×10^{-3}	8.10
100°C	60	3.854×10^{-3}	8.75
100°C	120	3.517×10^{-3}	8.66

(iii) Effect of varying the temperature of decomposition.

The effect of preirradiation with X-rays is best seen when the initial reaction is studied. Rate constants over the range of temperatures 100 - 125°C were determined for this reaction. The irradiation time was 1 hr. The results are given in TABLE 18. Rate constants, k_1, are listed in TABLE 19.

TABLE 18.

100°C 60 min. X-rays. Run 1.					37.4 mg.
t	p	t	p	t	p
2	0.07	30	2.57	70	14.66
4	0.13	32	3.00	75	16.50
6	0.19	34	3.47	80	18.67
8	0.27	36	3.96	85	20.97
10	0.39	38	4.39	90	23.16
12	0.52	40	5.07	95	25.18
14	0.69	42	5.54	100	27.33
16	0.82	44	6.04	105	28.97
18	0.97	46	6.69	110	30.66
20	1.18	48	7.24	115	31.82
22	1.42	50	7.81	120	33.59
24	1.67	55	9.48	130	36.04
26	1.94	60	11.31	140	38.24
28	2.25	65	12.75	160	42.52

105°C 60 min. X-rays. Run 2.					37.0 mg.
t	p	t	p	t	p
2	0.81	34	7.24	66	27.75
4	1.00	36	8.40	68	28.97
6	1.24	38	9.32	70	30.09

TABLE 18 cont/.....

TABLE 18 cont.

t	p	t	p	t	p
8	1.36	40	10.46	75	33.00
10	1.48	42	11.67	80	36.04
12	1.67	44	12.93	85	39.21
14	1.88	46	14.27	90	41.84
16	2.10	48	15.47	95	44.56
18	2.33	50	16.71	100	47.37
20	2.74	52	18.01	105	49.53
22	3.10	54	19.35	110	52.11
24	3.47	56	20.64	115	54.38
26	3.97	58	22.18	120	56.30
28	4.61	60	23.67	125	57.87
30	5.42	62	25.20	130	59.45
32	6.43	64	26.51	140	62.28

110°C 60 min. X-rays. Run 3.					37.0 mg.
t	p	t	p	t	p
2	0.07	28	12.02	54	40.19
4	0.22	30	14.27	56	41.84
6	0.60	32	16.50	60	45.26
8	1.30	34	18.90	65	49.43
10	1.81	36	21.21	70	52.86
12	2.25	38	23.66	75	56.30
14	2.60	40	25.72	80	59.06
16	3.28	42	27.86	85	61.47
18	4.07	44	30.09	90	64.34
20	5.18	46	32.11	95	66.87
22	6.43	48	34.20	100	68.99
24	8.10	50	36.35	105	71.15
26	9.96	52	38.56	110	72.91

115°C 60 min. X-rays. Run 4.					37.6 mg.
t	p	t	p	t	p
2	0.02	20	9.92	38	42.52
4	0.07	22	13.56	40	45.26
6	0.22	24	17.57	42	48.09
8	0.87	26	21.69	44	50.63
10	1.54	28	25.72	46	52.86
12	2.02	30	29.24	48	54.76
14	3.10	32	33.00	50	56.30
16	4.72	34	36.04	55	61.06
18	6.97	36	39.53	60	65.17

TABLE 18 cont/.....

TABLE 18 cont.

120°C 60 min. X-rays. Run 5.					37.4 mg.
t	p	t	p	t	p
2	0.10	20	22.18	38	45.61
4	0.39	22	26.25	40	47.01
6	1.18	24	29.52	45	50.26
8	1.81	26	32.70	50	53.24
10	2.74	28	35.72	55	55.53
12	4.95	30	38.24	60	57.87
14	8.40	32	40.19	70	61.87
16	12.75	34	42.18	80	64.34
18	17.57	36	43.88	90	66.43

125°C 60 min. X-rays. Run 6.					37.2 mg.
t	p	t	p	t	p
2	0.02	12	10.63	22	55.53
4	0.08	14	21.21	24	61.47
6	0.69	16	31.82	26	66.01
8	1.67	18	41.84	28	69.42
10	3.87	20	49.53	30	72.47

TABLE 19.

Temperature °C	k_1 $cm^{1/2} min.^{-1}$
100°	1.800×10^{-3}
105°	2.740×10^{-3}
110°	4.663×10^{-3}
115°	7.722×10^{-3}
120°	9.980×10^{-3}
125°	1.849×10^{-2}

(iv) Visual observations.

In contrast to sunlight and γ-ray irradiations no colour change was observable on irradiating mercuric oxalate with X-rays.

(v) Mathematical analysis of the results and evaluation of activation energies.

A plot of the initial reaction for the isothermal decomposition of X-irradiated mercuric oxalate is shown

in FIGURE 15 cont/.....

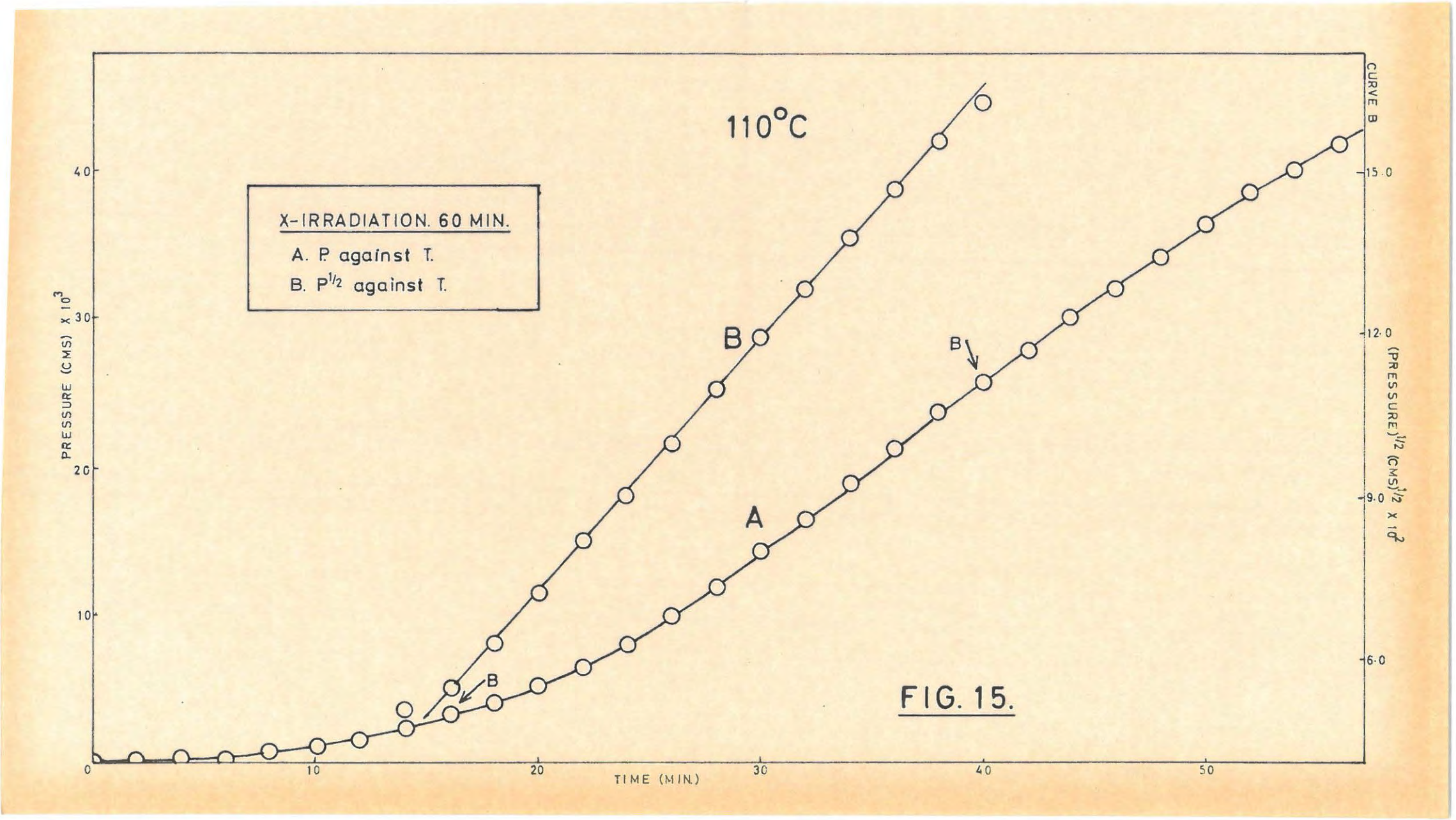
110°C
X-IRRADIATION. 60 MIN.
A. P against T.
B. P^1/2 against T.
PRESSURE (CMS) X 10^3
TIME (MIN.)
CURVE B
(PRESSURE)^1/2 (CMS)^1/2 X 10^2
A
B
B
B
0
10
20
30
40
50
10
20
30
40
6·0
9·0
12·0
15·0

FIG. 15.

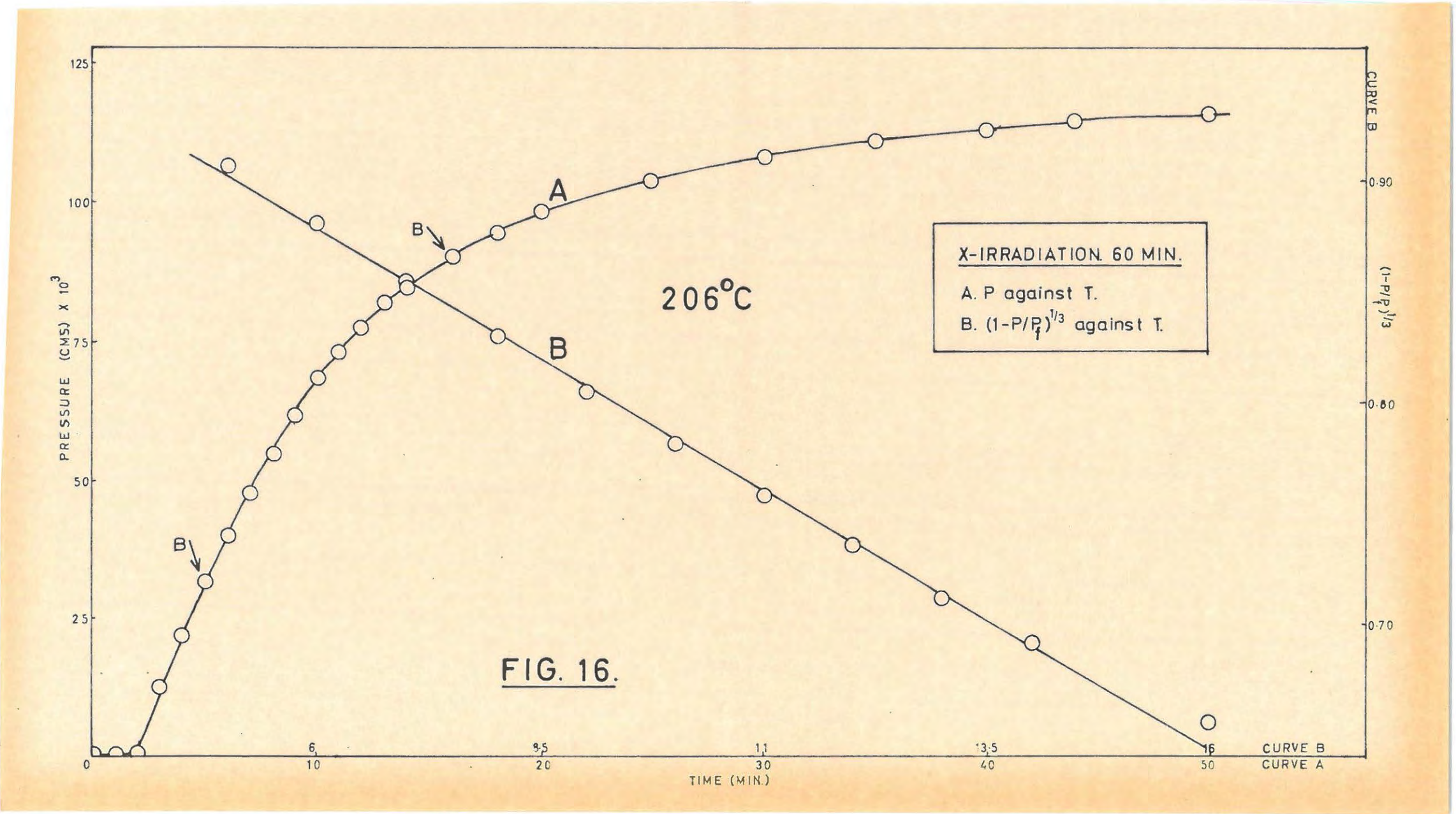
125
100
75
50
25
0
PRESSURE (CMS.) X 10^3
CURVE B
0·90
0·80
0·70
$(1-P/P_f)^{1/3}$
A
B
B
B
206°C
X-IRRADIATION. 60 MIN.
A. P against T.
B. $(1-P/P_f)^{1/3}$ against T.
6
9·5
11
13·5
16
10
20
30
40
50
TIME (MIN.)
CURVE B
CURVE A

FIG. 16.

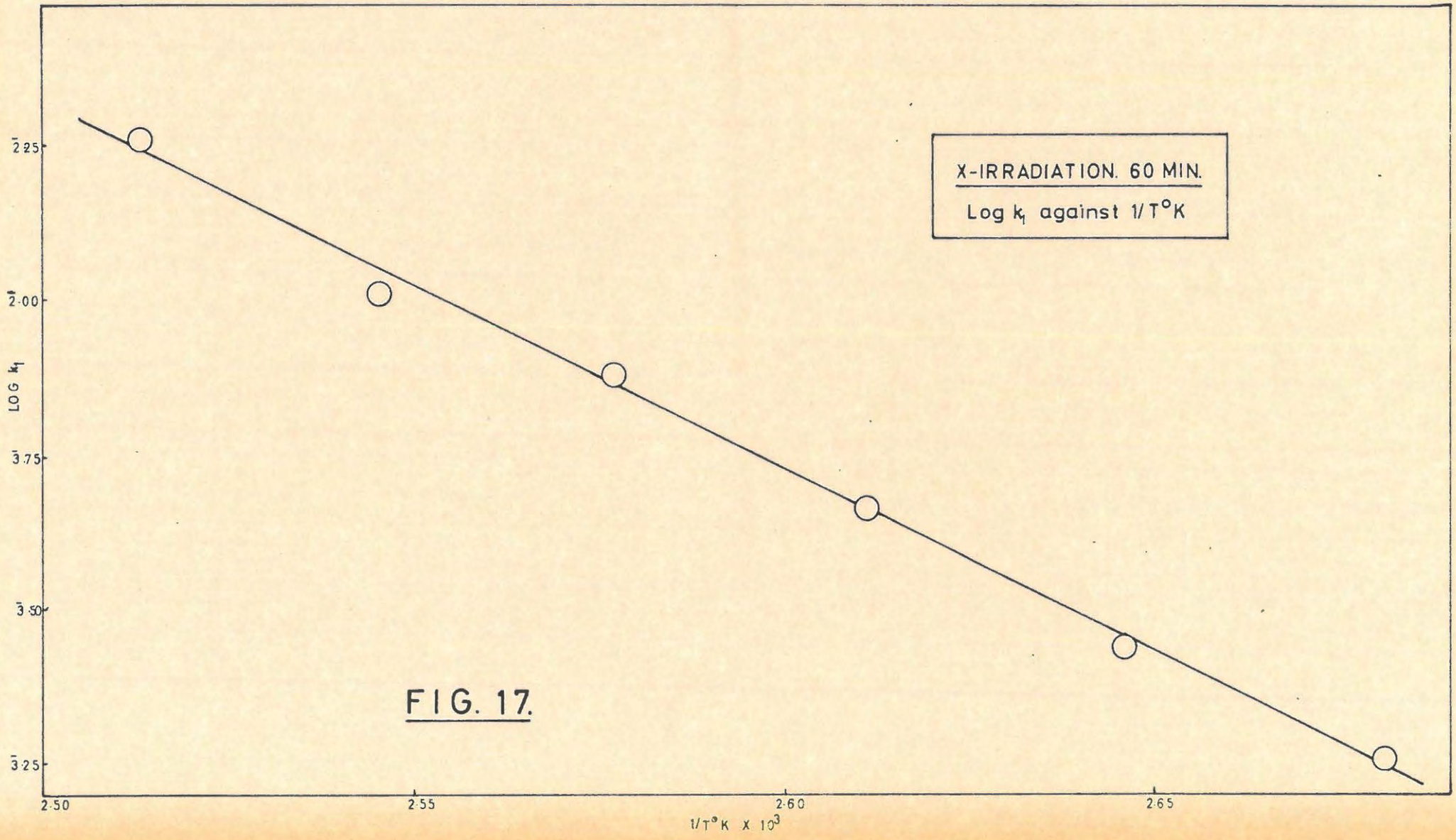
X-IRRADIATION. 60 MIN.
Log k_1 against $1/T°K$
LOG k_1
$\bar{2}.25$
$\bar{2}.00$
$\bar{3}.75$
$\bar{3}.50$
$\bar{3}.25$
2·50
2·55
2·60
2·65
$1/T°K \times 10^3$

FIG. 17.

in FIGURE 15. The acceleratory period conforms to the power law with n = 2 i.e.

$$p^{1/2} = k_1 t + c_1 \quad \ldots\ldots\ldots\ldots\ldots\ldots\ldots\ldots (1)$$

This analysis is also shown in FIGURE 15.

There was no real "decay" reaction as was found with mercuric oxalate preirradiated with sunlight.

The p/t plot for a complete decomposition is shown in FIGURE 16. There appears to be a fast almost linear evolution of gas with time prior to the main decay reaction when the complete decomposition is followed. The decay period obeys the contracting sphere formula viz

$$(1 - p/p_f)^{1/3} = k_7 t + c_7 \quad \ldots\ldots\ldots\ldots\ldots\ldots (2)$$

The extent of fit is however less than for the decomposition of unirradiated mercuric oxalate viz. from $\alpha \simeq 0.31$ to $\alpha \simeq 0.71$ for the irradiated salt as compared to $\alpha \simeq 0.35$ to $\alpha \simeq 0.91$ for the unirradiated salt.

The plot of log k_1 vs $1/T$ gave a value of 27.70 kcals.mole^{-1} as the activation energy for the processes occurring during the acceleratory period of the initial reaction. The plot is shown in FIGURE 17.

(vi) Percentage decomposition.

This was unchanged compared to that for the decomposition of unirradiated mercuric oxalate.

5.1.5. Preirradiated (γ-rays) Mercuric Oxalate.

(i) Preliminary investigation.

Irradiations were done in sealed evacuated pyrex ampoules as described previously. Preliminary work was done on a sample of salt preirradiated with a dose of 50 Mrad. The initial reaction and the complete decomposition were again studied at 100°C and 206°C respectively.

The results cont/.....

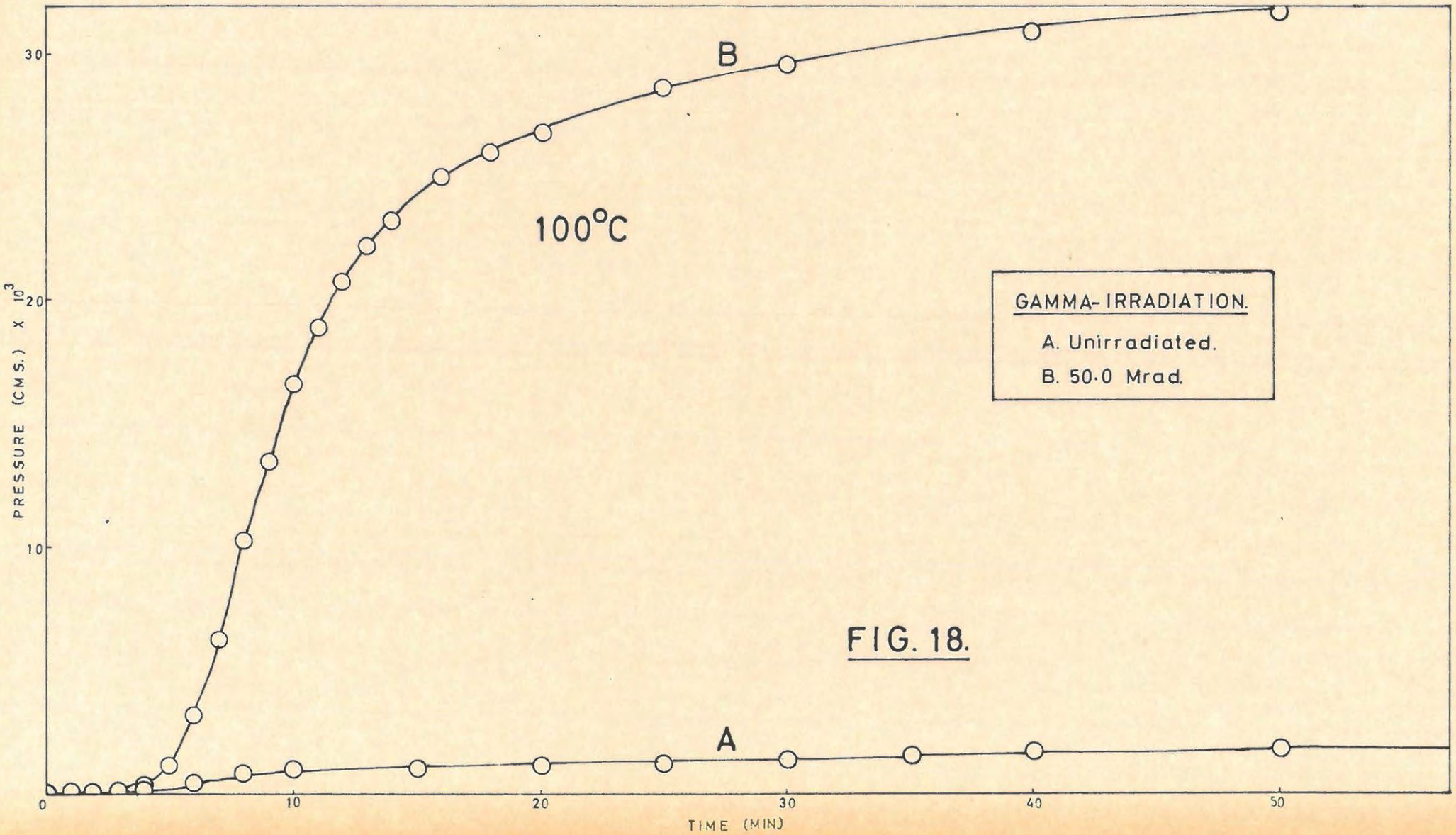
B
100°C
GAMMA-IRRADIATION.
A. Unirradiated.
B. 50·0 Mrad.
A
PRESSURE (CMS.) X 10^3
TIME (MIN)
0
10
20
30
40
50
10
20
30

FIG. 18.

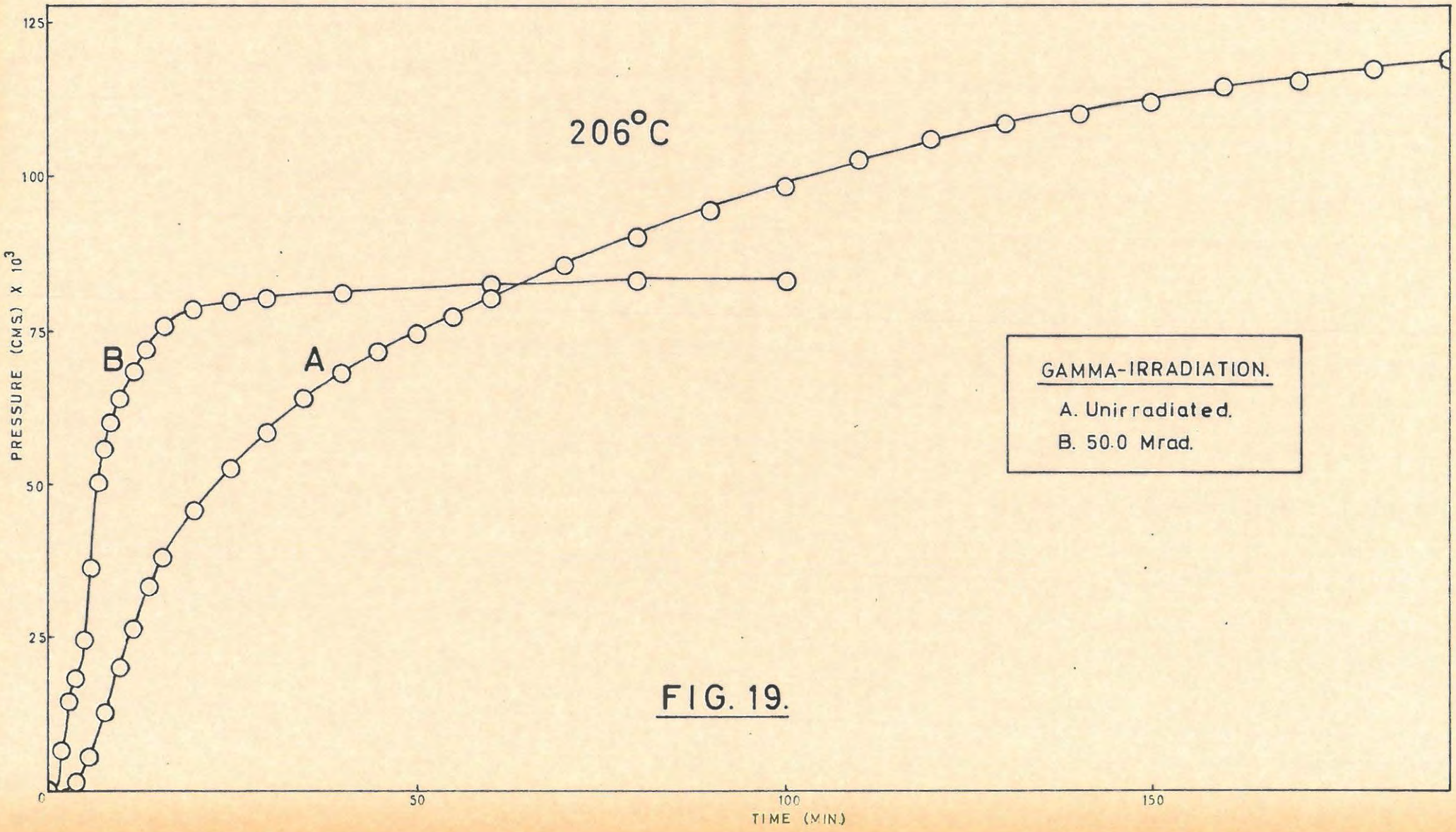
206°C
B
A
GAMMA-IRRADIATION.
A. Unirradiated.
B. 50.0 Mrad.
PRESSURE (CM.S.) X 10^3
TIME (MIN.)
0
25
50
75
100
125
50
100
150

FIG. 19.

The results are shown in FIGURES 18 and 19 respectively and tabulated in TABLE 20. Pressures are not normalised.

TABLE 20.

100°C 50 Mrad. Run 1					33.1 mg.
t	p	t	p	t	p
1	0.05	10	16.71	30	29.52
2	0.10	11	18.90	40	30.95
3	0.13	12	20.74	50	31.82
4	0.32	13	22.18	60	32.70
5	1.07	14	23.16	80	33.50
6	3.10	16	24.94	100	34.80
7	6.30	18	25.98	120	36.04
8	10.29	20	26.78		
9	13.50	25	28.69		

206°C 50 Mrad. Run 2.					5.5 mg.
t	p	t	p	t	p
1	0.07	9	60.26	30	80.15
2	6.70	10	64.34	40	81.08
3	14.67	11	67.28	60	82.48
4	18.45	12	69.41	80	83.43
5	25.72	14	72.91	100	83.63
6	36.36	16	75.13	p_a	83.90
7	50.26	20	77.85		
8	55.53	25	79.23		

The p/t plot for the initial reaction resembles that for the decomposition of mercuric oxalate preirradiated by sunlight. The complete decomposition shows an initial burst of gas followed by an acceleration and decay which are considerably faster than in the decomposition of the unirradiated salt. There is a marked decrease in the final pressure in the complete decomposition of the pre-irradiated salt.

(ii) Effect of varying γ-ray doses.

The effect of various doses of γ-rays was studied

on both the initial cont/.....

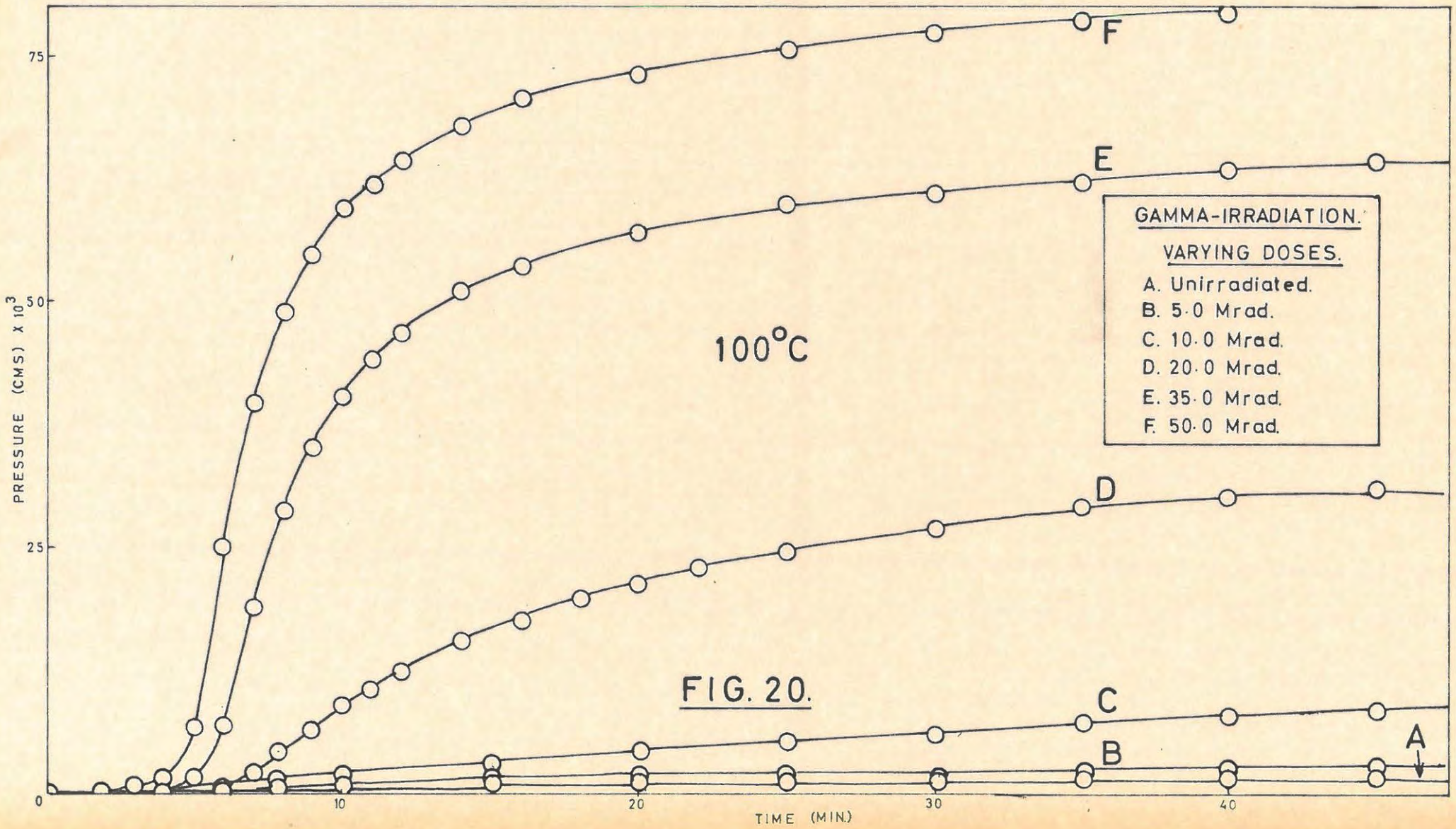
GAMMA-IRRADIATION.
VARYING DOSES.
A. Unirradiated.
B. 5·0 Mrad.
C. 10·0 Mrad.
D. 20·0 Mrad.
E. 35·0 Mrad.
F. 50·0 Mrad.
100°C
PRESSURE (CMS) X 10³
TIME (MIN.)
0
25
50
75
10
20
30
40
A
B
C
D
E
F

FIG. 20.

on both the initial reaction and the complete decomposition. The results are given in TABLES 21 and 22 and illustrated in FIGURES 20 and 21. Pressures are not normalised.

TABLE 21.

100°C 5 Mrad. Run 1. 34.8 mg.					
t	p	t	p	t	p
1	0.02	14	0.88	50	2.92
2	0.02	16	0.97	55	3.19
3	0.05	18	1.24	60	3.47
4	0.10	20	1.36	70	4.28
5	0.17	22	1.54	80	5.42
6	0.27	24	1.67	90	6.56
7	0.38	26	1.81	100	7.66
8	0.52	30	1.88	110	9.01
9	0.60	35	2.02	120	10.97
10	0.69	40	2.25	140	14.75
12	0.77	45	2.57		

100°C 10 Mrad. Run 2. 34.9 mg.					
t	p	t	p	t	p
1	0.04	12	2.25	45	8.25
2	0.10	14	2.74	50	8.85
3	0.21	16	3.28	60	9.96
4	0.39	18	3.77	70	10.97
5	0.60	20	4.28	80	11.84
6	0.77	22	4.72	90	12.75
7	1.00	24	5.07	100	13.50
8	1.24	26	5.42	110	14.27
9	1.42	30	6.17	120	14.86
10	1.67	35	6.97		
11	1.95	40	7.66		

100°C 20 Mrad. Run 3. 34.8 mg.					
t	p	t	p	t	p
1	0.03	11	10.43	30	27.05
2	0.04	12	12.38	35	28.97
3	0.07	13	14.08	40	30.09
4	0.10	14	15.47	50	32.40
5	0.19	15	16.71	60	34.20

TABLE 21 cont/.....

TABLE 21 cont.

t	p	t	p	t	p
6	0.60	16	17.57	70	35.42
7	2.02	18	19.81	80	36.35
8	4.28	20	21.45	100	37.92
9	6.43	22	22.91	120	39.86
10	8.70	25	24.68		

100°C 35 Mrad. Run 4. 35.1 mg.					
t	p	t	p	t	p
1	0.02	9	35.42	30	61.06
2	0.04	10	40.52	40	63.51
3	0.10	11	44.22	50	65.17
4	0.39	12	46.67	60	66.43
5	1.54	14	51.00	80	68.56
6	6.97	16	53.62	100	70.28
7	18.90	20	57.08	120	72.03
8	28.97	25	59.45		

100°C 50 Mrad. Run 5. 34.7 mg.					
t	p	t	p	t	p
1	0.04	9	54.76	30	77.39
2	0.52	10	59.45	40	79.69
3	0.87	11	61.87	50	81.55
4	1.54	12	64.34	60	82.49
5	6.70	14	67.70	80	84.85
6	24.94	16	70.73	100	87.30
7	39.86	20	72.91	120	89.18
8	48.81	25	75.58		

TABLE 22.

206°C 5 Mrad. Run 1. 5.1 mg.					
t	p	t	p	t	p
1	0.02	11	62.97	60	94.12
2	0.44	12	65.43	80	101.72
3	6.29	14	69.21	90	103.79
4	16.77	16	71.79	100	105.90
5	27.27	20	75.74	120	109.08
6	36.49	25	79.35	140	112.31

TABLE 22 Cont/.....

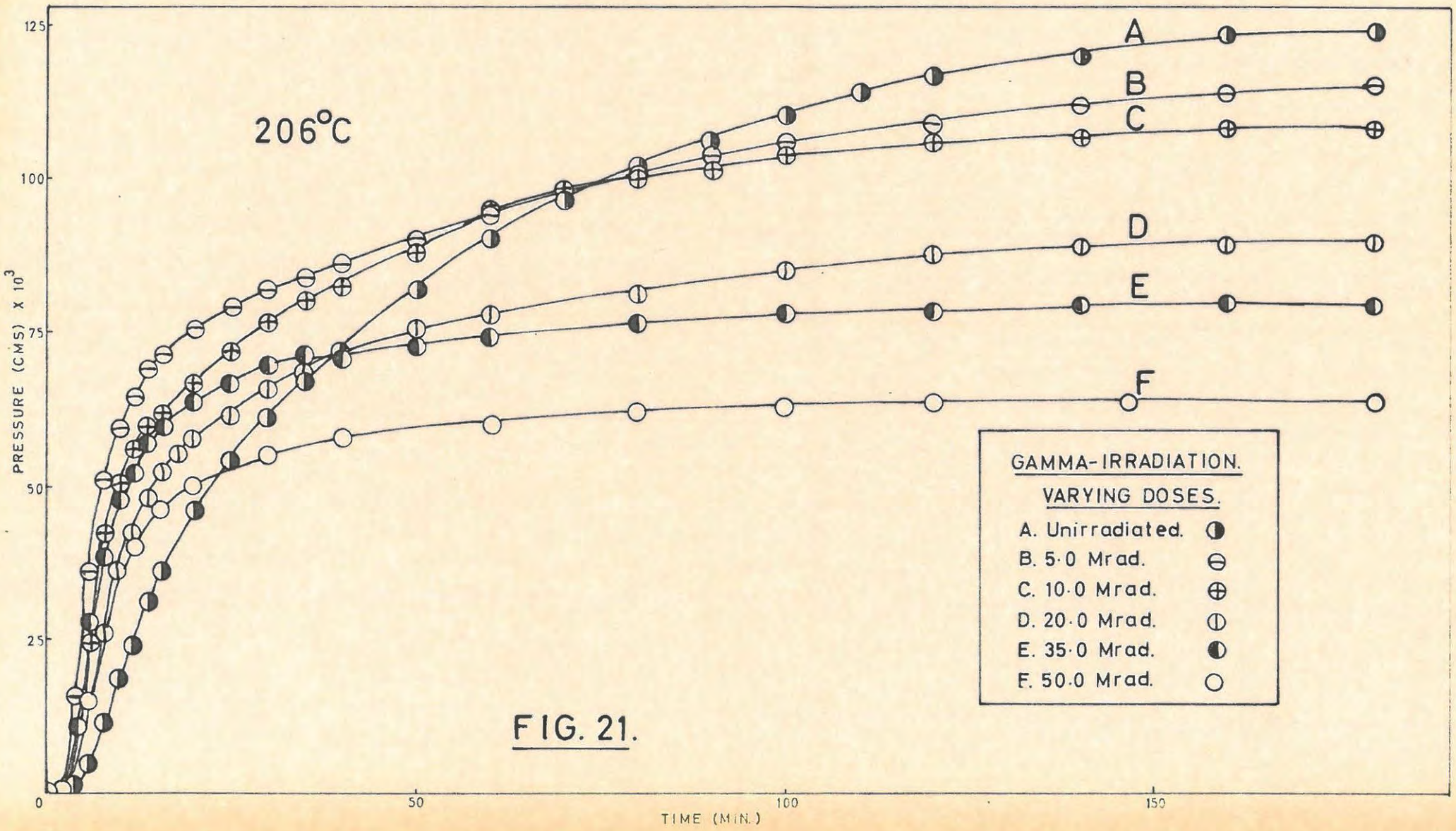
206°C
A
B
C
D
E
F
PRESSURE (CMS) X 10³
TIME (MIN.)
0
25
50
75
100
125
50
100
150
GAMMA-IRRADIATION.
VARYING DOSES.
A. Unirradiated.
B. 5·0 Mrad.
C. 10·0 Mrad.
D. 20·0 Mrad.
E. 35·0 Mrad.
F. 50·0 Mrad.

FIG. 21.

TABLE 22 cont.

t	p	t	p	t	p
7	44.29	30	82.11	160	114.49
8	51.00	35	84.45	180	116.14
9	55.87	40	86.34	200	117.80
10	59.76	50	90.19	p_a	117.83

206°C 10 Mrad. Run 2. 5.0 mg.					
t	p	t	p	t	p
1	0.13	11	54.76	60	94.65
2	0.32	12	56.69	70	98.72
3	4.07	14	60.26	80	100.79
4	11.31	16	62.69	90	102.88
5	19.81	20	67.28	100	104.99
6	28.97	25	72.03	120	106.58
7	37.28	30	76.49	140	107.66
8	43.88	35	80.13	160	108.19
9	48.45	40	82.95	180	108.73
10	51.74	50	88.71	p_a	109.27

206°C 20 Mrad. Run 3. 5.0 mg.					
t	p	t	p	t	p
1	0.13	11	39.86	40	71.15
2	0.69	12	43.19	50	75.58
3	4.72	13	45.96	60	77.85
4	7.52	14	48.81	80	81.08
5	10.97	16	52.86	100	84.85
6	15.47	18	55.92	120	87.73
7	20.74	20	58.27	140	89.19
8	26.25	25	62.69	160	89.68
9	31.82	30	66.43	p_a	90.77
10	36.35	35	68.99		

206°C 35 Mrad. Run 4. 5.0 mg.					
t	p	t	p	t	p
1	0.13	10	48.45	40	72.47
2	5.42	11	51.74	50	73.79
3	9.64	12	54.38	60	74.69
4	12.38	14	57.87	80	76.35

TABLE 22 cont/.....

TABLE 22 cont.

t	p	t	p	t	p
5	15.88	16	60.66	100	78.31
6	22.18	20	64.34	120	78.76
7	27.86	25	67.70	140	79.27
8	38.56	30	70.28	p_a	79.64
9	43.88	35	71.59		

206°C 50 Mrad. Run 5. 5.1 mg.					
t	p	t	p	t	p
1	0.09	9	32.51	30	55.51
2	6.42	10	35.77	35	57.03
3	11.19	11	38.24	40	58.19
4	14.07	12	40.14	50	60.14
5	17.27	14	44.09	60	60.93
6	21.27	16	46.47	80	62.52
7	25.18	20	50.35	100	63.37
8	28.87	25	53.27	p_a	63.74

The value of p_f' for the initial reaction increases as the dose increases. Rate constants, k_2 (equation 6), for the acceleratory region of the initial reaction are given in TABLE 23.

If a constant weight of salt is irradiated it is found that radiolysis occurs since, after opening the ampoule, there is a progressive loss in weight with increasing dose. This is accompanied by a corresponding fall in the final pressure, Δp_a, for the complete decomposition. These results are listed in TABLE 24. The following expressions relating the dose, Υ, the loss in mass, m, and the drop in the final pressure, Δp_f, were found to hold

(a) $\log \Upsilon = km + c$

(b) $\log \Upsilon = k \Delta p_f + c$

(c) $\Delta p_f = km + c$

Plots of $\log \Upsilon$ vs Δp_f, and Δp_f vs m, for b and c respectively, are shown in FIGURE 22.

TABLE 23 cont/.....

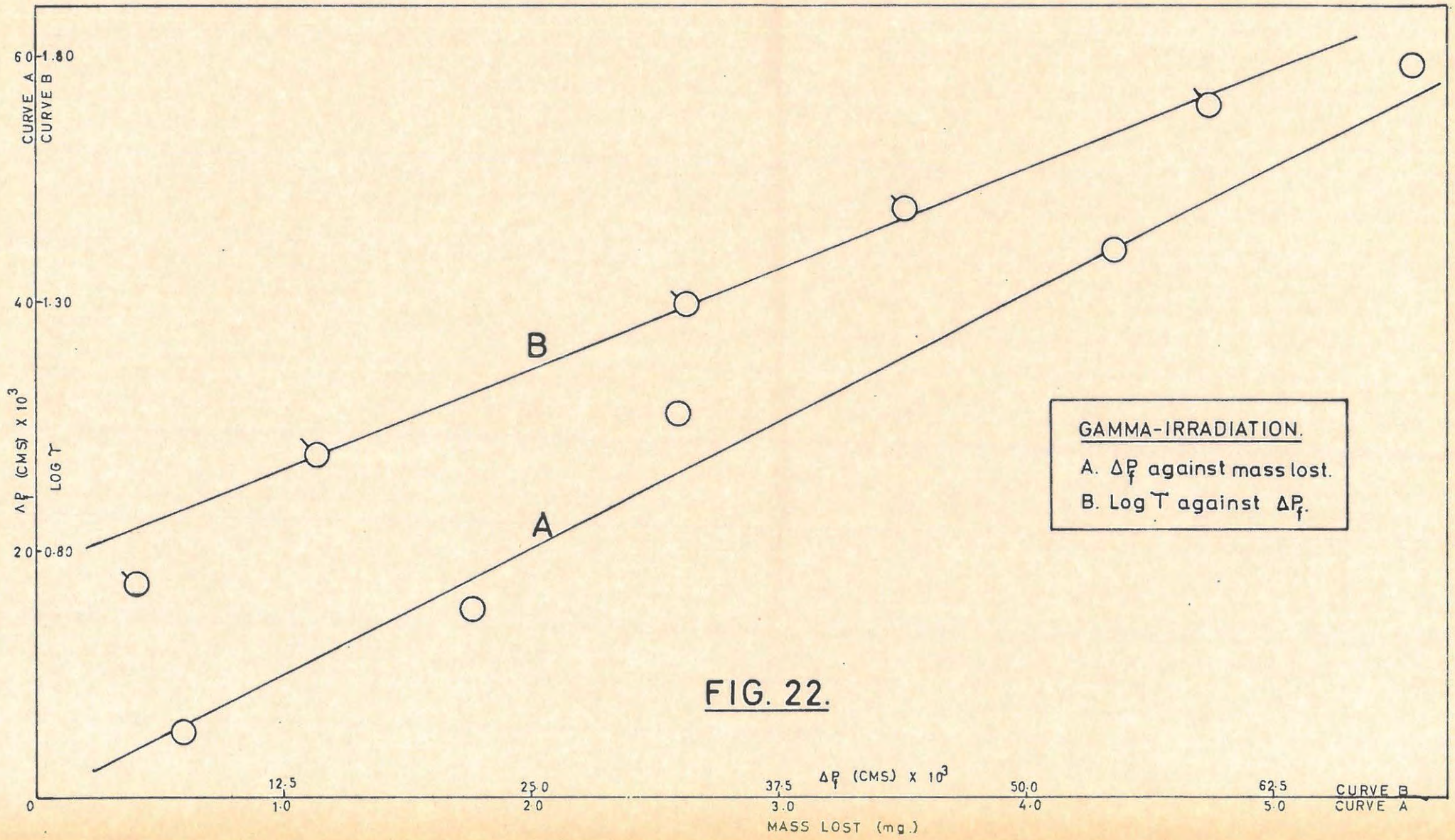
CURVE A
CURVE B
60
1.80
40
1.30
20
0.80
0
ΔP_f (CMS) X 10^3
LOG τ
B
A
GAMMA-IRRADIATION.
A. ΔP_f against mass lost.
B. Log τ against ΔP_f.
12.5
1.0
25.0
2.0
37.5
3.0
50.0
4.0
62.5
5.0
ΔP_f (CMS) X 10^3
MASS LOST (mg.)
CURVE B
CURVE A

FIG. 22.

TABLE 23.

Dose Mrad.	k_2 cm. min.$^{-1}$
5	6.93×10^{-2}
10	9.24×10^{-2}
20	1.525×10^{-1}
35	6.00×10^{-1}
50	6.4×10^{-1}

TABLE 24.

Dose Mrad.	Mass irradiated mg.	Loss in mass mg.	p_a	Δp_a
0	34.8	0	123.19	0
5	34.9	0.6	117.83	5.36
10	34.8	1.8	109.27	13.92
20	34.8	2.6	90.77	32.42
35	34.9	4.4	79.64	43.55
50	34.7	5.5	63.74	59.45

(iii) Effect of varying the temperature of decomposition.

The initial reaction was studied in the range 70°C - 95°C and the complete decomposition in the range 200 - 220°C. The specimens were preirradiated by γ-rays with a dose of 50 Mrad. The results are tabulated in TABLES 25 and 26, and the rate constants, k_2 and k_9, (equations 6 and 7) which were obtained, are given in TABLE 27. Pressures are not normalised for the initial decomposition.

TABLE 25.

70°C 50 Mrad. Run 1.					35.2 mg.
t	p	t	p	t	p
1	0.06	17	10.97	36	37.29
2	0.13	18	12.93	38	38.56
3	0.19	19	15.06	40	39.53
4	0.32	20	17.14	42	40.19
5	0.45	21	18.90	45	41.84
6	0.60	22	20.74	50	43.88
7	0.82	23	22.67	55	45.26

TABLE 25 cont/.....

TABLE 25 cont.

85°C 50 Mrad. Run 4. 35.3 mg.					
t	p	t	p	t	p
1	0.13	10	21.18	22	52.49
2	0.24	11	27.86	25	54.76
3	0.32	12	33.33	30	57.87
4	0.52	13	37.29	35	60.66
5	1.00	14	40.52	40	62.69
6	1.95	15	43.19	45	64.34
7	3.87	16	45.26	50	65.60
8	7.81	18	48.45	60	68.56
9	14.27	20	50.63		

90°C 50 Mrad. Run 5. 35.4 mg.					
t	p	t	p	t	p
1	0.09	9	33.00	25	64.34
2	0.22	10	39.21	30	66.85
3	0.38	11	43.88	35	68.56
4	0.77	12	47.37	40	69.85
5	1.95	13	50.26	50	73.81
6	5.18	14	52.49	60	74.69
7	11.23	16	55.53		
8	23.16	20	60.26		

95°C 50 Mrad. Run 6. 35.3 mg.					
t	p	t	p	t	p
1	0.13	8	40.52	20	70.72
2	0.22	9	48.81	25	73.79
3	0.38	10	53.24	30	76.03
4	0.87	11	57.08	35	77.39
5	2.57	12	59.45	40	78.31
6	11.31	14	63.92	50	80.61
7	28.11	16	66.85	60	82.95

TABLE 26.

200°C 50 Mrad. Run 1. 10.6 mg.					
t	p	t	p	t	p
1	0.06	10	43.88	35	83.43
2	5.43	11	48.09	40	85.81

TABLE 26 cont/.....

TABLE 26 cont.

t	p	t	p	t	p
3	13.88	12	51.74	50	89.68
4	17.14	14	57.87	60	91.16
5.	20.27	16	62.69	80	92.63
6	24.68	18	66.85	p_f	93.14
7	29.52	20	69.42	p_a	93.14
8	34.20	25	75.59		
9	38.88	30	79.69		

205°C 50 Mrad. Run 2. 10.5 mg.					
t	p	t	p	t	p
1	0.09	9	51.47	40	89.24
2	8.62	10	56.35	50	90.70
3	16.69	12	64.18	70	92.64
4	21.12	14	68.43	80	92.99
5	26.60	16	71.85	p_f	93.14
6	33.59	20	78.04	p_a	92.81
7	40.42	25	82.62		
8	46.47	30	85.90		

211°C 50 Mrad. Run 3. 10.2 mg.					
t	p	t	p	t	p
1	0.01	8	45.96	18	81.55
2	0.03	9	53.24	20	84.37
3	11.67	10	59.06	25	87.73
4	16.29	11	63.92	30	90.17
5	20.97	12	67.70	50	92.65
6	28.41	14	73.79	p_f	93.14
7	37.60	16	77.85	p_a	90.16

216°C 50 Mrad. Run 4. 10.5 mg.					
t	p	t	p	t	p
1	0.01	7	47.00	16	84.84
2	5.67	8	56.69	20	88.70
3	14.27	9	63.52	25	91.67
4	18.90	10	68.56	30	92.66
5	25.72	12	76.48	p_f	93.14
6	35.43	14	81.09	p_a	94.01

TABLE 26 cont/.....

TABLE 26 cont.

220°C 50 Mrad. Run 5. 10.2 mg.					
t	p	t	p	t	p
1	0.02	7	59.73	20	89.94
2	10.08	8	69.81	30	91.56
3	18.51	9	74.78	40	92.33
4	23.48	10	78.44	p_f	93.14
5	34.21	12	83.57	p_a	88.76
6	48.09	15	87.58		

TABLE 27.

Temp. °C	k_2 cm $min.^{-1}$	k_9 $min.^{-1}$ (initial reaction)	k_9 $min.^{-1}$ (complete reaction)
70	1.24×10^{-1}	3.35×10^{-2}	
75	1.60×10^{-1}	4.25×10^{-2}	
80	2.46×10^{-1}	4.60×10^{-2}	
85	2.90×10^{-1}	7.90×10^{-2}	
90	3.60×10^{-1}	8.40×10^{-2}	
95	4.75×10^{-1}	9.30×10^{-2}	
200			2.40×10^{-2}
205			3.42×10^{-2}
211			5.41×10^{-2}
216			7.40×10^{-2}
220			9.75×10^{-2}

(iv) Visual observations.

Mercuric oxalate darkens on exposure to γ-rays. There is a steady increase in the degree of darkening with increasing dose. The unirradiated salt is white. After a dose of 5 Mrad it is an off-white colour. The colour continues to change through light brown, brown, dark brown to almost black as the dose increases i.e. 10, 20, 35 and 50 Mrad.

(v) Analysis of the gas(es) evolved.

A liquid air trap placed in the line condensed virtually all the evolved gas. The condensed gas proved to be CO_2.

This is shown cont/.....

This is shown in TABLE 28. The γ dose was 50 Mrad.

TABLE 28.

206°C 50 Mrad. Run 1. 4.7 mg.					
t	p	t	p	t	p
1	0.09	11	38.24	80	62.52
2	6.42	12	40.14	100	63.37
3	11.19	14	44.09	120	63.74
4	14.07	16	46.47	140	63.74
5	17.27	20	50.35	Liquid air trap.	
6	21.27	25	53.27	142	58.60
7	25.18	30	55.51	144	2.16
8	28.87	40	58.19	145	2.01
9	32.51	50	60.14	146	2.01
10	35.77	60	60.93	150	2.01

(vi) Mathematical analysis of the results and evaluation of activation energies.

A pressure vs. time plot for the complete thermal decomposition of mercuric oxalate preirradiated with a dose of 50 Mrad is shown in FIGURE 23. The decomposition temperature was 200°C. An initial burst of gas is followed by a fast reaction when the evolution of gas is almost linear with time. After this the main decay process commences. At high temperatures only the decay reaction can be successfully analysed. It conforms to the unimolecular decay law, viz.

$$\log (p_f - p) = k_9 t + c_9 \quad \ldots\ldots\ldots\ldots\ldots\ldots (7)$$

The plot of log $(p_f - p)$ vs t is shown in FIGURE 23.

FIGURE 24 shows the p/t plot for the initial reaction at 80°C and with a dose of 50 Mrad. The acceleratory period is fitted by the exponential law,

$$\log p = k_2 t + c_2 \quad \ldots\ldots\ldots\ldots\ldots\ldots\ldots\ldots (6)$$

The unimolecular decay law fits the decay period, i.e.

$$\log (p_f' - p) = k_9 t + c_9 \quad \ldots\ldots\ldots\ldots\ldots\ldots (7)$$

Plots of log cont/.....

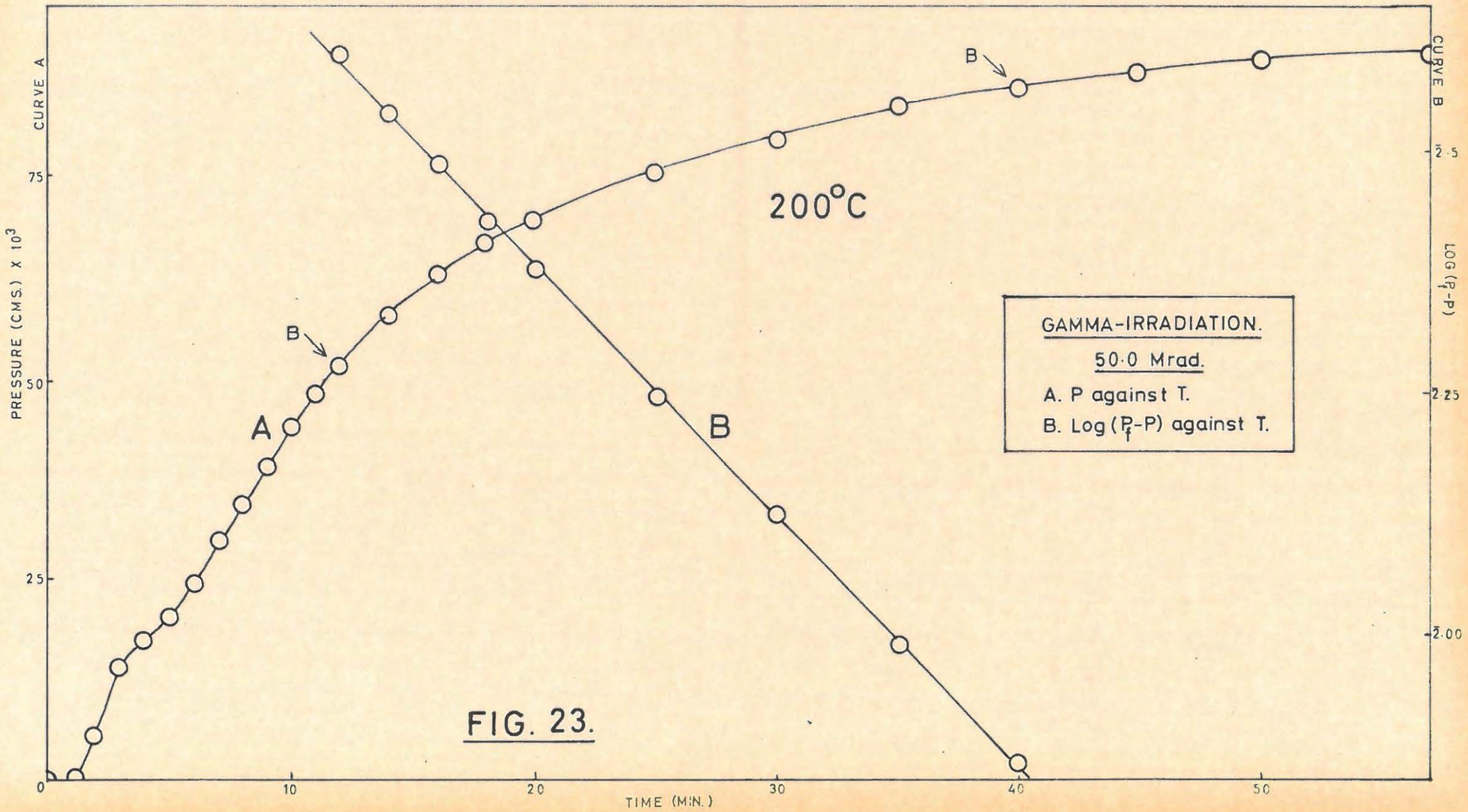
PRESSURE (CMS.) X 10^3
CURVE A
CURVE B
LOG (P_f-P)
TIME (MIN.)
0
10
20
30
40
50
25
50
75
2·5
2·25
2·00
200°C
A
B
B
B
GAMMA-IRRADIATION.
50·0 Mrad.
A. P against T.
B. Log (P_f-P) against T.

FIG. 23.

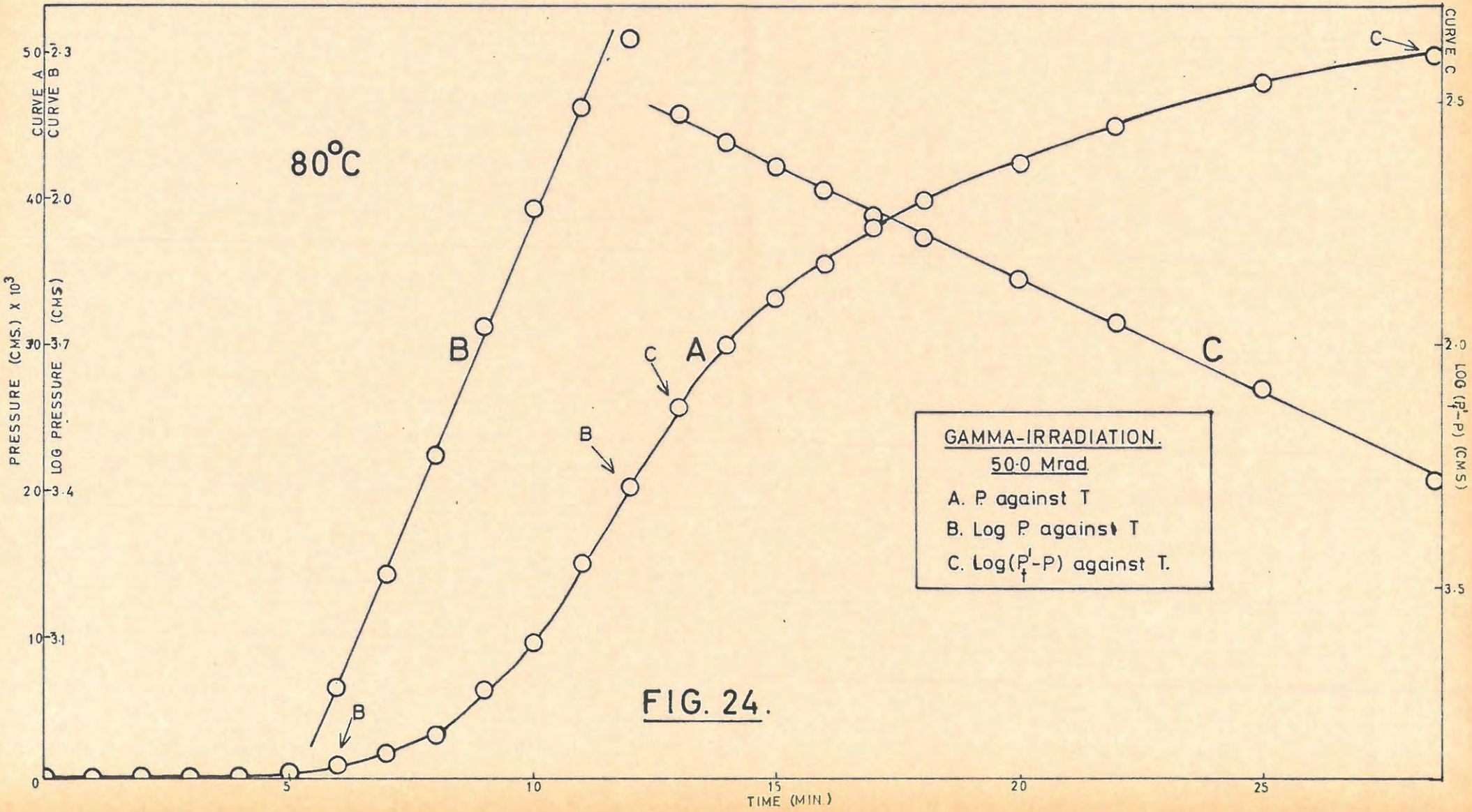
80°C
PRESSURE (CMS.) X 10³
LOG PRESSURE (CMS)
CURVE A
CURVE B
CURVE C
LOG (P'f-P) (CMS)
TIME (MIN.)
A
B
C
GAMMA-IRRADIATION.
50·0 Mrad.
A. P against T
B. Log P against T
C. Log(P'f-P) against T.

FIG. 24.

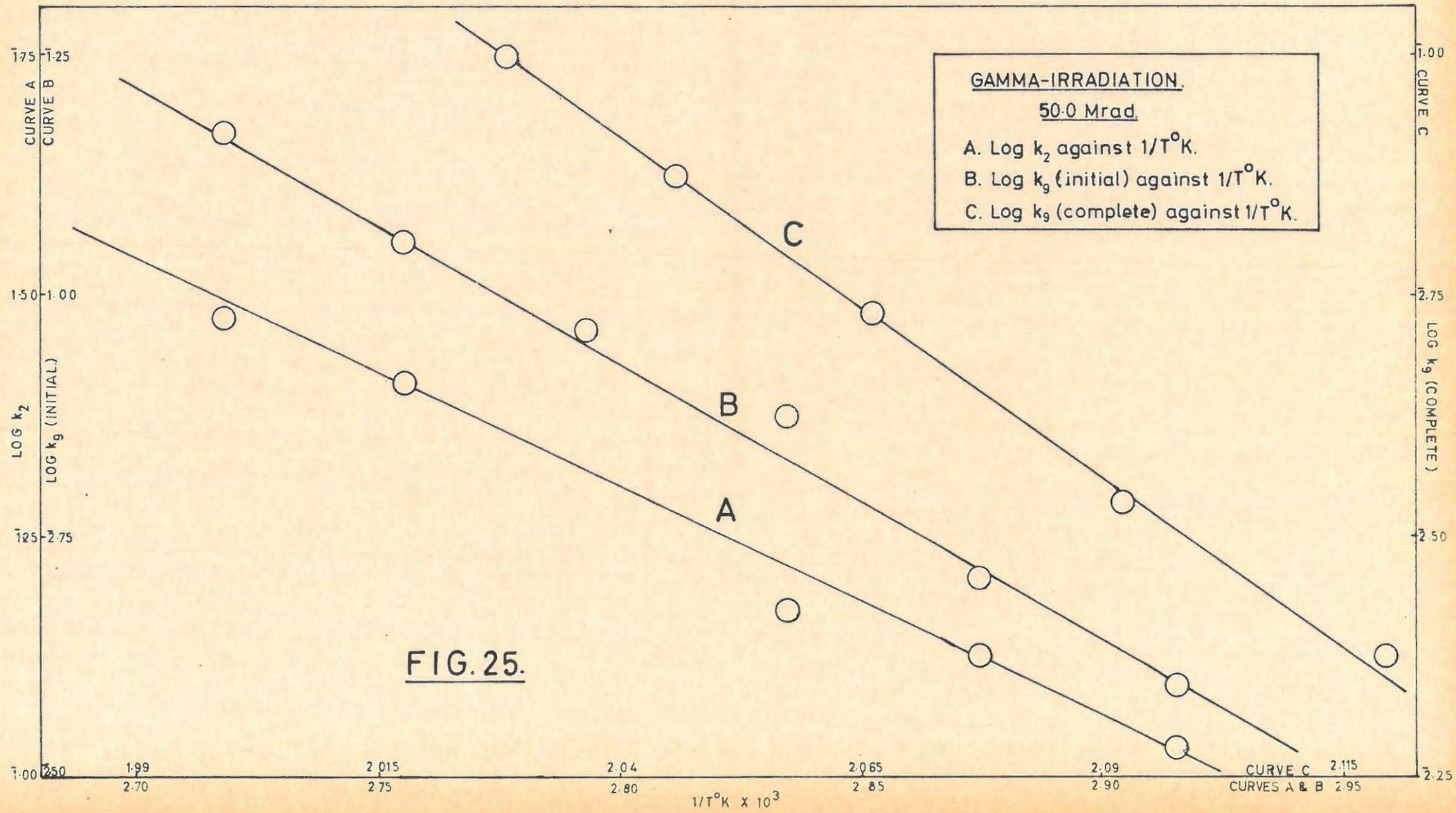
GAMMA-IRRADIATION.
50·0 Mrad.
A. Log k_2 against $1/T^{\circ}K$.
B. Log k_9 (initial) against $1/T^{\circ}K$.
C. Log k_9 (complete) against $1/T^{\circ}K$.
CURVE A
CURVE B
CURVE C
LOG k_2
LOG k_9 (INITIAL)
LOG k_9 (COMPLETE)
$\bar{1}\cdot75$
$\bar{1}\cdot50$
$\bar{1}\cdot25$
$\bar{1}\cdot00$
$\bar{1}\cdot25$
$\bar{1}\cdot00$
$\bar{2}\cdot75$
$\bar{2}\cdot50$
$\bar{2}\cdot25$
2·50
1·99
2·70
2·015
2·75
2·04
2·80
2·065
2·85
2·09
2·90
CURVE C 2·115
CURVES A & B 2·95
$1/T^{\circ}K \times 10^3$
A
B
C

FIG. 25.

Plots of log p vs. t and log $(p_f' - p)$ vs. t are shown in FIGURE 24.

Plots of log k_9 vs $^1/_T$ for the complete decomposition and log k_2 and log k_9 vs $^1/_T$ for the initial reaction are shown in FIGURE 25. The following activation energies were obtained:

(i) Complete decomposition:

Main decay period : 35.7 kcals. $mole^{-1}$.

(ii) Initial reaction:

Acceleratory period: 12.5 kcals. $mole^{-1}$.

Decay period: 11.9 kcals. $mole^{-1}$.

(vii) Percentage decomposition.

The percentage decomposition of mercuric oxalate preirradiated with γ-rays could not be determined since considerable radiolysis occurred during irradiation.

5.1.6. Superimposed Irradiations.

(i) Superimposed γ-ray and sunlight irradiations.

A thermal decomposition of mercuric oxalate which had been preirradiated for one hour followed by 35 min. preirradiation in sunlight was done. The results together with blank runs for singly irradiated salt are shown in TABLE 29. The initial reaction only was studied. The doubly irradiated material behaved as though it had been irradiated by sunlight only, in so far as the sigmoid portion was almost unchanged, although the rate of reaction after completion of the initial reaction was faster. This is illustrated in FIGURE 26. Pressures are not normalised.

TABLE 29/.....

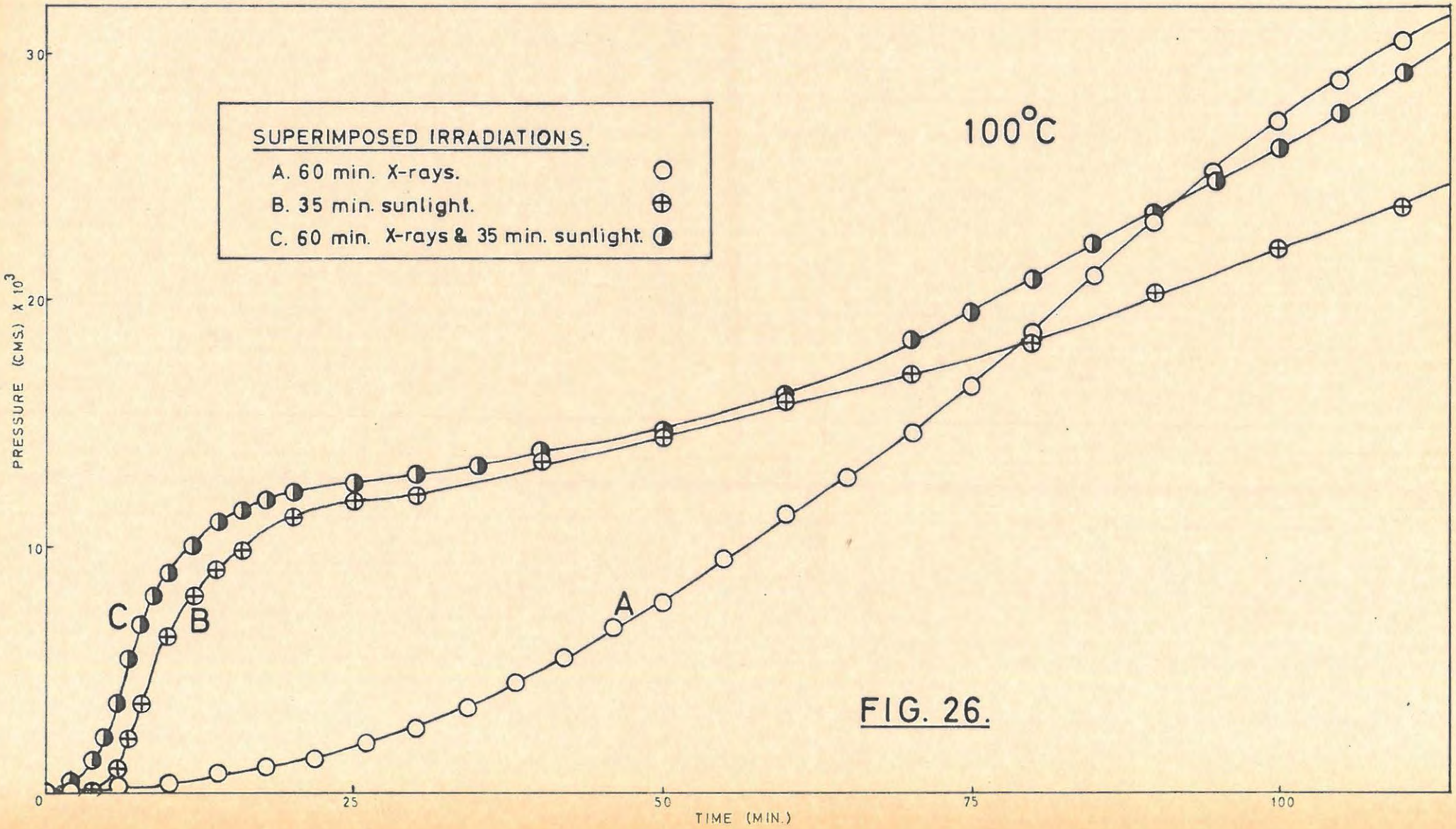
SUPERIMPOSED IRRADIATIONS.
A. 60 min. X-rays.
B. 35 min. sunlight.
C. 60 min. X-rays & 35 min. sunlight.
100°C
A
B
C
PRESSURE (CMS.) X 10³
TIME (MIN.)
0
10
20
30
25
50
75
100

FIG. 26.

TABLE 29

100°C 1 hr. X-rays. 35 min. sunlight. Run 1. 38.6 mg.					
t	p	t	p	t	p
1	0.27	16	11.52	90	23.41
2	0.78	18	11.87	95	24.90
3	0.93	20	12.22	100	26.18
4	1.24	25	12.58	105	27.76
5	2.16	30	12.94	110	29.39
6	3.71	35	13.33	115	30.75
7	5.43	40	13.49	120	32.20
8	6.80	50	14.63	125	33.95
9	8.05	60	16.02	130	35.44
10	8.93	70	18.35	140	38.20
11	9.55	75	19.43	150	40.76
12	10.02	80	20.79		
14	11.01	85	22.20		

100°C 35 min. sunlight. Run 2.					38.6 mg.
t	p	t	p	t	p
1	0.03	11	7.29	70	16.91
2	0.06	12	7.97	80	18.46
3	0.07	14	9.05	90	20.35
4	0.16	16	9.80	100	22.04
5	0.52	20	11.19	110	23.81
6	0.96	25	11.82	120	25.96
7	2.17	30	12.11	140	29.59
8	3.62	40	13.56	160	33.30
9	4.88	50	14.48	180	36.49
10	6.33	60	15.92		

100°C 1 hr. X-rays. Run 3.					37.4 mg.
t	p	t	p	t	p
2	0.07	30	2.57	70	14.66
4	0.13	32	3.00	75	16.50
6	0.19	34	3.47	80	18.67
8	0.27	36	3.96	85	20.97
10	0.39	38	4.39	90	23.16
12	0.52	40	5.07	95	25.18
14	0.69	42	5.54	100	27.33
16	0.82	44	6.04	105	28.97

TABLE 29 cont/.....

TABLE 29 cont.

t	p	t	p	t	p
18	0.97	46	6.69	110	30.66
20	1.18	48	7.24	115	31.82
22	1.42	50	7.81	120	33.59
24	1.67	55	9.48	130	36.04
26	1.94	60	11.31	140	38.24
28	2.25	65	12.75	160	42.52

5.1.7. Comparison of Irradiation Effects.

FIGURE 27 shows a comparison of the effect of sunlight, X-rays and γ-ray preirradiation on the initial reaction of the thermal decomposition of mercuric oxalate.

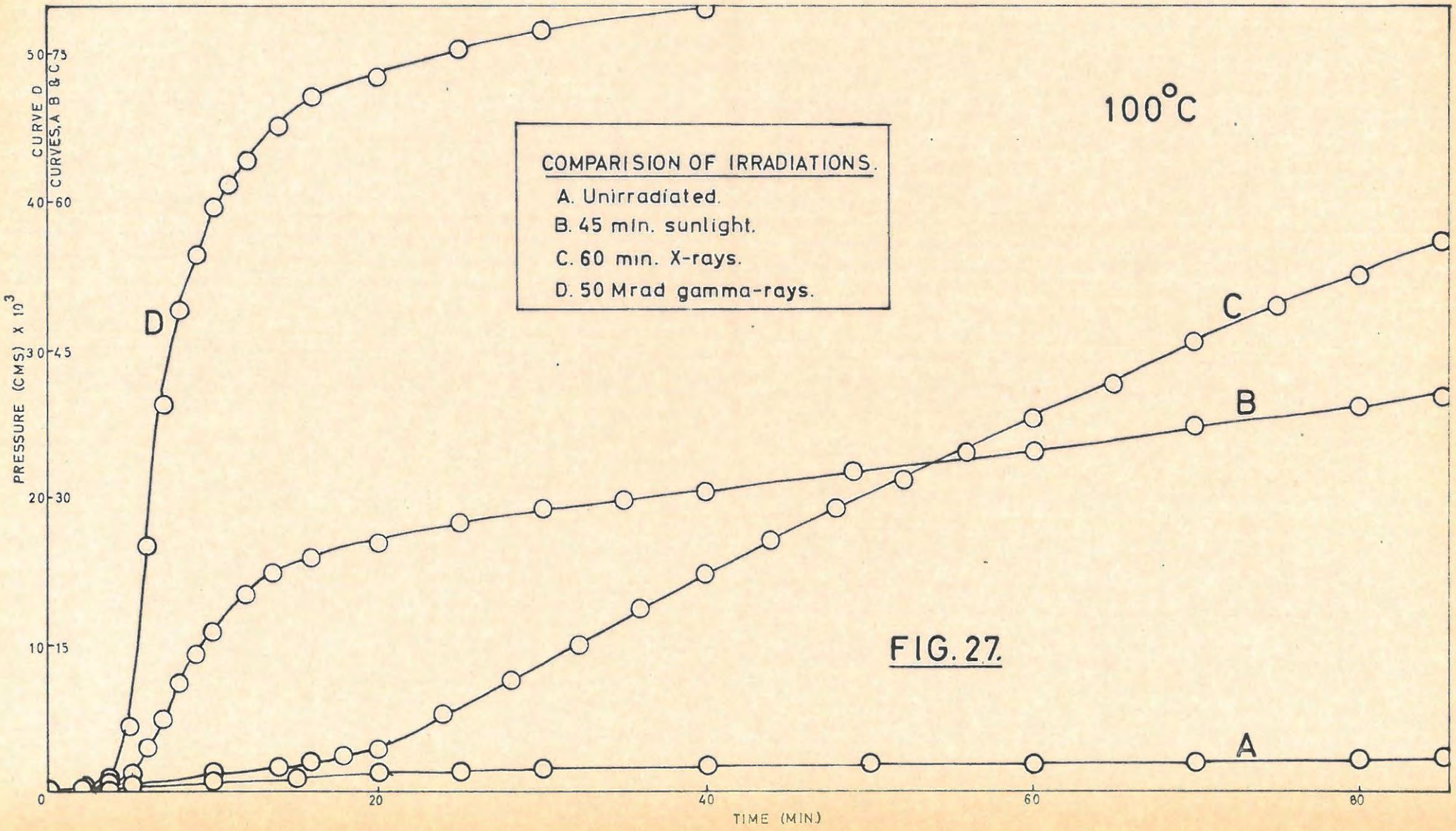
100°C
COMPARISION OF IRRADIATIONS.
A. Unirradiated.
B. 45 min. sunlight.
C. 60 min. X-rays.
D. 50 Mrad gamma-rays.
D
C
B
A
PRESSURE (CMS) X 10³
CURVE D
CURVES, A B & C
TIME (MIN.)
0
10
20
30
40
50
15
30
45
60
75
20
40
60
80

FIG. 27.

5.2. DISCUSSION.

5.2.1. Unirradiated Mercuric Oxalate.

The results obtained for the thermal decomposition of unirradiated mercuric oxalate confirm the earlier work of Prout and Tompkins,[12] except that a new chemical equation for the decomposition is proposed. The short acceleratory period is due to the two-dimensional growth of reaction centres, or nuclei, from many favourable sites on the surface of the particle. The reaction is confined to the surface during this stage, and there is no inward penetration of the reaction interface. There is a deceleratory region immediately after the inflexion point in the p/t plot where equation (2) does not apply; this must be the time during which the surface nuclei have touched and the decomposition comprises a contracting two-dimensional growth on the surface accompanied by the commencement of three-dimensional inward movement of the reaction interface. Once complete surface coverage is achieved the decomposition proceeds solely by the inward movement of the reaction interface and the decay period consists of the decomposition of approximately spherical particles by a contracting sphere mechanism.

The acceleratory and decay reactions are distinguished by different activation energies. The difference may be associated, during the decay period, with a process of activated gaseous diffusion which is absent during the acceleratory period when the reaction is confined to the surface of the particle.

5.2.2. Preirradiation by Sunlight.

The effect of preirradiation by sunlight is to create an "irradiation product" which forms and grows under the action of light from surface nuclei which may be located at emergent dislocations or steps on the crystal surface. The nature of the irradiation product and its mode of formation is, however,

uncertain and/.....

uncertain and it is considered that it is not possible to make any definite suggestion about these because of the unknown crystal structure of mercuric oxalate. The single molecule should be covalently bound. However, the salt may be composed of giant molecules where the bonds may possess a high degree of ionic character. It has been established that there is no measurable gas evolution during irradiation and it is suggested, as before[12], that there is an electron transference process to produce the unstable"irradiation product". An electron freed from a surface oxalate group could be trapped by a mercuric "ion", which would lead to the production of a lower-valent mercury compound which is identified as the "irradiation product", and which may be mercurous oxalate. Unfortunately, no information is available about the thermal decomposition of mercurous oxalate, in particular the activation energy of the decomposition is unknown. As the salt is darkened by exposure to sunlight, it is probable that mercury is produced during the change as well.

No activation energy was determined previously for the decomposition of this surface product. This decomposition was thus studied in greater detail by a series of low temperature runs. The fit of equations (1) and (4) for these p/t plots indicate the growth of two-dimensional reaction centres within the areas of the "irradiation product" on the surface during the acceleratory period, followed by decomposition in reaction centres which contract in a two-dimensional manner during the "decay" period. This latter process occurs when the initial reaction centres touch each other at the time corresponding to the inflexion point in the p/t plot (FIGURE 9). The activation energies for the acceleratory and "decay" periods are sufficiently close to suggest the same chemical reaction and have an average value of 12.0 kcals.mole^{-1}. At the end of the decomposition of the "irradiation product" the amount of reaction product will be greater than that resulting from the growth

of normal/.....

of normal reaction centres, and thus the product/reactant interface and consequently the rate of decomposition at this time should be greater than with the unirradiated salt. This is seen to be so in FIGURE 6. The activation energy for the decomposition after the initial reaction is 26.1 kcals.mole^{-1} which is approximately the same as for the acceleratory period of unirradiated material where reaction is confined, in the main, to the surface of the particle.

The fact that the decay region for a given temperature is practically unchanged after irradiation, except for a shift to shorter times, indicates the correctness of the original assumption that the acceleratory region in the decomposition of unirradiated material is confined to the external surfaces of the particles.

5.2.3. Preirradiation by X-rays.

The effect of preirradiation by X-rays appears to be an increase in the number of potential nuclei in the oxalate particle. This will occur on the surface and within the particle, e.g. at grain boundaries. The period of acceleration is reduced and the rate of acceleration is increased with increasing dose. This is shown in FIGURE 13 where there is a drop in the inflexion point with time of irradiation. The fit of equation (1) indicates, again, two dimensional growth of reaction centres from the nuclei. The fact that the activation energy for this process is approximately the same as that for the reaction during the corresponding period in the decomposition of the unirradiated material indicates the same chemical reaction in both cases. The fall in the inflexion point (α_i) is due to the fact that more nuclei are created. The reaction centres will thus touch earlier. If the nuclei are planar and grow two-dimensionally there should not be a drop in α_i as the irradiation dose increases. However, with only a few nuclei it is likely that they will not all touch at the same time. Consequently there/.....

sequently there will be a transition period before the decay proper begins and thus the α_i will not be a true one. This is the case for low irradiation doses. However, with a heavy dose, and hence a large number of nuclei, the transition period will shrink and a true inflexion point will be found which should be low for two-dimensional growth. If the additional nuclei are confined to the surface then the p/t plots for the decay reaction for the complete decomposition should be transferred to shorter times but otherwise be unchanged as compared to the unirradiated decay. This is not so (FIGURE 12). Thus it is concluded that after irradiation by X-rays internal nuclei are also formed. These will be formed in regions of stress in the particle such as grain boundaries.

Irradiation of X-ray irradiated material by light destroys the majority of the nuclei created on or very near the surface of the particle by X-rays since the sigmoid portions of the p/t plots for material preirradiated with sunlight only and with X-rays followed by sunlight, are almost identical (FIGURE 26 plots B and C). The increased rate of decomposition after the initial reaction with the doubly irradiated material, as compared to that irradiated by sunlight only, must be due to the additional reaction centres stemming from nuclei created within the particle by X-rays. This is further evidence for internal nucleation.

The fractional decomposition, α, at any time, t, calculated from the model of a contracting sphere[179] is given by

$$u/r = [1-(1-\alpha)^{1/3}]/t \qquad \ldots\ldots(12)$$

where u is the linear rate of penetration of the interface, which can be transformed to

$$dp/dt = 3kp_f/r(1-\frac{ut}{r})^2 \qquad \ldots\ldots(13)$$

where k is a velocity constant. The value of u is,

$$u = \frac{-Sr}{I} \qquad \ldots\ldots(14)$$

where I and S/.....

where I and S are the intercept and slope respectively, of the plot $(\frac{dp}{dt})^{1/2}$ vs t, which is a further expression for a contracting sphere. From the measured value of r for the spherical particle the value of u at 206°C for the decomposition of unirradiated salt is 1.010×10^{-8} cm. min^{-1}. Assuming this value for the rate of movement of the interface in the decay period for the decomposition of irradiated material, at the same temperature, the calculated value of r is 3×10^{-7} cm. Thus the decomposition in the acceleratory phase considerably reduces the particle size at the commencement of the decay reaction as compared to the size at the corresponding stage in the decomposition of unirradiated mercuric oxalate. This is expected since the acceleratory reaction occurs internally, possibly along grain boundaries, as well as on the surface of the particle, whereas with unirradiated material the acceleratory reaction is confined to the surface of the original particle.

The nature of the nuclei created by X-rays is uncertain, but they may be aggregates of vacancies created from dislocations. Esterman et alia, in a study of the effect of X-ray bombardment of potassium chloride concluded that vacancies were produced in the crystal by the X-rays. It has been suggested[180] that these may be vacancies which have been "boiled off" from jogs in dislocations by electrons generated by the X-rays which, in passing near these regions, supply sufficient local heating to free the vacancies. A similar mechanism may operate here and the vacancies produced may aggregate to produce centres around which the activation energy for decomposition of mercuric oxalate would be lowered.

5.2.4. Preirradiation by γ-rays.

During preirradiation by γ-rays damage will occur throughout the solid, although it is most likely to be at discontinuities in the crystal structure such as dislocations and grain boundaries. The effect of γ-rays will be the internal

bombardment of/.....

bombardment by electrons of widely varying energy. The pre-irradiation by γ-rays, unlike light and X-ray irradiation, is accompanied by a measurable decomposition of mercuric oxalate with the evolution of gaseous product(s). The difference in the final pressures for the decomposition of equal masses of unirradiated and irradiated salt (weighed before irradiation) may be as high as 48% (dose 50 Mrad) of the final pressure for the unirradiated salt. The loss of mass is directly proportional to the drop in the final pressure indicating that the nature of the radiolysis is independent of dose.

In addition to the radiolysis an "irradiation product" is formed which decomposes on heating. The decomposition was studied in detail at low temperatures. The "irradiation product" does not appear to be the product of radiolysis only, since the same relationship which exists between the dose and Δp_f does not hold between dose and p_f'. It is probable that the "irradiation product" is similar to that produced by the action of light since the average activation energy associated with the acceleratory and "decay" portions of the initial reaction is very close to the corresponding value for light irradiated salt, (12.2 and 12.0 kcals.mole^{-1} respectively).

The analysis of the initial reaction on heating (FIGURE 24) indicates that the acceleratory reaction occurs through a branching chain mechanism.[25] In the analysis of the mechanism of decomposition of silver oxalate[27] it was proposed that chain branching is facilitated by the presence of dislocations in the crystal. It is considered for mercuric oxalate that the initial acceleratory reaction occurs internally in the particle of mercuric oxalate through decomposition by a branching chain mechanism, of the irradiation product formed along dislocations. The "decay" reaction obeys the unimolecular law and would indicate the decomposition of "irradiation product" not favourably placed for chain branching.

The initial/.....

The initial decomposition of the "irradiation product" on heating constitutes as much as 22% (dose 50 Mrad) of the total gas evolved in the complete thermal decomposition of mercuric oxalate. Thus, at the commencement of the main decay reaction, a particle of the solid will contain in addition to the undecomposed mercuric oxalate, the products of radiolysis and of the thermal decomposition of the "irradiation product". Therefore it is not surprising that the activation energy for decomposition during this period is different from that for the corresponding period with unirradiated mercuric oxalate. The decomposition follows the unimolecular decay law.

5.2.5. General Observations.

The nature of the influence exerted by two of the types of radiation as compared to the third is essentially different. The action of sunlight is limited to the surface layer only and irradiation is effective in the initial stage of reaction i.e. only the period of acceleration is changed. The action of X-rays and γ-rays, however, results in the formation of active centres not only on the surface but also in the interior of the crystal, and so affects not only the initial stage but also the further course of the thermal decomposition.

The applicability of equation (1) to the acceleratory period of unirradiated and X-ray irradiated specimens suggests that the growth of the decomposition nuclei is similar in both cases. In addition, the agreement between the activation energies over this period indicates the same chemical reaction stemming from the nuclei. In a very insoluble salt, formed by rapid precipitation, a highly irregular form of particle will be produced and the surface will be pitted and stepped. Such regions will be centres around which deformation of the crystal structure will occur and decomposition will be favoured. It has been suggested that during X-ray irradiation aggregates of vacancies are formed in the crystal and on or very near the

surface, and/.....

surface, and these will produce similar regions of stress at which reaction will be favoured.

It is not clear why the "irradiation product" should be formed with sunlight and γ-rays, and that the salt should darken, whereas neither of these effects is detectable with X-ray irradiation. During γ-ray irradiation the salt will be internally bombarded with electrons varying from very slow to very fast and it is possible that a large number of these will have, or at some stage be slowed down to, an energy equal to that required for the production of the "irradiation product". Electrons will also be present during X-ray bombardment and there may be a similar production of radiation product, but with the irradiation doses used the amount may have been insignificant.

6. THE THERMAL DECOMPOSITION OF BARIUM AZIDE.

6.1. RESULTS.

6.1.1. Preparation.

Barium azide (L. Light and Co.) was recrystallized several times from high purity conductance water. During crystallization the solution was maintained acid (phenolphtholien) by the dropwise addition of 3% hydrazoic acid. Small crystals of the monohydrate $Ba(N_3)_2 . H_2O$ were obtained. These were dehydrated in a vacuum dessicator over P_2O_5 with continuous pumping for 48 hours. The barium azide thus obtained was finely ground in a WIG-L-BUG for 15 minutes. Nylon grinding balls were used. The powder was stored in vacuo over P_2O_5 in a darkened dessicator.

A second preparation (Prep. II) was later prepared in the same manner but with 5 minutes grinding. This preparation was used in studies on the effect of ultra-violet light on the thermal decomposition.

6.1.2. Unirradiated Barium Azide.

(i) Reproducibility.

Approximately 6.5 mg. of material was used in each run. Three runs at 125°C were done to check the reproducibility of the results. These are shown in TABLE 30 and FIGURE 28. Reproducibility was of a high order. The induction period was 58 min. in each case. Rate constants, k_3 and k_7 (equations 8 and 2) for the acceleratory and decay periods, respectively, were as follows:

(i) Acceleratory period: 1.30, 1.34 and 1.35 x 10^{-2} $min.^{-1}$ respectively.

(ii) Decay period: 9.45, 9.32 and 9.48 x 10^{-2} $min.^{-1}$ respectively.

TABLE 30/.....

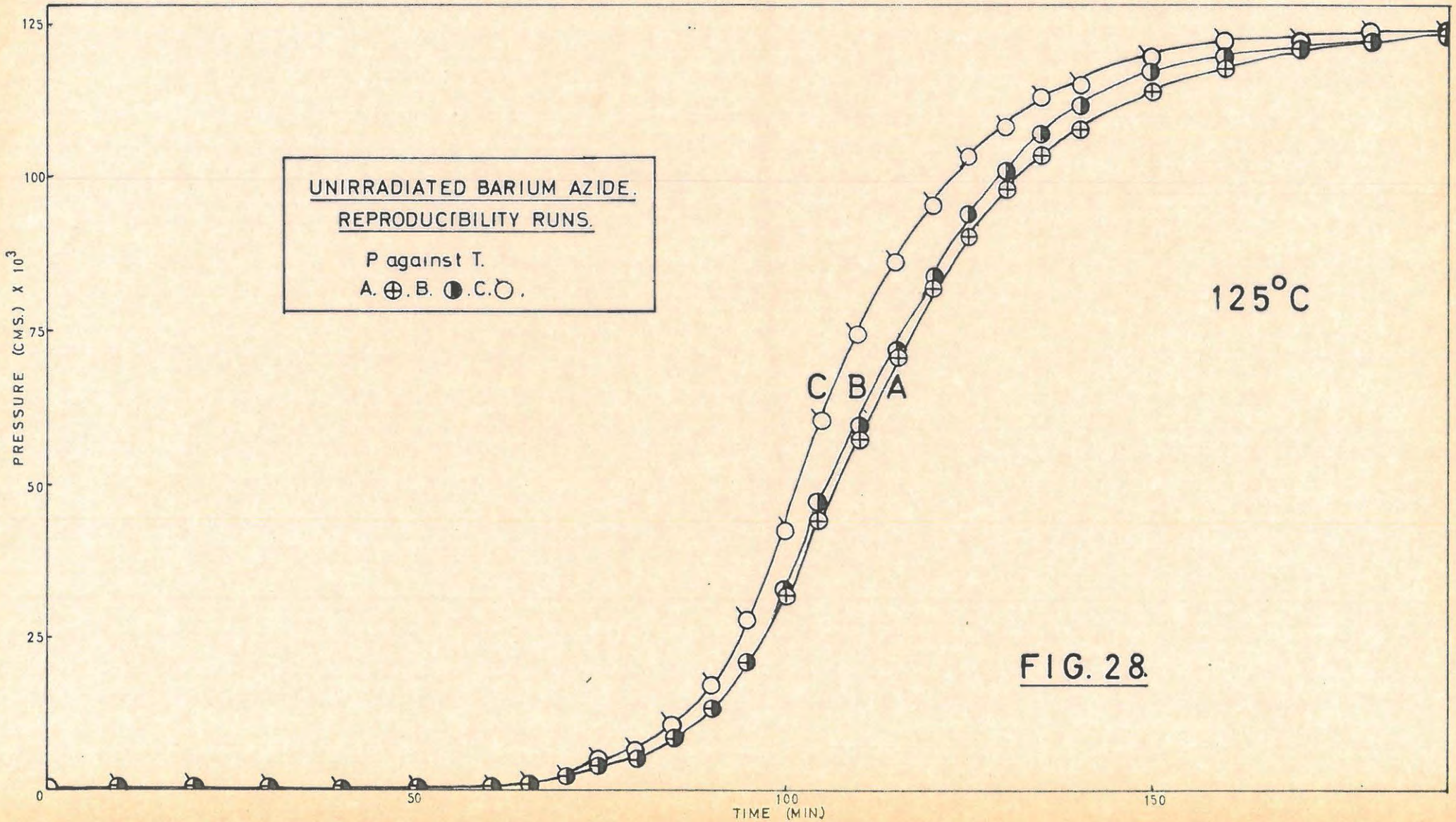
UNIRRADIATED BARIUM AZIDE.
REPRODUCIBILITY RUNS.
P against T.
A. ⊕. B. ◑. C. ○.
125°C
C
B
A
PRESSURE (CMS.) X 10³
TIME (MIN.)
0
25
50
75
100
125
50
100
150

FIG. 28.

TABLE 30.

125°C	Run 1.				6.6 mg.
t	p	t	p	t	p
10	0.04	80	6.11	130	101.93
20	0.07	85	9.14	135	107.31
30	0.10	90	13.74	140	111.71
40	0.15	95	21.41	150	117.34
50	0.33	100	32.55	160	120.20
55	0.54	105	43.90	170	121.94
60	1.00	110	57.34	200	125.45
65	1.59	115	71.23	220	126.63
70	2.49	120	84.19	p_f	127.20
75	3.79	125	94.16	p_a	123.21

125°C	Run 2.				6.3 mg.
t	p	t	p	t	p
10	0.03	80	6.58	130	108.59
20	0.03	85	10.98	140	115.89
30	0.04	90	17.38	150	120.03
40	0.09	95	27.99	160	122.39
50	0.26	100	42.51	180	123.57
55	0.48	105	61.30	200	124.76
60	0.92	110	74.04	220	125.95
65	1.58	115	86.31	250	126.57
70	2.57	120	95.65	p_f	127.20
75	4.13	125	103.11	p_a	119.23

125°C	Run 3.				6.4 mg.
t	p	t	p	t	p
10	0.11	85	8.43	140	108.05
20	0.15	90	13.11	150	114.46
30	0.19	95	21.57	160	118.64
40	0.27	100	33.06	170	121.06
50	0.44	105	47.00	180	122.89
55	0.68	110	59.29	200	125.36
60	0.99	115	71.56	220	126.60
65	1.48	120	81.72	p_f	127.20
70	2.31	125	90.44	p_a	122.41
75	3.53	130	97.95		
80	5.52	135	103.50		

(ii) Effect of/.....

(ii) Effect of interrupting a decomposition.

The effect of interrupting a decomposition, allowing the sample to cool, and then continuing the run after one hour, was studied at 120°C. During interruption the salt was kept in vacuo at 25°C and the run was recommenced at the same temperature as before. Interruptions were done at six stages in the decomposition viz. half way along the induction period, at the end of the induction period and at α =0.07, 0.30, 0.51 and 0.71. A pressure of approximately 0.60 x 10^{-3} cm.Hg, was taken as representing the end of the induction period. Apart from a small heating lag there was no effect. The results appear in TABLE 31.

TABLE 31.

120°C Uninterrupted blank. Run 1.					6.9 mg.
t	p	t	p	t	p
20	0.10	105	10.36	155	109.51
40	0.15	110	16.24	160	113.99
60	0.20	115	24.72	165	117.36
70	0.33	120	35.28	170	120.21
75	0.50	125	48.45	175	121.37
80	0.79	130	62.04	180	122.52
85	1.27	135	74.57	190	124.27
90	2.22	140	86.29	210	126.27
95	3.75	145	94.90	p_f	127.20
100	6.44	150	103.53	p_a	124.37

120°C			Run 2.		6.6 mg.
t	p	t	p	t	p
20	0.06	100	4.44	155	108.36
35	0.07	105	7.29	160	114.00
Interrupted		110	11.92	165	117.31
50	0.07	115	18.45	170	120.19
60	0.08	120	26.96	180	123.09
70	0.13	125	38.03	190	124.86
75	0.25	130	51.76	200	126.04
80	0.43	135	66.74	210	126.63
85	0.80	140	80.28	p_f	127.20
90	1.47	145	91.51	p_a	118.45
95	2.58	150	101.34		

TABLE 31 cont/.....

TABLE 31 cont.

120°C		Run 3.			6.7 mg.
t	p	t	p	t	p
20	0.06	95	3.69	150	108.82
40	0.08	100	6.44	155	114.24
50	0.12	105	10.60	160	118.17
60	0.29	110	16.41	165	119.79
65	0.41	115	24.47	170	121.48
70	0.67	120	35.97	180	123.75
Interrupted		125	49.32	190	125.47
75	0.68	130	63.96	200	126.62
80	0.73	135	78.65	p_f	127.20
85	0.80	140	91.90	p_a	126.66
90	1.92	145	101.47		

120°C		Run 4.			6.7 mg.
t	p	t	p	t	p
20	0.08	105	8.70	145	92.12
40	0.09	Interrupted		150	102.12
60	0.11	110	8.73	155	109.27
70	0.17	115	11.20	160	115.31
80	0.48	120	24.59	170	121.53
85	0.92	125	34.17	180	124.35
90	1.67	130	49.66	200	126.49
95	3.00	135	64.78	p_f	127.20
100	5.18	140	80.58	p_a	121.46

120°C		Run 5.			6.8 mg.
t	p	t	p	t	p
20	0.04	Interrupted		190	117.52
40	0.06	125	41.22	200	121.12
60	0.17	130	58.67	210	123.56
80	0.72	135	75.17	220	125.41
90	2.22	140	86.41	230	126.66
100	7.84	145	95.08	p_f	127.20
110	14.08	150	101.26	p_a	126.40
115	25.21	160	108.87		
120	38.66	170	114.86		

TABLE 31 cont/.....

TABLE 31 cont.

120°C		Run 6.			6.4 mg.
t	p	t	p	t	p
20	0.21	115	5.92	165	72.11
40	0.25	120	9.01	170	83.42
60	0.39	125	13.56	175	92.87
70	0.45	130	19.35	180	100.10
80	0.52	135	26.51	190	110.40
85	0.64	140	34.50	200	117.00
90	0.82	145	43.53	210	120.97
95	1.07	150	53.62	220	124.33
100	1.61	155	64.34	240	126.67
105	2.41	Interrupted		p_f	127.20
110	3.87	160	65.10	p_a	122.64

120°C		Run 7.			6.4 mg.
t	p	t	p	t	p
20	0.05	125	20.65	175	96.30
40	0.07	130	28.20	180	102.30
60	0.10	135	37.28	185	107.12
70	0.20	140	47.23	190	110.93
80	0.55	145	57.71	200	115.54
90	1.10	150	67.36	210	119.32
100	2.53	155	76.51	230	123.84
105	3.95	160	84.66	240	125.74
110	6.25	165	91.05	250	126.71
115	9.41	Interrupted		p_f	127.20
120	14.27	170	91.79	p_a	122.53

(iii) Effect of admitting water vapour onto the salt in an interrupted decomposition.

These are termed "water interruptions". The technique has been described in detail earlier. At the point of interruption the line was pumped hard and water vapour (17.0 mm. pressure) was admitted onto the sample at room temperature for ten minutes and then pumped off. The run was then continued after pumping for one hour. The decomposition temperature was 124°C in all cases. Interruptions along the induction period and in the acceleratory period resulted in

the apparent/.....

the apparent return of the decomposition reaction to zero time. A new induction period was produced followed by acceleratory and decay periods. The rate constants were, however, reduced in magnitude. Interruption at the inflexion point or beyond destroyed any further decomposition.

Interruption at the end of the induction period resulted in a new induction period. A second interruption at the end of this induction period caused yet another new induction period. The procedure could be repeated as often as desired with the same result. However, on allowing the reaction to proceed $\frac{1}{6}$ after interruptions the acceleration of the reaction is very slow.

The final pressures obtained after "water interruptions" were considerably lower than normal. The lost gas could, however, be completely recovered by heating at 300°C in vacuo.

The results are tabulated in TABLE 32 and shown graphically in FIGURE 29. TABLE 33 gives the rate constants, k_3, (equation 8) which were obtained, and the lengths of the induction periods. Pressures are not normalised.

TABLE 32.

124°C	Run 1.				6.5 mg.
t	p	t	p	t	p
20	0.30	120	1.74	210	66.40
35	0.39	130	3.48	220	75.97
Water Interruption		140	6.31	230	82.45
50	0.40	150	11.01	240	87.68
60	0.41	160	17.52	250	90.14
70	0.42	170	25.06	260	92.06
90	0.48	180	33.98	270	93.22
100	0.60	190	44.26	p_a	93.73
110	0.99	200	55.92		

TABLE 32 cont/.....

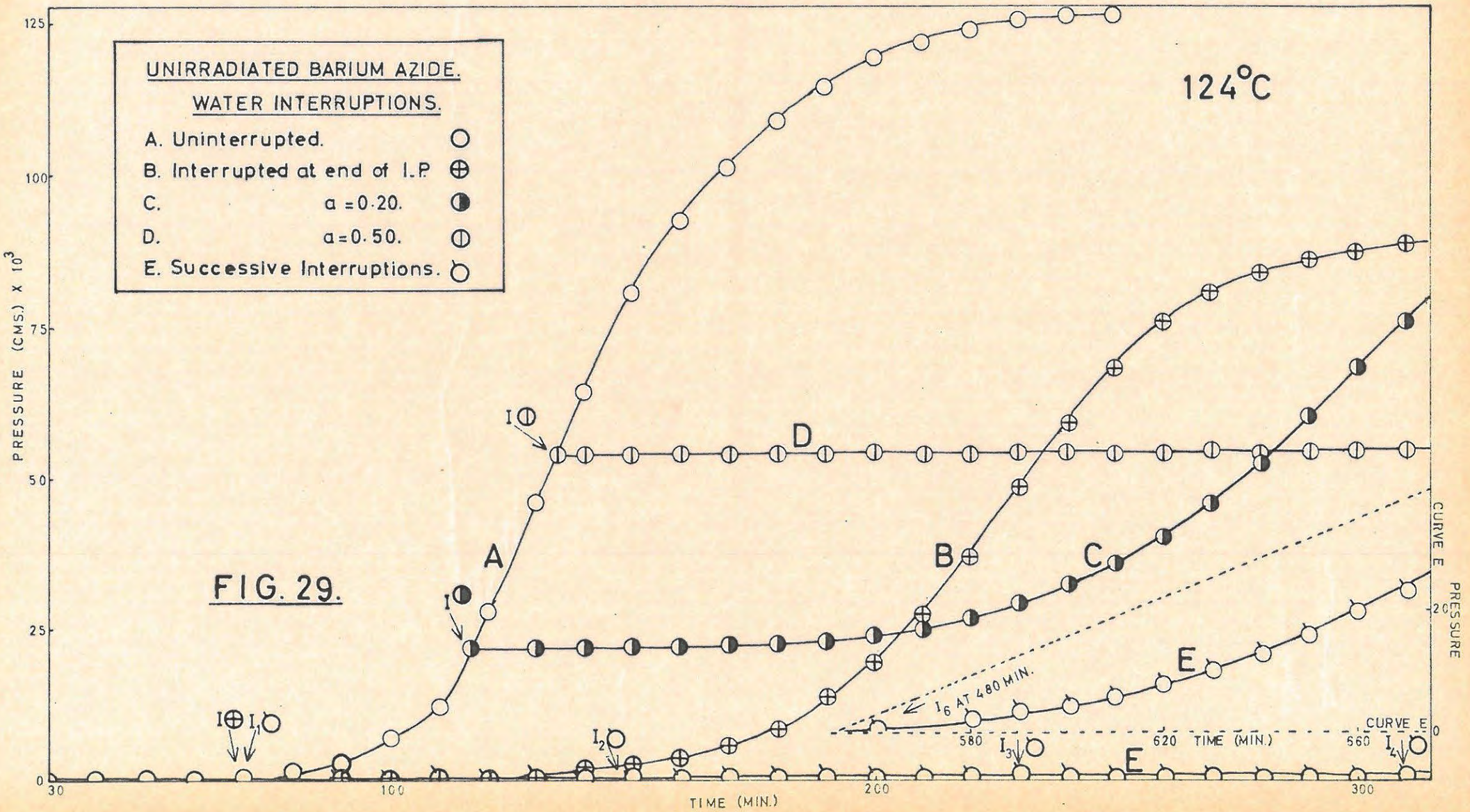
UNIRRADIATED BARIUM AZIDE.
WATER INTERRUPTIONS.
A. Uninterrupted.
B. Interrupted at end of I.P.
C. a = 0·20.
D. a = 0·50.
E. Successive Interruptions.
124°C
PRESSURE (CMS.) X 10³
TIME (MIN.)
CURVE E
PRESSURE
I₆ AT 480 MIN.
620 TIME (MIN.)
A
B
C
D
E

FIG. 29.

TABLE 32 cont.

124°C		Run 2.			6,6 mg.
t	p	t	p	t	p
20	0,07	130	0,93	230	48,69
40	0,11	140	1,29	240	59,00
60	0,39	150	2,02	250	68,25
70	0,61	160	3,52	260	75,41
Water Interruption		170	5,55	270	80,66
80	0,61	180	8,70	280	83,74
90	0,62	190	13,35	290	86,04
100	0,65	200	19,05	300	87,92
110	0,67	210	27,38	320	89,06
120	0,73	220	37,26	p_a	90,40

124°C		Run 3.			6,2 mg.
t	p	t	p	t	p
20	0,14	160	21,91	290	60,58
40	0,28	170	22,14	300	68,71
60	0,38	180	22,47	310	76,07
80	1,54	190	23,11	320	82,35
90	3,67	200	24,10	330	87,70
100	8,10	210	25,36	340	91,97
110	14,86	220	27,11	350	94,61
117	21,69	230	29,21	360	96,83
Water Interruption		240	31,99	370	98,63
120	21,72	250	35,19	380	100,00
130	21,73	260	39,70	390	100,92
145,	21,75	270	45,61	p_a	101,38
150	21,79	280	52,64		

124°C		Run 4.			6,3 mg
t	p	t	p	t	p
20	0,09	130	24,17	220	54,81
40	0,35	140	34,20	240	54,86
60	0,56	150	44,22	260	54,93
80	0,87	160	54,76	280	55,03
90	2,17	Water Interruption		300	55,65
100	4,72	170	54,77	320	55,36
110	9,16	180	54,77	340	55,49
120	15,06	200	54,79	p_a	55,59

TABLE 32 cont/.....

TABLE 32 cont.

124°C		Run 5.			6.3 mg.
t	p	t	p	t	p
20	0.10	290	0.83	610	5.46
40	0.14	300	0.85	620	7.55
60	0.21	310	0.94	630	10.09
70	0.45	Water Interruption		640	12.87
Water Interruption		360	1.00	650	16.05
100	0.46	380	1.01	660	19.39
120	0.48	390	1.01	670	23.08
130	0.50	400	1.12	680	27.10
140	0.52	Water Interruption		700	36.47
150	0.54	450	1.14	720	47.34
Water Interruption		480	1.38	740	57.30
180	0.56	Water Interruption		760	65.72
210	0.61	540	1.45	780	71.18
220	0.68	560	1.71	800	75.18
230	0.77	580	2.29	840	81.07
Water Interruption		590	2.93	880	84.14
280	0.81	600	3.96	p_a	87.19

TABLE 33.

Point of Interruption.	k_3 min.$^{-1}$	Induction Period min.	Number of Interruptions.	Induction Period min.
Uninterrupted	1.59×10^{-2}	70	0	70
$\frac{1}{2}$ along Induction P.	6.35×10^{-3}	75	1	80
End of Induction P.	6.25×10^{-3}	70	2	80
$\alpha = 0.20$	5.20×10^{-3}	63	3	80
$\alpha = 0.50$	No reaction	No reaction.	4	90
6 consecutive	3.60×10^{-3}	80	5	80
			6	80

(iv) Effect of varying the temperature of decomposition.

To obtain the critical increment of the process(es) occurring, decompositions were done over a range of temperatures (110° - 140°C) and the rate constants determined at each temperature. These runs are listed in TABLE 34 while the rate constants, k_3 and k_7 (equations 8 and 2) obtained appear in TABLE 35.

TABLE 34/.....

TABLE 34.

110°C	Run 1.				6.2 mg.
t	p	t	p	t	p
30	0.04	270	4.15	400	77.84
60	0.09	280	5.50	410	84.89
90	0.15	290	7.80	420	92.24
120	0.17	300	11.04	430	98.79
140	0.20	305	12.97	440	103.85
160	0.25	310	15.28	450	107.87
180	0.38	315	17.54	460	111.97
190	0.45	320	19.96	480	117.35
200	0.56	330	25.23	500	122.24
210	0.75	340	31.49	520	124.10
220	0.95	350	38.73	540	125.34
230	1.25	360	46.41	p_f	127.20
240	1.65	370	53.92	p_a	118.10
250	2.19	380	61.99		
260	2.90	390	70.11		

115°C	Run 2.				6.0 mg.
t	p	t	p	t	p
30	0.07	190	11.16	260	72.23
60	0.14	195	14.00	265	76.84
80	0.18	200	17.16	270	81.12
100	0.23	205	20.64	275	85.51
110	0.29	210	24.44	280	89.51
120	0.41	215	28.57	290	97.25
130	0.60	220	32.71	300	104.23
140	0.93	225	37.13	310	109.75
150	1.39	230	41.83	320	114.28
160	2.24	235	46.81	340	120.07
170	3.91	240	52.07	360	123.01
175	5.28	245	57.20	380	124.80
180	6.86	250	62.16	p_f	127.20
185	8.80	255	67.32	p_a	116.76

120°C	Run 3.				5.9 mg.
t	p	t	p	t	p
30	0.07	135	10.09	195	93.90
60	0.16	140	13.54	200	100.16
80	0.28	145	18.17	205	105.53

TABLE 34 cont/.....

TABLE 34 cont.

t	p	t	p	t	p
90	0.44	150	23.73	210	109.93
95	0.59	155	29.75	220	116.12
100	0.86	160	37.08	230	119.57
105	1.24	165	44.87	240	121.90
110	1.75	170	53.01	260	123.66
115	2.52	175	61.42	280	126.02
120	3.63	180	70.00	p_f	127.20
125	5.18	185	78.20	p_a	116.76
130	7.29	190	86.36		

125°C	Run 4.			6.2 mg.	
t	p	t	p	t	p
10	0.03	70	1.27	120	89.95
20	0.07	75	2.17	125	102.13
30	0.10	80	4.05	130	110.86
35	0.12	85	7.61	135	116.57
40	0.14	90	12.12	140	120.65
45	0.14	95	20.26	150	124.21
50	0.14	100	31.36	160	126.00
55	0.21	105	44.86	170	126.61
60	0.29	110	59.53	p_f	127.20
65	0.73	115	74.88	p_a	121.50

130°C	Run 5.			6.1 mg.	
t	p	t	p	t	p
10	0.04	58	16.23	80	90.27
20	0.15	60	21.01	85	105.65
30	0.25	62	26.13	90	114.99
35	0.48	64	32.12	95	120.41
40	1.06	66	38.03	100	123.48
43	1.78	68	45.20	110	125.34
45	2.33	70	52.98	120	126.59
48	3.78	72	60.94	p_f	127.20
50	5.32	74	68.99	p_a	122.64
53	8.03	76	76.58		
55	11.30	78	85.53		

TABLE 34 cont/.....

TABLE 34 cont.

135°C		Run 6.			6.0 mg.
t	p	t	p	t	p
5	0.05	42	18.04	64	104.68
10	0.08	44	24.64	66	109.82
15	0.11	46	32.27	70	116.86
20	0.13	48	40.93	75	121.62
25	0.37	50	49.84	80	124.13
30	1.47	52	58.77	90	125.98
32	2.22	54	67.54	100	126.60
34	2.73	56	76.42	p_f	127.20
36	5.89	58	85.35	p_a	122.07
38	8.87	60	93.16		
40	12.85	62	99.11		

140°C		Run 7.			6.3 mg.
t	p	t	p	t	p
10	0.07	28	48.79	45	122.98
15	0.36	30	65.60	50	124.79
18	1.85	32	81.43	60	126.62
20	4.27	34	94.68	p_f	127.20
22	9.60	36	105.00	p_a	124.94
24	18.91	38	112.36		
26	32.58	40	117.61		

TABLE 35.

Temperature °C	Induction Period min.	k_3 min.$^{-1}$	k_7 min.$^{-1}$
110°	180	3.599×10^{-3}	4.00×10^{-3}
115°	120	4.980×10^{-3}	5.10×10^{-3}
120°	90	7.440×10^{-3}	8.15×10^{-3}
125°	60	1.285×10^{-2}	1.40×10^{-2}
130°	37	1.660×10^{-2}	1.91×10^{-2}
135°	25	2.250×10^{-2}	2.26×10^{-2}
140°	15	4.125×10^{-2}	3.85×10^{-2}

(v) Effect of mixing barium azide with the solid end product (Ba).

The mixing was done by decomposing a sample of barium azide and adding to it some fresh sample. The two were mixed

together as/.....

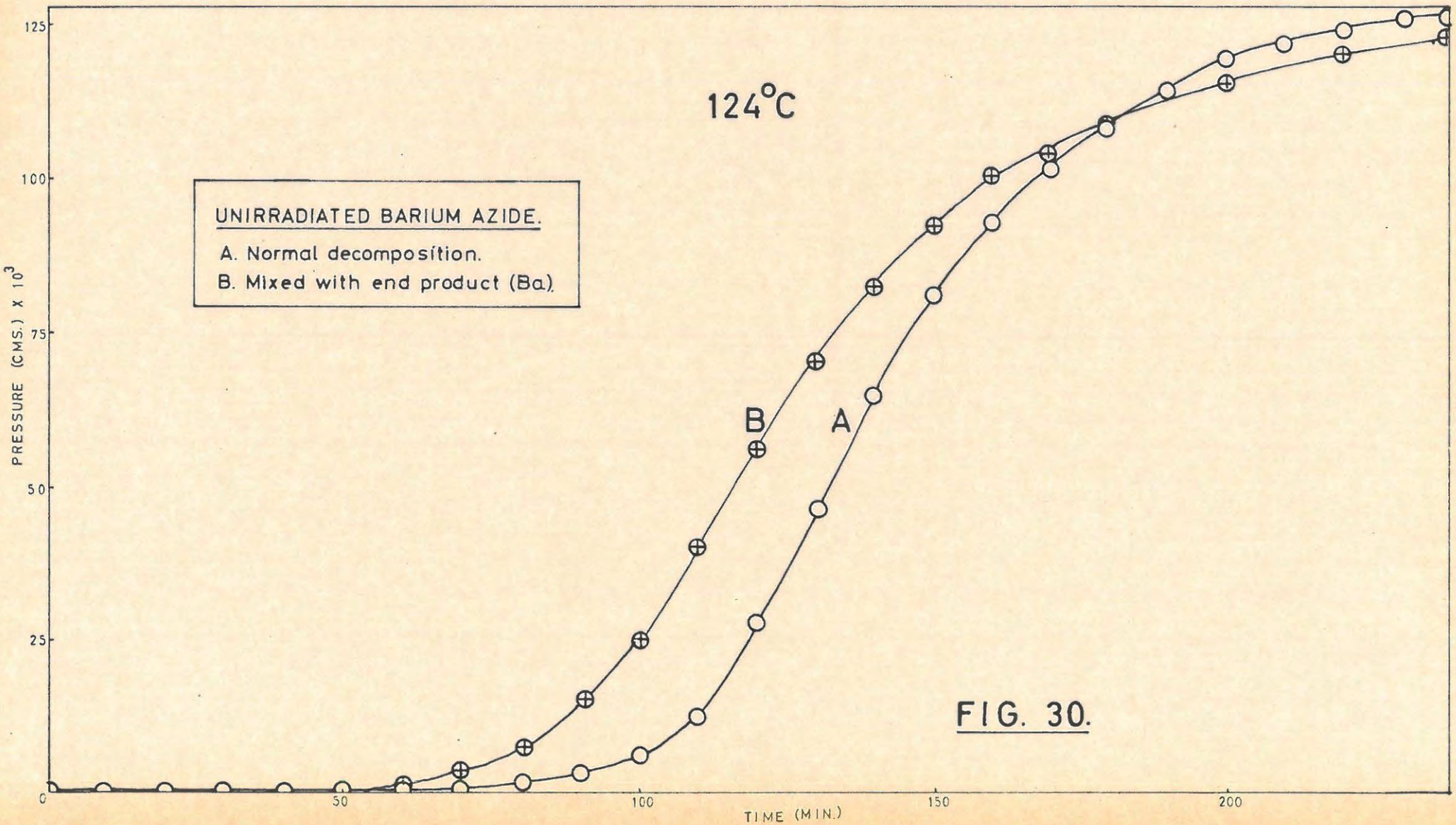
124°C
UNIRRADIATED BARIUM AZIDE.
A. Normal decomposition.
B. Mixed with end product (Ba).
B
A
PRESSURE (CMS.) X 10³
TIME (MIN.)
0
25
50
75
100
125
50
100
150
200

FIG. 30.

together as well as possible in an atmosphere of dry nitrogen. The resulting mixture was then decomposed at a temperature of 124°C. The induction period appeared to terminate a little earlier than usual, but otherwise no effect was obtained. TABLE 36 and FIGURE 30 illustrate the results.

TABLE 36.

124°C Blank run.		Run 1.			6.7 mg.
t	p	t	p	t	p
10	0.04	100	6.97	190	114.75
20	0.06	110	12.25	200	119.23
30	0.08	120	27.86	210	122.64
40	0.10	130	45.96	220	124.94
50	0.13	140	64.75	230	126.10
60	0.19	150	80.61	p_f	127.20
70	0.52	160	92.65	p_a	127.21
80	1.18	170	101.83		
90	2.92	180	109.21		

124°C Mixture		Run 2.			6.5 mg.
t	p	t	p	t	p
10	0.19	90	15.45	170	103.93
20	0.32	100	25.98	180	108.39
30	0.43	110	40.59	200	115.27
40	0.61	120	56.00	220	120.57
50	1.00	130	70.19	240	123.57
60	3.20	140	82.01	260	125.38
70	5.30	150	92.12	p_f	127.20
80	7.95	160	99.55	p_a	115.86

(vi) Decomposition along the induction period.

As is shown in FIGURE 28 apparently no gas is evolved during the induction period. It was considered (see Discussion) that some nitrogen may be produced during this time. A more detailed investigation into the nature of the induction period was thus carried out.

It was possible that with the apparatus used and the small

amount of/.....

amount of azide, that any gas evolved during the induction period might not be detected. Consequently a decomposition was performed using 500 x the normal weight of barium azide. Decomposition was only followed to the onset of the accelera-tory period. No gas was evolved during the induction period. This is shown in FIGURE 31 and TABLE 37. The temperature of decomposition was 110°C.

TABLE 37.

110°C		Run 1.			3.089 g.
t	p	t	p	t	p
5	0.01	60	0.02	115	0.49
10	0.01	65	0.02	120	1.00
15	0.01	70	0.02	125	1.54
20	0.01	75	0.04	130	2.74
25	0.01	80	0.04	135	4.72
30	0.01	85	0.04	140	8.10
35	0.01	90	0.04	145	13.12
40	0.01	95	0.06	150	22.18
45	0.02	100	0.10	155	31.53
50	0.02	105	0.17	160	61.87
55	0.02	110	0.27	165	102.88

It is possible that all of the nitrogen which may be pro-duced could be adsorbed on the azide surface, remembering that the salt is a very fine powder. Therefore a large weight (3.0 g) of barium azide was placed in the decomposition chamber at 110°C. The line was pumped hard and then dry nitrogen at a pressure of 3.7×10^{-2} cm. Hg was admitted onto the salt. The change in gas pressure was then recorded over a period of one hour after which time the pressure had dropped to a value of 2.0×10^{-2} cm.Hg. This result is shown in TABLE 38 and FIGURE 32. The volume of nitrogen was 1.8 litres.

TABLE 38/.....

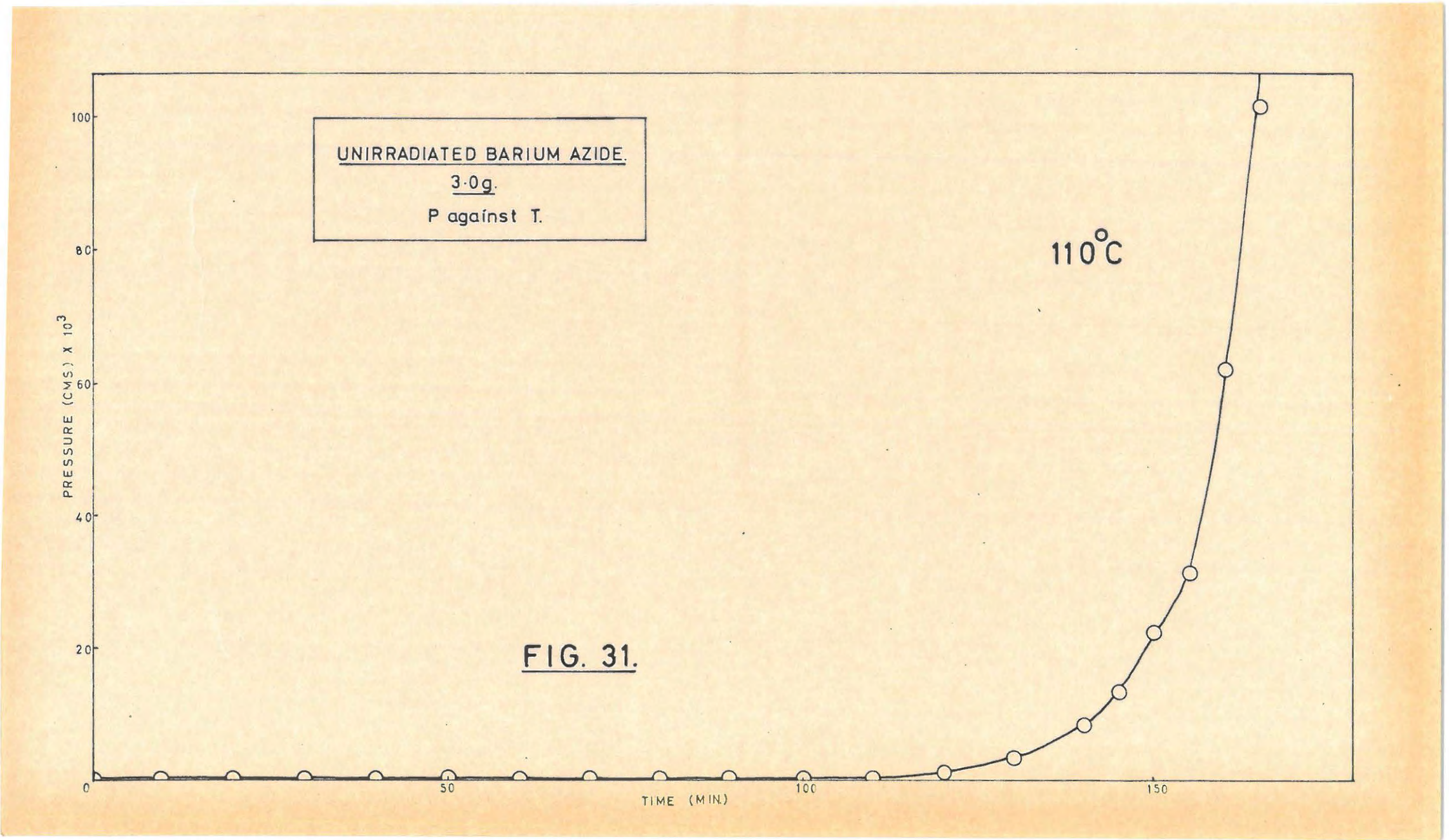
UNIRRADIATED BARIUM AZIDE.
3·0g.
P against T.
110°C
PRESSURE (CMS) X 10³
TIME (MIN.)
0
20
40
60
80
100
50
100
150

FIG. 31.

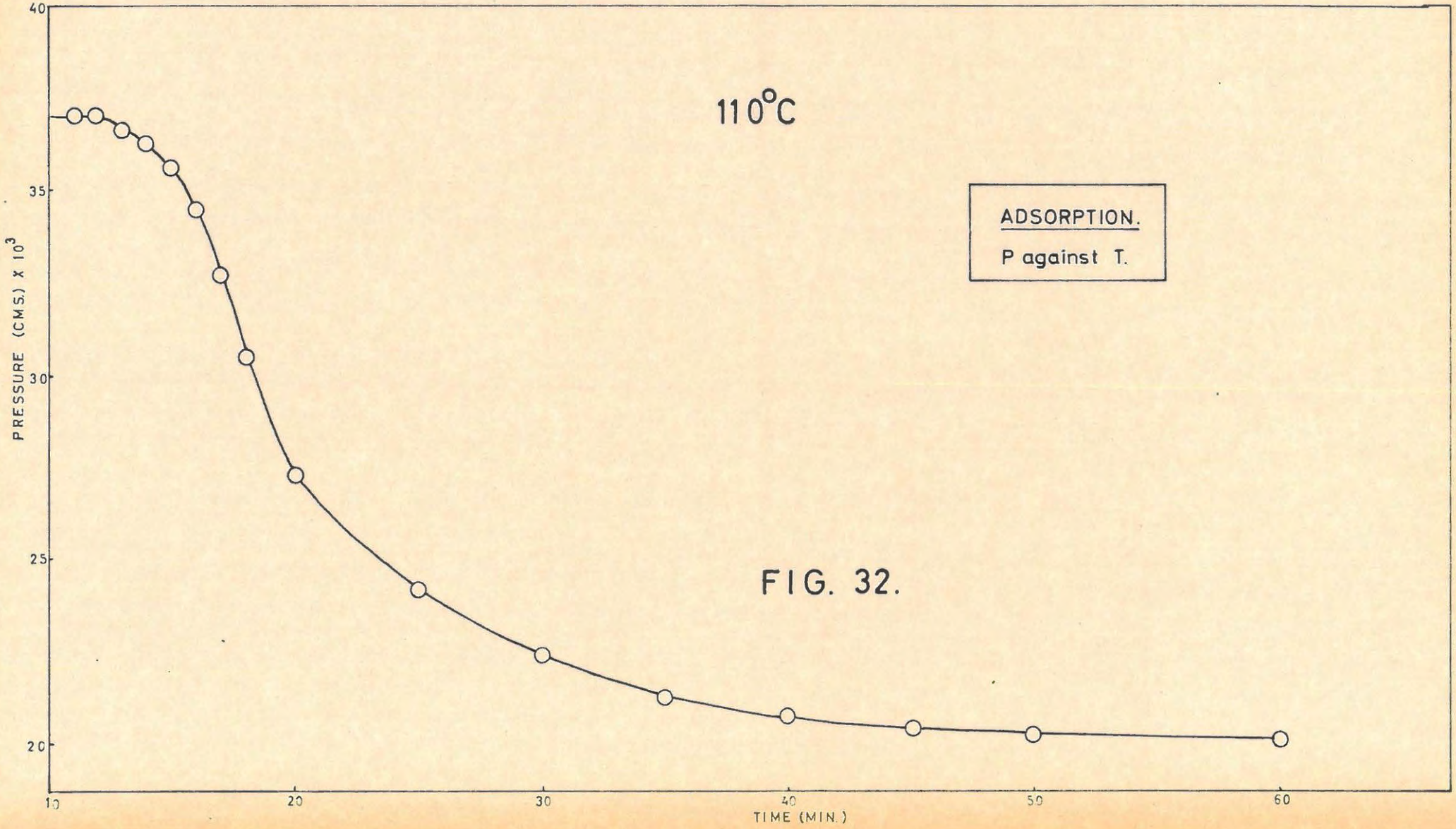
110°C
ADSORPTION.
P against T.
PRESSURE (CMS.) X 10^3
40
35
30
25
20
10
20
30
40
50
60
TIME (MIN.)

FIG. 32.

TABLE 38.

110°C		Run 1.			3.042 g.
t	p	t	p	t	p
10	0.0	15	35.72	30	22.42
Nitrogen Admitted		16	34.50	35	21.21
11	36.97	17	32.70	40	20.74
12	36.97	18	30.66	45	20.50
13	36.66	20	27.32	50	20.34
14	36.35	25	24.17	70	20.03

(vii) Visual observations.

These centred upon the colour of the salt at various stages of decomposition. The colour remained white up to the end of the induction period. The colour started to change as soon as the decomposition entered the acceleratory phase. At the onset of the acceleratory period the sample was a very light grey. The colour darkened as the reaction proceeded until by $\alpha = 0.30$ it was dark grey and at $\alpha = 0.50$ the salt was black

(viii) Mathematical analysis of the results.

A typical pressure vs. time plot for the thermal decomposition of unirradiated barium azide is shown in FIGURE 33. There is a well defined induction period with no gas evolution, followed by a period of acceleration and a relatively short decay. The inflexion point is at $\alpha = 0.62$.

The power law was frequently used by earlier workers to analyse the acceleratory period.[1,3,60] A value of n = 6 was most commonly used. However with the results obtained a plot of $p^{1/6}$ vs. t gave curved plots and the fit was only $\alpha = 0.02$ to $\alpha = 0.24$.

Using the equation in the form $(p - p_o)^{1/4}$ vs. t, where p_o is a small correction pressure, $\alpha = 0.005$, the extent of fit improved to cover the range $\alpha = 0.02$ to $\alpha = 0.35$ but did not describe the whole of the acceleratory period. (FIGURE 33).

The Avrami-Erofeyev/.....

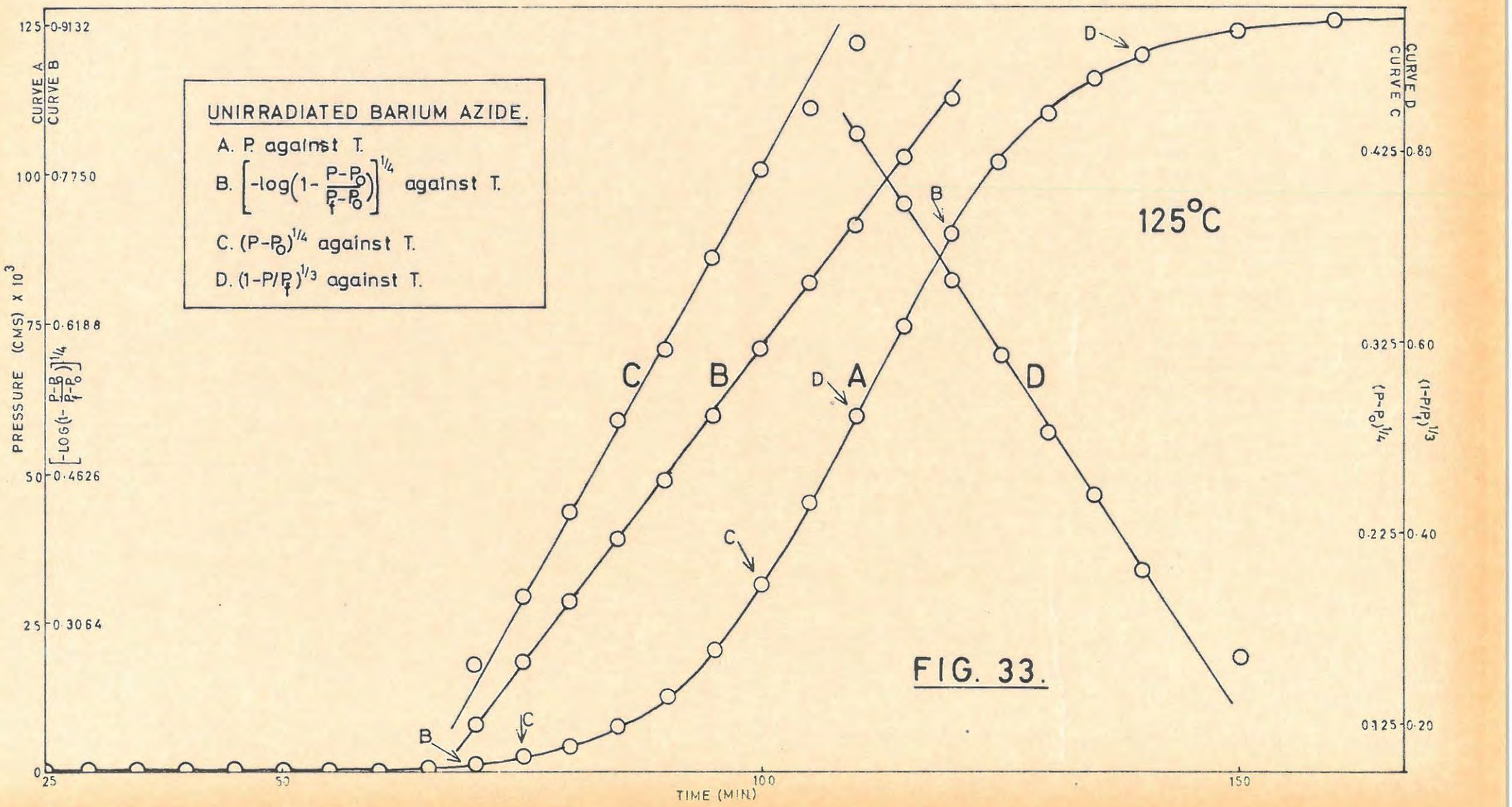
UNIRRADIATED BARIUM AZIDE.
A. P against T.
B. $\left[-\log\left(1-\frac{P-P_0}{P_f-P_0}\right)\right]^{1/4}$ against T.
C. $(P-P_0)^{1/4}$ against T.
D. $(1-P/P_f)^{1/3}$ against T.
125°C
PRESSURE (CMS) X 10^3
CURVE A
CURVE B
CURVE C
CURVE D
$\left[-\log\left(1-\frac{P-P_0}{P_f-P_0}\right)\right]^{1/4}$
$(P-P_0)^{1/4}$
$(1-P/P_f)^{1/3}$
TIME (MIN)
125
100
75
50
25
0
0·9132
0·7750
0·6188
0·4626
0·3064
0·425
0·325
0·225
0·125
0·80
0·60
0·40
0·20
25
50
100
150
A
B
C
D
FIG. 33.

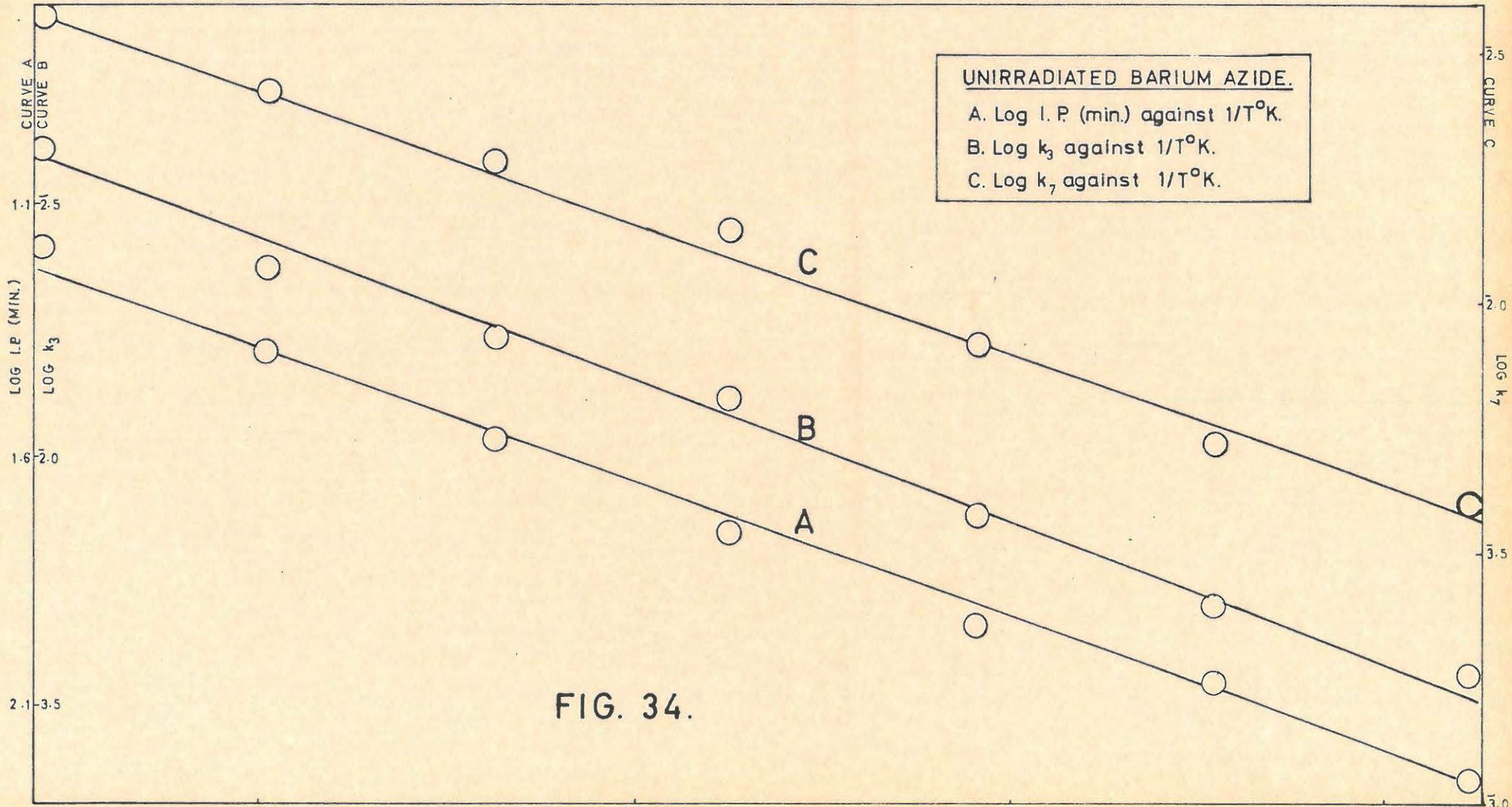
UNIRRADIATED BARIUM AZIDE.
A. Log I. P. (min.) against 1/T°K.
B. Log k_3 against 1/T°K.
C. Log k_7 against 1/T°K.
CURVE A
CURVE B
CURVE C
LOG I.P (MIN.)
LOG k_3
LOG k_7
1·1 $\bar{2}$·5
1·6 $\bar{2}$·0
2·1 $\bar{3}$·5
$\bar{2}$·5
$\bar{2}$·0
$\bar{3}$·5
$\bar{3}$·0
C
B
A
2·45
2·50
2·55
2·60
1/T°K X 10^3

FIG. 34.

The Avrami-Erofeyev equation with n = 4 i.e.

$$\left[-\log\left(1 - {}^{p}/_{p_f}\right)\right]^{1/4} = k_3 t + c_3 \quad \ldots\ldots\ldots\ldots (8)$$

described the whole of the acceleratory period. The fit (α = 0.10 to α = 0.66) is excellent, especially if a small correction factor p_o is applied, viz. the equation is used in the form

$$\left[-\log\left(1 - \frac{p - p_o}{p_f - p_o}\right)\right]^{1/4} = k_3 t + c_3 \quad \ldots\ldots\ldots (8)$$

The term p_o is usually of the order of 6.0×10^{-3} mm. Hg which is equivalent to α = 0.005. The plot of $\left[-\log\left(1 - \frac{p - p_o}{p_f - p_o}\right)\right]^{1/4}$ vs. t is shown in FIGURE 33.

The decay reaction is well described by the contracting sphere formula,

$$\left(1 - {}^{p}/_{p_f}\right)^{1/3} = k_7 t + c_7 \quad \ldots\ldots\ldots\ldots\ldots\ldots (2)$$

This fit is also shown in FIGURE 33 and is from α = 0.62 to α = 0.90.

The critical increment of the chemical process(es) was determined from the Arrhenius equation. Plots of log I.P. (min), log k_3 and log k_7 vs. ${}^{1}/_{T}$ ($^{\circ}$K) are shown in FIGURE 34. The following activation energies were obtained:

(i) Induction period: 24.7 kcals.mole^{-1}

(ii) Acceleratory period: 26.8 kcals. mole^{-1}

(iii) Decay period: 24.3 kcals. mole^{-1}

(ix) Electrical conductivity measurements.

These were made by Mr. C.A.R. Phillpotts. From the plot of log σ vs. ${}^{1}/_{T}$ ($^{\circ}$K) the activation energy in the temperature range 20° - 60°C for an unirradiated pellet was found to be 11.6 kcals. mole^{-1}. The Arrhenius plot is shown in FIGURE 35.

(x) Percentage decomposition.

This was calculated assuming the equation for decomposition to be

$$Ba(N_3)_2 \quad Ba + 3N_2.$$

The results/.....

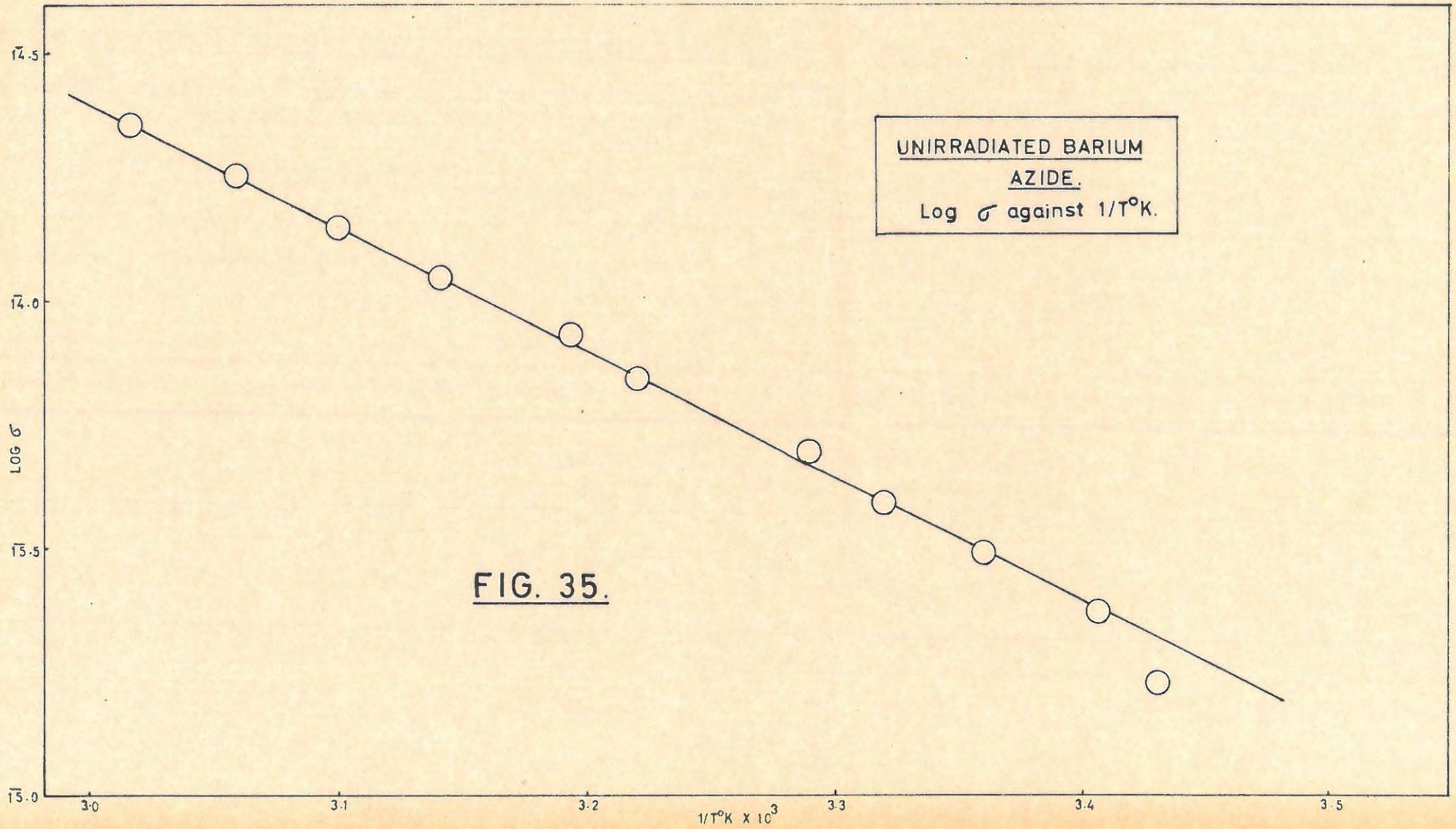
UNIRRADIATED BARIUM AZIDE.
Log σ against 1/T°K.
LOG σ
$\bar{1}4.5$
$\bar{1}4.0$
$\bar{1}5.5$
$\bar{1}5.0$
3·0
3·1
3·2
3·3
3·4
3·5
1/T°K X 10^3

FIG. 35.

The results of a series of determinations are summarized in TABLE 39. The average percentage decomposition was 93% of the theoretical value.

TABLE 39.

Temperature °C.	Wt used mg.	% decomposition.
120°	5.3	93.41
120°	5.5	90.73
120°	5.9	94.98
130°	6.1	95.72
130°	6.1	90.04

(xi) Measurement of particle size.

The average particle size, as determined microscopically, was 5.0×10^{-4} cm.

6.1.3. Preirradiated (Ultra-Violet Light) Barium Azide.

(i) Preliminary investigations.

Prep. II was used in all work on the effect of ultra-violet preirradiation on the thermal decomposition of barium azide. A preliminary investigation was done by irradiating a sample of barium azide for 15 min. from a distance of 10 cm. The apparatus used has been described previously. The salt was decomposed at 110°C. Results are shown in FIGURE 36 and TABLE 40. There is a shortening of the induction period and an increase in the rate. By trial and error an irradiation height of 40 cm. was selected as being the most suitable.

TABLE 40.

110°C Unirradiated blank. Run 1.					6.3 mg.
t	p	t	p	t	p
30	0.03	160	10.62	235	101.51
60	0.05	165	13.53	240	106.02
70	0.07	170	16.89	245	109.68
80	0.09	175	21.27	250	112.79

TABLE 40/.....

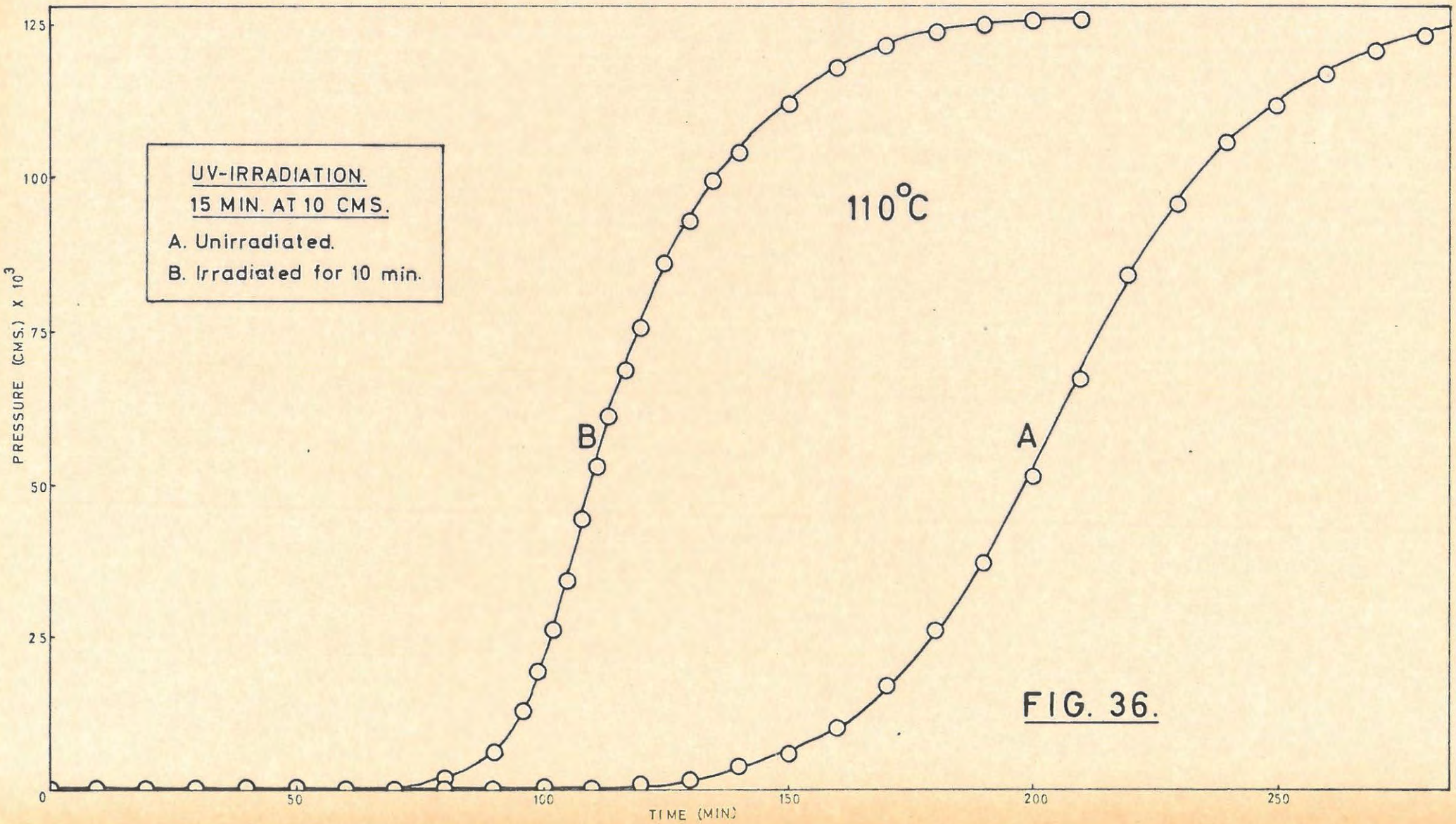
UV-IRRADIATION.
15 MIN. AT 10 CMS.
A. Unirradiated.
B. Irradiated for 10 min.
110°C
B
A
PRESSURE (CMS.) X 10^3
TIME (MIN)
0
25
50
75
100
125
50
100
150
200
250

FIG. 36.

TABLE 40 cont.

t	p	t	p	t	p
90	0.13	180	26.24	255	115.46
100	0.24	185	31.90	260	117.54
110	0.49	190	37.23	265	119.64
120	1.00	195	43.73	270	121.01
125	1.31	200	51.15	275	122.57
130	1.85	205	60.03	280	123.71
135	2.53	210	67.37	290	125.04
140	3.56	215	75.42	300	126.06
145	4.56	220	84.87	p_f	127.20
150	6.21	225	89.86	p_a	119.47
155	8.02	230	95.65		

110°C 15 min. U.V. 10 cm. Run 2.					6.4 mg.
t	p	t	p	t	p
10	0.04	90	6.59	130	92.91
20	0.04	93	9.46	135	96.46
30	0.06	96	13.30	140	104.70
40	0.07	99	19.20	145	109.62
45	0.08	102	26.41	150	112.60
50	0.09	105	34.97	155	115.86
55	0.14	108	44.44	160	118.06
60	0.19	111	53.10	165	120.16
65	0.35	114	61.13	175	123.40
70	0.62	117	68.97	185	125.30
75	1.12	120	75.50	195	126.56
80	2.07	123	81.41	p_f	127.20
85	3.66	126	87.01	p_a	121.88

(ii) Effect of varying doses of ultra-violet light.

The effect of different doses of ultra-violet light on the thermal decomposition of barium azide was studied at a decomposition temperature of 120°C. Irradiation times ranged from 1 min. to 90 min. The results appear in TABLE 41 and are shown graphically in FIGURE 37.

On increasing the dose the duration of the induction period decreased, the acceleratory rate constants, k_3 and k_4,

(equation 8 and 9)/.....

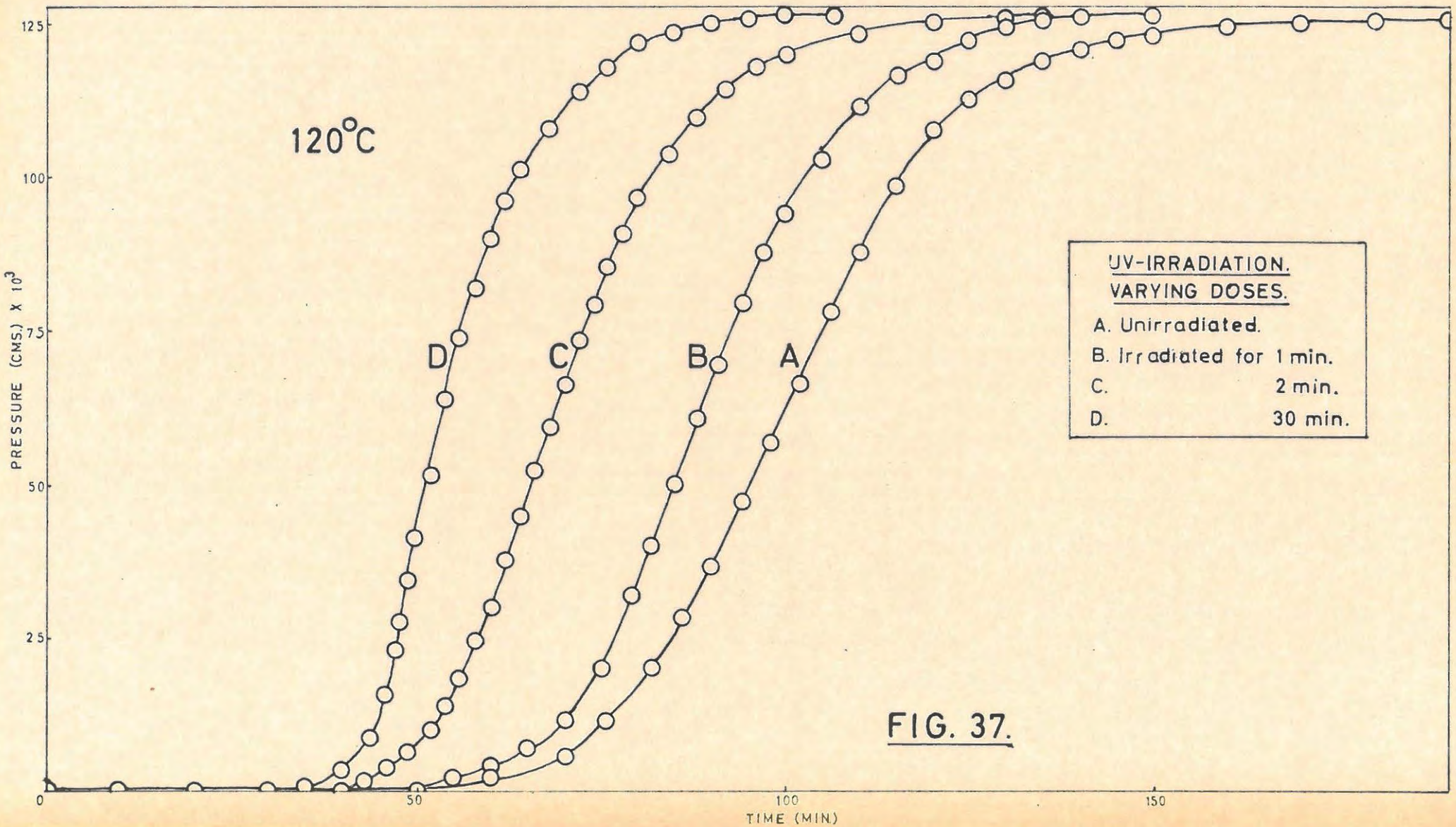
120°C
D
C
B
A
UV-IRRADIATION.
VARYING DOSES.
A. Unirradiated.
B. Irradiated for 1 min.
C. 2 min.
D. 30 min.
PRESSURE (CMS.) X 10³
TIME (MIN.)
0
25
50
75
100
125
50
100
150

FIG. 37.

(equation 8 and 9) increased and the inflexion point in the p/t plots dropped. These features are summarized in TABLE 42.

TABLE 41.

120°C Ultra-violet dose = 0. Run 1.					6,5 mg.
t	p	t	p	t	p
20	0.12	90	37.22	116	100.98
40	0.18	92	42,34	118	104.15
50	0,44	94	47.00	120	107.76
60	2,67	96	51.71	125	112,88
65	3,61	98	56.82	130	116,60
70	6,28	100	61.90	135	119,76
73	8,57	102	66,93	140	121,11
76	11,67	104	72,77	145	122,34
79	15,28	106	77,91	155	124,08
82	19,79	108	83,23	170	125,96
84	24,21	110	88,26	190	126,96
86	28,52	112	92,72	p_f	127,20
88	32,82	114	97,08	p_a	128,51

120°C 1 min. U.V. Run 2.					6.4 mg.
t	p	t	p	t	p
20	0,10	66	7,66	97	87,75
40	0,21	68	9,41	100	94,53
45	0,57	70	11,75	103	101,00
48	0,77	72	14,23	106	104,67
50	0,89	74	17,80	110	111,68
52	1,29	76	23,85	115	116,85
54	1,89	79	32,23	120	118,85
56	2,31	82	40,34	125	122,96
58	3,09	85	50,21	130	124,91
60	3,95	88	60,91	135	126,00
62	4,91	91	69,80	p_f	127,20
64	6,13	94	79,23	p_a	120,36

120°C 2 min. U.V. Run 3.					6,6 mg.
t	p	t	p	t	p
10	0.01	60	30,73	84	103,82
20	0,01	62	37,96	88	109,84

TABLE 41 cont/.....

TABLE 41 cont.

t	p	t	p	t	p
30	0.04	64	45.07	92	114.51
40	0.96	66	52.71	96	118.58
43	1.95	68	59.39	100	119.83
46	3.70	70	66.87	110	123.81
49	6.28	72	73.45	120	125.35
52	10.49	74	79.65	130	126.69
54	14.03	76	85.56	p_f	127.20
56	18.77	78	91.12	p_a	121.50
58	24.37	80	93.75		

120°C 5 min. U.V. Run 4. 6.5 mg.					
t	p	t	p	t	p
5	0.03	53	9.59	70	75.79
10	0.04	54	11.95	72	82.68
20	0.04	55	14.05	74	88.41
30	0.06	56	17.28	76	93.65
35	0.19	57	20.54	80	101.94
37	0.30	58	24.71	85	110.09
39	0.51	59	29.21	90	115.76
41	0.83	60	34.58	95	120.56
43	1.40	61	39.17	100	122.27
45	1.92	62	44.09	105	123.56
47	2.97	63	48.26	110	124.91
49	4.49	64	53.04	120	125.84
50	5.28	65	57.25	130	127.06
51	7.19	66	61.50	p_f	127.20
52	8.11	68	65.85	p_a	126.69

120°C 30 min. U.V. Run 5. 6.4 mg.					
t	p	t	p	t	p
5	0.01	49	34.81	68	108.39
10	0.02	50	41.13	70	111.99
15	0.03	51	47.15	72	114.41
20	0.05	52	53.29	74	115.95
25	0.07	53	59.04	76	118.08
30	0.19	54	64.52	80	121.89
35	0.78	55	69.38	85	123.22
38	2.65	56	74.05	90	125.27
40	3.14	57	78.86	95	126.30

TABLE 41 cont/.....

TABLE 41 cont.

t	p	t	p	t	p
42	5.24	58	82.47	100	126.60
44	8.83	60	90.47	110	126.94
46	15.49	62	96.17	p_f	127.20
47	23.50	64	101.13	p_a	123.79
48	28.98	66	105.45		

120°C 90 min. U.V. Run 6.					6.5 mg.
t	p	t	p	t	p
5	0.01	47	33.05	62	101.97
10	0.01	48	39.66	65	108.32
15	0.01	49	46.56	68	113.41
20	0.03	50	52.47	71	116.87
25	0.03	51	58.99	75	120.19
30	0.19	52	64.77	80	123.75
35	0.85	53	70.16	85	125.35
38	2.09	54	75.05	90	126.19
40	3.65	55	79.40	95	126.51
42	6.21	56	83.24	100	126.64
44	10.62	57	87.11	110	126.90
45	14.48	58	90.52	p_f	127.20
46	20.81	60	97.09	p_a	118.10

TABLE 42.

Dose min.	k_3 min^{-1}	Induction period min.	Inflexion point.
0	2.25×10^{-2}	55	0.60
	k_4 $min.^{-1}$		
1	1.180×10^{-2}	47	0.51
2	1.645×10^{-2}	39	0.35
5	2.320×10^{-2}	40	0.31
30	2.650×10^{-2}	33	0.32
90	3.470×10^{-2}	32	0.27

With irradiation times greater than 90 min. the salt went a buff colour. The thermal decomposition of these samples gave low final pressures, indicating that photolysis had taken place.

(iii) Effect of/.....

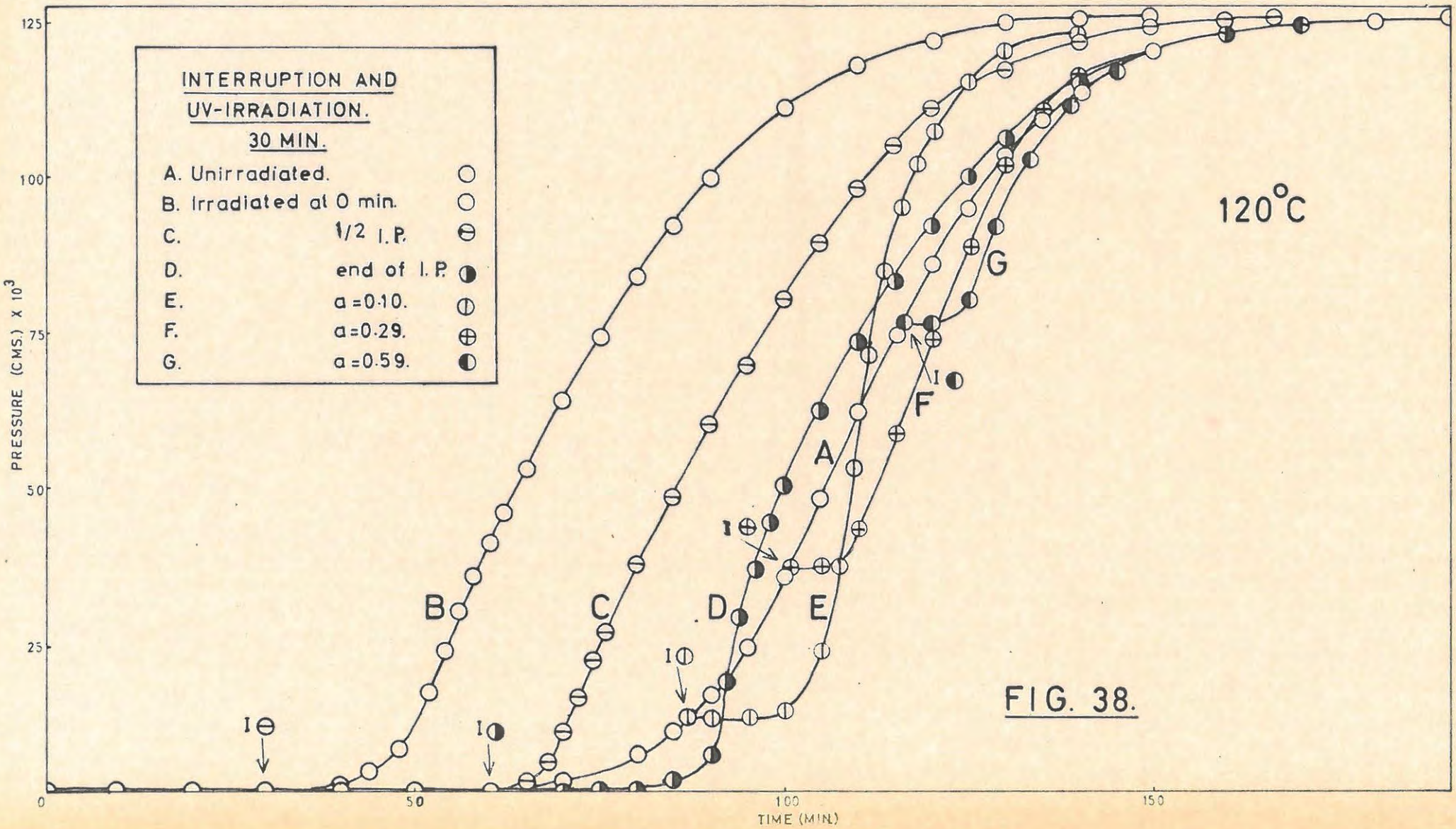
INTERRUPTION AND
UV-IRRADIATION.
30 MIN.
A. Unirradiated.
B. Irradiated at 0 min.
C. 1/2 I.P.
D. end of I.P.
E. a=0·10.
F. a=0·29.
G. a=0·59.
120°C
PRESSURE (CMS.) X 10³
TIME (MIN.)
0
50
100
150
25
75
100
125
A
B
C
D
E
F
G
I
I
I
I
I

FIG. 38.

(iii) Effect of interrupting a thermal decomposition and irradiating the salt.

The decomposition was interrupted at various stages of a run and the sample irradiated. The technique used has been described earlier. The irradiation time was 30 min. and the decomposition temperature was 120°C. The results are given in TABLE 43 and illustrated in FIGURE 38. A quartz ampoule was used in place of the usual pyrex one, and hence blank runs for both unirradiated and irradiated samples were first done. At the point of interruption and irradiation of the salt, the word "Irradiation" is written in the table.

TABLE 43.

120°C Unirradiated blank. Run 1.					6.6 mg.
t	p	t	p	t	p
20	0.13	90	16.03	140	114.24
40	0.20	95	24.48	145	117.59
50	0.29	100	35.05	150	120.55
55	0.47	105	48.21	155	121.82
60	0.79	110	62.00	160	123.00
65	1.26	115	74.56	170	124.41
70	2.04	120	86.31	180	125.14
75	3.71	125	94.92	190	126.27
80	6.39	130	103.59	p_f	127.20
85	10.21	135	109.78	p_a	119.97

120°C Irradiated blank. Run 2.					6.7 mg.
t	p	t	p	t	p
10	0.01	50	10.88	80	83.88
20	0.03	52	16.28	85	92.17
30	0.17	54	23.33	90	99.66
35	0.54	56	29.68	100	111.15
38	1.06	58	35.39	110	118.73
40	1.68	60	40.84	120	122.61
42	2.44	62	45.88	130	125.23
44	3.44	65	53.34	140	126.55
46	4.88	70	64.16	p_f	127.20
48	7.18	75	74.45	p_a	124.18

TABLE 43 cont/.....

TABLE 43 cont.

120°C 30 min. U.V. Run 3. 6.6 mg.					
t	p	t	p	t	p
20	0.08	70	10.18	110	98.23
30	0.10	72	15.90	115	105.46
Irradiation		74	21.82	120	111.06
50	0.11	76	26.87	130	117.76
55	0.16	80	37.15	140	122.13
60	0.55	85	48.30	150	124.66
62	0.83	90	59.14	160	125.94
64	1.50	95	69.64	p_f	127.20
66	2.73	100	79.99	p_a	121.50
68	5.06	105	89.42		

120°C 30 min. U.V. Run 4. 6.5 mg.					
t	p	t	p	t	p
20	0.32	92	18.85	125	100.19
40	0.45	94	28.70	130	106.50
60	0.51	96	36.75	140	114.80
Irradiation		98	43.90	150	119.68
70	0.51	100	49.69	160	122.16
75	0.54	105	62.33	180	125.93
80	0.62	110	73.47	p_f	127.21
85	2.15	115	83.39	p_a	119.17
90	6.73	120	92.44		

120°C 30 min. U.V. Run 5. 6.4 mg.					
t	p	t	p	t	p
20	0.08	95	12.08	120	95.17
40	0.19	100	12.32	122	102.41
50	0.51	105	13.76	125	109.36
60	0.75	110	23.64	130	116.56
70	1.58	112	37.25	135	120.26
75	2.32	113	44.97	140	122.77
80	3.78	114	53.73	150	125.30
85	6.01	115	62.65	160	126.57
90	10.04	116	71.06	p_f	127.20
92	12.03	117	78.15	p_a	118.10
Irradiation		118	84.62		

TABLE 43 cont/.....

TABLE 43 cont.

120°C 30 min. U.V. Run. 6. 6.3 mg.					
t	p	t	p	t	p
20	0.11	Irradiation		150	120.67
40	0.31	105	37.38	160	122.83
60	0.62	110	43.04	170	124.47
70	1.66	115	58.56	180	125.57
80	4.21	120	74.98	190	126.67
85	7.58	125	91.20	p_f	127.20
90	12.77	130	103.94	p_a	116.98
95	21.70	135	111.32		
100	37.13	140	116.45		

120°C 30 min. U.V. Run 7. 6.4 mg.					
t	p	t	p	t	p
20	0.14	105	36.20	145	113.25
40	0.29	110	47.73	150	119.97
50	0.48	115	61.31	155	123.52
60	1.20	120	74.59	160	124.74
70	2.79	Irradiation		170	125.97
80	6.42	125	75.06	180	126.80
90	13.37	130	80.04	p_f	127.20
95	18.65	135	92.25	p_a	120.93
100	26.26	140	103.26		

Up to a value of $\alpha = 0.10$ for the point of irradiation there is a pronounced increase in the acceleratory rate after approximately 20 - 30 min. after an interrupted and irradiated decomposition is allowed to continue. At values of $\alpha > 0.30$ there is virtually no effect on the subsequent thermal decomposition.

(iv) Effect of admitting water vapour onto the salt in an interrupted decomposition.

The technique of "water interruptions" has been described. An irradiation time of 30 min. was chosen and the subsequent decomposition temperature was 120°C.

Interruptions during the induction period and in the

acceleratory period/.....

acceleratory period resulted in a new induction period being formed when decomposition was resumed. The duration of the new induction period was greater than with the decomposition of preirradiated salt. The subsequent reaction was considerably slower.

Successive interruptions and admission of water vapour, in which the point of interruption was taken as the time for the pressure to equal 6.0×10^{-4} mm. Hg were carried out. Five such interruptions were performed and then the reaction was allowed to proceed normally. Each new induction period was longer than the previous one and eventually equalled that for normal decomposition of unirradiated barium azide at the same temperature.

In all these runs the final pressure was lower than that normally expected. The lost gas could be recovered by heating at 300°C in vacuo. The results are shown in TABLE 44 and FIGURE 39. Pressures are not normalised. Data on the acceleratory rate constants, k_3 and k_4, (equation 8 and 9) and induction period lengths is given in TABLE 45.

TABLE 44.

120°C Irradiated blank. Run 1.					6.6 mg.
t	p	t	p	t	p
10	0.26	52	14.13	80	105.86
20	0.32	54	23.91	85	112.36
30	0.46	56	31.96	90	117.20
35	0.62	58	40.09	100	122.78
40	1.21	60	48.35	110	124.99
42	1.69	62	56.96	120	125.23
44	2.33	64	64.44	p_a	125.88
46	3.48	66	71.91		
48	5.24	70	84.91		
50	8.31	75	96.76		

TABLE 44 cont/.....

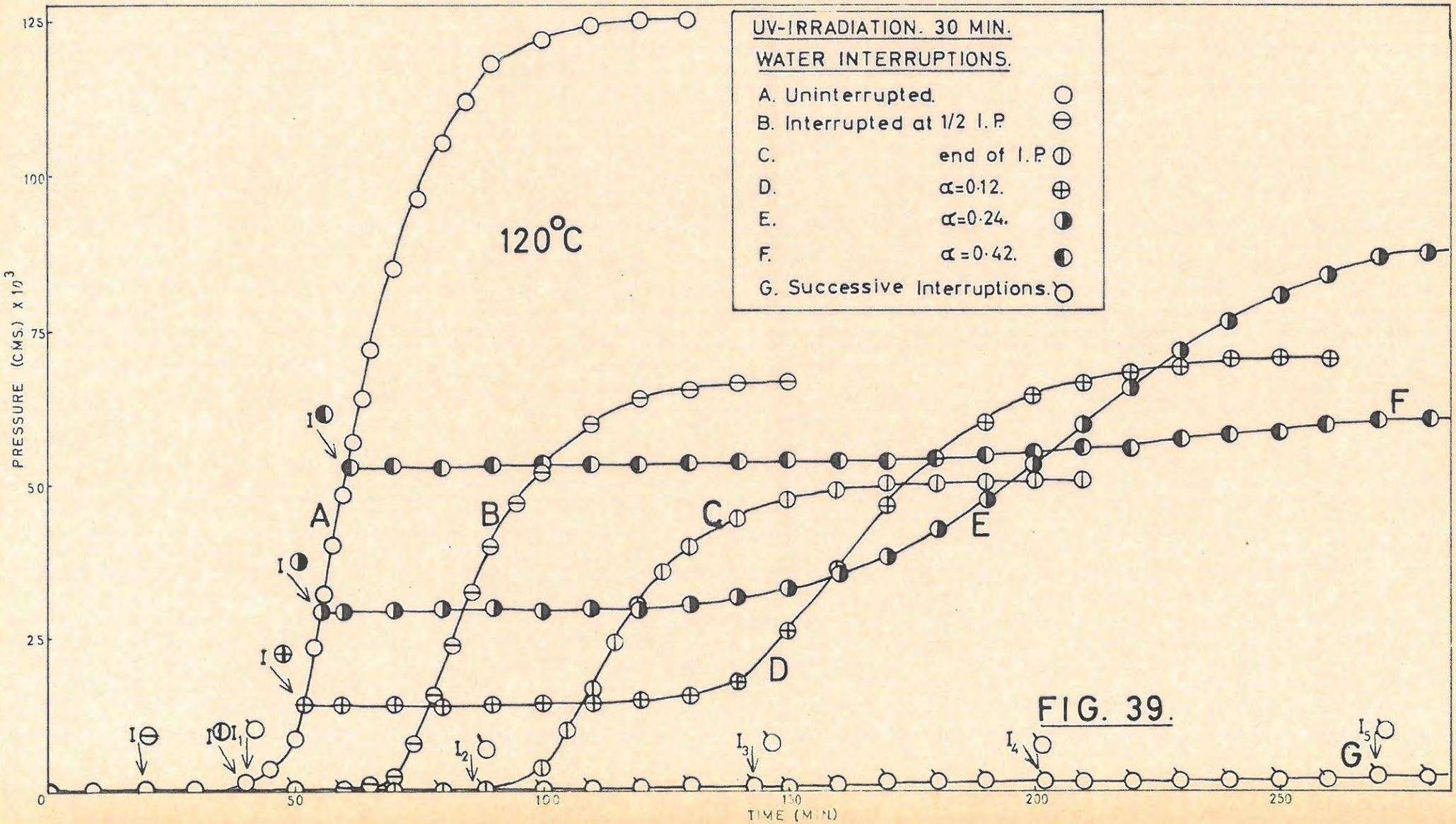
UV-IRRADIATION. 30 MIN.
WATER INTERRUPTIONS.
A. Uninterrupted.
B. Interrupted at 1/2 I.P.
C. end of I.P.
D. α=0·12.
E. α=0·24.
F. α=0·42.
G. Successive Interruptions.
120°C
PRESSURE (C.M.S.) X 10³
TIME (MIN)
0
25
50
75
100
125
50
100
150
200
250
A
B
C
D
E
F
G
I
I₁
I₂
I₃
I₄
I₅

FIG. 39.

TABLE 44 cont.

120°C 30 min. U.V. Run 2. 6.5 mg.					
t	p	t	p	t	p
18	0.17	70	2.21	95	46.75
Water Interruption 72			3.90	100	51.95
20	0.17	74	7.86	110	59.67
30	0.17	76	11.59	120	63.71
40	0.18	78	15.59	130	65.55
50	0.19	80	20.17	140	66.48
60	0.33	82	23.93	p_a	66.95
65	0.84	85	30.49		
68	1.51	90	39.62		

120°C 30 min. U.V. Run 3. 6.6 mg.					
t	p	t	p	t	p
10	0.04	95	1.18	125	35.30
20	0.07	100	3.61	130	39.15
30	0.10	102	5.81	140	44.33
40	0.64	104	8.57	150	47.45
Water Interruption 106			11.47	170	50.66
60	0.66	108	14.35	200	52.31
70	0.68	110	17.56	220	53.15
80	0.70	112	20.56	p_a	53.56
85	0.81	115	24.37		
90	0.92	120	30.68		

120°C 30 min. U.V. Run 4. 6.6 mg.					
t	p	t	p	t	p
10	0.07	80	14.68	170	46.48
20	0.13	90	14.69	175	50.70
30	0.27	110	14.80	180	54.20
35	0.48	120	15.08	190	60.27
40	1.12	130	15.90	200	64.20
42	1.67	135	16.76	210	66.41
44	2.41	140	18.53	220	67.91
46	3.57	145	21.63	230	69.04
48	5.30	150	26.00	240	69.54
50	8.40	155	31.17	p_a	70.20
52	14.66	160	36.36		
Water Interruption 165			41.44		

TABLE 44 cont/.....

TABLE 44 cont.

120°C 30 min. U.V. Run 5. 6.7 mg.					
t	p	t	p	t	p
20	0.07	90	29.57	220	65.87
30	0.19	110	29.79	230	71.37
40	0.86	120	30.05	240	76.19
45	2.02	130	30.65	250	80.52
48	3.37	140	31.83	285	88.98
50	4.61	150	33.08	300	91.40
52	6.43	155	34.14	310	92.21
54	9.48	160	35.58	320	92.62
56	13.50	170	38.53	330	93.45
58	19.80	180	42.83	340	93.86
60	26.51	190	47.75	p_a	94.28
61	29.52	200	53.44		
Water Interruption		210	59.61		

120°C 30 min. U.V. Run 6. 6.6 mg.					
t	p	t	p	t	p
20	0.12	68	48.09	230	57.53
30	0.19	70	53.24	240	58.19
40	0.77	Water Interruption		250	58.78
45	1.74	110	53.27	280	60.07
50	3.86	150	53.51	290	60.48
55	8.70	170	53.93	300	60.76
58	15.88	180	54.31	310	60.91
60	23.66	190	54.78	320	61.19
62	30.66	200	55.42	330	61.33
64	36.66	210	56.07	340	61.49
66	42.85	220	56.81	p_a	61.64

120°C 30 min. U.V. Run 7. 6.6 mg.					
t	p	t	p	t	p
40	0.60	Water Interruption		385	22.82
Water Interruption		325	3.34	390	24.96
80	0.77	330	3.54	400	28.20
88	1.20	335	3.88	410	31.42
Water Interruption		340	4.43	420	33.39
130	1.38	345	5.11	430	34.83
143	1.81	350	6.11	440	35.71

TABLE 44 cont/.....

TABLE 44 cont.

t	p	t	p	t	p
Water Interruption		355	7.62	450	36.31
190	1.87	360	9.57	470	37.21
202	2.41	365	11.71	480	37.51
Water Interruption		370	14.33	p_a	37.82
260	2.80	375	17.48		
270	3.01	380	20.15		

TABLE 45.

Point of Interruption.	k_4 min.$^{-1}$	Induction period min.	Number of Interruptions.	Induction period min.
Uninterrupted	2.330×10^{-2}	35	0	40
	k_3 min.$^{-1}$		1	48
$1/2$ along I.P.	2.530×10^{-2}	44	2	55
End of I.P.	2.075×10^{-2}	55	3	59
$\alpha = 0.12$	1.320×10^{-2}	60	4	68
$\alpha = 0.24$	5.500×10^{-3}	65	5	65
$\alpha = 0.42$	4.830×10^{-3}	90		
5 consecutive	9.900×10^{-3}	65		

(v) Effect of varying the temperature of decomposition.

An irradiation time of 30 min. was selected. Decompositions were performed in the temperature range 100° - 125°C. These results are given in TABLE 46. TABLE 47 lists the rate constants, k_4 and k_7, (equation 9 and 12) obtained from these runs.

TABLE 46.

100°C 30 min. U.V. Run 1.					6.2 mg.
t	p	t	p	t	p
60	0.03	260	5.73	390	77.49
90	0.05	270	7.87	400	83.39
120	0.07	280	10.36	410	89.03
140	0.09	290	13.59	420	93.76
160	0.14	300	17.71	440	101.93

TABLE 46 cont/.....

TABLE 46 cont.

t	p	t	p	t	p
180	0.25	310	22.65	460	109.27
190	0.33	320	28.48	480	115.69
200	0.55	330	35.31	500	120.47
210	0.82	340	42.87	520	123.51
220	1.27	350	50.37	540	125.34
230	1.97	360	57.23	560	126.59
240	2.91	370	64.52	p_f	127.20
250	4.14	380	71.32	p_a	112.58

105°C 30 min. U.V. Run 2.					6.4 mg.
t	p	t	p	t	p
20	0.07	180	8.46	270	89.98
40	0.10	190	13.26	280	96.27
60	0.14	200	20.36	290	101.68
80	0.19	205	25.01	300	106.67
100	0.21	210	30.44	310	110.64
120	0.39	215	36.08	320	113.52
130	0.62	220	42.20	330	115.85
140	0.96	230	53.46	340	118.20
150	1.77	240	63.85	390	126.62
160	3.03	250	73.77	p_f	127.20
170	5.09	260	82.41	p_a	123.79

110°C 30 min. U.V. Run 3.					6.4 mg.
t	p	t	p	t	p
20	0.13	120	10.77	190	106.38
40	0.18	125	15.77	200	112.14
60	0.30	130	22.24	210	116.86
70	0.41	135	30.42	220	119.86
80	0.60	140	39.88	230	122.29
85	0.73	145	49.06	240	124.13
90	1.04	150	57.93	250	125.36
95	1.61	155	66.63	260	126.60
100	2.30	160	74.03	p_f	127.20
105	3.52	165	80.82	p_a	124.94
110	5.11	170	86.88		
115	7.30	180	97.47		

TABLE 46 cont/.....

TABLE 46 cont.

115°C 30 min. U.V. Run 4.					6.4 mg.
t	p	t	p	t	p
10	0.08	72	10.11	100	85.26
20	0.11	74	13.36	105	93.09
30	0.15	76	18.36	110	100.15
40	0.24	78	24.76	115	105.19
50	0.48	80	32.17	120	109.78
55	0.93	82	39.03	130	116.24
60	2.07	84	45.50	140	120.45
62	2.66	86	51.66	150	123.51
64	3.53	88	57.38	160	125.36
66	4.65	90	62.95	170	126.60
68	5.92	92	67.87	p_f	127.20
70	7.49	95	74.40	p_a	122.64

120°C 30 min. U.V. Run 5.					6.6 mg.
t	p	t	p	t	p
10	0.19	58	16.51	77	90.28
20	0.29	59	22.19	80	97.05
30	0.38	60	27.83	85	106.28
35	0.49	61	31.95	90	113.04
40	0.69	62	36.03	95	117.08
45	1.27	63	40.01	100	120.60
48	2.03	64	44.20	105	122.96
50	2.97	66	52.42	110	125.38
52	4.29	68	60.51	120	126.59
54	6.40	70	68.73	p_f	127.20
56	9.92	72	76.06	p_a	128.44
57	12.62	74	81.79		

125°C 30 min. U.V. Run 6.					6.5 mg.
t	p	t	p	t	p
10	0.03	36	9.56	48	88.07
20	0.15	37	14.55	50	95.00
25	0.31	38	26.83	52	101.06
28	0.79	39	34.20	55	108.47
30	1.43	40	41.74	60	117.35
31	1.94	41	49.25	67	122.23

TABLE 46 cont/.....

TABLE 46 cont.

t	p	t	p	t	p
32	2.61	42	55.70	70	125.32
33	3.59	43	62.11	75	126.51
34	4.84	44	67.95	p_f	127.20
35	6.56	46	78.91	p_a	122.92

TABLE 47.

Temperature °C	Induction period min.	k_4 min.$^{-1}$	k_7 min.$^{-1}$
100°	205	3.100×10^{-3}	2.990×10^{-3}
105°	130	4.960×10^{-3}	4.220×10^{-3}
110°	80	8.125×10^{-3}	6.630×10^{-3}
115°	52	1.490×10^{-2}	9.900×10^{-3}
120°	40	2.310×10^{-2}	1.520×10^{-2}
125°	26	3.300×10^{-2}	2.355×10^{-2}

(vi) Percentage decomposition.

The percentage decomposition (for irradiation times of less than 90 min.) was the same as that obtained with the unirradiated salt.

(vii) Mathematical analysis of the results and evaluation of activation energies.

The acceleratory period was fitted by the Avrami-Erofeyev equation but the value of n increased from 4 to 6 when the salt was preirradiated with ultra-violet light. The equation was thus used in the form,

$$\left[- \log \left(1 - \frac{p-p_o}{p_f-p_o}\right) \right]^{1/6} = k_4 t + c_4 \quad \ldots\ldots\ldots (9)$$

The extent of fit was $\alpha = 0.05$ to $\alpha = 0.35$ on a sample preirradiated for 2 minutes.

The contracting sphere equation,

$$(1 - p/p_f)^{1/3} = k_7 t + c_7 \quad \ldots\ldots\ldots\ldots\ldots\ldots (2)$$

fitted the decay reaction

FIGURE 40/.....

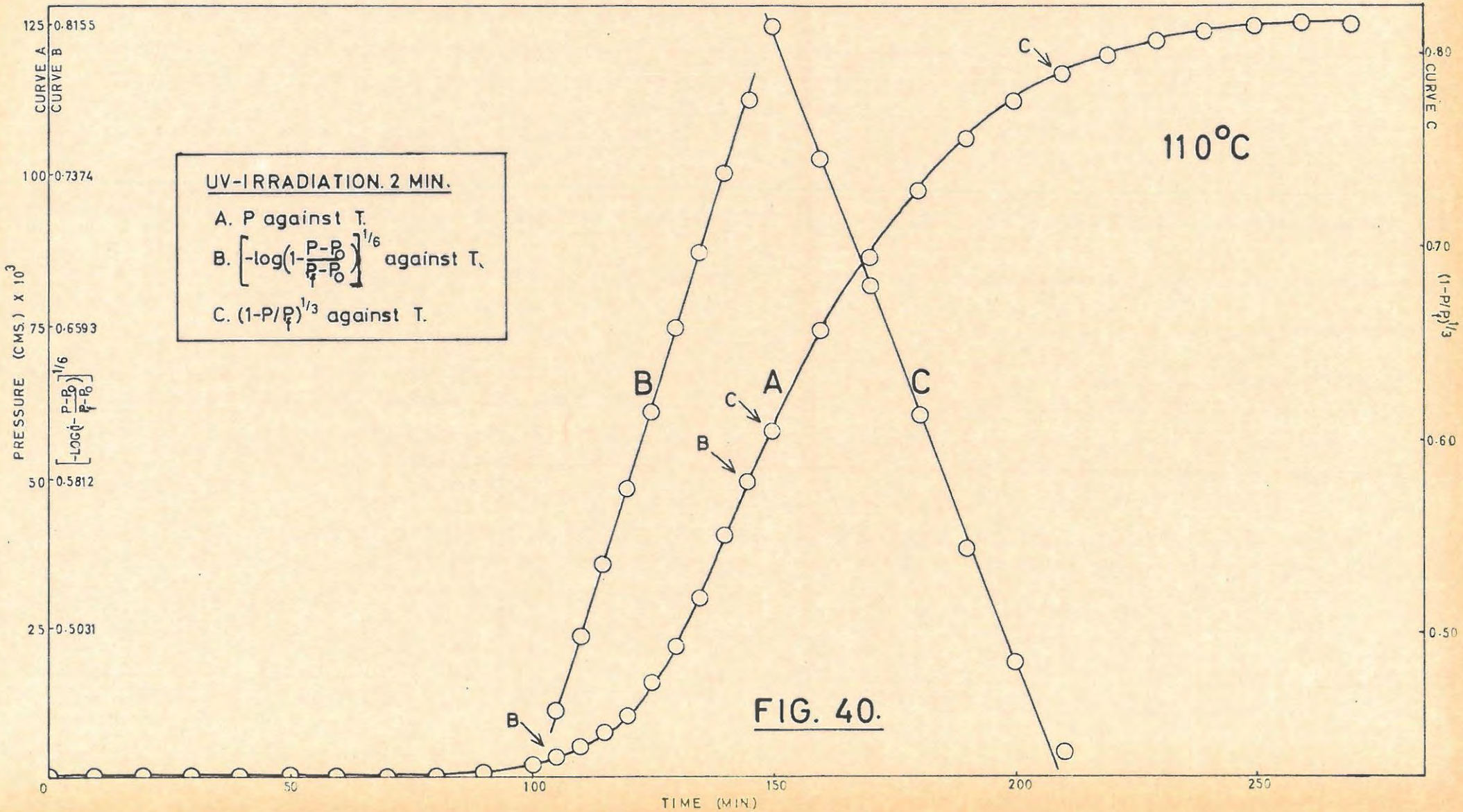
UV-IRRADIATION. 2 MIN.
A. P against T.
B. $\left[-\log\left(1-\frac{P-P_0}{P_f-P_0}\right)\right]^{1/6}$ against T.
C. $(1-P/P_f)^{1/3}$ against T.
110°C
A
B
C
PRESSURE (CMS.) x 10^3
CURVE A
CURVE B
$\left[-\log\left(1-\frac{P-P_0}{P_f-P_0}\right)\right]^{1/6}$
CURVE C
$(1-P/P_f)^{1/3}$
TIME (MIN.)
125
100
75
50
25
0
0.8155
0.7374
0.6593
0.5812
0.5031
0.80
0.70
0.60
0.50
50
100
150
200
250

FIG. 40.

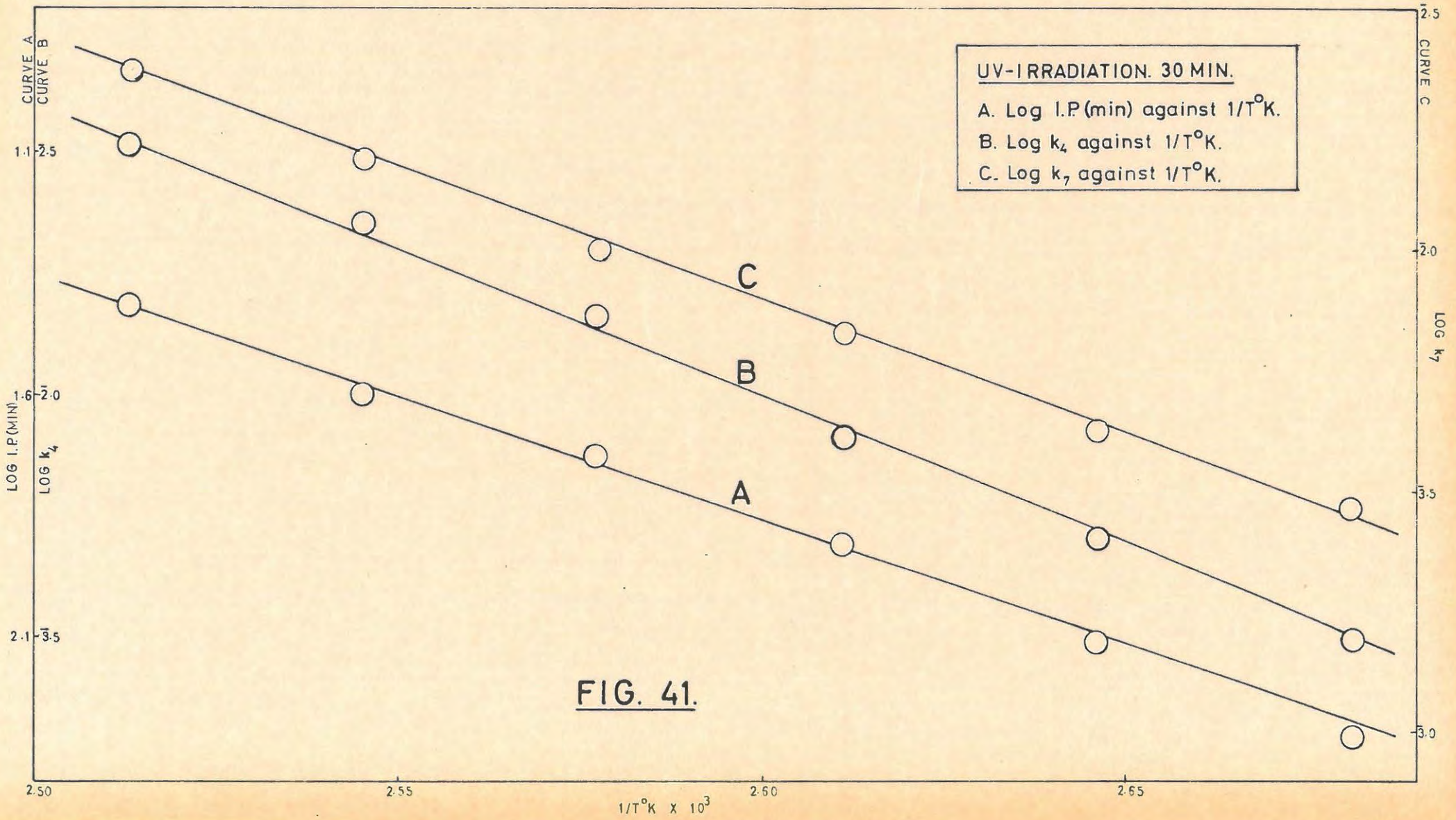
UV-IRRADIATION. 30 MIN.
A. Log I.P(min) against 1/T°K.
B. Log k_4 against 1/T°K.
C. Log k_7 against 1/T°K.
CURVE A
CURVE B
CURVE C
LOG I.P(MIN)
LOG k_4
LOG k_7
1·1 2·5
1·6 2·0
2·1 3·5
2·5
2·0
3·5
3·0
C
B
A
2·50
2·55
2·60
2·65
1/T°K X 10^3

FIG. 41.

FIGURE 40 shows a typical p/t plot with the analysis for the thermal decomposition of irradiated barium azide.

When water vapour is admitted onto the salt in an interrupted run, the subsequent acceleratory period is described by the Avrami-Erofeyev equation with n = 4. The equation thus becomes,

$$\left[- \log \left(1 - \frac{p - p_o}{p_f - p_o}\right)\right]^{1/4} = k_3 t + c_3 \ldots\ldots (8)$$

The analysis is thus the same as for the unirradiated salt once more.

Plots of log I.P. (min.), log k_4 and log k_7 vs $^1/_T$ ^oK are shown in FIGURE 41. The following activation energies were obtained:

(i) Induction period: 23.10 kcals.mole^{-1}

(ii) Acceleratory period: 27.70 kcals.mole^{-1}

(iii) Decay period: 25.00 kcals.mole^{-1}.

6.1.4. Preirradiated (γ-rays) Barium Azide.

(i) Preliminary investigations.

Irradiations were done in sealed, evacuated pyrex ampoules as has been described earlier. An initial decomposition was done at 125^{o}C on a sample which had received a dose of 20 Mrad. The results are tabulated in TABLE 48 and the p/t plots are shown in FIGURE 42

TABLE 48.

125^{o}C Unirradiated blank. Run 1.					6.2 mg.
t	p	t	p	t	p
10	0.03	70	1.27	120	89.95
20	0.07	75	2.17	125	102.13
30	0.10	80	4.04	130	110.86
35	0.12	85	7.61	135	116.51
40	0.14	90	12.12	140	120.65
45	0.14	95	20.26	150	124.21

TABLE 48 cont/.....

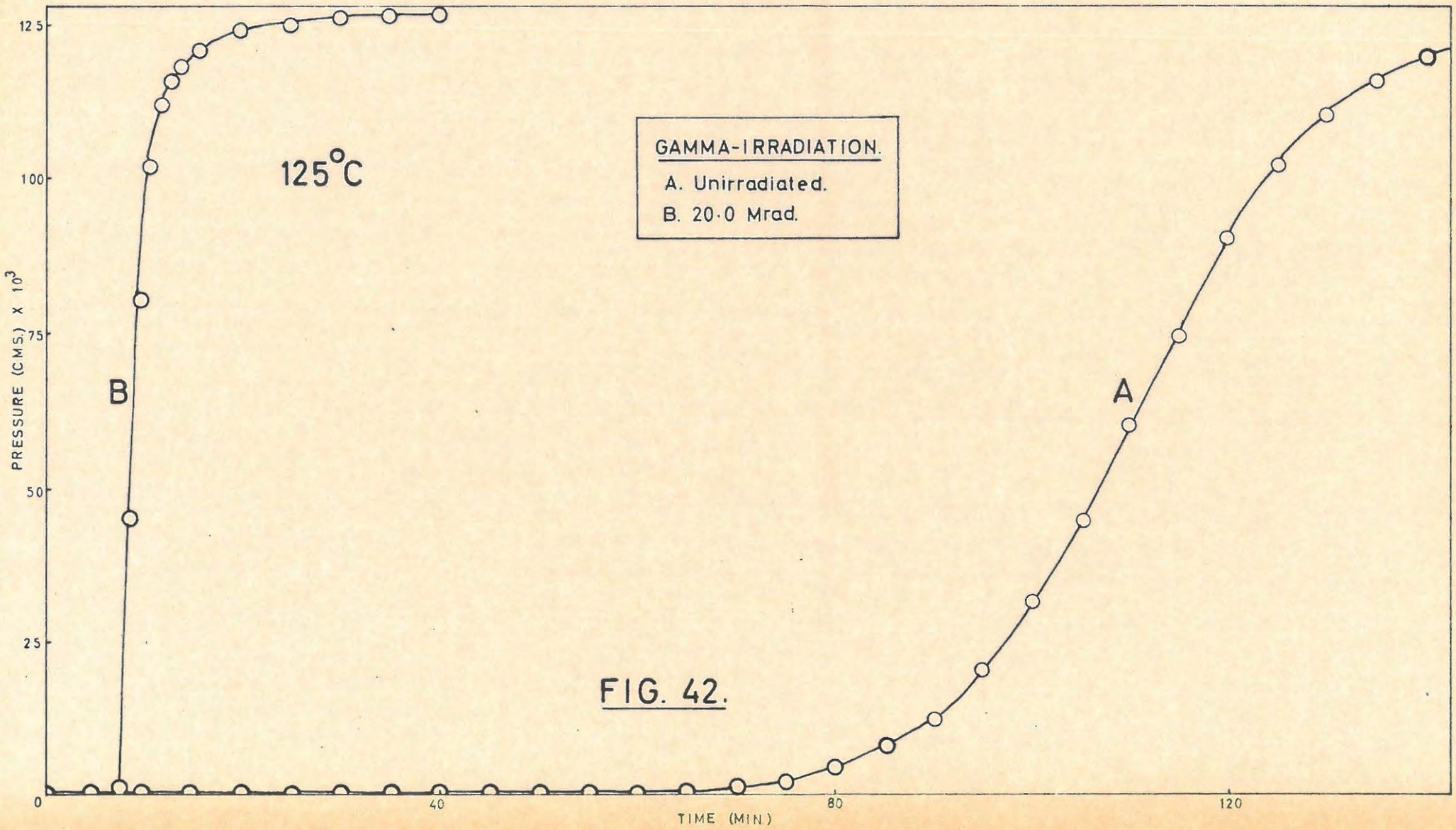
125°C
GAMMA-IRRADIATION.
A. Unirradiated.
B. 20·0 Mrad.
B
A
PRESSURE (CMS.) X 10³
TIME (MIN.)
0
25
50
75
100
125
40
80
120

FIG. 42.

TABLE 48 cont.

t	p	t	p	t	p
50	0.14	100	31.36	160	126.00
55	0.21	105	44.86	170	126.61
60	0.29	110	59.53	p_f	127.20
65	0.73	115	74.88	p_a	121.50

125°C 20 Mrad.		Run 2.			6.3 mg.
t	p	t	p	t	p
1	0.04	8	0.37	16	121.71
2	0.07	9	45.79	20	124.14
3	0.12	10	80.18	25	125.67
4	0.14	11	102.34	30	126.43
5	0.16	12	112.25	p_f	127.20
6	0.19	13	116.64	p_a	118.69
7	0.22	14	118.86		

(ii) Effects of air, nitrogen and argon.

Decompositions were done on samples where the ampoules had been opened in air, dry nitrogen, and dry argon, respectively. No difference in the subsequent decompositions was found. The dose given was 1 Mrad and the decomposition temperature was 110°C. The results appear in TABLE 49.

TABLE 49.

110°C 1 Mrad.		Run 1.		Argon.	6.5 mg.
t	p	t	p	t	p
10	0.38	60	8.28	105	107.56
20	0.53	65	13.38	110	115.77
25	0.62	70	20.82	115	120.85
30	0.87	75	31.36	120	122.98
35	0.99	80	45.09	130	125.45
40	1.19	85	59.30	140	126.62
45	1.82	90	72.32	p_f	127.20
50	3.02	95	85.68	p_a	126.68
55	4.97	100	97.58		

TABLE 49 cont/.....

TABLE 49 cont.

110°C 1 Mrad.		Run 2.		Nitrogen.	6.4 mg.
t	p	t	p	t	p
10	0.12	60	8.06	105	109.22
20	0.18	65	13.80	110	116.08
25	0.41	70	21.18	115	119.70
30	0.63	75	32.86	120	122.40
35	0.72	80	46.51	130	125.42
40	0.86	85	62.54	140	126.61
45	1.43	90	78.09	p_f	127.20
50	2.54	95	90.76	p_a	120.93
55	4.76	100	101.60		

110°C 1 Mrad.		Run 3.		Air.	6.5 mg.
t	p	t	p	t	p
10	0.19	60	7.93	105	108.02
20	0.23	65	12.87	110	115.21
25	0.35	70	18.99	115	119.96
30	0.59	75	30.02	120	122.14
35	0.81	80	43.78	130	125.41
40	1.02	85	57.82	140	126.68
45	1.45	90	71.41	p_f	127.20
50	2.87	95	85.01	p_a	118.10
55	4.12	100	97.65		

(iii) Effect of varying doses of γ-rays.

The effect of an increasing dose of γ-rays on the subsequent thermal decomposition is given in TABLE 50 and shown graphically in FIGURE 43. All irradiations in this series were done in the Co^{60} source at Wantage. The decomposition temperature was 110°C throughout the series. Doses ranged from 1,000 rad to 20 Mrad. A marked decrease in the induction period and an increase in the acceleratory and decay rate constants, k_3 and k_7 (equation 8 and 2), are the main consequences of increasing the dose. TABLE 51 lists these effects.

A further feature is a decrease of the inflexion point of the p/t plot with increasing dose. This is well illustrated

in FIGURE 44/.....

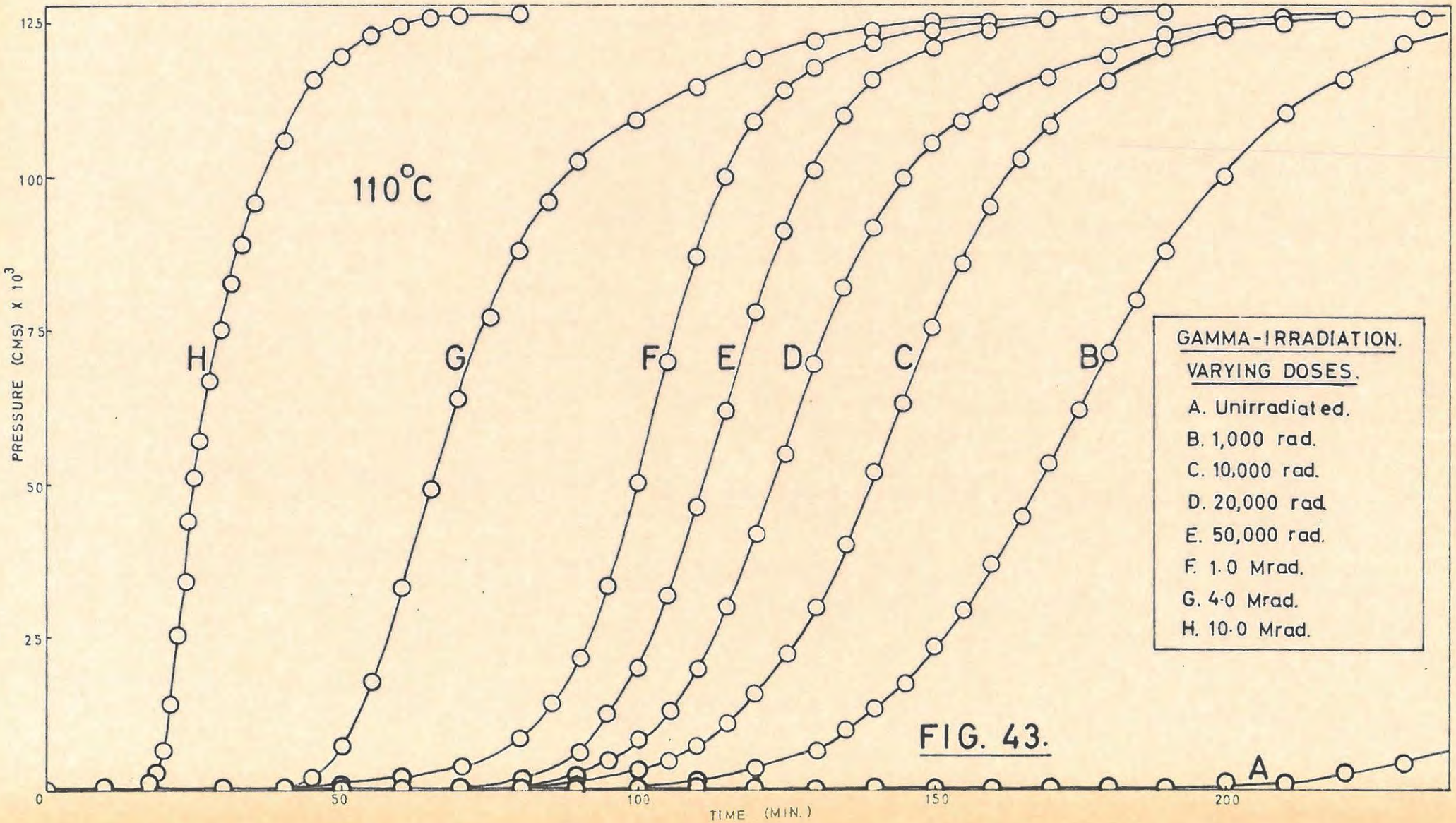
110°C
H
G
F
E
D
C
B
A
GAMMA-IRRADIATION.
VARYING DOSES.
A. Unirradiated.
B. 1,000 rad.
C. 10,000 rad.
D. 20,000 rad.
E. 50,000 rad.
F. 1·0 Mrad.
G. 4·0 Mrad.
H. 10·0 Mrad.
PRESSURE (CMS) X 10³
TIME (MIN.)
0
25
50
75
100
125
50
100
150
200

FIG. 43.

in FIGURE 44, which shows the p/t plot for the decomposition of a sample after a dose of 20 Mrad. The mathematical analysis of the plot is also shown.

TABLE 50.

110°C Unirradiated blank. Run 1.					6.7 mg.
t	p	t	p	t	p
30	0.06	235	6.71	320	82.15
60	0.09	240	8.49	330	90.47
90	0.09	245	10.96	340	96.73
120	0.13	250	13.76	350	102.70
140	0.20	255	17.08	360	107.29
160	0.30	260	20.99	370	111.99
170	0.41	265	25.30	380	115.17
180	0.50	270	30.01	390	117.32
190	0.90	275	35.12	400	118.94
200	1.31	280	40.63	420	121.67
205	1.68	285	46.21	440	124.64
210	2.01	290	51.43	460	126.11
215	2.46	295	56.92	480	126.67
220	3.12	300	62.70	p_f	127.20
225	4.07	305	68.34	p_a	131.98
230	5.36	310	73.36		

110°C 1000 rad. Run 2.					6.4 mg.
t	p	t	p	t	p
20	0.02	145	17.61	200	100.55
40	0.03	150	23.26	210	110.62
60	0.06	155	29.40	220	116.43
80	0.10	160	36.92	230	121.18
100	0.50	165	44.56	240	123.60
110	1.44	170	53.33	250	124.81
120	3.21	175	62.44	260	125.42
130	6.84	180	71.35	280	126.64
135	9.82	185	79.88	p_f	127.20
140	13.32	190	87.86	p_a	114.75

TABLE 50 cont/.....

TABLE 50 cont.

110°C	10,000 rad.	Run 3.			6.5 mg.
t	p	t	p	t	p
20	0.02	115	11.08	165	103.03
40	0.03	120	16.01	170	108.55
50	0.05	125	22.33	180	116.52
60	0.07	130	30.60	190	121.21
70	0.16	135	40.84	200	124.18
80	0.29	140	51.79	210	125.38
90	1.15	145	63.60	240	126.59
100	3.14	150	75.69	p_f	127.20
105	4.61	155	85.82	p_a	118.10
110	7.21	160	95.01		

110°C	20,000 rad.	Run 4.			6.8 mg.
t	p	t	p	t	p
20	0.03	105	12.93	155	109.43
30	0.05	110	20.10	160	112.38
40	0.06	115	30.37	170	116.38
50	0.08	120	41.83	180	119.44
60	0.10	125	55.13	200	123.54
70	0.35	130	69.88	220	125.62
80	0.78	135	82.08	240	126.47
90	2.59	140	91.65	p_f	127.20
95	5.02	145	99.88	p_a	138.00
100	8.38	150	105.56		

110°C	50,000 rad	Run 5.			6.4 mg.
t	p	t	p	t	p
10	0.01	95	12.55	140	116.43
20	0.01	100	20.46	150	121,18
30	0.03	105	31,51	160	124.81
40	0.05	110	46.40	170	126.03
50	0.09	115	62.44	180	126.64
60	0.14	120	77.94	p_f	127.20
70	0.61	125	91.47	p_a	114.75
80	1.64	130	101.64		
90	6.56	135	110.05		

TABLE 50 cont/.....

TABLE 50 cont

110°C	1.0 Mrad.	Run 6.			6.3 mg.
t	p	t	p	t	p
10	0.18	85	14.54	125	114.90
20	0.30	90	21.78	130	118.36
30	0.41	95	33.79	140	122.45
40	0.58	100	50.31	150	124.12
50	1.13	105	70.10	160	125.42
60	2.39	110	87.10	180	126.42
70	4.11	115	100.52	p_f	127.20
80	8.92	120	109.25	p_a	119.79

110°C	4.0 Mrad.	Run 7.			6.2 mg.
t	p	t	p	t	p
5	0.05	55	18.07	100	109.85
10	0.13	60	33.49	110	114.86
15	0.28	65	49.47	120	119.33
20	0.48	70	64.49	130	122.59
30	0.68	75	77.41	140	124.55
40	0.89	80	88.15	160	126.33
45	2.18	85	96.06	p_f	127.20
50	7.38	90	103.15	p_a	121.49

110°C	20 Mrad.	Run 8.			6.7 mg.
t	p	t	p	t	p
5	0.01	22	25.93	40	106.80
10	0.10	23	34.96	45	116.24
12	0.25	24	44.32	50	120.57
14	0.48	25	51.54	55	123.06
15	0.63	26	57.77	60	124.96
16	0.71	27	63.20	65	126.08
17	0.89	28	67.61	70	126.64
18	1.42	30	75.60	p_f	127.20
19	2.69	32	82.67	p_a	135.57
20	6.41	34	89.58		
21	14.64	36	95.33		

TABLE 51/.....

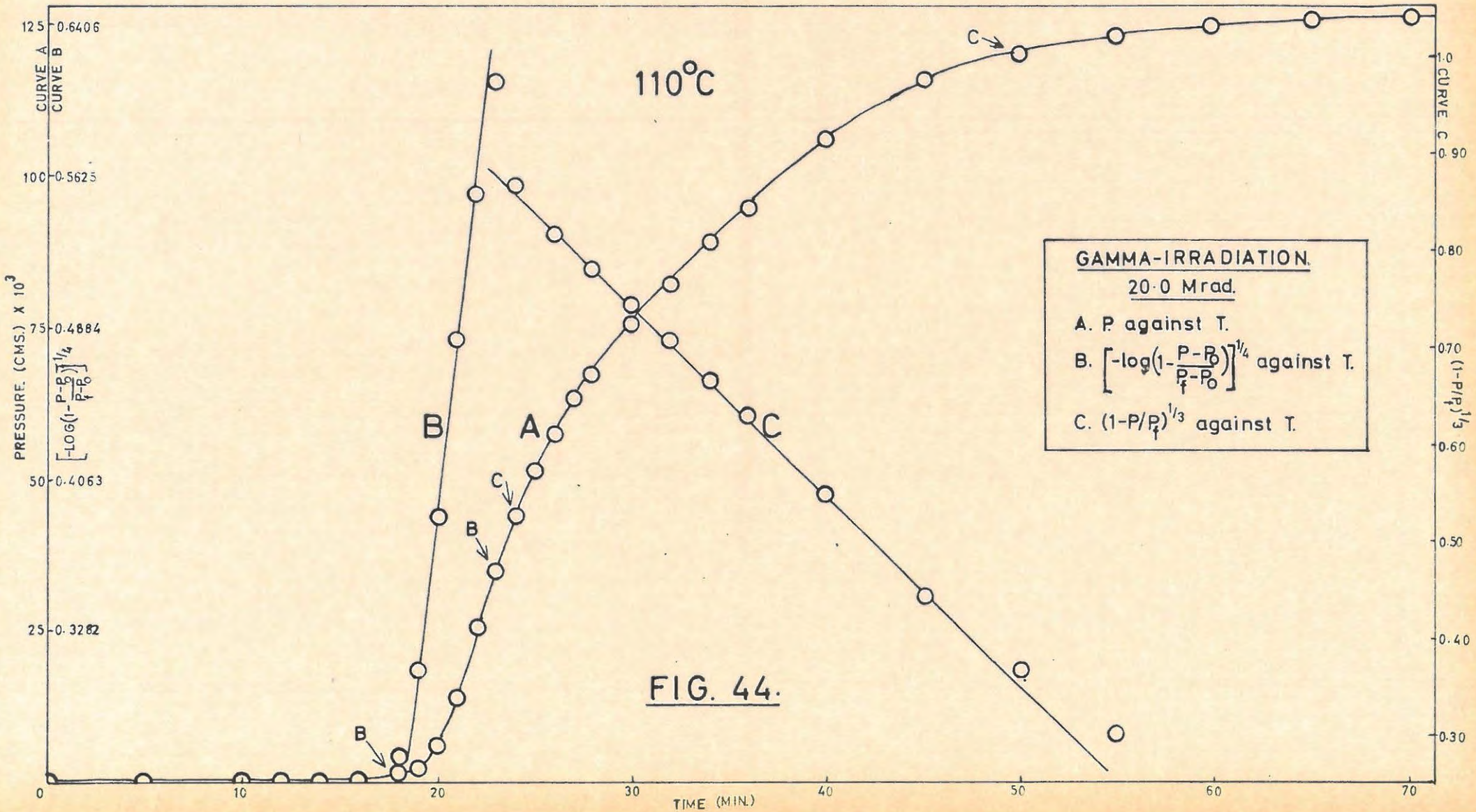
110°C
GAMMA-IRRADIATION.
20·0 Mrad.
A. P against T.
B. $\left[-\log\left(1-\frac{P-P_0}{P_f-P_0}\right)\right]^{1/4}$ against T.
C. $(1-P/P_f)^{1/3}$ against T.
PRESSURE. (CMS.) X 10^3
CURVE A
CURVE B
CURVE C
$\left[-LOG\left(1-\frac{P-P_0}{P_f-P_0}\right)\right]^{1/4}$
$(1-P/P_f)^{1/3}$
TIME (MIN.)
A
B
C
0
10
20
30
40
50
60
70
25
50
75
100
125
0.3282
0.4063
0.4884
0.5625
0.6406
0.30
0.40
0.50
0.60
0.70
0.80
0.90
1.0

FIG. 44.

TABLE 51.

Dose.	Induction period min.	k_3 min^{-1}	k_7 min^{-1}
0	185	5.220×10^{-3}	4.400×10^{-3}
1,000 rad	102	7.610×10^{-3}	8.300×10^{-3}
10,000 rad	85	9.500×10^{-3}	1.095×10^{-2}
20,000 rad	78	1.085×10^{-2}	1.105×10^{-2}
50,000 rad	70	1.385×10^{-2}	1.440×10^{-2}
1.0 Mrad	42	1.550×10^{-2}	1.662×10^{-2}
4.0 Mrad	30	1.920×10^{-2}	1.070×10^{-2}
20.0 Mrad	15	8.30×10^{-2}	1.88×10^{-2}

(iv) Effect of interrupting a thermal decomposition and irradiating the salt.

The method used and precautions taken in performing this type of experiment are described elsewhere. It has also been pointed out that it is impossible to prevent water vapour from coming out of the walls of the ampoule. The vapour reacts with any metal present at the point of interruption and this affects the subsequent decomposition.

Interruptions were done at five points on the p/t plots as shown in FIGURE 45. The decomposition temperature was 110°C and the γ-ray dose 4.0 Mrad. The results obtained are tabulated in TABLE 52 and shown in FIGURE 45.

TABLE 52.

110°C Unirradiated blank. Run 1.					6.2 mg.
t	p	t	p	t	p
20	0.02	210	4.79	310	82.04
40	0.03	220	7.25	320	90.99
60	0.05	230	10.76	330	98.09
80	0.11	240	15.87	340	104.29
100	0.15	250	22.21	380	119.93
120	0.20	260	30.24	400	123.43
140	0.25	270	39.49	420	125.31
160	0.43	280	49.98	460	126.57
180	1.14	290	61.71	p_f	127.20
200	3.02	300	72.74	p_a	121.41

TABLE 52 cont/.....

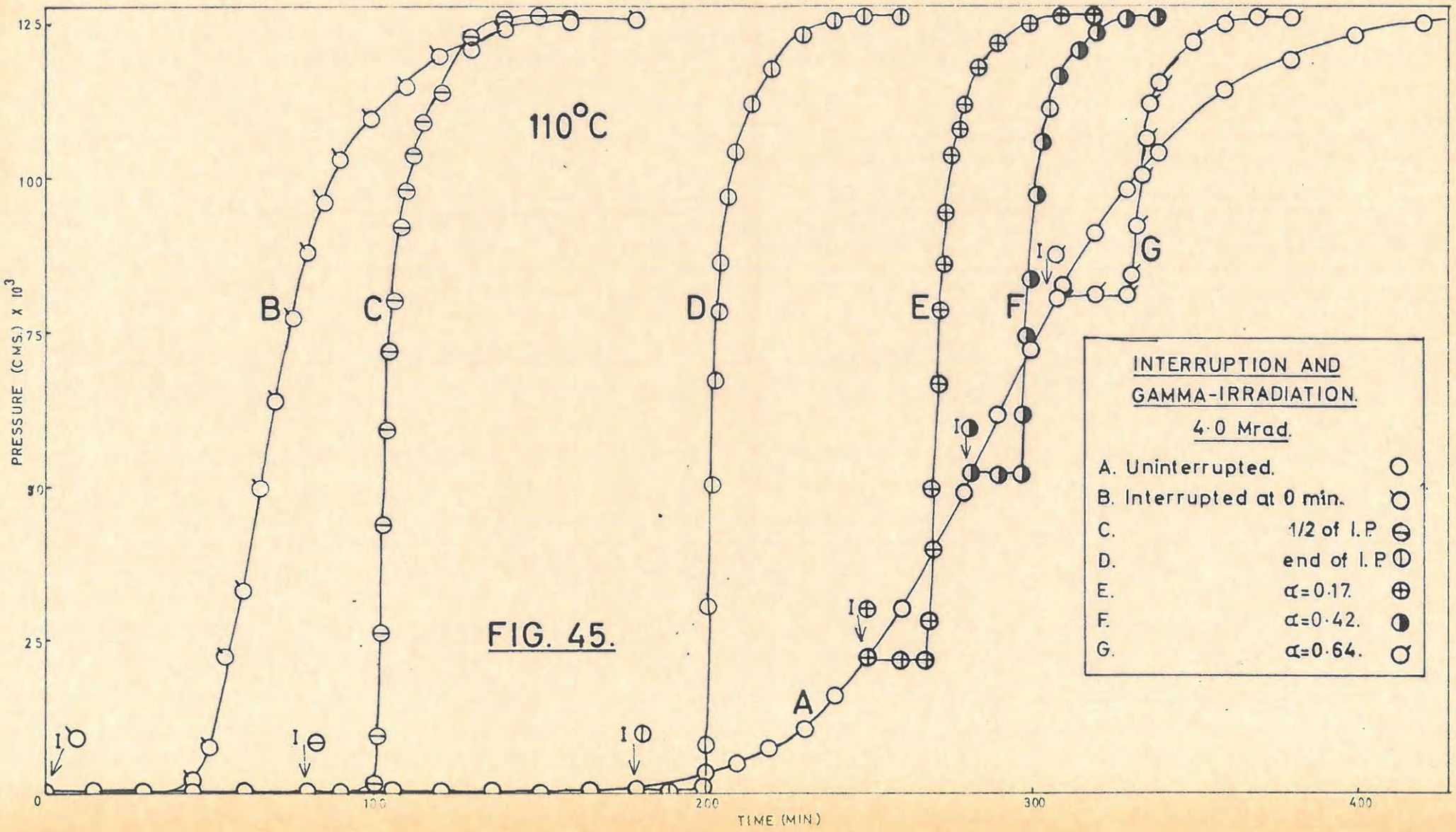
110°C
B
C
D
E
F
G
A
I
PRESSURE (CMS.) X 10³
TIME (MIN)
0
25
50
75
100
125
100
200
300
400
INTERRUPTION AND
GAMMA-IRRADIATION.
4·0 Mrad.
A. Uninterrupted.
B. Interrupted at 0 min.
C. 1/2 of I.P
D. end of I.P
E. α=0·17.
F. α=0·42.
G. α=0·64.

FIG. 45.

TABLE 52 cont.

110°C 4.0 Mrad.		Run 2.			6.5 mg.
t	p	t	p	t	p
20	0.06	100	1.81	110	98.65
40	0.07	101	9.72	112	104.19
60	0.09	102	26.36	115	109.24
80	0.13	103	43.57	120	114.41
Irradiation		104	59.78	130	121.04
90	0.13	105	72.18	140	125.11
95	0.17	106	80.73	150	126.48
98	0.30	107	86.88	p_f	127.20
99	0.73	108	92.08	p_a	112.48

110°C 4.0 Mrad.		Run 3.			6.5 mg.
t	p	t	p	t	p
60	0.12	198	0.46	208	97.88
100	0.16	199	0.50	210	104.39
140	0.23	200	1.25	215	112.36
160	0.31	201	8.84	220	118.05
180	0.45	202	30.97	230	123.22
Irradiation		203	50.35	240	125.18
185	0.45	204	67.00	250	126.52
190	0.45	205	78.55	p_f	127.20
195	0.46	206	86.57	p_a	113.82

110°C 4.0 Mrad.		Run 4.			6.5 mg.
t	p	t	p	t	p
60	0.08	255	21.48	278	108.95
100	0.13	260	21.57	280	112.35
140	0.27	265	21.65	285	118.16
180	0.98	268	22.08	290	122.33
200	2.51	269	27.47	295	124.14
210	3.72	270	49.28	300	125.36
220	6.26	271	66.58	310	126.46
230	10.14	272	78.52	p_f	127.20
240	15.01	273	86.97	p_a	111.45
250	21.42	274	93.94		
Irradiation		276	103.43		

TABLE 52 cont/.....

TABLE 52 cont.

110°C	4.0 Mrad.		Run 5.		6.5 mg.
t	p	t	p	t	p
60	0.12	270	43.12	302	97.40
100	0.17	280	53.56	304	106.05
140	0.41	Irradiation		306	111.55
180	1.58	290	54.07	310	117.14
200	4.13	295	54.63	315	121.61
220	8.24	297	55.45	320	124.37
230	12.01	298	61.95	325	125.77
240	17.32	299	74.53	330	126.71
250	24.79	300	83.38	p_f	127.20
260	33.81	301	91.41	p_a	118.31

110°C	4.0 Mrad.		Run 6.		6.5 mg.
t	p	t	p	t	p
60	0.09	310	81.95	335	102.24
120	0.26	Irradiation		336	106.20
180	1.02	315	82.04	338	112.15
220	7.98	320	82.18	340	115.54
240	17.62	325	82.31	345	119.84
260	31.88	330	83.05	350	122.48
270	40.86	331	83.69	360	125.59
280	50.13	332	87.72	370	126.79
290	62.01	333	92.27	p_f	127.20
300	72.81	334	97.42	p_a	115.54

At all points on the p/t plot interruption and irradiation of the salt results in a new, short, induction period followed by a period of extremely rapid acceleration. The short induction period is almost certainly due to water vapour effects. Confirmation of this was obtained by carrying out a decomposition where water vapour was deliberately admitted onto the sample at the point of interruption. Irradiation was then carried out. The resultant decomposition was exactly the same as in the runs without water admission as can be seen in TABLE 53 and FIGURE 46. In addition a sample of partially

decomposed salt/.....

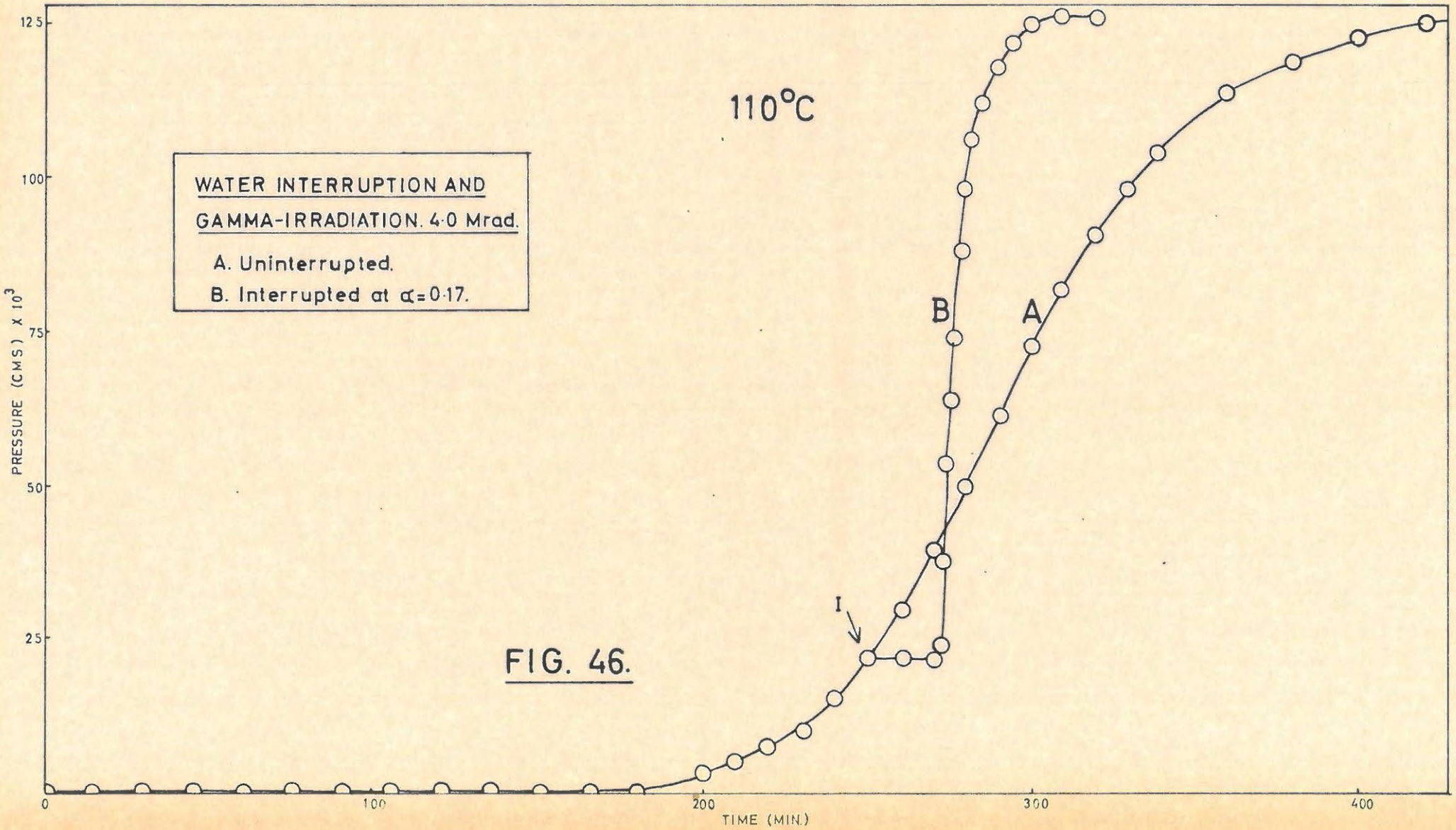
110°C
WATER INTERRUPTION AND
GAMMA-IRRADIATION. 4·0 Mrad.
A. Uninterrupted.
B. Interrupted at α=0·17.
B
A
I
PRESSURE (CMS) X 10³
TIME (MIN.)
125
100
75
50
25
0
100
200
300
400

FIG. 46.

decomposed salt kept in a sealed evaucated ampoule turned white after 1 week, whereas one kept open in the high vacuum line with continuous pumping and liquid air traps in position for fourteen days remained black.

TABLE 53.

110°C 4.0 Mrad. Run 1. Water vapour. 6.5 mg.					
t	p	t	p	t	p
60	0.08	269	21.56	280	98.91
120	0.14	270	21.71	282	106.07
180	0.83	271	22.06	285	112.53
220	6.17	272	23.95	290	118.70
230	10.02	273	38.53	295	122.93
240	14.88	274	53.62	300	125.08
250	21.40	275	64.66	310	126.71
Irradiation		276	73.81	p_f	127.20
260	21.45	277	82.19	p_a	122.21
265	21.47	278	88.98		

(v) Effect of admitting water vapour onto the salt in an interrupted decomposition.

"Water interruptions" were performed at several stages in the decomposition. The γ-ray dose for irradiation was 4.0 Mrad, and the decomposition temperature was 110°C.

The effect of "water interruption" is to produce a new induction period at the point of interruption which is longer than the normal induction for the decomposition of the irradiated salt. As the value of α at which the interruption is performed increases, so does the duration of the induction period. Rate constants, k_3, (equation 8) for the reaction are reduced. Interruption in the decay period virtually destroys the reaction.

Interruption at the end of the induction period followed by repeated interruption at the end of each new induction period formed, results in a progressive increase in the length of this period, until eventually the unirradiated induction

period is/.....

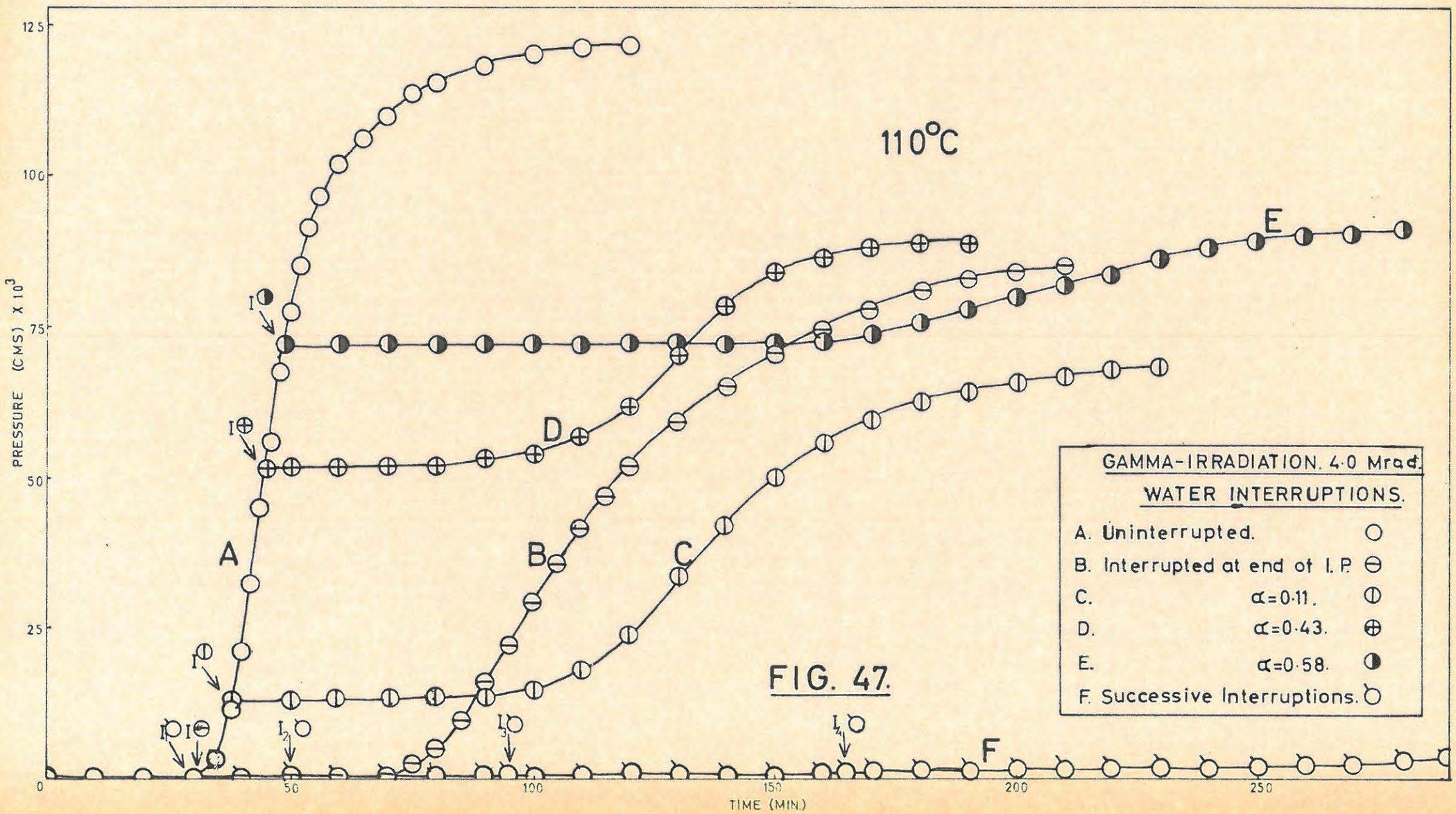
110°C
PRESSURE (CMS) X 10³
TIME (MIN.)
125
100
75
50
25
0
50
100
150
200
250
A
B
C
D
E
F
I
I
I
I
I₂
I₃
I₄
GAMMA-IRRADIATION. 4·0 Mrad.
WATER INTERRUPTIONS.
A. Uninterrupted.
B. Interrupted at end of I. P.
C. α=0·11.
D. α=0·43.
E. α=0·58.
F. Successive Interruptions.

FIG. 47.

period is reached.

Final pressures were always lower than normal but the residual gas was evolved if the residue was heated to 300°C in vacuo.

These results are given in TABLE 54 and appear graphically in FIGURE 47. TABLE 55 gives the rate constants obtained and the lengths of the induction periods. Pressures are not normalised.

TABLE 54.

110°C 4.0 Mrad. Run 1. Blank run. 6.5 mg.					
t	p	t	p	t	p
10	0.07	46	56.73	70	110.98
20	0.13	48	67.89	75	113.77
30	0.61	50	77.19	80	115.63
35	3.42	52	85.25	90	118.73
38	11.14	54	91.45	100	120.28
40	21.39	56	96.41	110	121.37
42	32.87	60	102.44	120	121.83
44	44.95	65	106.64	p_a	122.45

110°C 4.0 Mrad. Run 2. 6.4 mg.					
t	p	t	p	t	p
10	0.07	80	5.18	140	65.59
20	0.29	85	9.96	150	70.72
30	0.47	90	16.08	160	74.69
Water Interruption		95	22.91	170	78.31
40	0.48	100	29.52	180	81.08
50	0.49	105	35.72	190	82.95
60	0.51	110	41.84	200	84.37
65	0.54	115	47.37	210	85.33
70	0.77	120	51.74	p_a	85.81
75	2.09	130	59.06		

110°C 4.0 Mrad. Run 3. 6.5 mg.					
t	p	t	p	t	p
10	0.10	90	13.63	190	64.12
20	0.22	95	14.19	200	65.99
30	0.87	100	15.07	210	67.12

TABLE 54 cont/.....

TABLE 54 cont.

t	p	t	p	t	p
35	4.07	110	18.19	220	67.88
38	13.12	120	24.09	230	68.65
Water Interruption		130	33.93	240	69.43
45	13.13	140	42.09	250	70.21
50	13.13	150	50.41	260	70.99
60	13.14	160	55.98	p_a	71.79
70	13.17	170	59.78		
80	13.25	180	62.29		

110°C 4.0 Mrad. Run 4. 6.3 mg.					
t	p	t	p	t	p
10	0.10	Water Interruption		120	62.74
20	0.15	50	52.14	130	71.01
30	0.87	60	52.16	140	78.39
35	8.70	70	52.27	150	83.35
38	21.49	80	52.57	160	85.71
40	32.11	90	53.29	170	87.22
42	42.52	100	54.52	p_a	87.57
44	52.11	110	57.07		

110°C 4.0 Mrad. Run 5. 6.4 mg.					
t	p	t	p	t	p
10	0.07	Water Interruption		170	74.38
20	0.21	60	70.73	180	75.90
30	0.77	70	70.73	190	78.10
35	3.10	80	70.76	200	80.36
38	9.64	90	70.78	210	82.56
40	18.70	100	70.82	220	84.60
42	28.41	110	70.93	230	86.59
44	38.88	120	71.13	240	88.07
46	49.17	130	71.40	250	88.94
48	58.66	140	71.79	260	89.61
50	66.85	150	72.39	270	90.06
51	70.72	160	73.13	p_a	90.29

110°C 4.0 Mrad. Run 6. 6.3 mg.					
t	p	t	p	t	p
10	0.13	120	1.83	290	3.48
20	0.42	130	1.85	300	4.29

TABLE 54 cont/.....

TABLE 54 cont.

t	p	t	p	t	p
25	0.60	140	1.89	310	5.60
Water Interruption		150	1.94	320	7.71
40	0.65	155	2.02	330	10.81
45	0.73	160	2.13	340	15.34
50	1.21	165	2.41	350	21.08
Water Interruption		Water Interruption		360	27.35
60	1.23	180	2.42	370	33.36
70	1.25	200	2.43	380	38.45
80	1.27	220	2.43	390	42.60
85	1.34	240	2.48	400	43.61
90	1.47	250	2.54	420	48.90
95	1.81	260	2.63	440	54.90
Water Interruption		270	2.86	460	57.17
110	1.83	280	3.10	p_a	57.94

TABLE 55.

Point of Interruption.	k_3 min^{-1}	Induction Period min.	Number of Interruptions.	Induction Period min.
Uninterrupted	4.00×10^{-2}	30	0	25
End of I.P.	1.350×10^{-2}	40	1	25
$\alpha = 0.11$	1.150×10^{-2}	53	2	45
$\alpha = 0.43$	1.275×10^{-2}	40	3	70
$\alpha = 0.58$	6.05×10^{-3}	80	4	115
4 consecutive	5.95×10^{-3}	115		

(vi) Effect of thermal annealing.

An irradiated (0.25 Mrad) specimen was thermally annealed at 70°C for 2 hours in vacuo before being decomposed at 110°C. TABLE 56 shows that this has no effect on the subsequent decomposition.

TABLE 56.

110°C 0.25 Mrad. Run 1. Annealed 2 hrs. 70°C 6.5 mg.					
t	p	t	p	t	p
20	0.11	135	26.26	190	111.98
40	0.22	140	34.20	200	116.75
60	0.38	145	43.51	210	119.77

TABLE 56 cont/.....

TABLE 56 cont.

t	p	t	p	t	p
80	0.70	150	54.05	220	121.61
100	1.64	155	65.22	240	124.08
110	3.48	160	74.53	260	125.32
115	5.47	165	83.74	280	126.57
120	8.55	170	92.30	p_f	127.20
125	13.31	175	98.24	p_a	118.63
130	19.36	180	103.88		

110°C 0.25 Mrad. Run 2. Blank run 6.4 mg.					
t	p	t	p	t	p
20	0.11	135	23.77	190	111.68
40	0.19	140	31.21	200	118.46
60	0.33	145	39.34	210	121.93
80	0.71	150	48.40	220	124.27
100	1.74	155	57.60	240	126.04
110	3.80	160	66.74	260	126.69
115	5.63	165	76.55	p_f	127.20
120	8.56	170	85.56	p_a	122.64
125.	12.28	175	94.56		
130	17.78	180	101.34		

(vii) Effect of varying the temperature of decomposition.

Two irradiation doses, viz. 0.5 Mrad and 4.0 Mrad, were chosen and the critical increments for thermal decomposition were determined. Decompositions were carried out over a range of temperatures (100° - 125°C) and the rate constants, k_3 and k_7, (equation 8 and 2) determined at each temperature. The p/t values are given in TABLE 57 and the derived rate constants in TABLE 58.

TABLE 57.

100°C 0.5 Mrad. Run 1. 6.3 mg.					
t	p	t	p	t	p
30	0.03	220	5.57	330	75.74
60	0.11	230	8.35	340	83.07
80	0.25	240	11.87	350	90.17
100	0.35	250	16.23	360	95.65

TABLE 57 cont/.....

TABLE 57 cont.

t	p	t	p	t	p
120	0.42	260	21,01	380	106.23
140	0.89	270	27.28	400	112.06
160	1.24	280	34,04	440	119.78
180	1.78	290	41,55	480	125.38
190	2.25	300	49,80	500	126.24
200	2.87	310	57,96	p_f	127.20
210	4.00	320	67,81	p_a	123.72

105°C 0.5 Mrad. Run 2. 6.3 mg.					
t	p	t	p	t	p
30	0.02	145	6.39	230	97.84
60	0.33	150	8.51	240	105.68
70	0.48	155	11.12	250	112.06
80	0.59	160	14.28	260	116.22
90	0.67	170	23.37	280	121.06
100	0.98	180	33.42	300	124.14
110	1.29	190	46.71	p_f	127.20
120	1.93	200	60.52	p_a	117.56
130	2.88	210	74.19		
140	4.81	220	86.63		

110°C 0.5 Mrad. Run 3. 6.4 mg.					
t	p	t	p	t	p
20	0.15	100	6.34	140	108.23
40	0.33	105	10.44	145	112.83
60	0.66	110	17.78	150	116.35
70	1.08	115	31.19	160	120.52
80	1.52	120	50.28	170	122.23
85	1.87	125	71.10	210	125.99
90	2.70	130	87.66	p_f	127.20
95	4.10	135	100.95	p_a	129.62

115°C 0.5 Mrad. Run 4. 6.2 mg.					
t	p	t	p	t	p
20	0.11	80	9.42	100	89.94
30	0.34	82	12.33	105	106.36
40	0.60	84	17.43	110	115.09
50	0.88	86	24.49	115	119.88

TABLE 57 cont/.....

TABLE 57 cont.

t	p	t	p	t	p
60	1.35	88	33.39	120	122.23
70	2.75	90	44.03	140	126.64
75	4.77	92	55.32	p_f	127.20
78	6.90	95	69.72	p_a	123.79

120°C 0.5 Mrad. Run 5. 6.4 mg.					
t	p	t	p	t	p
20	0.26	60	11.89	78	100.69
30	0.62	62	17.50	80	107.03
40	1.03	64	25.60	85	117.81
45	1.41	66	36.25	90	123.40
50	2.33	68	49.14	95	125.29
52	2.88	70	62.19	100	126.56
54	4.09	72	73.35	p_f	127.20
56	5.64	74	83.87	p_a	126.10
58	7.99	76	93.45		

125°C 0.50 Mrad. Run 6. 6.5 mg.					
t	p	t	p	t	p
10	0.04	43	22.04	52	100.22
20	0.29	44	31.20	54	110.18
30	0.89	45	41.96	56	116.50
35	1.82	46	53.08	60	122.40
38	3.88	47	62.94	65	125.98
40	6.85	48	71.79	p_f	127.20
41	10.48	49	80.26	p_a	120.36
42	15.10	50	87.67		

105°C 4.0 Mrad. Run 7. 6.4 mg.					
t	p	t	p	t	p
5	0.01	65	3.95	140	80.16
10	0.03	70	9.05	150	88.70
15	0.06	75	13.76	160	96.16
20	0.08	80	18.50	180	109.51
25	0.11	85	23.47	200	117.78
30	0.16	90	29.02	220	122.02
35	0.21	95	34.71	240	124.60

TABLE 57 cont/.....

TABLE 57 cont

t	p	t	p	t	p
40	0.29	100	40.90	260	126.34
45	0.37	105	46.53	p_f	127.20
50	0.52	110	51.97	p_a	115.86
55	0.68	120	61.93		
60	1.87	130	71.39		

110°C 4.0 Mrad. Run 8. 6.2 mg.					
t	p	t	p	t	p
5	0.08	48	16.99	80	98.08
10	0.11	50	22.04	85	106.20
15	0.17	52	27.74	90	112.18
20	0.25	54	34.43	95	116.47
25	0.51	56	40.39	100	118.95
30	0.70	58	46.03	110	121.46
35	2.39	60	51.22	120	123.36
40	4.52	62	56.68	140	125.89
42	6.79	65	64.25	p_f	127.20
44	9.21	70	77.74	p_a	128.44
46	12.60	75	89.24		

115°C 4.0 Mrad. Run 9. 6.4 mg.					
t	p	t	p	t	p
5	0.14	37	22.68	65	94.95
10	0.18	38	25.64	70	104.23
15	0.31	40	31.79	75	110.37
20	0.68	42	37.59	80	115.71
25	2.49	44	43.87	85	119.27
28	3.90	46	49.10	90	122.28
30	5.95	48	54.62	95	124.10
32	9.23	50	60.42	100	125.32
33	11.33	52	65.64	110	126.46
34	13.65	54	70.60	p_f	127.20
35	16.41	56	74.81	p_a	124.26
36	19.66	60	84.58		

TABLE 57 cont/.....

TABLE 57 cont.

120°C 4.0 Mrad Run 10. 6.1 mg.					
t	p	t	p	t	p
5	0.12	26	29.43	50	110.12
10	0.38	28	39.46	55	116.97
15	0.64	30	48.94	60	120.86
20	5.38	32	56.72	65	125.02
22	11.01	35	68.57	70	125.62
23	15.13	40	85.46	p_f	127.20
24	19.59	45	100.60	p_a	115.86

125°C 4.0 Mrad. Run 11. 6.5 mg.					
t	p	t	p	t	p
5	0.31	21	19.96	32	95.63
10	0.51	22	30.23	34	103.74
12	1.13	23	38.65	36	110.20
14	1.48	24	46.39	40	119.58
16	2.15	25	53.91	45	123.71
17	2.84	26	60.52	50	125.10
18	4.25	27	67.01	60	126.51
19	6.40	28	73.28	p_f	127.20
20	11.17	30	84.95	p_a	121.85

TABLE 58

Dose Mrad.	Temperature. °C.	Induction Period (Min.).	k_3 min^{-1}	k_7 min^{-1}
0.5	100°	130	3.825×10^{-3}	7.375×10^{-3}
0.5	105°	90	6.250×10^{-3}	6.250×10^{-3}
0.5	110°	60	1.650×10^{-2}	1.020×10^{-2}
0.5	115°	40	2.420×10^{-2}	2.100×10^{-2}
0.5	120°	30	2.950×10^{-2}	2.520×10^{-2}
0.5	125°	25	5.250×10^{-2}	3.795×10^{-2}
4.0	105°	55	7.90×10^{-3}	4.650×10^{-3}
4.0	110°	30	1.760×10^{-2}	1.150×10^{-2}
4.0	115°	20	2.350×10^{-2}	1.225×10^{-2}
4.0	120°	15	3.640×10^{-2}	1.700×10^{-2}
4.0	125°	11	6.600×10^{-2}	2.925×10^{-2}

(viii) Percentage/.....

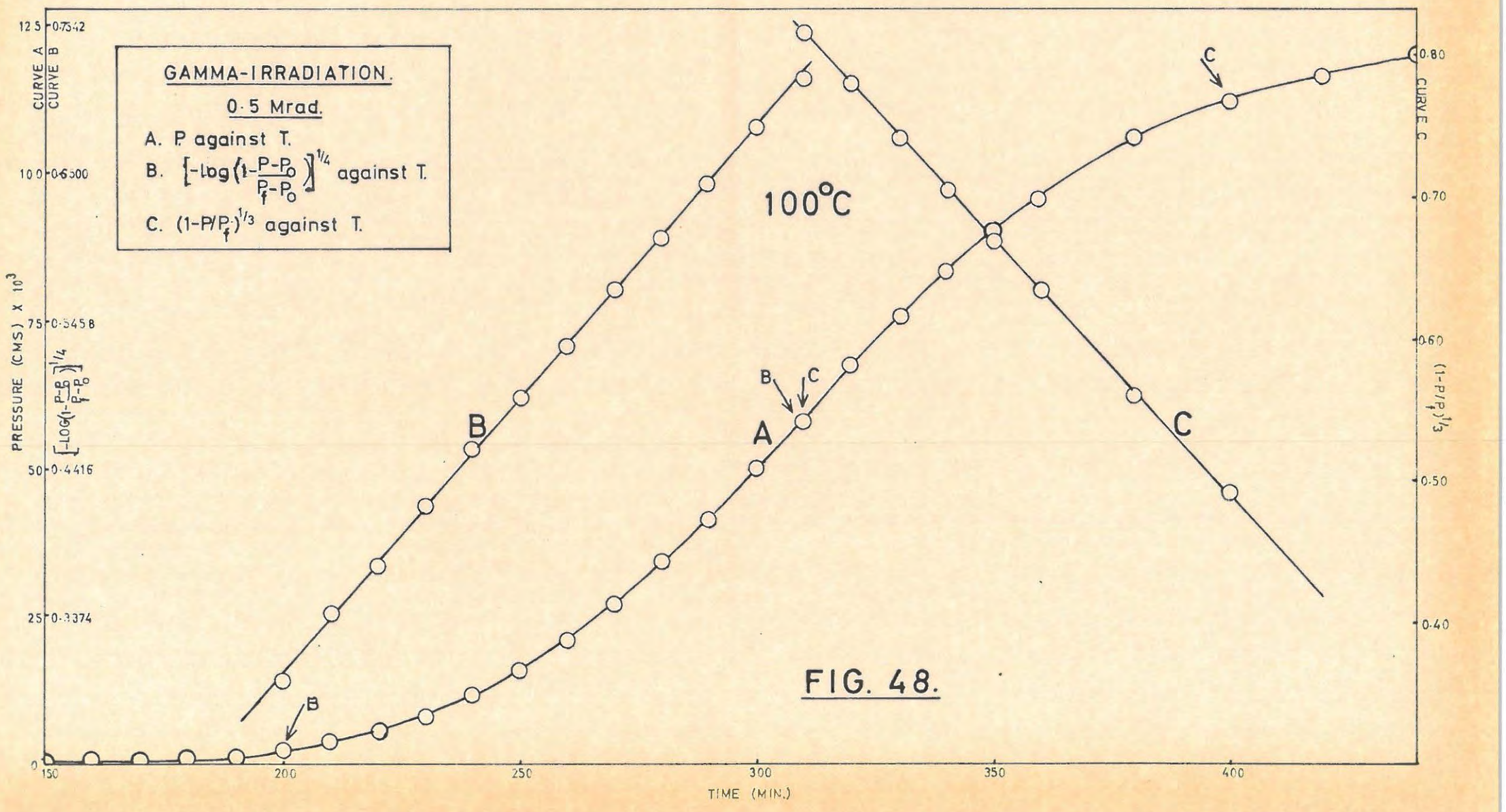
GAMMA-IRRADIATION.
0·5 Mrad.
A. P against T.
B. $\left[-\log\left(1-\frac{P-P_0}{P_f-P_0}\right)\right]^{1/4}$ against T.
C. $(1-P/P_f)^{1/3}$ against T.
100°C
A
B
C
PRESSURE (CMS) X 10^3
CURVE A
CURVE B
CURVE C
$\left[-\log\left(1-\frac{P-P_0}{P_f-P_0}\right)\right]^{1/4}$
$(1-P/P_f)^{1/3}$
TIME (MIN.)
12·5
10·0
7·5
5·0
2·5
0
0·7542
0·6500
0·5458
0·4416
0·3374
0·80
0·70
0·60
0·50
0·40
150
200
250
300
350
400

FIG. 48.

(viii) Percentage decomposition.

The percentage decomposition was approximately the same as for the decomposition of unirradiated barium azide.

(ix) Mathematical analysis of the results and evaluation of activation energies.

The acceleratory period is once again described by the Avrami-Erofeyev equation with n = 4 i.e.

$$\left[-\log\left(1-\frac{p-p_o}{p_f-p_o}\right)\right]^{1/4} = k_3 t + c_3 \quad \ldots\ldots\ldots\ldots (8)$$

The degree of fit is α = 0.03 to α = 0.54 for a dose of 0.5 Mrad.

The decay stage is described by the contracting sphere equation, viz.

$$(1 - {}^{p}/_{p_f})^{1/3} = k_7 t + c_7 \quad \ldots\ldots\ldots\ldots\ldots\ldots (2)$$

The above equations are applicable irrespective of the γ-ray dose used. FIGURE 48 shows the p/t plot for the decomposition of a specimen preirradiated with a dose of 0.50 Mrad. The corresponding analyses are also given.

The Arrhenius plots of log I.P., log k_3 and log k_7 vs $^{1}/_{T}\ ^{o}K$, respectively, gave the following activation energies:

(a) 0.5 Mrad.

(i) Induction period	21.90 kcals.mole^{-1}
(ii) Acceleratory period	28.40 kcals.mole^{-1}
(iii) Decay period	27.00 kcals.mole^{-1}

(b) 4.0 Mrad.

(i) Induction period	20.60 kcals.mole^{-1}
(ii) Acceleratory period	26.80 kcals.mole^{-1}
(iii) Decay period	27.50 kcals.mole^{-1}

FIGURES 49 and 50 show the Arrhenius plots.

6.2. DISCUSSION/.....

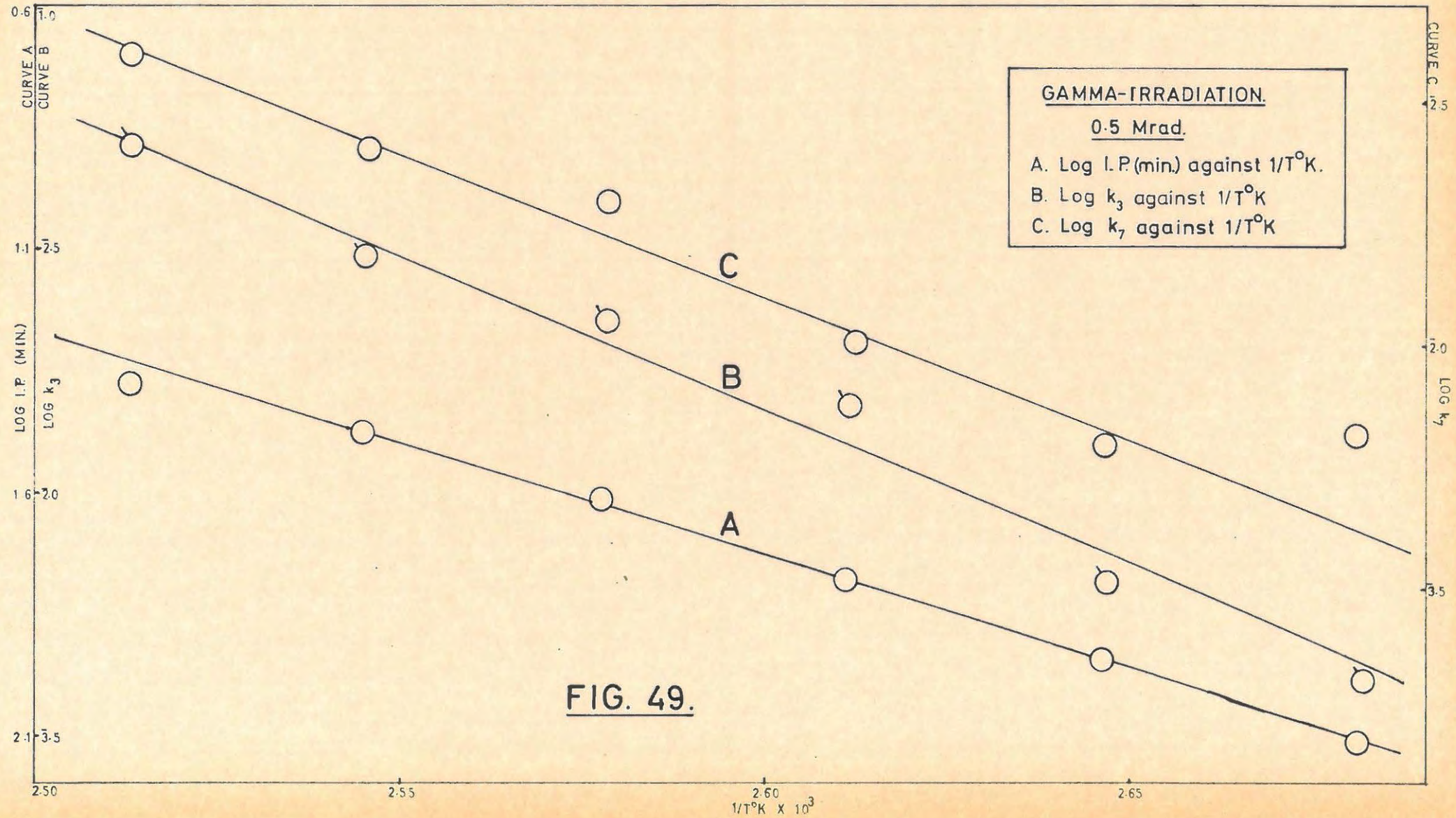
GAMMA-IRRADIATION.
0·5 Mrad.
A. Log I.P.(min.) against 1/T°K.
B. Log k_3 against 1/T°K
C. Log k_7 against 1/T°K
CURVE A
CURVE B
CURVE C
LOG I.P (MIN.)
LOG k_3
LOG k_7
0·6
1·0
1·1
2·5
1·6
2·0
2·1
3·5
2·0
2·5
3·5
C
B
A
2·50
2·55
2·60
2·65
1/T°K X 10^3

FIG. 49.

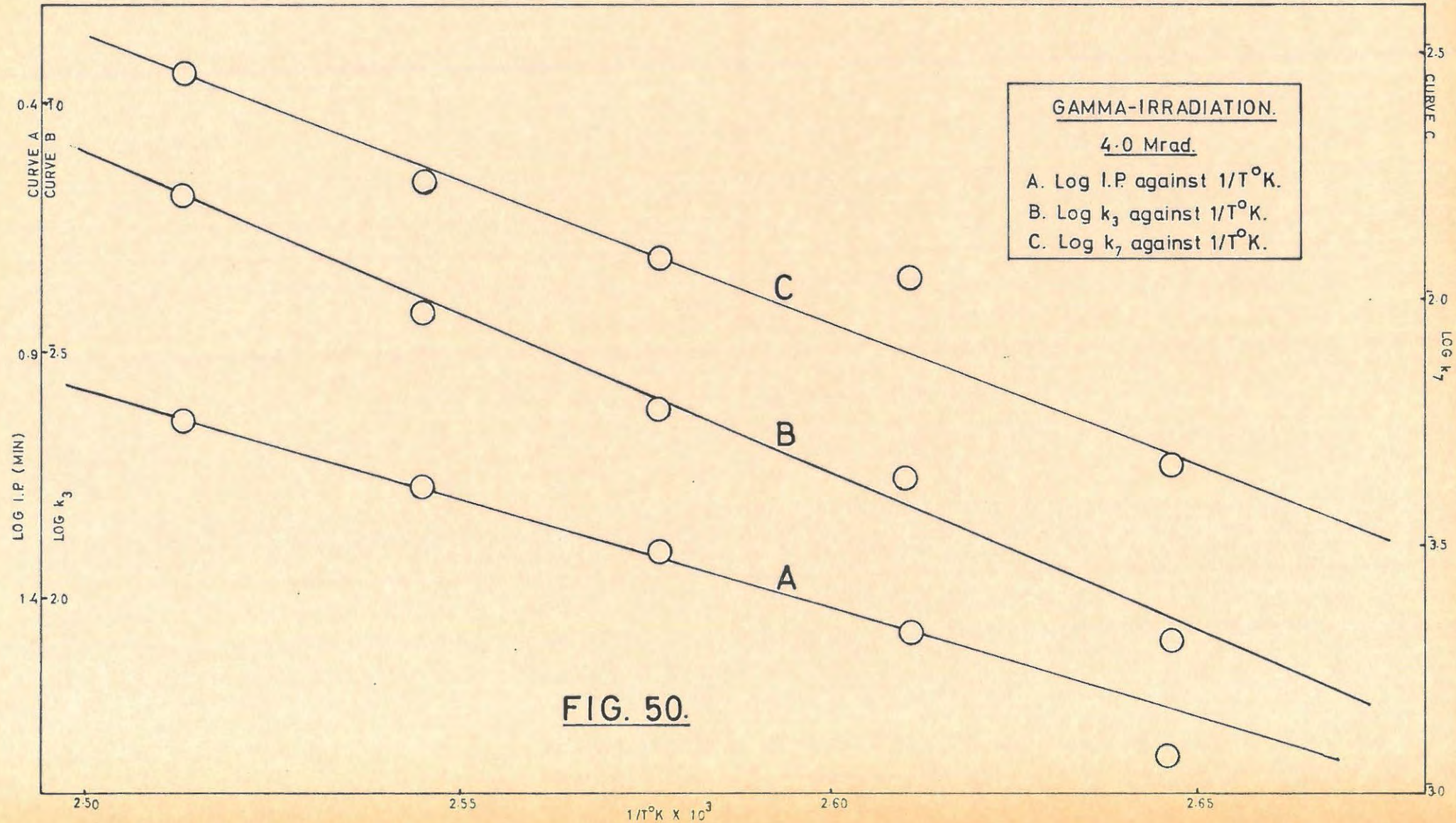
GAMMA-IRRADIATION.
4·0 Mrad.
A. Log I.P. against 1/T°K.
B. Log k3 against 1/T°K.
C. Log k7 against 1/T°K.
CURVE A
CURVE B
CURVE C
LOG I.P (MIN)
LOG k3
LOG k7
0·4
0·9
1·4
2·0
2·5
3·0
3·5
2·50
2·55
2·60
2·65
1/T°K X 10³
A
B
C

FIG. 50.

6.2. DISCUSSION.

6.2.1. Unirradiated Barium Azide.

(i) Mathematical analysis of the pressure-time plots.

The power law;

$$p = Ct^n \quad \ldots\ldots\ldots\ldots\ldots\ldots\ldots\ldots\ldots\ldots\ldots\ldots (15)$$

where C and n are constants, has been most commonly applied to the kinetics of the decomposition of barium azide.[1,3] An obvious solution of this expression is $p = 0$, $t = 0$. One of the features of the decomposition of barium azide using the masses normally employed is that it shows an induction period during which no measurable amount of gas is evolved. Consequently the method of evaluating n by plotting log p against log t where the values of t include those from $t = 0$ to the end of the induction period must be incorrect. In fact unless the induction period is non-existent, or very short, the plot should be curved. This explains the fact that Harvey[1] and Wischin[3] found that p varies as the 7th - 10th and 6th - 8th power of time, respectively. Thomas and Tompkins[60] apparently overcame this difficulty by applying a "slow growth" correction, y, viz

$$p = C\,(t-y)^6 \quad \ldots\ldots\ldots\ldots\ldots\ldots\ldots\ldots\ldots\ldots\ldots\ldots (16)$$

The value of $n = 6$ was chosen in the light of Wischin's results (see later). It is not possible to determine whether $y = t_i$, nor is it possible to determine the extent of applicability of this equation from the published results. When attempting to determine the value of n, by adjusting y, its value is very sensitive to changes in y, as has been demonstrated by Jach.[10]

Attempts were made to fit the pressure-time plots in the manner used by Thomas and Tompkins. It was found that y is approximately $^1/_4\ t_i$. However, the plots of p versus $(t-y)^6$ are curved and the extent of "fit" in the temperature range 110°C to 140°C is only $\alpha = 0.02$ to $\alpha = 0.24$ which means that a very large part of the acceleratory period is not defined by the

equation/.....

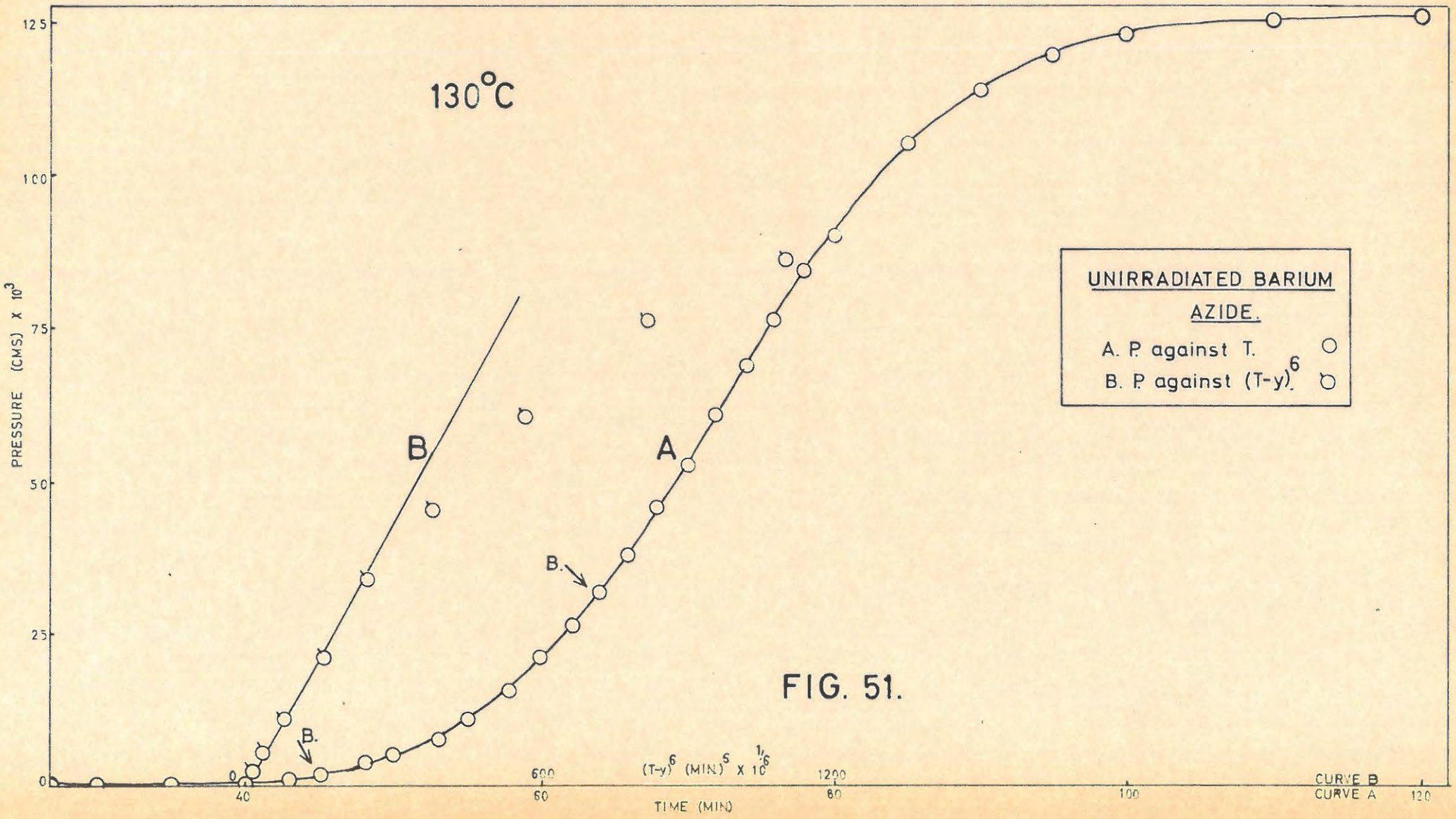
130°C
UNIRRADIATED BARIUM AZIDE.
A. P against T.
B. P against (T-y)^6
PRESSURE (CMS) X 10^3
TIME (MIN)
(T-y)^6 (MIN)^5 X 1/6
CURVE B
CURVE A
B
A
B.
B.
0
25
50
75
100
125
40
60
80
100
120
600
1200

FIG. 51.

equation (FIGURE 51). In any case, Thomas and Tompkins followed only the first 10% to 20% of decomposition. Thus it was concluded that the power law in the form of either of the two equations above is not applicable to the decomposition of ground barium azide.

The power law describes decomposition occuring at centres which are increasing according to a fixed power of time and growing 1, 2 or 3-dimensionally, but takes no account of overlap of nuclei, or ingestion of nuclei by each other. Avrami[35] made such allowances and derived the kinetic expression;

$$-\ln (1 - \alpha) = k_{10} t^{n} \quad \ldots\ldots\ldots\ldots\ldots\ldots\ldots\ldots (17)$$

where k_{10} and n are constants, the value of n being determined by whether growth is 1, 2 or 3-dimensional and on the rate of increase in the number of nuclei. The equation is usually referred to as the Avrami-Erofeyev (A-E) equation.

In attempting to test the applicability of the Avrami-Erofeyev equation it should be applied in the form:

$$[-\ln (1 - \alpha)] = (k_{11} t)^{n} \quad \ldots\ldots\ldots\ldots\ldots\ldots\ldots\ldots (18)$$

or, alternatively, as used in this work, i.e.

$$[-\log(1 - \alpha)]^{1/n} = k_{11} t \quad \ldots\ldots\ldots\ldots\ldots\ldots\ldots\ldots (19)$$

and integral values of n tried. It was found that the best fit, viz. $\alpha = 0.01$ to $\alpha = 0.66$ is obtained when $n = 4$. However, if n is determined by plotting $\log [-\log(1 - \alpha)]$ against $\log t$ with values of t from $t = 0$ and drawing the best straight line through the slightly curved plot, n varies between 7.7 and 9.4 (TABLE A).

TABLE A.

Temperature °C	t_i	n
140	15	8.3
135	25	7.4
130	37	7.7
115	120	8.9
110	180	9.4

The variations/.....

The variations in n found by Erofeyev and Sviridov[114] in a study of the thermal decomposition of unirradiated ($n = 7.9$ to 12.0) and preirradiated (X-rays, $n = 3$ to 15) barium azide are probably due to the Avrami-Erofeyev equation being misapplied in the manner described above.

For small values of α, $\log(1-\alpha) \simeq \alpha$, and thus $\alpha = k(t-t_i)^4$ should fit the early part of the main decomposition; the plot of $p^{1/4}$ versus t is a straight line from $\alpha = 0.01$ to $\alpha = 0.35$ (FIGURE 33).

(ii) Activation energies.

Wischin[3] found that during the thermal decomposition of a dehydrated single crystal of barium azide the following expressions were obeyed,

$$r = k_{12}t \quad \ldots\ldots (20)$$

(r = radial growth of a visible Ba nucleus)

$$N = k_{13}t^3 \quad \ldots\ldots (21)$$

(N = number of visible Ba nuclei at time t)

$$p = k_{14}t^6 \quad \ldots\ldots (22)$$

(p = pressure of N_2 evolved over the acceleratory period).

The derived activation energies, as determined from the plots of log k vs $^1/_T$ °K are

$Ek_{12} = 23.5$ kcal.mole^{-1}

$Ek_{13} = 74$ kcal.mole^{-1}

$Ek_{14} = 166$ kcal.mole^{-1}

It must be pointed out that these last two values are not true (or conventional) activation energies since the Arrhenius activation energies, E, is obtained from the expression;

$$k = \text{const.}\ e^{-E/RT} \quad \ldots\ldots (23)$$

where k is a rate constant, i.e. with the dimensions of (time)$^{-1}$.

Consequently/........

Consequently equations (21) and (22) should be written

$$N^{1/3} = k'_{13}t \quad \ldots\ldots\ldots\ldots\ldots\ldots\ldots\ldots\ldots\ldots\ldots\ldots(24)$$

$$p^{1/6} = k'_{14}t \quad \ldots\ldots\ldots\ldots\ldots\ldots\ldots\ldots\ldots\ldots\ldots\ldots(25)$$

and the activation energies should be obtained from the plots of $\log k'_{13}$ or $\log k'_{14}$ versus $^{1}/_{T}\ ^{o}K$. Wischins values would then become;

$Ek_{12} = 23.5$ kcal.mole^{-1} (radial growth)

$Ek'_{13} = 24.6$ kcal.mole^{-1} (nucleus formation)

$Ek'_{14} = 27.7$ kcal.mole^{-1} (pressure evolution)

Similarly, the activation energy obtained by Thomas and Tompkins[60] using equation (16) reduces from 145 kcal.mole^{-1} to 24.2 kcal.mole^{-1}. Wischins value of 74.0 kcal.mole^{-1} for nucleus formation was accepted by Mott[57] and Thomas and Tompkins[60] and created difficulties in their theoretical speculations.

When the kinetic expressions are used in their correct form it is found that there is a general agreement in the values of the activation energies obtained by various workers. These values are listed in TABLE B.

TABLE B.

Reference	Conditions	Equation used	Activation energies kcal.mole^{-1}.
This work	Unirradiated	$[-\log(1-\alpha)]^{1/4} = k_3t + c_3$	26.8
	Irradiated 0.5 Mrad.		27.0
	Irradiated 4.0 Mrad.		26.8
This work	Unirradiated	$(1-\alpha)^{1/3} = k_7t + c_7$	26.1
	Irradiated 0.5 Mrad.		28.4
	Irradiated 4.0 Mrad.		27.4
	Irradiated U.V.		25.0

TABLE B cont/.....

TABLE B.cont.

Reference	Conditions	Equation used	Activation energies $kcal.mole^{-1}$.
This work	Unirradiated		26.5
	Irradiated 0.5 Mrad.	t_1(for $\alpha = 0.005$)	21.9
	Irradiated 4.0 Mrad.		20.6
	Irradiated U.V.		23.1
This work	Irradiated U.V.	$[-\log(1-\alpha)]^{1/6} = k_4 t + c_4$	27.7
Wischin[3]	Unirradiated	$r = k_{12} t$	23.5
		$N^{1/3} = k'_{13} t$	24.6
		$p^{1/6} = k'_{14} t$	27.7
Harvey[1]	Unirradiated	$\log p = k_2 t + c_2$	21.0
Thomas and Tompkins[60]	Unirradiated	$p^{1/6} = C(t-y)$	24.1
		$y = k$	29.0
Erofeyev and Sviridov[114]	Unirradiated	t for $\alpha = 0.25$	26.7
	Unirradiated	t for $\alpha = 0.02$	29.5
	Irradiated X-rays.	t for $\alpha = 0.25$	29.0

(iii) Mechanism of thermal decomposition.

(a) Nucleus formation.

A theoretical treatment of nuclear formation involving the production of a nucleus, either by alternate trapping of conduction electrons and interstitial Ba^{++} ions[57], or the bimolecular aggregation of interstitial atoms[181], has been made. However these theories have been rejected by Thomas and Tompkins[60] as improbable. Instead they propose that two adjacent azide groups on the surface of the crystal are electronically excited by receipt of sufficient thermal energy and decompose to give nitrogen. In order that the overall experimental activation energy of 74 $kcal.mole^{-1}$ (Wischin[3]) should not be ex-

ceeded it was/.....

ceeded it was suggested that a positive hole is formed by the ejection of an electron into the conduction band of the crystal followed by the trapping of the positive hole at some surface defect. If an adjacent azide ion receives sufficient thermal energy to create an exciton this reacts with the positive hole to give $3N_2$. The first excitation process is considered to be rate determining; i.e. the overall experimental activation energy of 74 kcal.mole^{-1} will not be exceeded. The remaining complex dissociates to give a free F-centre and a vacant anion site. The F-centres aggregate as in Mitchell's theory[49] forming double F-centres which are regarded as nuclei.

However, the estimated thermal energy for the ejection of an electron from the azide full band to the conduction band is approximately 70 kcal.mole^{-1}.[64] This is considerably more than the true (corrected Wischin value) activation energy of 24.6 kcal.mole^{-1}.

Mott[57] has suggested that there is a slow evaporation of nitrogen from the surfaces of barium azide crystals which is constant at constant temperature and that, as a result of this evaporation, barium atoms are left on the surface in a number proportional to time. Although there is no experimental evidence that it occurs in the case of barium azide there is ample evidence that it occurs in potassium and sodium azide[15] and mercury fulminate[182] during the "induction period". The experiments done in this work indicate that it is likely that if this slow decomposition takes place in barium azide the nitrogen is adsorbed on the surface of the particle.

An emergent edge dislocation, either isolated or in a grain boundary terminating at the surface, will have a core near which the lattice is severely strained and thus this region will be one at which decompositions will be favoured. Singh[183] has discussed mechanisms for preferential decomposition at the surface during the slow thermal decomposition of mercury fulminate crystals. Etch pits on the surface produced during

decomposition/.....

decomposition were supposed to occur at points where edge dislocations emerged. Similarly Dreyfus and Levy[184] showed that decomposition of potassium azide during γ-ray irradiation occurs preferentially at steps produced artificially by subjecting the crystal to shock or strain. Such steps will contain a large number of dislocations.

The stresses induced in barium azide during the preparation used in this work (dehydration and grinding) will have generated a large number of dislocations which will have grouped to form high angle grain boundaries. The crystal structure of barium azide is not known but it is likely to be similar to strontium azide[185] which has a layer structure (the azides of sodium, potassium and silver also possess layer structures). It is highly probably that a large number of the incomplete planes of the edge dislocations in an emergent grain boundary will contain only azide ions or Ba^{2+} ions. The decomposition of two adjacent azide ions at the core of a dislocation will be favoured, particularly if they both lie on the surface.[167] Decomposition will produce a barium atom and $3N_2$. It is assumed that the latter are adsorbed on the surface. The dislocation will then climb along the surface (and also down the core) producing barium atoms which, initially, will be at the interatomic spacing in the azide which is greater than in barium metal. When a critical concentration of barium atoms is reached a barium metal speck will crystallize to form what is now considered to be a "nucleus" and will have the electronic properties of the metal. At this stage growth proper will begin (see below) and the reaction will accelerate, reaction occuring at a rapidly expanding metal/salt interface.

It seems clear from the experiments with water vapour, when the barium atoms or metal specks were destroyed, that the induction period and the subsequent nuclear growth are definitely related to the presence of barium. Destruction of barium atoms during the induction period returns the reaction to zero time

and this process/.....

and this process can be repeated many times indicating a slow surface decomposition. Obviously from FIGURE 29 plot D, when the "emergent" grain boundaries are covered by the product of reaction between barium and water, decomposition of the surface azide ions is practically undetectable. This is probably due to the fact that any additional vibrational energy which these azide ions aquire thermally, and which might lead to decomposition, can be transferred to the product, i.e. the azide ion is no longer an ion at a "free" surface.

The concept of nuclear formation given here is thus, in essence, similar to that of Thomas and Tompkins except that it is considered that barium atoms are formed when the nitrogen is evolved whereas they propose that two F-centres aggregate to form a "nucleus", after evolution of nitrogen. Such a centre, however, will not constitute the metal speck which they assume to be necessary for continuous decomposition, i.e. growth. Such a centre would probably not be destroyed by water vapour.

Previous visual observations of barium nuclei formed during the decomposition of dehydrated single crystals have shown that the nuclei are approximately spherical.[1,3,170] If the nuclei in this study also grow thre dimensionally then the applicability of the Avrami-Erofeyev equation and $p = k(t-t_i)^4$ indicates that the nuclei are formed linearly with time i.e. the crystallization and formation of nuclei of barium metal occurs linearly with time. If the rate of initiation of climb at an edge dislocation decreases slowly with time but is approximately constant during the induction period, and if the size of the nucleus when it is first formed is also constant, then the deduced rate of nucleation will result. The decrease in k_3, after "water interruption(s)" is associated with a decrease in the number of nuclei formed, or in the process of forming at the end of the induction period, the original ones having been destroyed. The apparent approximate constancy of the time taken for α to reach 0.005 in plot E of FIGURE 29 is probably

due to the/.....

due to the difficulty in distinguishing, by pressure measurements, between say $\alpha = 0.005$ and $\alpha = 0.0025$. The reason for the lower p_f is discussed later in connection with the preirradiated salt.

Harvey[1] was unable to determine the rate of nucleation by visual observations, but Wischin[3] found that the number increased as a power of time between 2.5 and 3.5. Bartlett et al[170] observed a dependence involving the third power of time. The difference between the deduced rate of nucleation in this work and the third power relationship is probably associated with the use by the above workers of carefully grown, fairly perfect, single crystals whereas in this work rapidly precipitated crystals which were ground to a powder were used.

Thomas and Tompkins[60] attribute the induction period as being due to partly, if not wholly, the slow growth of nuclei. Wischin[3] states that when the plot of the radius of the largest nucleus against time is extrapolated to $r = 0$, the extrapolation intersects the time axis very close to $t = 0$. Her plots of r versus t (FIGURE 3 of the publication) do not bear this out for the decompositions at 100°C and 115°C. Extrapolation of similar plots by Bartlett et al,[170] show too that growth does not begin at the commencement of heating. The visual observations done support this in that at the commencement of the acceleration (using 3.0 g of salt) the powder is still white and no nuclei are observable under low magnification (x40). The salt begins to darken immediately gas is detectable.

(b) Nuclear growth.

In potassium azide[15] the rate of emission of nitrogen measured in vacuo, so that the nuclei evaporate at once, is several thousand times less than in potassium vapour. Obviously contact between the metal and azide catalyses the reaction. Similarly the destruction of barium metal specks during the early part of the acceleratory period destroys growth and returns the reaction to zero times. It would appear further

that the metal/.....

that the metal must be intimately incorporated in the particle since mixing the salt with the end product of decomposition viz. Ba, has no effect on the decomposition. Mott[57] and Thomas and Tompkins[60] have stated that less energy is required to transfer an electron from the full band to the lowest vacant level of the metal nucleus than to eject it into the conduction band of the crystal. Consequently they assumed that growth occurs by the creation of an azide positive hole which reacts with an adjacent azide ion which has received sufficient thermal energy to raise it to an exciton level or, alternatively, with an azide ion whenever sufficient activation energy is available. It is considered that the latter is most probable since the energy required to raise an azide ion to an exciton level is approximately 50 $kcal.mole^{-1}$.[64] Mott and Thomas and Tompkins identify the activation energy for growth i.e. leV with the energy difference of the electron in the full band and in the lowest level of the metal. After liberation of the nitrogen the freed electrons are trapped in the newly formed anion sites forming an F-centre complex which is bound to the nucleus. On attaining a critical size the aggregate collapses to yield barium atoms which add on to the nucleus. The results obtained in this work support this mechanism of nuclear growth in that the "catalytic" importance of the barium metal has been shown.

If nucleation occurs only on the surface of the particles then the decay stage of the reaction, when the nuclei have so overlapped as to form a continuous interface with the salt, corresponds simply to the penetration of this interface into the particles. One therefore expects a contracting sphere formula of the type used here, viz. equation 2 to hold.

6.2.2. Preirradiated (γ-rays) Barium Azide.

Erofeyev and Sviridov[114] observed a decrease in the length of the induction period and an increase in the maximum velocity on preirradiation of barium azide with X-rays (Fe cathode, 35 kV, 14 mA)/.....

ode, 35 kV, 14 mA) in dry air. No decrease of the irradiation effect took place after six months. Similar effects were found by Osinovik[171] and Groocock and Tompkins[9] using fast electrons. The latter found that preirradiation did not affect the exponent in the power law (equation 16). These results are in general in agreement with the results obtained here for the decomposition of preirradiated (γ-rays) barium azide. However, as indicated, Erofeyev and Sviridov failed to obtain a satisfactory analysis of their pressure-time plots using the Avrami-Erofeyev equation. The possible reason for this failure has been suggested.

The significant features of the decomposition of preirradiated barium azide as the γ-ray dose is increased, are;

(i) the induction period is progressively shortened,

(ii) the value of the rate constant, k_3, in the Avrami-Erofeyev equation increases but the exponent n remains at 4,

(iii) the onset of the decay reaction commences at smaller α values.

In addition, there is a change in the ionic conductivity of a preirradiated pellet compared to that for an unirradiated pellet. The activation energy for the ionic (anionic) conductivity is unchanged.

The facts that the same kinetic expressions apply in the acceleratory and decay period and that the relevant activation energies agree, indicate that the mode of thermal decomposition during these phases of the reaction is unchanged by preirradiation, but that reaction now proceeds from many more nuclei. There is, however, a difference in the processes occurring during the induction period. This conclusion is supported by the lower activation energy (derived from t_i) for preirradiated salt and is confirmed by the fact that reaction of preirradiated salt occurs with irradiated barium azide which is almost coated with the product formed from the reaction of barium with water. Unirradiated barium azide once coated with

the product/.....

the product ceases to decompose. A comparison of the plots FIGURE 45G and FIGURE 29 D illustrates this point.

Previous work has indicated that in the solid phase azide radicals are formed during bombardment by X-rays[186] and γ-rays[184,187,109]. Kaufman[187] showed that nitrogen was liberated from α-lead azide with γ-ray doses greater than 10^6r and Heal[186] generated nitrogen by bombarding sodium azide crystals with X-rays. Electron spin resonance studies[188] show that nitrogen atoms are produced by γ-ray irradiation but are short lived above -170°C.

Irradiation of a solid with high energy γ-rays is, in effect, an internal bombardment by electrons varying in velocity from very fast to very slow and the possible reactions in the solid are numerous. The following changes are possible in barium azide during irradiation:

$$N_3^- \rightarrow N_3 + e^-$$

$$N_3 + e^- \rightarrow N_3^-$$

$$N_3 + N_3^{-*} \rightarrow 3N_2 + \boxed{A} + F$$

$$\boxed{A} + e^- \rightarrow F$$

$$N_3 + F \rightarrow N_3^- + \boxed{A}$$

$$N_3 + \boxed{C} + N_3 \rightarrow 3N_2 + \boxed{C} + 2\boxed{A}$$

where $\boxed{A}$ = anion vacancy

$\boxed{C}$ = cation vacancy

F = F-centre

N_3^{-*} = excited state (internal excitation or an exciton).

Thus, the barium azide after irradiation may contain nitrogen, cation and anion vacancies, and F centres. The increase in conductivity, but with no significant change in the activation energy, indicates that anion vacancies are formed. By

analogy with/.....

analogy with irradiation effects in sodium and potassium azides and the alkali halides, and from the buff colour of the salt after a heavy γ-ray dose, it is almost certain that there is a high concentration of F-centres after irradiation.

Nucleation may occur throughout, or on the surface of the particle as with the unirradiated salt. The lower inflexion point of the pressure-time plots for irradiated salt, and the steady fall in this point with increasing γ-ray dose, is indicative of surface nucleation, if one assumes that with increased dosage more nuclei are created but that the nuclear growth rate is constant.

The effect of irradiation on the subsequent thermal decomposition is considered to be associated with the production of F-centres. During the induction period these will aggregate and collapse to form barium atoms. The collapse could occur,

(i) within the particle after which the barium atoms would migrate along grain boundaries and accumulate on the surface where they would crystallize to form barium nuclei, or

(ii) at the surface, after the F-centres have migrated there and aggregated - crystallization occurring after collapse.

Mitchell[49] assumes that migration of an F-centre occurs as a result of a moving anion vacancy coming to within a few lattice sites of it. The electron may then jump across (by tunnel effect) and the original site diffuse away. The activation energy should thus approximate to that for the movement of an anion vacancy; in this case approximately 12 kcal.mole^{-1}. Scott et al[189], however, find that the activation energy for migration of F-centres in additively coloured potassium chloride is 0.43 eV, as compared with a value of 1.5 eV for the activation energy for the migration of anion vacancies.

If the activation energy derived from the variation of t_i with temperature (21.3 kcal.mole^{-1}) represents the energy for the slow stage during the nucleation period then it appears

that (i) above/.....

that (i) above occurs. The activation energy for the migration of barium atoms in barium azide has been estimated at 20-25 kcal.mole^{-1} [59] which supports this conclusion.

The effects of admitting water vapour show that the nuclei are on the surface and that, as with the unirradiated salt, the metal is essential for the propogation of the decomposition. The increase in the duration of the induction period on successive interruptions (FIGURE 47 plot F) may be interpreted as a steady consumption of the F-centres (which must be quite considerable in number) since there is a marked lengthening of the time required for α to equal 0.005. When the reaction is allowed to accelerate in this instance, it is probably mainly the normal unirradiated decomposition which occurs. The fact that 53% of the salt was undecomposed at the end of the run may be due to the complete removal of potential nuclear sites on the surface of a number of small particles. This would, in turn, indicate that with preirradiated salt aggregation of barium atoms, followed by recrystallization, takes place at sites where the nuclei would form with unirradiated salt, which is highly probable. The absence of an appreciable rate of decomposition after interruption in the decay reaction (FIGURE 47 plot E) shows that at this stage all F-centres are consumed and most nucleation sites are destroyed.

6.2.3. Preirradiated (Ultra-Violet Light) Barium Azide.

Preirradiation by ultra-violet light decreases the duration of the induction period and increases the rate of the thermal decomposition over the acceleratory period. The decay reaction is relatively unaffected. These effects are not nearly as marked as the corresponding changes after γ-ray irradiation. There is also a steady and substantial fall in the inflexion point with increasing dose. The exponent, n, in the Avrami-Erofeyev equation increases from 4 to 6 after irradiation. The decay equation is unchanged. The salt develops

a buff colour/.....

a buff colour and after prolonged irradiation the final pressure in the thermal decomposition is considerably lower than normal, indicating that photolysis has taken place.

Irradiation after interruption of the normal decomposition of unirradiated salt is only effective at low α values (FIGURE 38). This is due to the fact that the product layer on the surface will screen the unreacted azide from the ultra-violet light. The buff colour is indicative of F-centre formation, and it is suggested that the effects of irradiation are similar to those for γ-ray irradiation. F-centres formed will aggregate and collapse on heating to give barium atoms. These will migrate and accumulate at favourable sites, such as steps on the surface or emergent dislocation edges, where they will crystallize to give metal nuclei. Nuclear growth will then proceed by the same mechanism as for unirradiated barium azide.

The activation energy for the induction period, 23.1 kcal. $mole^{-1}$, is different from that for the unirradiated salt (26.5 $kcal.mole^{-1}$) and is close to that for the decomposition of unirradiated (0.5 Mrad) salt, namely 21.9 $kcal.mole^{-1}$. On successive interruptions with water vapour the duration of the induction period increases markedly and approaches the unirradiated value in a manner analogous to the γ-irradiated salt, where this is due to the steady consumption of F-centres. The acceleratory and decay period activation energies remain unaltered (within experimental error), as would be expected.

The increase in the exponent n in the Avrami-Erofeyev equation, from 4 - 6, is accounted for if one assumes that after irradiation the number of nuclei no longer increases linearly with time, but with the cube of the time. This is the value obtained by Wischin[3] in work on single crystals of barium azide. The linear rate is restored after "water interruptions due to the consumption of a large number of F-centres at the point of interruption.

The sharp fall in the inflexion point can be accounted

for in two/.....

for in two ways. Firstly the large increase in the number of nuclei, which are formed only at the surface, will result in rapid surface coverage and the decay reaction will commence before appreciable penetration of the nuclei into the interior of the particles. Secondly, since photolysis occurs at high doses, there will probably be some portion of the surface covered with barium hydroxide or barium carbonate. Thus, when surface coverage is complete, a smaller fraction will have decomposed. As the fall in the inflexion point is very marked, $\alpha_i = 0.60$ for unirradiated salt and $\alpha_i = 0.27$ after a dose of 90 minutes, a combination of both factors is likely.

7. THE THERMAL DECOMPOSITION OF STRONTIUM AZIDE.

7.1. RESULTS.

7.1.1. Preparation.

Six grams of strontium hydroxide (A.R.) were dissolved in a minimum quantity of water at 35°C. Hydrazoic acid[190] (3%) was added to the resulting solution until it was just acid to phenolphthalein (external indicator). The solution was then evaporated to dryness, the pH being kept just acid by the addition of hydrazoic acid. The resulting precipitate of strontium azide was then dried for 48 hours over P_2O_5 in a vacuum dessicator with constant pumping, after which it was finely ground. The salt was stored in vacuo over P_2O_5. In all subsequent handling light was excluded.

7.1.2. Unirradiated Strontium Azide.

(i) Reproducibility.

7.5 mg. of salt were used in each run. Three consecutive runs were done at 140°C. The results are given in TABLE 59. The reproducibility was satisfactory. In each run the induction period was 22-23 min. The rate constants, k_5 and k_7, (equation 10 and 2) for the acceleratory and decay periods, respectively, were as follows:

(i) Acceleratory period: 1.426, 1.406 and 1.406 x 10^{-2} cm.$Hg^{1/3}$ min^{-1} respectively.

(ii) Decay period: 9.75 x 10^{-3}, 1.115 and 1.115 x 10^{-2} $min.^{-1}$. respectively

TABLE 59.

140°C		Run 1.			7.6 mg.
t	p	t	p	t	p
5	0.04	38	25.98	70	112.54
10	0.04	40	34.20	75	115.86
15	0.07	42	42.52	80	119.27
20	0.35	45	55.53	85	121.50

TABLE 50 cont/.....

TABLE 59 cont.

t	p	t	p	t	p
25	1.67	48	66.85	90	123.79
30	5.92	50	74.24	95	124.94
32	9.01	55	89.19	100	126.10
34	13.31	60	99.75	p_f	127.20
36	18.90	65	107.12	p_a	127.27

140°C	Run 2.				7.7 mg.
t	p	t	p	t	p
5	0.05	38	23.25	75	112.12
10	0.05	40	30.16	80	116.56
15	0.09	42	37.31	85	119.47
20	0.29	45	47.77	90	123.01
25	1.45	48	58.70	95	125.40
28	3.13	50	65.02	100	126.60
30	5.18	55	78.63	p_f	127.20
32	8.06	60	89.94	p_a	118.64
34	11.94	65	99.31		
36	17.02	70	106.38		

140°C	Run 3.				7.6 mg.
t	p	t	p	t	p
5	0.04	38	23.47	75	112.45
10	0.07	40	30.15	80	116.48
15	0.10	42	37.66	85	119.99
20	0.29	45	48.22	90	122.96
25	1.28	48	58.84	95	125.36
28	2.96	50	65.20	100	126.57
30	4.87	55	78.89	p_f	127.20
32	7.84	60	90.78	p_a	117.54
34	11.87	65	99.72		
36	17.18	70	106.82		

(ii) Effect of interrupting a decomposition.

A series of decompositions was done where the decomposition was interrupted, the salt allowed to cool, and then kept in vacuo at 25°C for one hour before continuing with the run. Interruptions were done half way along the induction period, at

the end/.....

the end of the induction period, and at α = 0.13, 0.31, and 0.61, respectively. The results are given in TABLE 60, and from these it is seen that there was no effect on the subsequent decomposition apart from a short time lag necessary for reheating. The decomposition temperature was 125°C in all cases.

TABLE 60

125°C Unirradiated blank. Run 1.					7.6 mg.
t	p	t	p	t	p
20	0.11	115	16.46	190	98.52
40	0.18	120	21.89	200	104.52
60	0.32	125	28.10	220	112.98
70	0.49	130	34.76	240	118.80
80	0.71	140	48.69	260	122.98
90	2.21	150	61.52	280	125.41
100	5.41	160	73.51	300	126.59
105	8.22	170	83.57	p_f	127.20
110	11.98	180	91.67	p_a	116.42

125°C		Run 2.			7.6 mg.
t	p	t	p	t	p
20	0.04	110	8.71	200	102.41
40	0.06	120	16.47	210	106.72
Interrupted		130	28.34	220	111.12
50	0.07	140	41.35	240	117.31
60	0.10	150	55.23	260	121.35
70	0.25	160	67.61	280	124.14
80	0.63	170	78.41	300	126.48
90	1.74	180	88.02	p_f	127.20
100	4.01	190	95.59	p_a	122.64

125°C		Run 3.			7.5 mg.
t	p	t	p	t	p
20	0.02	120	10.53	210	104.52
40	0.04	130	19.20	220	108.99
60	0.21	140	31.04	240	115.87
70	0.42	150	44.27	260	120.58

TABLE 60 cont/.....

TABLE 60 cont.

t	p	t	p	t	p
80	0.64	160	57.35	280	123.56
Interrupted		170	70.30	300	125.38
90	0.84	180	81.60	320	126.59
100	1.83	190	90.12	p_f	127.20
110	4.80	200	97.99	p_a	116.42

125°C	Run 4.				7.6 mg.
t	p	t	p	t	p
20	0.05	115	17.72	210	113.83
40	0.09	120	23.12	220	116.84
60	0.31	130	37.99	230	119.39
70	0.57	140	52.83	240	121.44
80	1.53	150	66.75	260	124.57
90	3.76	160	78.86	280	126.15
100	8.84	170	99.66	p_f	127.20
108	16.26	180	98.09	p_a	134.12
Interrupted		190	105.08		
110	16.27	200	110.38		

125°C	Run 5.				7.5 mg.
t	p	t	p	t	p
20	0.08	140	40.06	220	112.17
40	0.14	Interrupted		230	116.26
60	0.23	145	40.69	240	119.52
70	0.40	150	45.45	260	122.84
80	0.85	160	59.46	280	124.77
90	1.95	170	73.11	300	126.22
100	4.34	180	84.23	p_f	127.20
110	8.42	190	93.43	p_a	122.46
120	15.65	200	101.22		
130	26.45	210	106.90		

125°C	Run 6.				7.5 mg.
t	p	t	p	t	p
20	0.13	140	38.26	220	109.45
40	0.22	150	52.07	230	113.52
60	0.42	160	65.36	240	117.15
70	0.67	170	78.22	250	119.61

TABLE 60 cont/.....

TABLE 60 cont.

t	p	t	p	t	p
80	1.00	Interrupted		260	122.04
90	1.99	175	78.80	270	123.49
100	4.25	180	82.70	280	125.33
110	8.58	190	91.83	300	126.45
120	15.69	200	98.74	p_f	127.20
130	25.46	210	104.79	p_a	115.72

(iii) Effect of admitting water vapour onto the salt in an interrupted decomposition.

A series similar to the above was done but in each case, on interruption, the line was pumped hard and water vapour (17.0 mm. pressure) was admitted onto the salt at room temperature, for ten minutes. The water vapour was then pumped off, and the run continued after pumping for one hour. Interruptions were done at similar points on the p/t plot as in the above series, and, in addition, a run was done where successive interruptions were performed at the end of each new induction period. The latter point was that time at which the pressure rose to 0.60×10^{-3} cm.Hg i.e. $\alpha = 0.005$. The temperature for all experiments was 130°C. The results are given in TABLE 61 and illustrated in FIGURE 52. From FIGURE 52 it is seen that the effect of "water interruptions" is to regenerate a further induction period of approximately the same duration of time as the original one, followed by the usual acceleratory and decay periods, but with lower rate constants. Repeated interruptions at the end of each induction period (FIGURE 52) shows that the induction period can be repeated a large number of times after which a normal p/t curve is obtained, with slightly slower rate than normal.

The above points are illusted in TABLE 62 where the acceleratory rate constants, k_5 (equation 10), and the lengths of the induction periods are listed.

A constant/.....

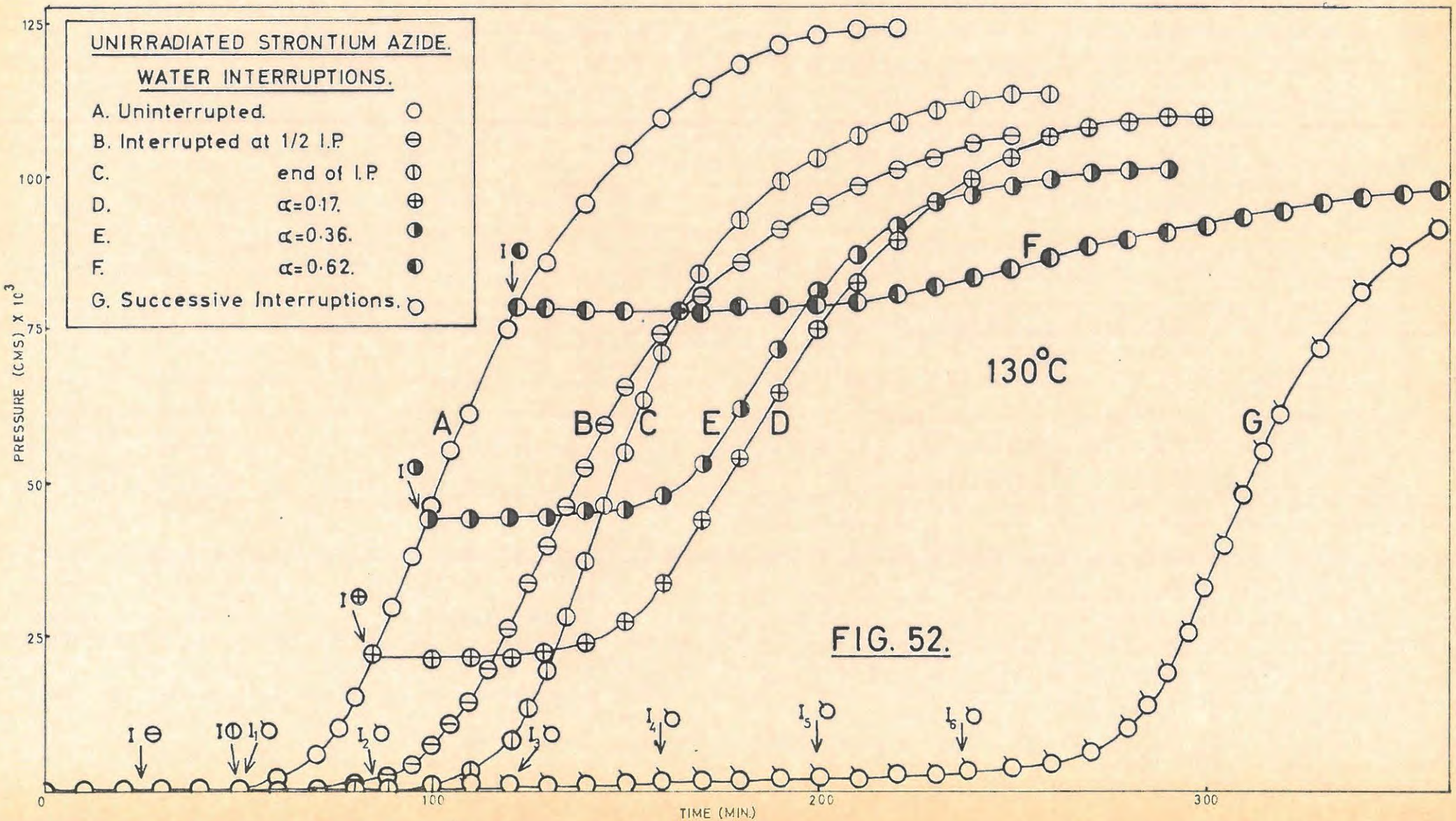
UNIRRADIATED STRONTIUM AZIDE.
WATER INTERRUPTIONS.
A. Uninterrupted.
B. Interrupted at 1/2 I.P.
C. end of I.P.
D. α=0·17.
E. α=0·36.
F. α=0·62.
G. Successive Interruptions.
PRESSURE (CMS) X 10³
TIME (MIN.)
130°C
A
B
C
D
E
F
G
I
I₁
I₂
I₃
I₄
I₅
I₆
0
25
50
75
100
125
100
200
300

FIG. 52.

A constant mass of salt was used in all the above experiments and it can be seen that the final pressure is always lower for an interrupted run than for an uninterrupted one. The lost gas can be regained by heating the salt at 300°C in vacuo.

TABLE 61.

130°C Blank run		Run 1.			7.6 mg.
t	p	t	p	t	p
20	0.09	80	15.18	150	103.48
30	0.14	85	22.16	160	109.62
40	0.32	90	30.16	170	114.78
50	0.61	95	38.72	180	118.87
55	1.11	100	46.11	190	121.84
60	2.13	110	61.56	200	123.64
65	3.69	120	74.95	210	125.11
70	6.20	130	86.62	p_a	125.40
75	9.85	140	95.92		

130°C		Run 2.			7.6 mg.
t	p	t	p	t	p
10	0.07	95	4.61	160	74.69
20	0.08	100	7.10	170	80.15
25	0.10	105	10.46	180	86.77
Water Interruption		110	14.86	190	91.65
30	0.11	115	20.27	200	95.66
40	0.12	120	26.78	210	98.72
50	0.13	125	33.59	220	101.31
60	0.15	130	39.86	230	103.93
70	0.27	135	45.96	240	106.05
80	0.97	140	52.49	250	107.12
85	1.67	145	59.45	p_a	107.66
90	2.74	150	65.17		

130°C		Run 3.			7.7 mg.
t	p	t	p	t	p
10	0.13	105	1.67	165	78.76
20	0.19	110	2.74	170	84.37
30	0.27	115	4.72	180	93.65

TABLE 61 cont/.....

TABLE 61 cont.

t	p	t	p	t	p
40	0.45	120	8.10	190	99.73
45	0.52	125	13.12	200	103.93
50	0.62	130	19.81	210	107.12
Water Interruption 135			28.41	220	109.27
60	0.63	140	37.29	230	111.45
80	0.66	145	46.66	240	113.09
90	0.70	150	55.53	250	114.20
95	0.77	155	63.92	260	114.41
100	1.07	160	71.59	p_a	114.75

130°C		Run 4.			7.6 mg.
t	p	t	p	t	p
10	0.08	90	8.13	210	63.63
20	0.10	100	8.14	220	69.57
30	0.11	110	8.21	230	74.95
40	0.22	120	8.52	240	78.82
50	0.73	130	9.23	250	82.34
55	1.30	140	11.28	260	85.50
60	2.41	150	15.48	270	87.78
65	4.28	160	22.37	280	89.18
70	7.24	170	31.26	290	90.11
71	8.10	180	40.50	p_a	90.58
Water Interruption 190			49.28		
80	8.13	200	57.30		

130°C		Run 5.			7.6 mg.
t	p	t	p	t	p
10	0.07	100	21.60	185	59.14
20	0.13	105	21.74	190	64.40
30	0.17	110	21.90	200	75.21
40	0.29	120	22.18	210	83.08
50	0.77	130	22.75	220	89.77
55	1.42	135	23.31	230	92.01
60	2.25	140	24.04	240	99.98
65	3.86	145	25.28	250	103.23
70	6.17	150	27.38	260	106.06
75	9.32	155	30.22	270	107.98
80	13.69	160	33.96	280	109.43
85	19.57	165	38.35	290	110.56

TABLE 61 cont/.....

TABLE 61 cont.

t	p	t	p	t	p
86	21.21	170	43.88	p_a	110.90
Water Interruption		175	49.35		
90	21.32	180	54.21		

130°C		Run 6.			7.6 mg.
t	p	t	p	t	p
10	0.02	95	36.04	190	72.70
20	0.03	100	44.56	200	81.22
30	0.05	Water Interruption		210	87.76
40	0.24	110	44.66	220	92.65
50	0.60	120	44.83	230	95.56
55	1.18	130	45.02	240	97.81
60	2.17	140	45.25	250	99.33
65	3.77	150	46.11	260	100.48
70	6.30	160	48.13	270	101.26
75	9.80	165	50.35	280	101.64
80	14.47	170	53.89	p_a	102.04
85	20.50	175	58.25		
90	27.84	180	62.57		

130°C		Run 7.			7.6 mg.
t	p	t	p	t	p
10	0.19	110	54.76	260	87.32
20	0.31	115	61.87	270	88.94
30	0.45	120	68.13	280	90.33
40	0.60	125	75.35	290	91.43
50	0.82	130	78.31	300	92.77
60	1.48	Water Interruption		310	94.19
65	2.25	170	78.63	320	95.45
70	3.66	180	78.91	330	96.31
75	5.79	190	79.18	340	97.20
80	9.32	200	79.72	370	100.48
85	14.66	210	80.41	380	101.47
90	21.69	220	81.40	390	101.97
95	30.37	230	82.59	400	102.48
100	39.21	240	83.97	410	102.99
105	47.37	250	85.54	p_a	103.24

TABLE 61 cont/.....

TABLE 61 cont

130°C		Run 8.			7.6 mg.
t	p	t	p	t	p
10	0.05	150	2.00	285	13.93
20	0.09	155	2.15	290	19.11
30	0.13	160	2.42	295	25.82
40	0.22	Water Interruption		300	33.16
45	0.45	180	2.46	305	40.30
48	0.61	190	2.59	310	48.20
Water Interruption		195	2.74	315	55.40
80	0.93	200	3.03	320	61.51
85	1.13	Water Interruption		330	72.63
88	1.21	210	3.07	340	81.49
Water Interruption		220	3.10	350	87.34
100	1.23	230	3.30	360	91.98
110	1.33	235	3.55	370	96.79
115	1.45	237	3.84	380	100.31
120	1.79	Water Interruption		390	102.36
122	1.83	250	4.16	400	104.91
Water Interruption		260	4.82	410	104.94
130	1.85	270	6.38	420	105.99
140	1.87	280	10.34	p_a	106.52

TABLE 62.

Point of Interruption.	k_5 $cm^{1/3}$ min^{-1}	Induction Period Min.	Number of Interruptions.	Induction Period Min.
Uninterrupted	6.207×10^{-3}	52	0	48
1/2 along I.P.	5.26×10^{-3}	50	1	40
End of I.P.	6.225×10^{-3}	48	2	34
$\alpha = 0.06$	4.920×10^{-3}	52	3	38
$\alpha = 0.17$	5.05×10^{-3}	30	4	40
$\alpha = 0.36$	5.30×10^{-3}	40	5	37
$\alpha = 0.62$	1.65×10^{-3}	50	6	25
5 consecutive	6.10×10^{-3}	25		

(iv) Effect of/.....

(iv) Effect of varying the temperature of decomposition.

The critical increment of the process(es) occurring during a thermal decomposition was determined by performing a series of separate decompositions at various fixed temperatures. These are shown in TABLE 63 below. TABLE 64 gives the rate constants, k_5 and k_7, (equations 10 and 2) for the acceleratory and decay periods, respectively, as well as the length of the induction period (min.) at each temperature.

TABLE 63.

120°C		Run 1.			7.7 mg.
t	p	t	p	t	p
10	0.01	140	6.46	270	105.11
20	0.01	150	10.19	280	109.59
30	0.02	160	15.17	290	113.60
40	0.02	170	22.16	300	116.50
50	0.07	180	31.05	310	118.84
60	0.16	190	40.10	320	120.03
70	0.21	200	51.00	330	123.01
80	0.32	210	61.54	340	124.82
90	0.47	220	70.78	350	126.05
100	0.68	230	79.21	360	126.64
110	1.55	240	87.10	p_f	127.20
120	2.55	250	93.79	p_a	116.42
130	4.01	260	99.64		

125°C		Run 2.			7.6 mg.
t	p	t	p	t	p
10	0.05	120	12.07	230	111.45
20	0.08	130	20.16	240	117.75
30	0.10	140	30.61	250	120.67
40	0.12	150	42.18	260	123.03
50	0.16	160	54.02	270	124.82
60	0.19	170	66.01	280	126.01
70	0.48	180	77.79	290	126.61
80	0.93	190	87.01	p_f	127.20
90	1.86	200	95.69	p_a	119.23
100	3.60	210	103.15		
110	7.00	220	108.65		

TABLE 63 cont/.....

TABLE 63 cont.

130°C	Run 3.				7.5 mg.
t	p	t	p	t	p
10	0,11	75	9,85	140	103,48
20	0,14	80	15,18	150	109,62
30	0,21	85	22,16	160	114,78
40	0,39	90	30,16	170	118,87
50	0,58	95	38,72	180	121,84
55	1,11	100	46,11	190	123,64
60	2,13	110	74,95	200	125,11
65	3,69	120	86,62	p_f	127,20
70	6,20	130	95,92	p_a	118,10

135°C	Run 4.				7,5 mg.
t	p	t	p	t	p
10	0,02	60	19,63	110	111,38
15	0,02	65	31,20	115	115,63
20	0,03	70	43,99	120	118,86
25	0,08	75	58,81	125	121,81
30	0,16	80	67,96	130	124,19
35	0,42	85	78,05	135	125,40
40	1,21	90	87,33	140	125,99
45	2,77	95	95,02	p_f	127,20
50	5,97	100	101,41	p_a	118,64
55	11,27	105	106,85		

140°C	Run 5.				7,6 mg.
t	p	t	p	t	p
5	0,05	38	23,25	75	112,12
10	0,05	40	30,16	80	116,56
15	0,09	42	37,31	85	119,47
20	0,29	45	47,77	90	123,01
25	1,45	48	58,70	95	125,40
28	3,13	50	65,02	100	126,60
30	5,18	55	78,63	p_f	127,20
32	8,06	60	89,94	p_a	119,17
34	11,94	65	99,31		
36	17,02	70	106,38		

TABLE 63 cont/.....

TABLE 63 cont.

145°C		Run 6.			7.6 mg.
t	p	t	p	t	p
5	0,01	32	31,06	52	106,11
10	0,02	34	41,87	55	110 50
15	0,08	36	52,37	60	116,13
18	0,47	38	62,37	65	120,73
20	1,12	40	71,88	70	123,65
22	2,43	42	80,65	75	125,42
24	4,62	44	87,42	80	126,60
26	8,44	46	93,45	p_f	127,20
28	14,07	48	98,63	p_a	122,07
30	21,61	50	102,87		

150°C		Run 7.			7,6 mg.
t	p	t	p	t	p
5	0,04	28	60,30	45	112,33
10	0,07	30	71,80	50	117,39
15	0,62	32	81,44	55	120,25
18	3,18	34	90,19	60	123,73
20	8,03	36	96,78	65	125,27
22	17,84	38	102,02	70	126,64
24	32,41	40	105,76	p_f	127,20
26	47,25	42	109,02	p_a	123,79

TABLE 64.

Temperature °C.	Induction Period min.	k_5 $cm^{1/3}$ $min.^{-1}$	k_7 $min.^{-1}$
120°	100	$3,010 \times 10^{-3}$	$4,10 \times 10^{-3}$
125°	75	$4,022 \times 10^{-3}$	$4,90 \times 10^{-3}$
130°	52	$6,207 \times 10^{-3}$	$5,90 \times 10^{-3}$
135°	37	$8,625 \times 10^{-3}$	$9,13 \times 10^{-3}$
140°	25	$1,406 \times 10^{-2}$	$1,15 \times 10^{-2}$
145°	19	$1,824 \times 10^{-2}$	$1,45 \times 10^{-2}$
150°	15	$2,939 \times 10^{-2}$	$2,22 \times 10^{-2}$

(v) Mathematical analysis of the results and evaluation of activation energies.

FIGURE 53 shows a typical p/t plot for the isothermal decomposition of strontium azide. The main features are (i) a

marked/.....

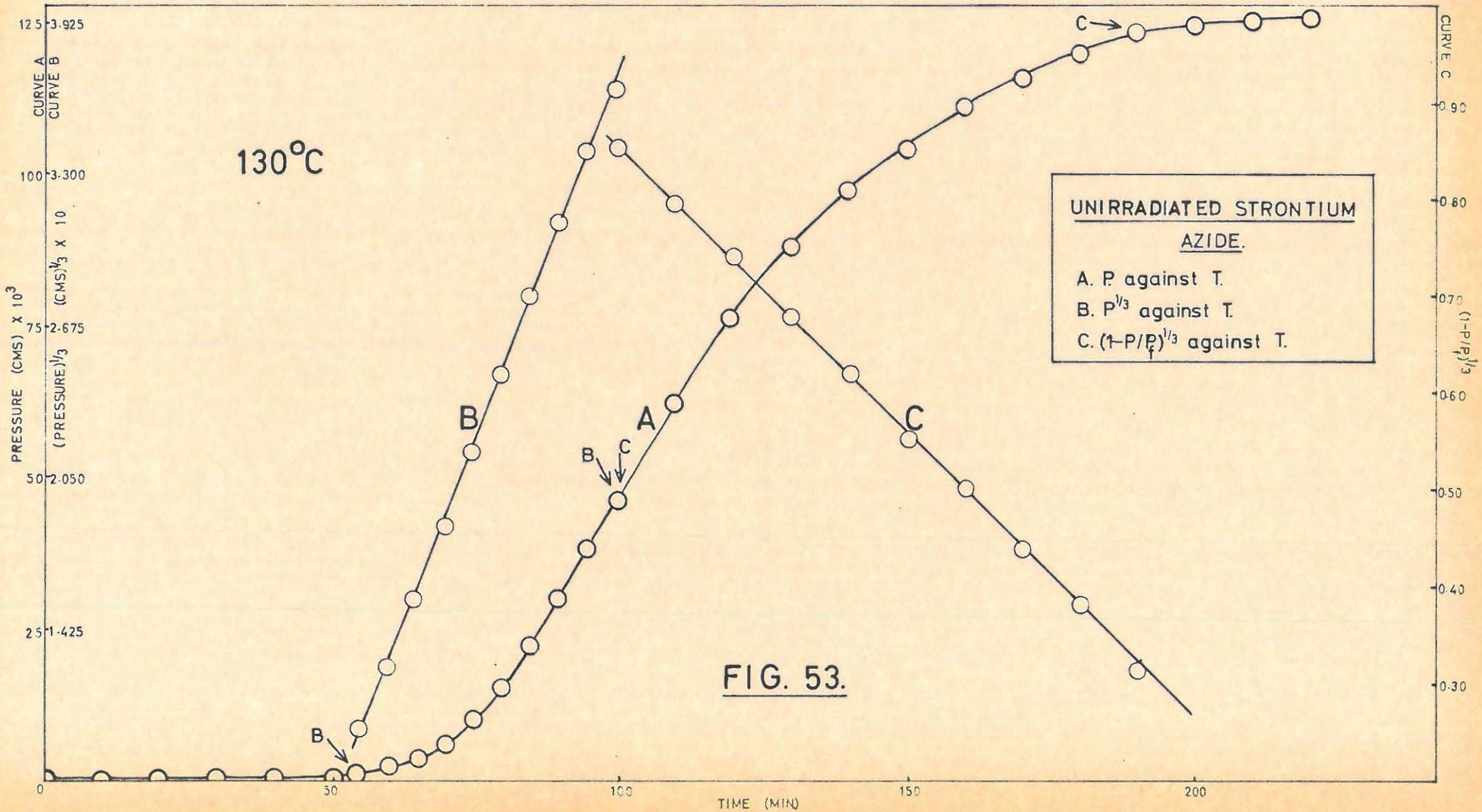
130°C
UNIRRADIATED STRONTIUM AZIDE.
A. P against T.
B. $P^{1/3}$ against T.
C. $(1-P/P_f)^{1/3}$ against T.
PRESSURE (CMS) X 10^3
CURVE A
CURVE B
$(PRESSURE)^{1/3}$ $(CMS)^{1/3}$ X 10
CURVE C
$(1-P/P_f)^{1/3}$
TIME (MIN)
125
100
75
50
25
3·925
3·300
2·675
2·050
1·425
0·90
0·80
0·70
0·60
0·50
0·40
0·30
0
50
100
150
200
A
B
C

FIG. 53.

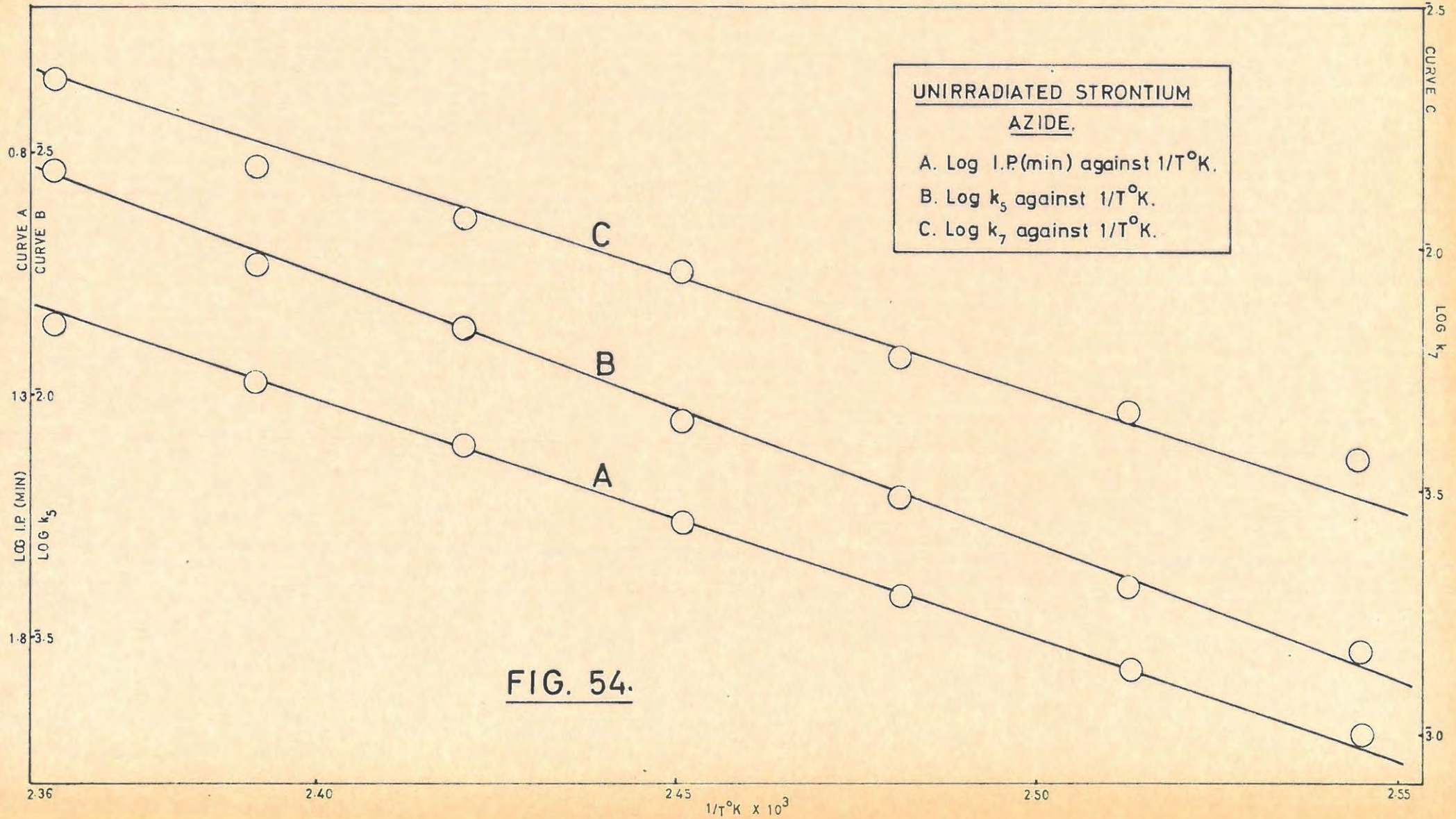
UNIRRADIATED STRONTIUM AZIDE.
A. Log I.P.(min) against 1/T°K.
B. Log k_5 against 1/T°K.
C. Log k_7 against 1/T°K.
CURVE A
CURVE B
CURVE C
LOG I.P. (MIN)
LOG k_5
LOG k_7
0·8
1·3
1·8
2·5
2·0
3·5
2·5
2·0
3·5
3·0
C
B
A
2·36
2·40
2·45
2·50
2·55
1/T°K x 10^3

FIG. 54.

marked induction period with no evolution of gas, followed by (ii) a well defined period of acceleration, and (iii) a decay period.

Since no gas was evolved no mathematical analysis of induction period was possible. For comparitive purposes the lengths of induction periods (min.) were used.

The acceleratory period was well described by the power law with n = 3 viz.

$$p^{1/3} = k_5 t + c_5 \quad \ldots\ldots\ldots\ldots\ldots\ldots\ldots\ldots\ldots\ldots\ldots\ldots (10)$$

The decay period was well fitted by the contracting sphere equation,

$$(1 - p/p_f)^{1/3} = k_7 t + c_7 \quad \ldots\ldots\ldots\ldots\ldots\ldots\ldots\ldots\ldots\ldots (2)$$

The extent of fit of the power law was from $\alpha = 0.02$ to $\alpha = 0.41$ and the contracting sphere from $\alpha = 0.42$ to $\alpha = 0.92$. This fit was approximately the same throughout the temperature range 120° - 150°C. A typical analysis is shown in FIGURE 53.

The Arrhenius plots of log I.P. (min.), log k_5, and log k_7, vs. $^1/_T$ °K respectively (FIGURE 54) gave the following activation energies:

(i) Induction period: 23.3 kcals.mole^{-1}

(ii) Acceleratory period: 25.0 kcals.mole^{-1}

(iii) Decay period: 21.7 kcals.mole^{-1}.

(vi) Percentage decomposition.

This was calculated using the equation,

$$Sr(N_3)_2 \rightarrow Sr + 3N_2$$

The results of a series of determinations are listed in TABLE 65.

TABLE 65/.....

TABLE 65.

Temperature °C.	Weight used mg.	% decomposition.
140°	6.4	65.70
140°	7.6	77.12
140°	7.7	69.87
130°	7.7	69.54
125°	7.6	70.81
145°	7.6	72.48
150°	7.7	72.85

The average percentage decomposition was evaluated as being 71.20% of the theoretical value.

7.1.3. Preirradiated (Ultra-Violet Light) Strontium Azide.

(i) Preliminary investigation.

In order to determine whether preirradiation by ultra-violet light would have any effect on the subsequent thermal decomposition, an initial run was done in which a sample of strontium azide was irradiated for one minute at a distance of 10 cms. The techniques employed in ultra-violet light irradiations have been described. The subsequent decomposition at 130°C is shown in FIGURE 55 and the results in TABLE 66. An unirradiated decomposition at the same temperature is also given for comparitive purposes.

TABLE 66.

130°C Unirradiated blank Run 1.					7.5 mg.
t	p	t	p	t	p
10	0.11	75	9.85	140	103.48
20	0.14	80	15.18	150	109.62
30	0.21	85	22.16	160	114.78
40	0.39	90	30.16	170	118.87
50	0.58	95	38.72	180	121.84

TABLE 66 cont/.....

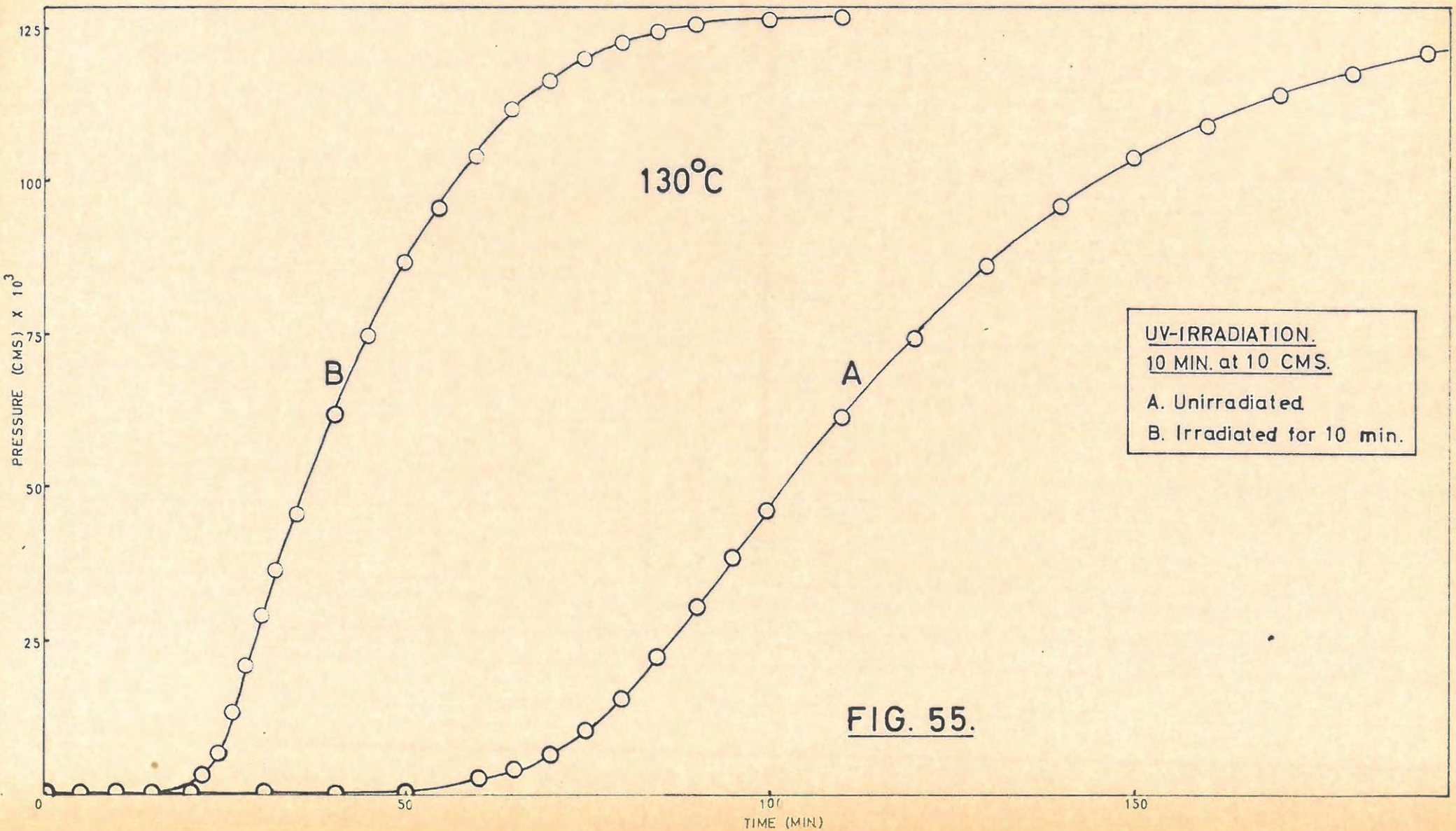
125
100
75
50
25
0
50
100
150
PRESSURE (CMS) X 10^3
TIME (MIN.)
130°C
B
A
UV-IRRADIATION.
10 MIN. at 10 CMS.
A. Unirradiated
B. Irradiated for 10 min.

FIG. 55.

TABLE 66 cont.

t	p	t	p	t	p
55	1.11	100	46.11	190	123.64
60	2.13	110	74.95	200	125.11
65	3.69	120	86.62	p_f	127.20
70	6.20	130	95.92	p_a	118.10

130°C 1 min. U.V. 10 cms. Run 2.					7.6 mg.
t	p	t	p	t	p
10	0.05	32	36.49	70	116.78
15	0.08	35	46.82	75	120.38
20	1.13	40	62.11	80	122.99
22	3.05	45	74.99	85	124.23
24.	6.98	50	86.87	90	126.15
26	13.21	55	96.35	p_f	127.20
28	20.96	60	104.87	p_a	152.97
30	28.94	65	111.74		

Preirradiation with ultra-violet light has a marked effect on the thermal decomposition. The induction period is shortened considerably, and the rate of decomposition is greatly accelerated. There is also an increase in the percentage decomposition.

By a method of trial and error it was decided to irradiate with the lamp at a distance of 80 cms from the sample.

(ii) Effect of varying the dose of ultra-violet light.

A series of decompositions were done at 120°C where the time of preirradiation varied from 2 secs. to 15 min. The results, in tabular form, are given in TABLE 67 and FIGURE 56 gives a graphical illustration of the results. The main features emerging from this are, that with increasing dose there is, (i) a decrease in the duration of the induction period, (ii) an increase in the rate in the acceleratory period, and (iii) a decrease in the inflexion point, α_i. The decay reaction is not affected to any extent. Rate constants, k_5,

(equation 10)/.....

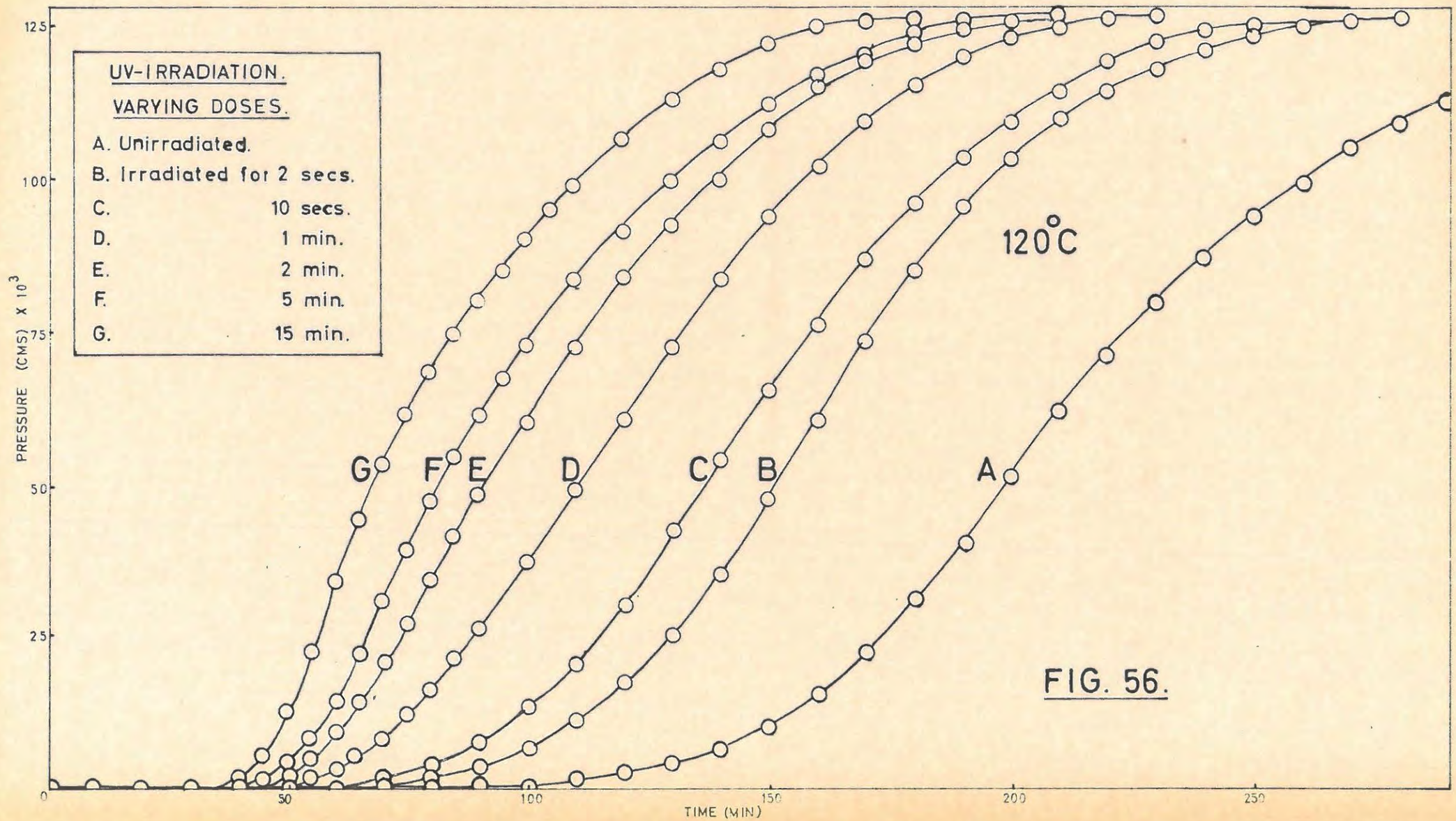
UV-IRRADIATION.
VARYING DOSES.
A. Unirradiated.
B. Irradiated for 2 secs.
C. 10 secs.
D. 1 min.
E. 2 min.
F. 5 min.
G. 15 min.
120°C
G
F
E
D
C
B
A
PRESSURE (CMS) X 10³
TIME (MIN)
0
25
50
75
100
125
50
100
150
200
250

FIG. 56.

(equation 10) for irradiation times of up to one minute, and k_1 (equation 1) for irradiation times exceeding one minute, are given in TABLE 68 together with the other effects mentioned.

TABLE 67.

120°C Unirradiated blank. Run 1.					7.7 mg.
t	p	t	p	t	p
10	0.01	140	6.46	270	105.11
20	0.01	150	10.19	280	109.59
30	0.02	160	15.17	290	113.60
40	0.02	170	22.16	300	116.50
50	0.07	180	31.05	310	118.84
60	0.16	190	40.10	320	120.03
70	0.21	200	51.00	330	123.01
80	0.32	210	61.54	340	124.82
90	0.47	220	70.78	350	126.05
100	0.68	230	79.21	360	126.64
110	1.55	240	87.10	p_f	127.20
120	2.55	250	93.79	p_a	116.42
130	4.01	260	99.64		

120°C 2 secs. U.V. Run 2.					6.8 mg.
t	p	t	p	t	p
10	0.01	110	11.13	210	109.92
20	0.03	120	17.06	220	114.97
30	0.05	130	25.04	230	118.41
40	0.07	140	35.17	240	121.31
50	0.14	150	47.75	250	123.65
60	0.37	160	60.59	260	125.42
70	0.86	170	73.13	270	126.61
80	1.97	180	84.89	p_f	127.20
90	3.74	190	95.44	p_a	121.50
100	6.59	200	103.36		

120°C 10 secs. U.V. Run 3.					6.9 mg.
t	p	t	p	t	p
10	0.05	110	20.61	210	114.75
20	0.07	120	30.54	220	119.07
30	0.08	130	42.06	230	122.17

TABLE 67 cont/.....

TABLE 67 cont.

t	p	t	p	t	p
40	0.09	140	53.74	240	124.65
50	0.23	150	65.03	250	125.94
60	0.67	160	75.91	260	126.57
70	1.75	170	86.68	p_f	127.20
80	3.90	180	95.73	p_a	122.64
90	7.63	190	103.61		
100	13.23	200	109.43		

120°C 1 min. U.V. Run 4. 7.1 mg.					
t	p	t	p	t	p
10	0.04	75	11.87	160	107.29
20	0.05	80	16.13	170	109.43
30	0.06	85	21.03	180	115.20
40	0.16	90	26.58	190	119.50
45	0.50	100	37.11	200	123.33
50	0.89	110	48.87	210	125.53
55	1.79	120	60.58	220	126.65
60	3.28	130	72.71	p_f	127.20
65	5.43	140	83.67	p_a	138.49
70	8.27	150	93.94		

120°C 2 min. U.V. Run 5. 6.9 mg.					
t	p	t	p	t	p
10	0.16	70	20.53	150	108.63
20	0.25	75	26.90	160	115.05
30	0.36	80	34.12	170	119.38
35	0.44	85	40.89	180	122.71
40	0.57	90	47.58	190	125.51
45	1.12	100	60.13	200	126.64
50	2.43	110	72.41	p_f	127.20
55	5.13	120	83.52	p_a	134.37
60	9.13	130	92.49		
65	14.26	140	100.90		

TABLE 67 cont/.....

TABLE 67 cont.

120°C 5 min. U.V. Run 6. 6.6 mg.					
t	p	t	p	t	p
10	0.02	70	30.95	140	106.58
20	0.04	75	38.88	150	111.99
30	0.07	80	46.66	160	116.98
35	0.24	85	54.00	170	120.93
40	0.56	90	61.06	180	123.79
45	1.74	95	66.85	190	125.52
50	4.18	100	72.03	200	126.69
55	8.40	110	82.95	p_f	127.20
60	14.47	120	91.65	p_a	127.27
65	22.18	130	99.75		

120°C 15 min. U.V. Run 7. 6.4 mg.					
t	p	t	p	t	p
10	0.03	70	52.86	130	113.09
20	0.04	75	61.06	140	118.10
30	0.13	80	68.13	150	122.64
35	0.49	85	74.24	160	124.94
40	1.88	90	79.69	170	126.10
45	5.79	95	84.85	180	126.65
50	12.93	100	89.68	p_f	127.20
55	22.67	105	94.65	p_a	127.69
60	33.89	110	98.72		
65	43.53	120	106.58		

TABLE 68.

U.V. Dose.	k_5 cm.$^{1/3}$ min.$^{-1}$	Induction period min.	Inflexion point α_i
0	3.010×10^{-3}	100	0.44
2 secs.	2.850×10^{-3}	66	0.43
10 secs.	3.094×10^{-3}	60	0.39
1 min.	4.222×10^{-3}	47	0.30
	k_1 cm.$^{1/2}$ min.$^{-1}$		
2 min.	4.663×10^{-3}	42	0.31
5 min.	5.602×10^{-3}	42	0.31
15 min.	7.362×10^{-3}	38	0.29

(iii) Effect of/.....

(iii) Effect of interrupting a decomposition and then irradiating the salt.

When an unirradiated run was interrupted and then continued no effect on the subsequent decomposition was found. It was of some significance therefore to determine whether irradiation at these points of interruption of the decomposition would affect the subsequent reaction. The technique for irradiating an interrupted decomposition has been described. All specimens were irradiated for 5 min. and the decomposition temperature was 120°C. Blank runs for the unirradiated and preirradiated salt were done, as a quartz ampoule was used in place of the normal pyrex one. The results are given in TABLE 69 and shown graphically in FIGURE 57.

It can be seen (FIGURE 57) that the rate of the subsequent reaction is increased only when irradiation is done at low α values. During the induction period, and at $\alpha = 0.14$, the subsequent rate is increased by irradiation, but for values of $\alpha \gtrsim 0.30$ the reaction rate is the same as for an unirradiated specimen.

TABLE 69

120°C Unirradiated blank Run 1.					7.4 mg.
t	p	t	p	t	p
20	0.08	125	15.46	200	97.76
40	0.14	130	20.22	210	103.24
60	0.22	135	26.52	220	108.98
70	0.36	140	33.01	240	115.41
80	0.54	145	40.23	260	121.20
90	0.72	150	47.85	280	123.76
100	1.98	160	61.01	300	125.92
110	4.76	170	72.98	320	126.68
115	7.39	180	82.67	p_f	127.20
120	10.98	190	91.04	p_a	118.09

TABLE 69 cont/.....

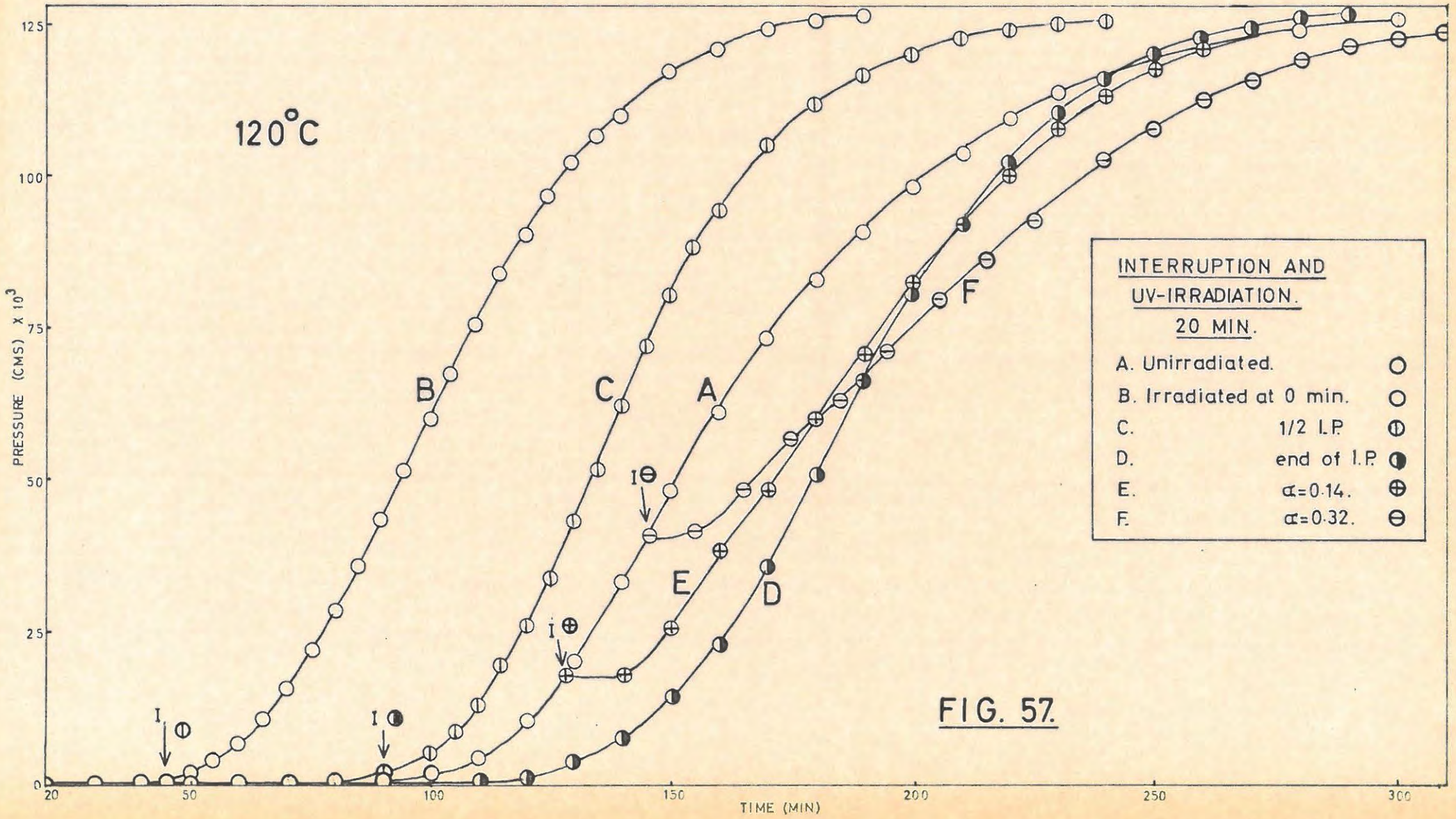
120°C
PRESSURE (CMS) X 10³
TIME (MIN)
0
25
50
75
100
125
20
50
100
150
200
250
300
A
B
C
D
E
F
I
INTERRUPTION AND
UV-IRRADIATION.
20 MIN.
A. Unirradiated.
B. Irradiated at 0 min.
C. 1/2 I.P.
D. end of I.P.
E. α=0.14.
F. α=0.32.

FIG. 57.

TABLE 69 cont.

120°C Irradiated blank. Run 2.					7.0 mg.
t	p	t	p	t	p
20	0.01	85	35,71	135	106,27
40	0,33	90	43.21	140	109,89
45	0,80	95	51,43	150	116,24
50	1,94	100	59,58	160	120.58
55	3,97	105	67,52	170	123.33
60	6,83	110	75.08	180	125,55
65	10.80	115	80.57	190	126,67
70	15,87	120	90.47	p_f	127,20
75	21,91	125	96,73	p_a	137.39
80	28,66	130	101,69		

120°C 5 min. U.V. Run 3.					7.0 mg.
t	p	t	p	t	p
20	0,11	100	5,36	155	87,88
40	0,14	105	8,58	160	94,03
45	0,19	110	12,98	170	105,65
Irradiation		115	19,05	180	111,23
50	0,21	120	25,98	190	116,23
60	0,23	125	34,33	200	120,05
70	0,31	130	43,45	240	126,55
80	0,42	135	53,21	p_f	127,20
85	0,88	140	62,57	p_a	123,79
90	1,74	145	71,68		
95	3,30	150	80,36		

120°C 5 min. U.V. Run 4.					7.0 mg.
t	p	t	p	t	p
20	0,02	130	3,60	195	73,49
40	0,04	135	5,18	200	80,59
60	0,06	140	7,32	205	87,07
70	0,09	145	10,15	210	93,32
80	0,24	150	14,01	220	102,83
90	0,61	155	18,26	230	110,14
Irradiation		160	22,82	240	115,51
100	0,62	165	29,29	250	119,35
105	0,64	170	35,92	260	122,12
110	0,68	175	43,57	270	123,91
115	0,87	180	50,86	280	126,64
120	1,41	185	58,71	p_f	127,20
125	2,38	190	66,31	p_a	133,17

TABLE 69 cont/.....

TABLE 69 cont.

120°C 5 min. U.V. Run 5. 6.8 mg.					
t	p	t	p	t	p
20	0.06	Irradiation		205	86.98
40	0.10	140	18.42	210	92.25
60	0.27	145	21.10	215	96.97
80	0.38	150	26.11	220	100.96
90	0.52	155	31.51	230	108.67
95	0.87	160	37.36	240	114.68
100	1.30	165	42.71	250	118.80
105	2.10	170	48.10	260	121.94
110	3.37	175	53.73	270	124.06
115	5.30	180	59.18	280	125.66
120	7.66	185	64.64	290	126.74
125	11.14	190	70.12	p_f	127.20
130	15.27	195	75.88	p_a	127.28
133	18.01	200	81.52		

120°C 5 min. U.V. Run 6. 7.0 mg.					
t	p	t	p	t	p
20	0.08	140	29.21	230	97.27
40	0.11	145	35.15	240	103.75
60	0.15	150	40.98	250	108.85
70	0.21	Irradiation		260	112.81
80	0.31	155	41.31	270	115.93
90	0.80	160	42.84	280	119.14
100	2.16	165	47.06	290	121.48
105	3.37	170	51.73	300	123.37
110	5.09	175	56.05	310	124.80
115	7.59	180	60.17	320	125.77
120	10.75	190	67.39	330	126.74
125	13.88	200	77.65	p_f	127.20
130	18.97	210	82.63	p_a	123.76
135	24.07	220	90.41		

120°C 5 min. U.V. Run 7. 7.0 mg.					
t	p	t	p	t	p
20	0.06	180	65.07	260	104.49
40	0.08	186	70.61	270	108.16
60	0.12	Irradiation		280	113.39
80	0.21	190	70.99	290	114.42

TABLE 69 cont/.....

TABLE 69 cont.

t	p	t	p	t	p
90	0.52	195	72.15	300	117.20
100	1.18	200	75.55	310	120.06
110	3.09	205	79.30	320	122.64
120	9.31	210	82.97	330	124.53
130	11.65	215	86.05	340	126.44
140	19.32	220	88.81	p_f	127.20
150	30.05	230	93.74	p_a	127.40
160	42.45	240	97.62		
170	53.92	250	101.22		

(iv) Effect of admitting water vapour onto the salt in an interrupted decomposition.

This was done in the same manner as before. The irradiation time was 20 min. and the decomposition temperature 115°C in all cases. The results appear in TABLE 70 and are illustrated in FIGURE 58. Results similar to the corresponding runs for the unirradiated salt were obtained, with a new induction period being regenerated, and the rate constants decreasing. The induction period was repeated with successive interruptions, and each new induction period was of approximately the same duration of time. TABLE 71 gives the rate constants, k_1 (equation 1) for interruptions in the induction period, and k_5 (equation 10) for interruptions in the accelerator and decay periods. The duration of each induction period formed is also given.

Again the final pressures are lower than normal, but the gas can be partially recovered by strong heating at 300°C in vacuo. Pressure are thus not normalised.

TABLE 70.

115°C Uninterrupted blank Run 1.					6.7 mg.
t	p	t	p	t	p
10	0.03	70	25.72	140	103.93
20	0.05	75	35.42	150	110.36
30	0.07	80	43.19	160	115.86

TABLE 70 cont/.....

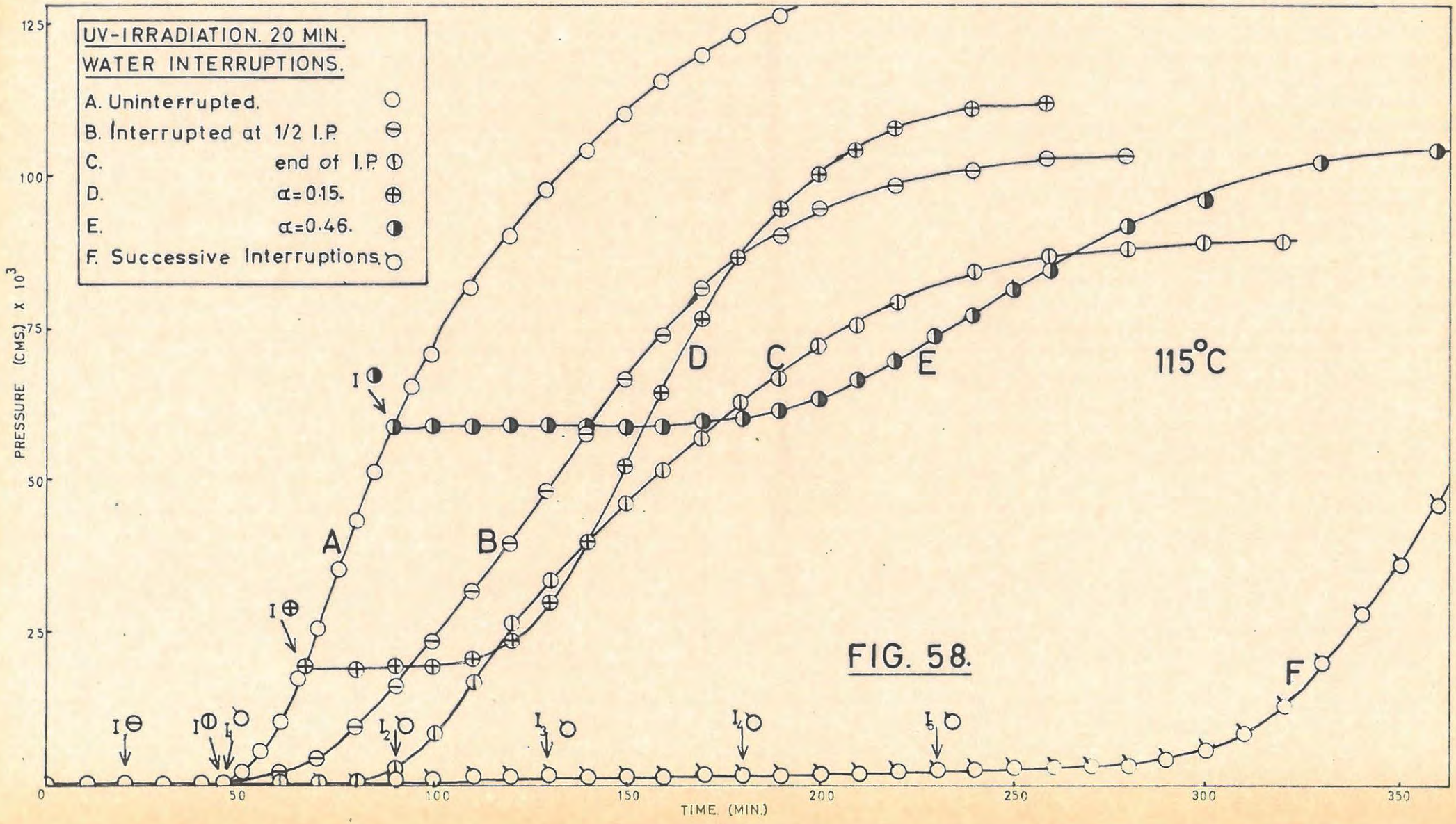
UV-IRRADIATION. 20 MIN.
WATER INTERRUPTIONS.
A. Uninterrupted.
B. Interrupted at 1/2 I.P.
C. end of I.P.
D. α=0.15.
E. α=0.46.
F. Successive Interruptions.
PRESSURE (CMS.) X 10³
TIME. (MIN.)
115°C
A
B
C
D
E
F
0
50
100
150
200
250
300
350
25
50
75
100
125

FIG. 58.

TABLE 70 cont.

t	p	t	p	t	p
35	0.11	85	51.37	170	120.93
40	0.22	90	58.66	180	125.52
45	0.69	95	65.17	190	129.03
50	2.02	100	71.59	200	130.80
55	5.18	110	81.56	210	131.98
60	10.29	120	90.07	p_a	132.57
65	17.35	130	97.70		

115°C 20 min. U.V. Run 2.					6.8 mg.
t	p	t	p	t	p
10	0.09	80	0.48	170	81.08
20	0.13	90	16.08	180	86.29
Water Interruption		100	23.41	190	90.67
30	0.14	110	31.24	200	94.65
40	0.17	120	39.53	220	98.72
60	1.18	130	48.09	240	101.31
65	2.41	140	57.08	260	102.88
70	4.39	150	66.43	280	103.93
75	6.70	160	74.24	p_a	104.46

115°C 20 min. U.V. Run 3.					6.7 mg.
t	p	t	p	t	p
20	0.04	85	1.02	170	56.69
30	0.05	90	2.74	180	61.87
35	0.07	95	5.30	190	66.85
40	0.15	100	8.70	200	71.59
45	0.45	105	12.93	210	75.71
46	0.56	110	17.35	220	78.77
Water Interruption		115	21.69	230	81.55
50	0.57	120	25.98	240	83.43
60	0.58	130	33.29	250	85.33
70	0.60	140	39.53	260	86.77
80	0.64	150	45.96	300	90.67
82	0.70	160	51.37	p_a	91.15

TABLE 70 cont/.....

TABLE 70 cont.

115°C 20 min. U.V. Run 4. 6.6 mg.					
t	p	t	p	t	p
20	0.24	80	18.97	160	64.56
30	0.41	90	19.07	170	75.98
40	0.87	95	19.19	180	86.17
50	2.10	100	19.46	190	94.03
55	4.50	110	20.78	200	100.44
60	8.10	120	24.20	210	104.70
65	14.47	130	30.22	220	107.59
68	18.90	140	39.87	240	111.54
Water Interruption		150	52.22	p_a	112.54

115°C 20 min. U.V. Run 5. 6.6 mg.					
t	p	t	p	t	p
20	0.05	Water Interruption		200	62.39
30	0.08	100	35.10	210	68.40
40	0.13	110	35.28	220	74.66
50	0.52	120	36.36	230	80.76
60	2.41	130	37.38	240	85.07
65	4.95	140	38.67	250	89.19
70	9.01	150	40.47	260	91.89
75	14.47	160	43.20	300	98.73
80	21.21	170	46.47	340	102.51
85	28.41	180	50.68	p_a	103.36
90	34.80	190	56.50		

115°C 20 min. U.V. Run 6. 6.7 mg.					
t	p	t	p	t	p
20	0.12	105	58.66	220	66.04
30	0.18	Water Interruption		230	69.63
40	0.27	110	58.68	240	73.52
50	1.54	120	58.70	250	77.33
60	6.97	130	58.70	260	81.33
65	12.02	140	58.72	270	84.64
70	18.01	150	58.76	310	96.26
75	25.20	160	58.83	340	102.19
80	31.82	170	58.98	370	105.32
85	37.60	180	59.34	410	106.78
90	43.53	190	60.08	440	108.19
95	48.81	200	61.23	p_a	110.40
100	54.06	210	63.38		

TABLE 70 cont/.....

TABLE 70 cont.

115°C 20 min. U.V. Run 7.					6.8 mg.
t	p	t	p	t	p
20	0.13	160	1.90	315	9.67
30	0.13	170	1.94	320	12.64
40	0.17	180	2.43	325	15.75
45	0.27	Water Interuuption		330	19.29
50	0.65	210	2.56	335	23.27
Water Interruption		220	2.65	340	27.68
60	0.67	230	3.00	350	36.59
80	0.87	Water Interruption		360	45.18
90	1.24	240	3.02	370	52.90
Water Interruption		250	3.04	380	59.69
100	1.28	260	3.07	390	64.87
110	1.29	270	3.13	400	69.01
120	1.46	280	3.35	420	74.15
130	1.83	290	4.07	440	77.69
Water Interruption		300	5.10	460	80.39
140	1.85	305	6.37	p_a	82.23
150	1.87	310	7.95		

TABLE 71.

Point of Interruption.	k_1 $cm^{1/2}$ $min.^{-1}$	Induction Period min.	Number of Interruptions.	Induction Period min.
Uninterrupted.	5.808×10^{-3}	45	0	50
$^1/_2$ along I.P.	3.436×10^{-3}	35	1	40
End of I.P.	4.136×10^{-3}	40	2	40
	k_5 $cm^{1/3}$ $min.^{-1}$		3	50
$\alpha = 0.15$	4.98×10^{-3}	32	4	50
$\alpha = 0.27$	2.370×10^{-3}	25	5	50
$\alpha = 0.46$	2.62×10^{-3}	65		
5 consecutive	4.110×10^{-3}	50		

(v) Effect of/.....

(v) Effect of varying the temperature of decomposition.

In order to evaluate the critical increment of the process-(es) taking place a number of decompositions at various temperatures were carried out. The azide was preirradiated for 20 min. The results are listed in TABLE 72. The rate constants, k_1 and k_7, (equation 1 and 2) which were obtained are given in TABLE 73 together with the lengths of the induction periods.

TABLE 72.

105°C 20 min. U.V. Run 1.					6.7 mg.
t	p	t	p	t	p
20	0.06	120	3.42	220	62.35
30	0.06	130	6.60	240	70.94
40	0.07	140	11.33	260	78.56
50	0.07	150	17.32	280	85.54
60	0.07	160	24.08	300	91.83
70	0.09	170	31.08	320	97.33
80	0.13	180	38.02	360	107.73
90	0.24	190	44.62	420	119.26
100	0.55	200	51.38	p_f	127.20
110	1.52	210	57.44	p_a	129.03

110°C 20 min. U.V. Run 2.					6.7 mg.
t	p	t	p	t	p
20	0.02	110	31.80	230	109.84
30	0.02	115	37.56	240	113.10
40	0.04	120	43.12	250	116.41
50	0.07	130	53.16	260	119.21
60	0.24	140	62.09	270	122.03
70	1.17	150	70.04	280	123.74
75	2.31	160	77.10	290	124.89
80	4.14	170	83.85	300	126.05
85	6.76	180	87.85	310	126.63
90	10.20	190	92.75	p_f	127.20
95	14.52	200	97.77	p_a	128.44
100	19.62	210	101.89		
105	25.47	220	106.09		

TABLE 72 cont/.....

TABLE 72 cont.

115°C 20 min. U.V. Run 3.					6.7 mg.
t	p	t	p	t	p
20	0,04	75	33,98	150	105,89
30	0.06	80	41,44	160	111,17
35	0,11	85	49,29	170	116,03
40	0,21	90	56,31	180	120,44
45	0,66	95	62,53	190	123,80
50	1,94	100	68,69	200	125,50
55	4,98	110	78,24	210	126,64
60	9,88	120	86,43	p_f	127,20
65	16,65	130	93,74	p_a	132,58
70	24,68	140	99,72		

120°C 20 min. U.V. Run 4.					6.9 mg.
t	p	t	p	t	p
10	0.09	60	42,76	115	112,78
20	0,16	65	52,91	120	116,58
30	0,31	70	62,13	125	119,32
35	0,74	75	69,95	130	122,01
40	2,97	80	77,35	135	123,80
45	8,64	85	83,71	140	124,93
48	14,26	90	89,37	145	126,07
50	18,56	95	94,72	150	126,64
52	23,19	100	99,72	p_f	127,20
54	28,33	105	104,33	p_a	132,58
57	35,78	110	108,51		

125°C 20 min. U.V. Run 5.					6.9 mg.
t	p	t	p	t	p
10	0.02	38	20,40	85	101,58
15	0,03	40	26,56	90	108,38
20	0,06	42	32,09	95	114,85
22	0,13	45	39,41	100	119,27
24	0,29	50	50,32	105	122,64
26	0,75	55	58,60	110	124,91
28	1,76	60	66,67	115	126,03
30	3,37	65	73,51	120	126,62
32	6,12	70	80,67	p_f	127,20
34	10,01	75	87,69	p_a	130,80
36	14,84	80	94,51		

TABLE 72 cont/.....

TABLE 72 cont.

130°C 20 min. U.V. Run 6. 6.8 mg.					
t	p	t	p	t	p
10	0.04	27	24.47	55	97.39
15	0.06	28	29.81	60	106.18
18	0.35	29	34.76	65	113.16
20	1.39	30	38.80	70	118.12
21	2.52	32	45.79	75	121.49
22	4.42	34	52.25	80	123.76
23	7.11	37	59.93	85	125.48
24	10.43	40	66.44	90	126.62
25	14.59	45	76.85	p_f	127.20
26	19.21	50	87.05	p_a	129.62

TABLE 73.

Temperature °C	Induction period min.	k_1 $cm^{1/2}$ $min.^{-1}$	k_7 $min.^{-1}$
105°	102	3.907×10^{-3}	1.830×10^{-3}
110°	65	5.808×10^{-3}	3.000×10^{-3}
115°	45	8.262×10^{-3}	4.440×10^{-3}
120°	34	1.104×10^{-2}	6.700×10^{-3}
125°	25	1.783×10^{-2}	1.250×10^{-2}
130°	19	2.503×10^{-2}	1.830×10^{-2}

(vi) Percentage decomposition.

The percentage decomposition increases on irradiation with ultra-violet light as compared to the unirradiated salt. As the irradiation time is increased so does the percentage decomposition, and an average limiting value of 87.33% of that calculated theoretically is reached. The limiting value is reached after a dose of 1 minute. TABLE 74 summarizes the results of a series of calculations.

TABLE 74/.....

TABLE 74.

Temperature °C	Dose.	Weight used mg.	% decomposition.
120°	2 secs.	7.7	71.52
120°	10 secs.	6.9	80.73
120°	1 min.	7.1	88.49
120°	2 "	6.9	88.52
120°	5 "	6.6	88.42
120°	15 "	6.4	90.03
105°	20 "	6.7	87.40
110°	20 "	6.7	87.02
115°	20 "	6.7	89.69
120°	20 "	6.9	87.41
125°	20 "	6.9	85.96
130°	20 "	6.8	86.47

The average percentage decomposition for a sample pre-irradiated for 20 min. is 87.33% of the theoretical value, assuming the equation for the thermal decomposition to be,

$$Sr(N_3)_2 \rightarrow Sr + 3N_2$$

(vii) Mathematical analysis of the results and evaluation of activation energies.

The acceleratory period of the p/t plot was described by the power law with n = 3 for low doses of irradiation,

$$p^{1/3} = k_5 t + c_5 \quad \ldots\ldots\ldots\ldots\ldots\ldots\ldots\ldots (10)$$

This is the same as for the unirradiated decomposition, and and is valid for irradiation time of up to 10 secs. As the irradiation time increases, however, the value of the exponent changes from $^1/_3$ to $^1/_2$. The equation thus becomes

$$p^{1/2} = k_1 t + c_1 \quad \ldots\ldots\ldots\ldots\ldots\ldots\ldots\ldots (1)$$

for heavily dosed samples.

An irradiation time of one minute appears to be the transition point. At this dose neither power law fits well; below it n = 3, and above it n = 2. FIGURE 59 shows the p/t

plots for/.....

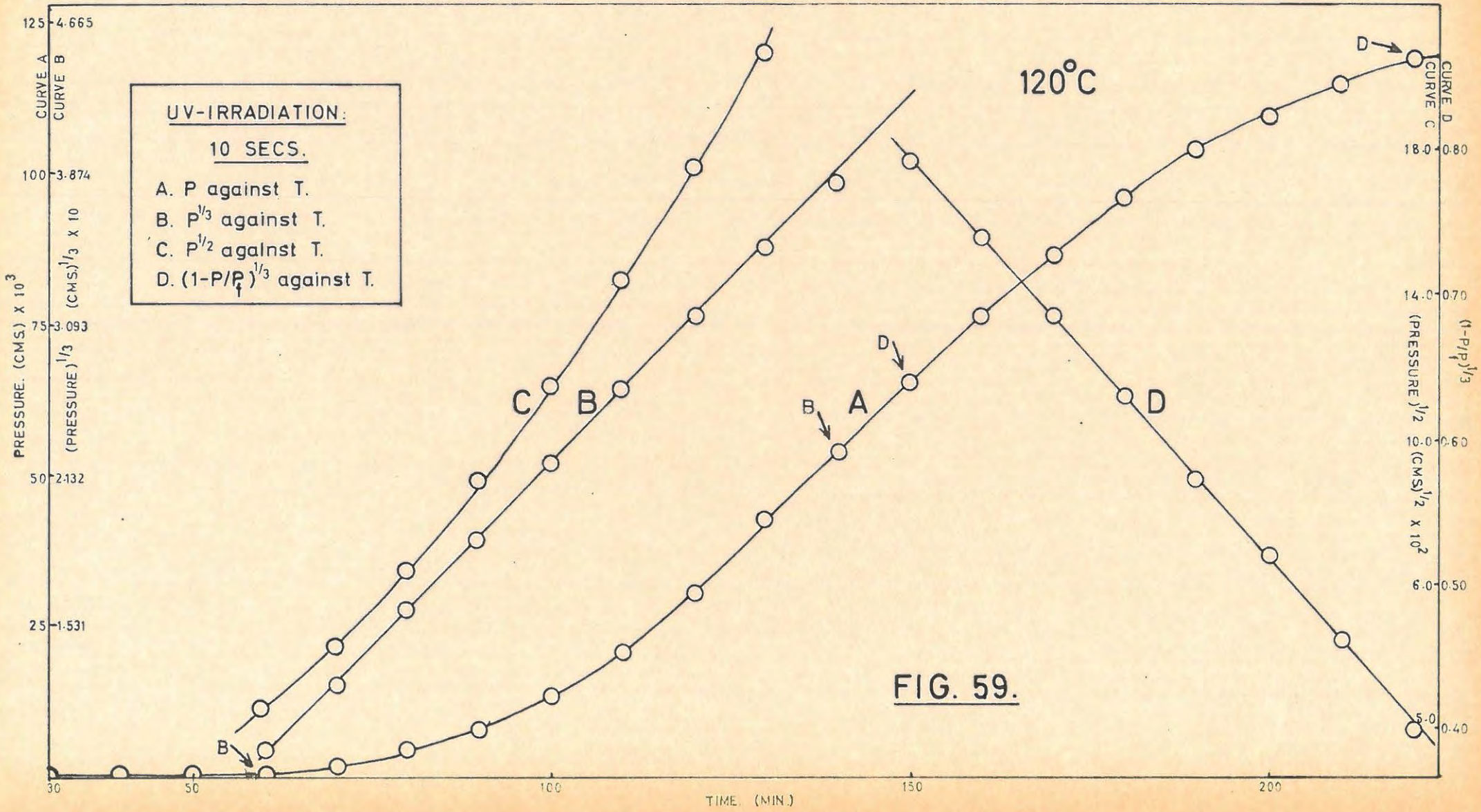
UV-IRRADIATION:
10 SECS.
A. P against T.
B. P^1/3 against T.
C. P^1/2 against T.
D. (1-P/Pf)^1/3 against T.
120°C
PRESSURE. (CMS.) X 10^3
CURVE A
CURVE B
(PRESSURE)^1/3 (CMS)^1/3 X 10
CURVE C
(PRESSURE)^1/2 (CMS)^1/2 X 10^2
CURVE D
(1-P/Pf)^1/3
TIME. (MIN.)
125
100
75
50
25
4.665
3.874
3.093
2.132
1.531
18.0
14.0
10.0
6.0
5.0
0.80
0.70
0.60
0.50
0.40
30
50
100
150
200
A
B
C
D

FIG. 59.

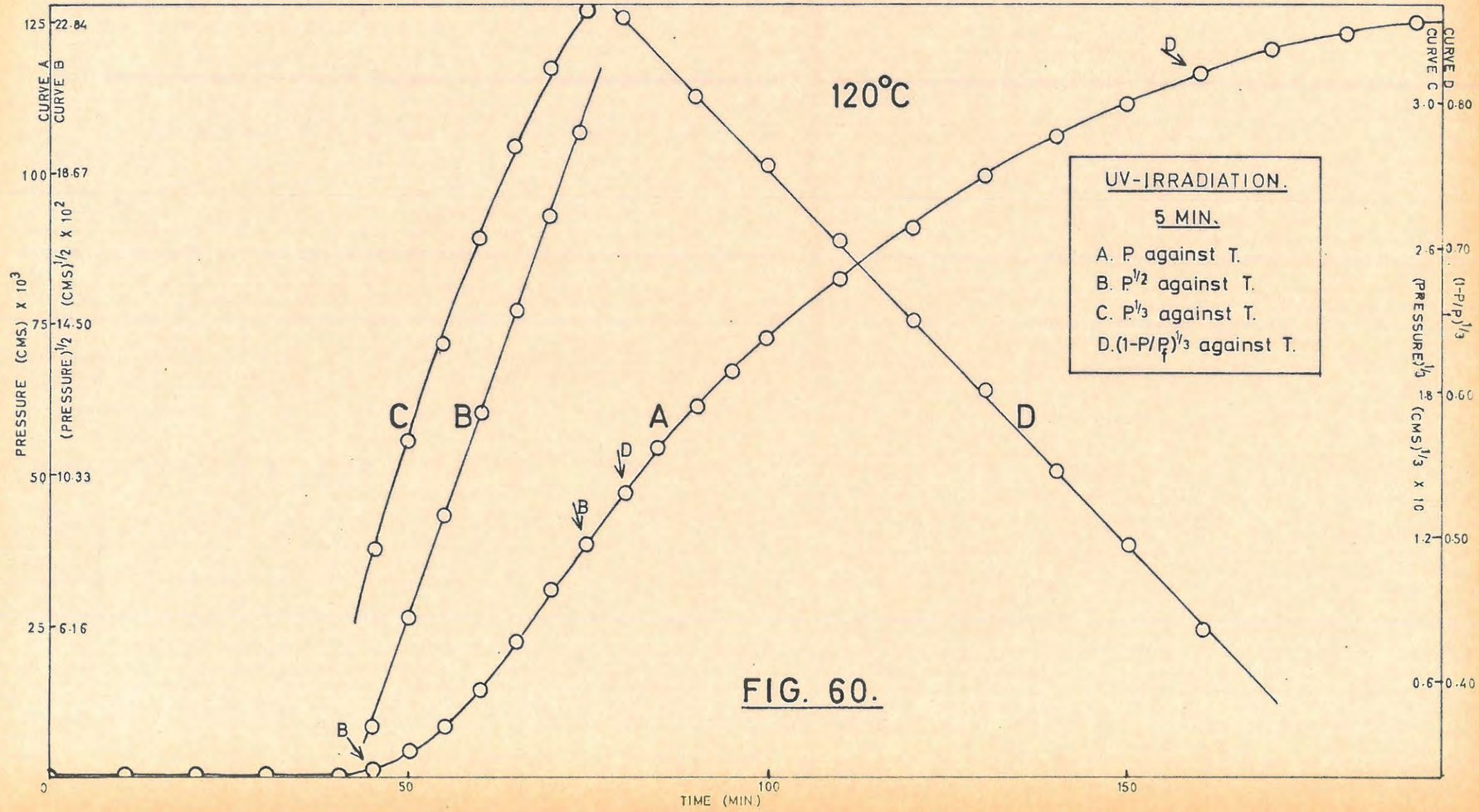
120°C
UV-IRRADIATION.
5 MIN.
A. P against T.
B. $P^{1/2}$ against T.
C. $P^{1/3}$ against T.
D. $(1-P/P_f)^{1/3}$ against T.
PRESSURE (CMS) X 10^3
CURVE A
CURVE B
$(PRESSURE)^{1/2}$ $(CMS)^{1/2}$ X 10^2
CURVE C
CURVE D
$(PRESSURE)^{1/3}$ $(CMS)^{1/3}$ X 10
$(1-P/P_f)^{1/3}$
TIME (MIN.)
A
B
C
D
125
100
75
50
25
0
22.84
18.67
14.50
10.33
6.16
3.0
2.6
1.8
1.2
0.6
0.80
0.70
0.60
0.50
0.40
50
100
150

FIG. 60.

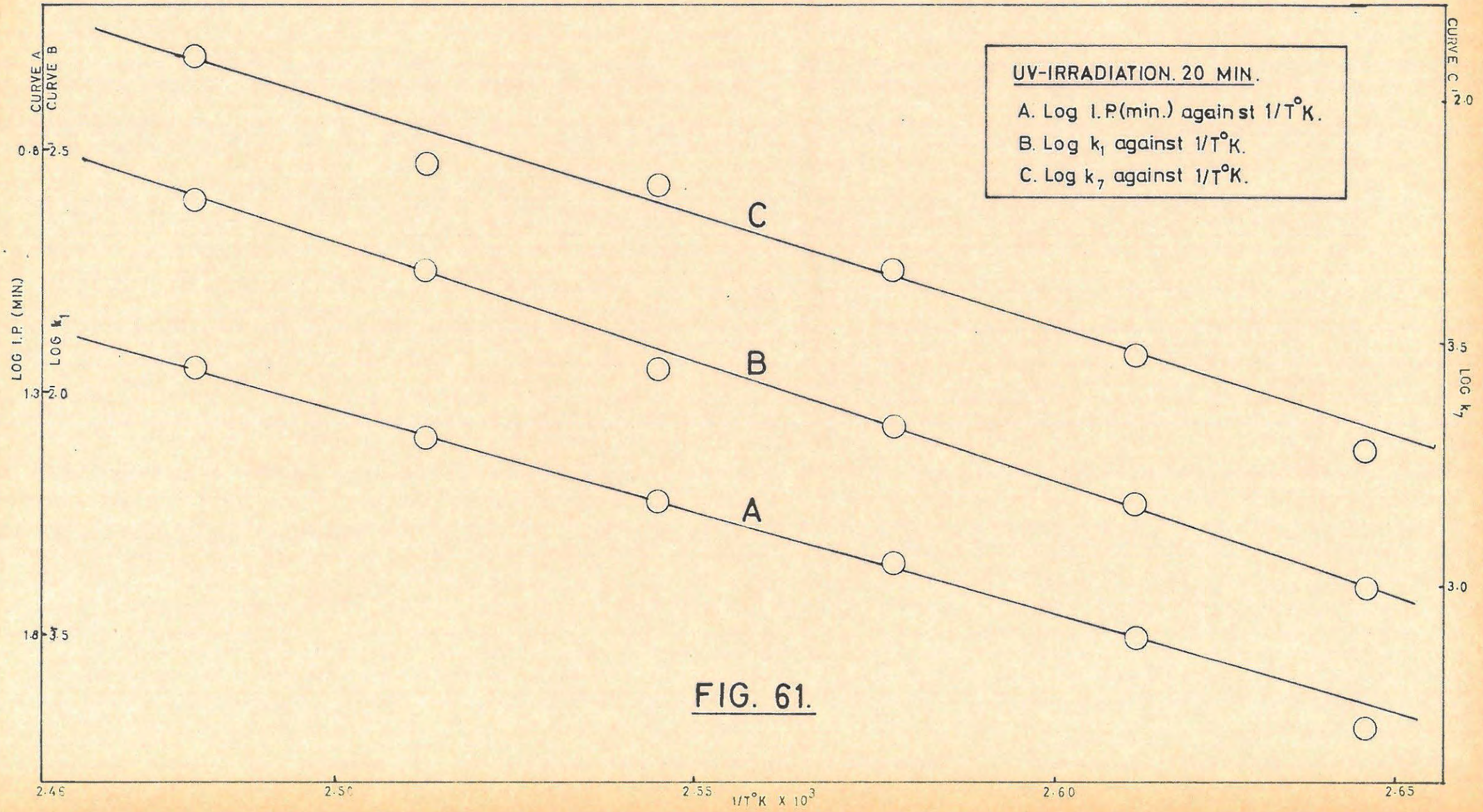
UV-IRRADIATION. 20 MIN.
A. Log I.P.(min.) against 1/T°K.
B. Log k_1 against 1/T°K.
C. Log k_7 against 1/T°K.
C
B
A
CURVE A
CURVE B
CURVE C
LOG I.P. (MIN.)
LOG k_1
LOG k_7
0·8
1·3
1·8
2·5
2·0
3·5
2·0
3·5
3·0
2·45
2·50
2·55
2·60
2·65
1/T°K X 10^3

FIG. 61.

plots for a low dose (10 secs.) with the corresponding analysis for n = 2 and 3, while FIGURE 60 shows the same plots for a high dose (5 min.).

The decay stage is fitted by the contracting sphere formula in all cases viz.

$$(1 - {}^{p}/_{p_f})^{1/3} = k_7 t + c_7 \quad \ldots\ldots\ldots\ldots\ldots\ldots\ldots\ldots (2)$$

The plot of $(1 - {}^{p}/_{p_f})^{1/3}$ vs t is also shown in FIGURES 59 and 60

The analysis of the p/t plots after water vapour has been admitted onto interrupted runs also shows a power change in the exponent in the power law. At the dose given (20 min.) the power law holds with n = 2. After one interruption at the end of the induction period n is still 2. However, after 5 consecutive interruptions n changes to 3. Also after any "water interruption" done in the acceleratory or decay periods n reverts back to 3 in the subsequent acceleratory period.

Plots of log I.P. (min.), log k_1, and log k_7, vs ${}^{1}/_{T}\ {}^{o}K$, respectively, are shown in FIGURE 61. From them the following activation energies were evaluated:

(i) Induction period: 19.50 kcals.mole^{-1}

(ii) Acceleratory period: 23.00 kcals. mole^{-1}

(iii) Decay period: 21.70 kcals.mole^{-1}.

7.1.4. Preirradiated (X-rays) Strontium Azide.

(i) Preliminary investigation.

The apparatus and techniques employed in X-ray irradiations have already been described. An initial run to test for any effect was done by irradiating a sample in air for five minutes with a beam current of 5 mA and an applied voltage of 10 kV. Decomposition was then carried out in vacuo at 120°C. The resulting p/t plot is shown in FIGURE 62 and the results are listed in TABLE 75.

TABLE 75/.....

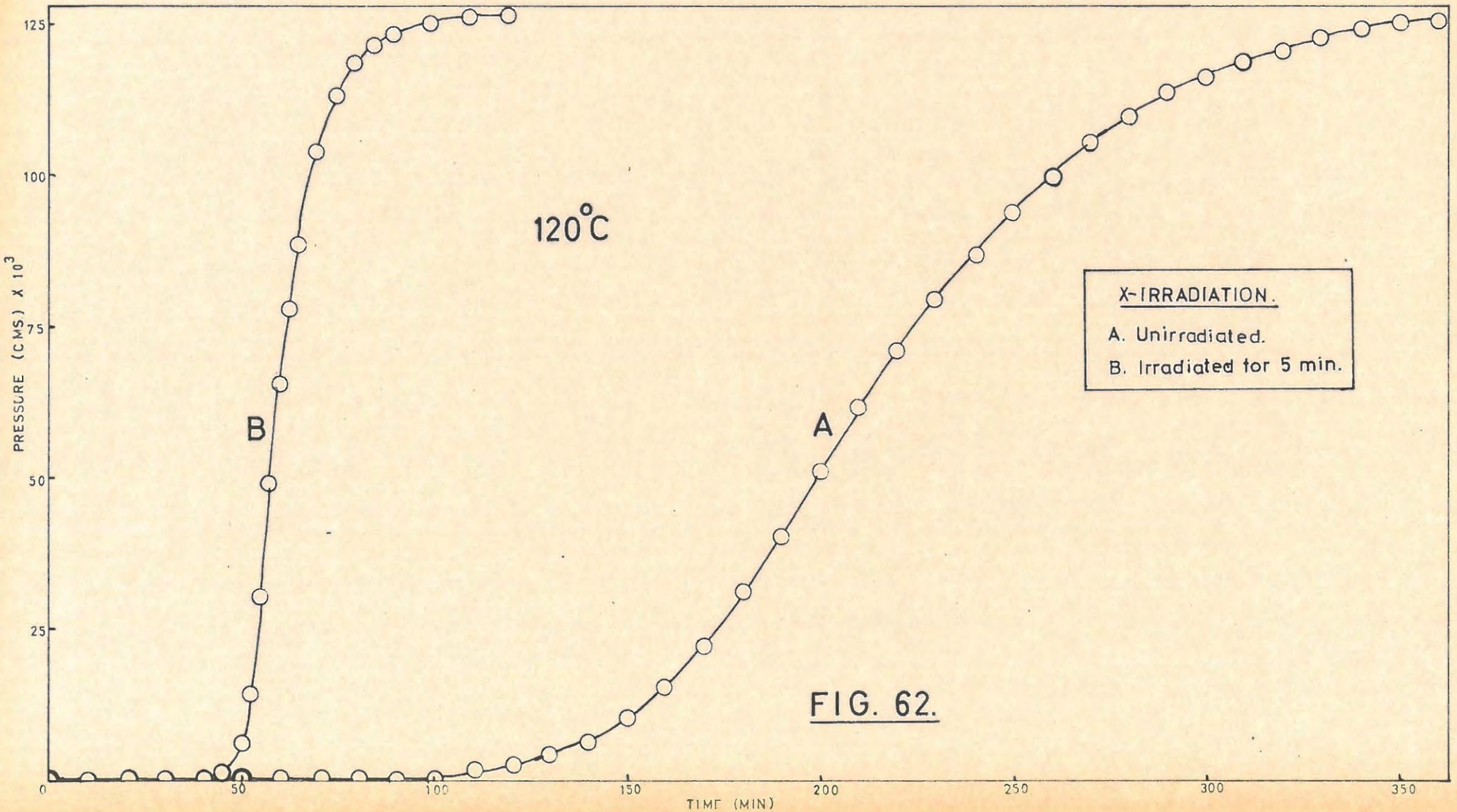
120°C
X-IRRADIATION.
A. Unirradiated.
B. Irradiated for 5 min.
A
B
PRESSURE (CMS) X 10³
TIME (MIN)
0
50
100
150
200
250
300
350
25
50
75
100
125

FIG. 62.

TABLE 75.

120°C Unirradiated blank Run 1.					7.7 mg.
t	p	t	p	t	p
10	0.01	140	6.46	270	105.11
20	0.01	150	10.19	280	109.59
30	0.02	160	15.17	290	113.60
40	0.02	170	22.16	300	116.50
50	0.07	180	31.05	310	118.84
60	0.16	190	40.10	320	120.03
70	0.21	200	51.00	330	123.01
80	0.32	210	61.54	340	124.82
90	0.47	220	70.78	350	126.05
100	0.68	230	79.21	360	126.64
110	1.55	240	87.10	p_f	127.20
120	2.55	250	93.79	p_a	116.42
130	4.01	260	99.64		

120°C 5 min. X-rays. Run 2.					6.2 mg.
t	p	t	p	t	p
10	0.07	53	17.30	70	104.84
15	0.14	54	23.29	75	113.76
20	0.14	55	30.46	80	118.94
30	0.18	56	38.27	85	121.87
40	0.31	57	45.87	90	123.64
45	1.14	58	52.22	100	125.42
48	3.10	60	65.28	110	126.62
50	6.28	62	76.03	p_f	127.20
51	8.92	64	85.61	p_a	119.79
52	12.39	66	93.69		

(ii) Effect of varying doses of X-rays.

The high sensitivity of strontium azide to X-rays made it necessary to insert an absorber to reduce the intensity. An aluminium absorber of thickness 0.43 mm. gave the required screening effect. A beam current of 5 mA and applied voltage of 10 kV was used in all the X-ray studies, unless otherwise stated.

The effect of increased dosage of X-rays on the thermal decomposition was studied at a decomposition temperature of 120°C

Irradiation/.....

Irradiation times ranged from 15 secs. to 4 hours. The results are listed in TABLE 76, and are shown in FIGURE 63. An unirradiated blank run is given in TABLE 75 (Run 1). A marked decrease in the duration of the induction period, and an increase in the acceleratory and decay rate constants, are the main features. The acceleratory rate constants, k_5, (equation 10) for exposure times of up to 30 min., and k_6 (equation 11) for longer exposures, are given in TABLE 77, together with the decay rate constants, k_7, (equation 2) and the lengths of the induction periods (min.).

TABLE 76.

120°C 15 secs. X-rays. Run 1.					6.7 mg.
t	p	t	p	t	p
10	0.03	110	7.38	220	102.35
20	0.03	120	13.50	240	110.36
30	0.04	130	22.42	270	118.10
40	0.07	140	33.59	310	122.64
50	0.10	150	45.96	340	124.94
60	0.13	160	57.87	360	126.10
70	0.24	170	68.56	380	126.68
80	0.60	180	78.31	p_f	127.20
90	1.54	190	86.29	p_a	127.27
100	3.57	200	92.65		

120°C 1 min. X-rays. Run 2.					6.2 mg.
t	p	t	p	t	p
10	0.06	100	7.44	180	101.03
20	0.09	105	10.70	190	107.29
30	0.12	110	15.63	200	112.54
40	0.16	115	21.11	210	116.71
50	0.20	120	27.38	220	120.35
60	0.25	125	34.19	230	122.81
65	0.36	130	41.73	240	124.67
70	0.52	135	49.23	250	125.91
75	0.79	140	56.94	260	126.54
80	1.37	145	64.30	p_f	127.20
85	2.10	150	71.18	p_a	109.81
90	3.18	160	83.92		
95	4.96	170	93.33		

TABLE 76 cont/.....

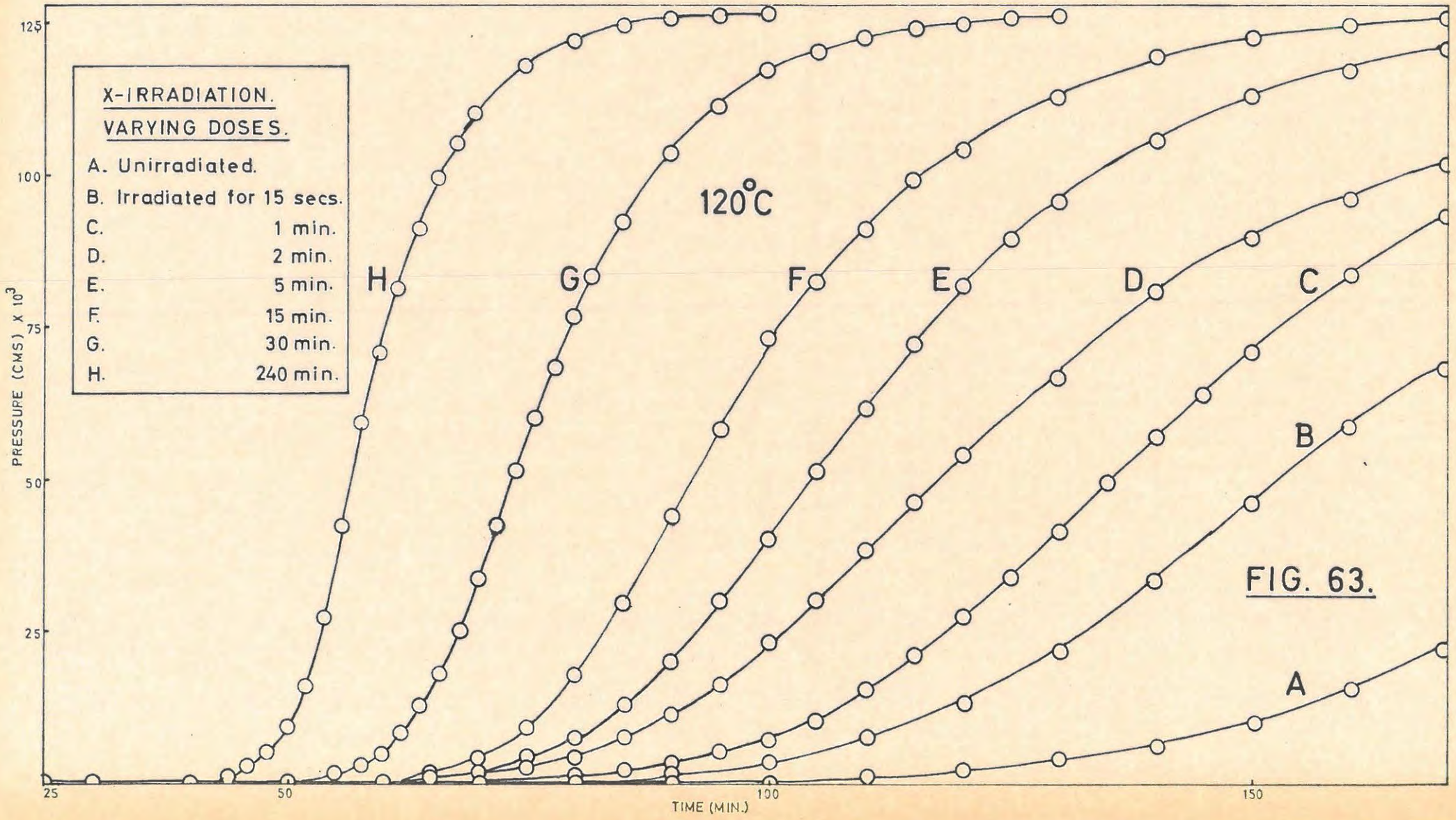
X-IRRADIATION.
VARYING DOSES.
A. Unirradiated.
B. Irradiated for 15 secs.
C. 1 min.
D. 2 min.
E. 5 min.
F. 15 min.
G. 30 min.
H. 240 min.
120°C
H
G
F
E
D
C
B
A
PRESSURE (CMS) X 10³
TIME (MIN.)
125
100
75
50
25
25
50
100
150

FIG. 63.

TABLE 76 cont.

120°C 2 min. X-rays. Run 3.					6.5 mg.
t	p	t	p	t	p
20	0.05	90	11.06	160	96.23
30	0.06	95	16.37	170	102.30
40	0.08	100	22.98	180	106.27
50	0.15	105	30.41	200	113.23
60	0.37	110	38.16	220	119.21
65	0.69	115	45.72	240	122.87
70	1.42	120	53.92	260	125.34
75	2.58	130	66.97	280	126.58
80	4.43	140	81.11	p_f	127.20
85	7.23	150	90.34	p_a	110.90

120°C 5 min. X-rays. Run 4.					6.7 mg.
t	p	t	p	t	p
10	0.06	85	12.98	140	106.39
20	0.07	90	20.35	150	113.30
30	0.07	95	29.96	160	117.44
40	0.19	100	40.37	170	121.05
50	0.19	105	51.14	180	123.48
60	0.51	110	61.88	190	125.32
65	1.09	115	72.23	200	126.55
70	2.12	120	81.39	p_f	127.20
75	4.25	125	89.53	p_a	112.54
80	7.54	130	95.88		

120°C 15 min. X-rays. Run 5.					6.4 mg.
t	p	t	p	t	p
10	0.02	78	13.86	120	104.79
20	0.03	80	17.77	130	113.95
30	0.03	85	29.37	140	119.27
40	0.07	90	43.87	150	122.88
50	0.15	95	58.32	160	125.32
60	0.67	100	71.53	170	126.55
65	1.87	105	82.58	p_f	127.20
70	4.33	110	91.25	p_a	113.64
75	9.07	115	99.26		

TABLE 76/.....

TABLE 76 cont.

120°C 30 min, X-rays. Run 6.					6.4 mg.
t	p	t	p	t	p
10	0.08	66	18.19	90	103.91
20	0.13	68	25.45	95	111.44
30	0.17	70	33.93	100	117.02
40	0.22	72	42.26	105	120.42
50	0.61	74	51.51	110	122.71
55	1.69	76	60.06	115	124.45
58	3.31	78	68.38	120	125.61
60	5.24	80	76.34	130	126.78
62	8.18	82	83.31	p_f	127.20
64	12.51	85	92.57	p_a	125.89

120°C 60 min, X-rays. Run 7.					6.6 mg.
t	p	t	p	t	p
10	0.04	62	11.59	85	100.05
20	0.07	64	17.22	90	109.85
30	0.10	66	24.48	95	116.07
40	0.14	68	33.32	100	120.12
45	0.28	70	42.82	105	123.65
50	0.77	72	52.35	110	125.43
52	1.25	74	62.00	115	126.62
54	1.91	76	71.11	p_f	127.20
56	3.18	78	78.94	p_a	120.36
58	4.99	80	86.19		
60	7.65	82	89.54		

120°C 240 min, X-rays. Run 8.					6.7 mg.
t	p	t	p	t	p
10	0.06	54	27.32	72	114.20
20	0.10	56	42.52	75	118.10
30	0.13	58	57.08	80	122.64
40	0.69	60	70.28	85	124.94
44	1.61	62	81.55	90	126.10
46	2.92	64	91.16	95	126.68
48	5.30	66	99.75	p_f	127.20
50	9.16	68	105.52	p_a	127.27
52	16.29	70	110.36		

TABLE 77/.....

TABLE 77.

Dose	Induction period (min.)	k_5 $cm^{1/3}$ $min.^{-1}$	k_7 $min.^{-1}$
0	100	3.010×10^{-3}	4.100×10^{-3}
15 secs.	80	4.280×10^{-3}	3.800×10^{-3}
1 min.	73	5.210×10^{-3}	5.625×10^{-3}
2 "	65	5.898×10^{-3}	5.100×10^{-3}
5 "	62	7.303×10^{-3}	8.550×10^{-3}
15 "	60	9.443×10^{-3}	1.050×10^{-2}
30 "	50	1.505×10^{-2}	1.760×10^{-2}
		k_6 $min.^{-1}$	
60 min.	48	2.875×10^{-2}	1.890×10^{-2}
240 min.	40	4.120×10^{-2}	2.660×10^{-2}

(iii) Effect of interrupting a decomposition and irradiating the salt.

The effect of irradiating at various stages during a decomposition was done in the same manner as before. The technique used, which involved irradiating through thin glass ampoules, has been described earlier. Because the pyrex ampoule absorbed a considerable amount of the X-rays the aluminium absorber was removed and the generator run at 16 kV and 8 mA. The irradiation time was 10 minutes and the decomposition temperature 120°C. TABLE 78 and FIGURE 64 give the results. An unirradiated blank run is given in TABLE 75. It is seen that in all cases the interrupted and irradiated salt continues decomposing in the normal manner for an unirradiated decomposition for a period of approximately 30 - 40 minutes. This is of the same order as the duration of the induction period for the preirradiated salt. At this point there is a distinct increase in the rate of acceleration and the remainder of the decomposition has the characteristics of the preirradiated decomposition.

TABLE 78/.....

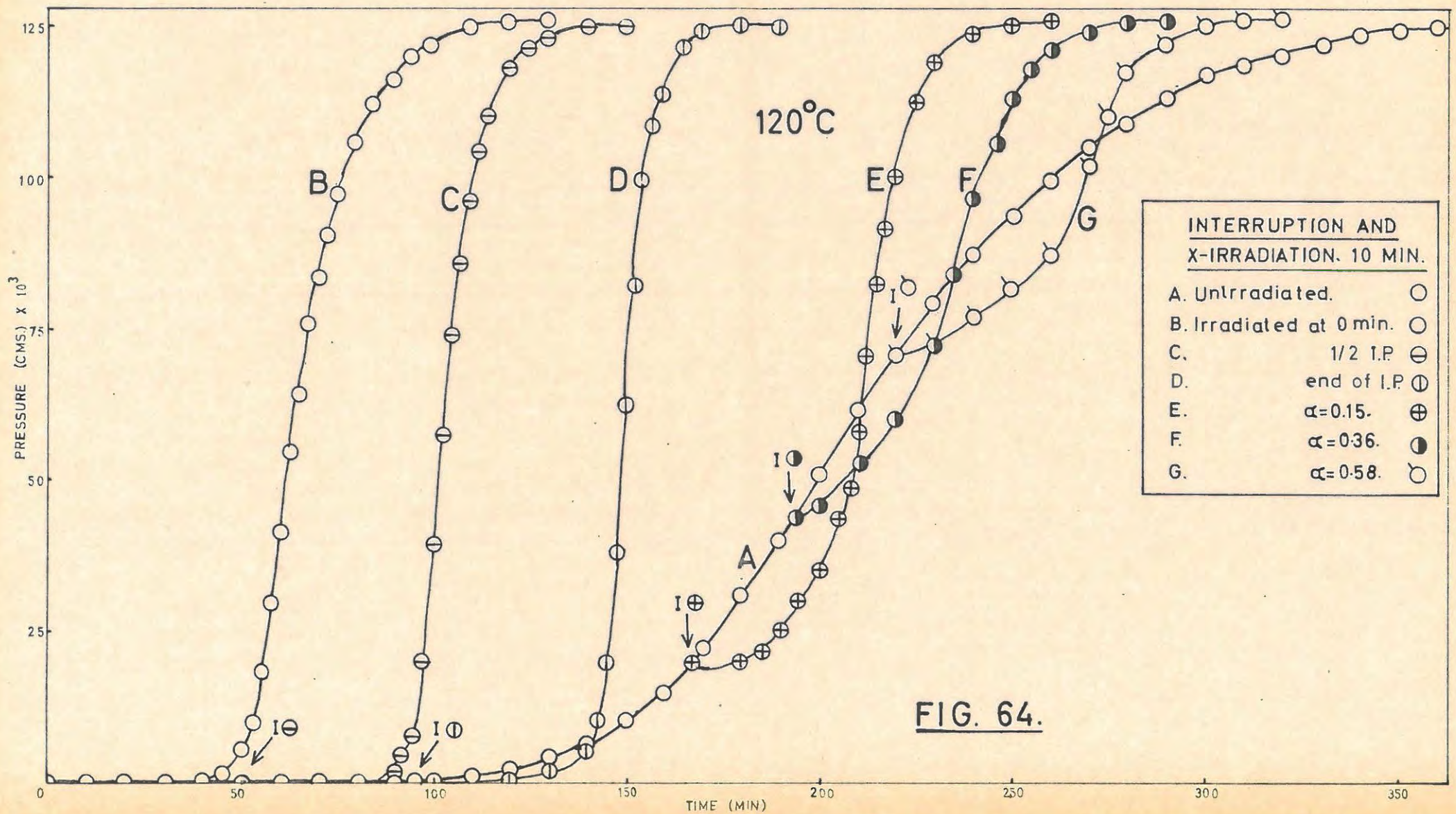
120°C
B
C
D
E
F
G
A
I⊖
I◑
I⊕
I○
INTERRUPTION AND
X-IRRADIATION. 10 MIN.
A. Unirradiated. ○
B. Irradiated at 0 min. ○
C. 1/2 I.P ⊖
D. end of I.P ◑
E. α=0.15. ⊕
F. α=0.36. ◑
G. α=0.58. ○
PRESSURE (CMS.) X 10³
TIME (MIN)
0
50
100
150
200
250
300
350
25
50
75
100
125

FIG. 64.

TABLE 78.

120°C Irradiated blank. Run 1.					7.0 mg.
t	p	t	p	t	p
10	0.01	54	15.16	80	106.35
20	0.01	56	22.60	85	112.53
30	0.03	58	31.81	90	116.56
35	0.07	60	41.54	95	120.06
40	0.29	62	51.42	100	122.43
43	0.74	65	64.48	110	125.42
46	1.95	68	76.65	120	126.62
48	3.34	70	83.87	p_f	127.20
50	5.84	72	89.37	p_a	118.10
52	9.71	75	97.14		

120°C 10 min. X-rays. Run 2.					6.9 mg.
t	p	t	p	t	p
20	0.02	96	11.10	108	88.97
40	0.05	97	16.19	110	96.88
50	0.07	98	22.97	112	103.03
Irradiation		99	30.65	115	110.44
70	0.08	100	39.12	120	118.11
80	0.09	101	46.84	125	122.61
85	0.24	102	54.12	130	124.89
90	1.16	103	61.69	134	126.04
92	2.53	104	67.70	140	126.61
94	5.20	105	73.73	p_f	127.20
95	7.66	106	79.11	p_a	129.61

120°C 10 min. X-rays. Run 3.					7.0 mg.
t	p	t	p	t	p
20	0.04	130	2.03	151	71.08
40	0.05	135	3.12	152	78.97
60	0.08	138	4.32	153	86.22
70	0.13	140	5.72	154	92.68
80	0.22	142	9.64	156	102.81
90	0.39	143	12.47	158	109.86
95	0.60	144	15.67	160	114.69
Irradiation		145	19.49	165	122.13
100	0.62	146	25.99	170	124.66

TABLE 78 cont/.....

TABLE 78 cont.

t	p	t	p	t	p
110	0.71	147	34.43	175	126.57
115	0.83	148	43.66	p_f	127.20
120	0.95	149	54.00	p_a	119.23
125	1.29	150	62.70		

120°C 10 min. X-rays. Run 4.					6.9 mg.
t	p	t	p	t	p
20	0.08	Irradiation		211	63.73
40	0.11	180	19.34	212	68.54
60	0.23	185	21.26	214	78.05
70	0.35	188	23.62	216	86.61
80	0.42	190	25.24	218	94.82
90	0.52	192	27.11	220	100.56
100	0.65	194	29.06	222	105.99
110	0.89	196	31.21	225	112.64
120	1.28	198	33.05	230	118.99
130	1.96	200	35.37	235	122.25
140	3.44	202	37.62	240	124.44
150	5.86	204	41.03	245	126.11
160	10.07	206	44.72	250	126.67
170	16.50	208	50.47	p_f	127.20
173	18.99	210	58.83	p_a	117.73

120°C 10 min. X-rays. Run 5.					6.9 mg.
t	p	t	p	t	p
20	0.02	180	36.79	234	81.71
40	0.07	190	45.91	236	86.79
60	0.11	Irradiation		238	91.83
80	0.25	195	46.27	240	96.76
90	0.43	200	47.49	242	101.14
100	0.63	202	48.51	245	106.55
110	1.19	204	49.89	250	113.55
120	2.26	206	51.18	255	118.11
130	4.54	208	52.65	260	121.40
135	6.18	210	53.99	265	123.31
140	8.23	215	57.39	270	124.76
145	10.75	220	60.54	280	126.22
150	13.81	225	64.90	p_f	127.20
160	20.32	230	72.58	p_a	114.09
170	28.38	232	76.98		

TABLE 78 cont/.....

TABLE 78 cont.

120°C 10 min. X-rays. Run 6.					6.9 mg.
t	p	t	p	t	p
20	0.05	180	39.30	260	87.38
40	0.09	190	49.05	265	94.12
60	0.12	200	58.14	270	102.79
80	0.21	210	66.15	275	110.22
90	0.43	220	73.70	280	116.26
100	0.58	Irradiation		285	119.64
110	0.76	225	74.28	290	122.62
120	1.83	230	74.98	295	124.75
130	3.91	235	76.03	300	125.97
140	7.66	240	77.61	310	126.79
150	13.27	245	79.74	p_f	127.20
160	20.67	250	81.68	p_a	113.64
170	29.40	255	83.88		

(iv) Effect of admitting water vapour onto the salt in an interrupted decomposition.

The procedure for this type of experiment has been given earlier. The time of X-ray irradiation was one hour, and the decomposition temperature 120°C throughout the series. These runs are tabulated in TABLE 79, and illustrated in FIGURE 65. Again a new induction period is generated, and the subsequent rate constants are decreased. Interruption and admission of water vapour in the decay region produces a flash of flame from the sample and further decomposition is virtually eliminated. Successive interruptions along the induction period results once more in producing new induction periods all of approximately the same duration.

Acceleratory rate constants, k_5, (equation 10) are given in TABLE 80, together with the lengths of the induction periods formed.

Reduced values for the final pressures are once more obtained. Partial recovery of the lost pressure occurs on heating to 300°C in vacuo. Pressures are thus not normalised in the tables.

TABLE 79/.....

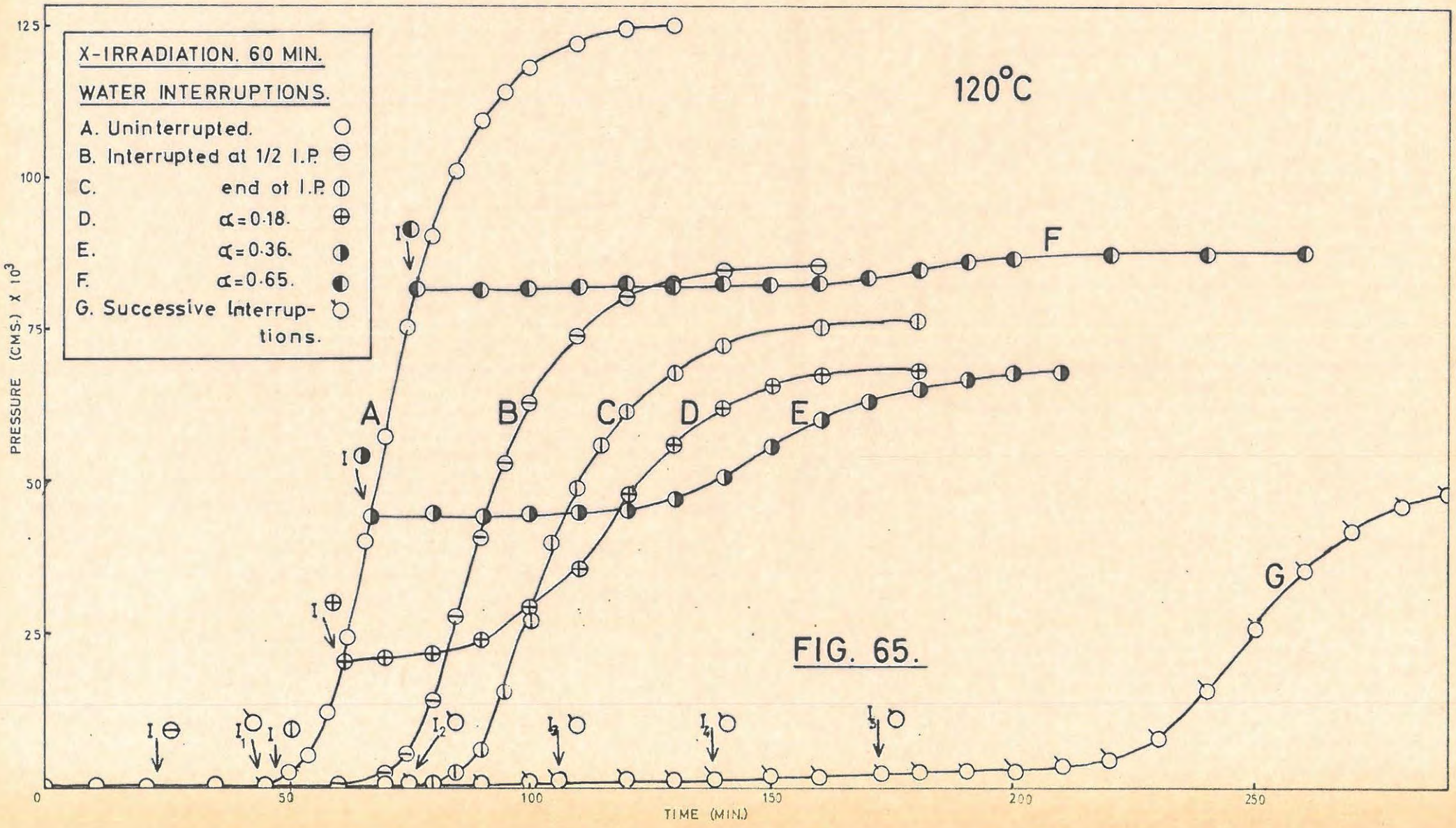
X-IRRADIATION. 60 MIN.
WATER INTERRUPTIONS.
A. Uninterrupted.
B. Interrupted at 1/2 I.P.
C. end of I.P.
D. α=0·18.
E. α=0·36.
F. α=0·65.
G. Successive Interruptions.
120°C
A
B
C
D
E
F
G
PRESSURE (CMS.) X 10³
TIME (MIN.)
0
25
50
75
100
125
50
100
150
200
250

FIG. 65.

TABLE 79.

120°C Irradiated blank. Run 1.					6.5 mg.
t	p	t	p	t	p
10	0.04	60	17.79	90	109.27
20	0.06	62	24.68	95	114.20
30	0.13	64	32.40	100	118.10
40	0.21	66	40.52	105	120.93
45	0.60	68	48.81	110	122.64
50	1.95	70	57.08	115	123.79
52	3.28	72	64.75	120	124.37
54	5.30	75	75.58	p_a	124.94
56	8.25	80	90.17		
58	12.38	85	101.31		

120°C 60 min. X-rays. Run 2.					6.4 mg.
t	p	t	p	t	p
10	0.05	78	10.29	105	68.99
20	0.09	80	14.27	110	73.79
23	0.13	82	19.12	120	79.23
Water Interruption		84	24.42	130	82.48
40	0.14	86	30.37	140	83.90
50	0.32	88	35.72	150	84.85
60	0.60	90	40.84	160	85.81
65	1.00	92	45.96	170	86.29
70	1.95	95	53.24	p_a	86.77
75	5.67	100	62.28		

120°C 60 min. X-rays. Run 3.					6.5 mg.
t	p	t	p	t	p
10	0.11	88	4.28	115	55.92
20	0.17	90	6.56	120	61.06
30	0.22	92	9.80	130	67.70
40	0.29	94	13.88	140	71.59
50	0.60	96	18.45	150	73.79
Water Interruption		98	23.16	160	75.58
60	0.62	100	27.86	170	76.49
70	0.65	102	32.70	p_a	76.94
80	0.69	105	39.21		
85	2.02	110	48.45		

TABLE 79 cont/.....

TABLE 79 cont.

120°C 60 min. X-rays. Run 4.					6.5 mg.
t	p	t	p	t	p
10	0.21	60	18.23	110	36.60
20	0.32	61	21.93	115	41.74
30	0.41	Water Interruption		120	47.13
40	0.60	70	22.20	125	52.02
45	0.86	75	22.39	130	56.43
48	1.36	80	22.80	140	61.79
50	2.02	85	23.41	150	65.47
52	3.28	90	24.42	180	68.24
54	5.18	95	26.01	210	70.38
56	8.40	100	28.38	p_a	72.56
58	12.57	105	31.90		

120°C 60 min. X-rays. Run 5.					6.5 mg.
t	p	t	p	t	p
10	0.12	66	19.35	135	49.40
20	0.18	68	25.72	140	50.99
30	0.27	70	33.00	145	53.73
40	0.39	72	39.86	150	55.79
45	0.52	73	44.56	155	58.25
50	0.87	Water Interruption		160	60.03
52	1.24	80	44.57	170	63.46
54	1.81	90	44.58	180	65.54
56	2.74	100	44.63	190	66.74
58	4.07	110	44.86	200	67.73
60	6.17	120	45.64	210	68.27
62	9.32	125	46.52	p_a	68.48
64	13.69	130	47.75		

120°C 60 min. X-rays. Run 6.					6.5 mg.
t	p	t	p	t	p
10	0.03	68	24.17	140	82.69
20	0.04	70	32.70	150	83.10
30	0.10	72	42.18	160	83.66
40	0.17	74	51.37	170	84.57
45	0.27	76	60.66	180	85.03
50	0.56	78	69.85	190	86.06
52	0.88	80	77.85	200	86.51
54	1.36	81	81.56	220	86.98

TABLE 79 cont/.....

TABLE 79 cont.

t	p	t	p	t	p
56	2.10	Water Interruption		240	87.22
58	3.28	90	81.69	260	87.35
60	5.07	100	81.78	280	87.42
62	7.95	110	81.89	p_a	87.47
64	12.02	120	82.01		
66	17.35	130	82.32		

120°C 60 min. X-rays. Run 7.					6.5 mg.
t	p	t	p	t	p
10	0.14	120	1.82	220	4.14
20	0.21	130	1.91	225	5.41
30	0.32	135	2.13	230	7.72
40	0.41	138	2.40	235	11.10
45	0.60	Water Interruption		240	15.57
Water Interruption		150	2.41	245	20.79
60	0.69	160	2.46	250	25.91
70	0.87	165	2.56	255	31.14
75	1.20	170	2.78	260	35.46
Water Interruption		173	3.00	270	41.88
90	1.31	Water Interruption		280	46.19
100	1.33	190	3.01	320	54.37
105	1.65	200	3.03	330	55.86
106	1.81	210	3.27	340	56.62
Water Interruption		215	3.59	p_a	57.00

TABLE 80.

Point of Interruption.	k_5 $cm^{1/3}$ $min.^{-1}$	Induction period min.	Number of Interruptions.	Induction period min.
Uninterrupted.	1.450×10^{-2}	45	0	45
½ along I.P.	1.231×10^{-2}	40	1	30
End of I.P.	1.289×10^{-2}	30	2	31
$\alpha = 0.18$	5.479×10^{-3}	20	3	32
$\alpha = 0.36$	4.287×10^{-3}	40	4	35
$\alpha = 0.65$	1.160×10^{-3}	50	5	40
5 consecutive.	6.372×10^{-3}	40		

(v) Effect of/.....

(v) Effect of varying the temperature of decomposition.

An irradiation time of two hours was selected for these runs. A series of decompositions in the temperature range 100°-130°C were carried out and the necessary rate constants determined at each temperature. The results appear in TABLE 81. The acceleratory and decay period rate constants, k_6 and k_7 (equations 11 and 2) respectively, and the induction periods (min.) are given in TABLE 82.

TABLE 81.

100°C 2 hrs. X-rays. Run 1.					6.5 mg.
t	p	t	p	t	p
60	0.07	240	4.21	340	84.58
120	0.11	250	6.90	350	92.30
140	0.15	260	10.97	360	99.26
160	0.15	270	16.86	380	108.75
180	0.24	280	24.81	400	115.71
190	0.36	290	34.31	440	123.49
200	0.55	300	44.24	460	125.32
210	0.86	310	55.02	480	126.56
220	1.52	320	66.08	p_f	127.20
230	2.52	330	75.76	p_a	113.64

105°C 2 hrs. X-rays. Run 2.					6.4 mg.
t	p	t	p	t	p
20	0.08	180	8.10	240	92.15
40	0.10	185	12.20	250	101.83
60	0.10	190	17.14	260	109.81
80	0.17	195	23.16	270	115.30
90	0.17	200	30.09	280	119.79
100	0.17	205	37.60	290	122.64
110	0.22	210	45.96	300	124.94
120	0.26	215	54.76	310	126.10
140	0.68	220	63.51	320	126.69
160	1.95	225	71.15	p_f	127.20
170	3.67	230	78.77	p_a	127.70

TABLE 81/cont.....

TABLE 81 cont.

110°C 2 hrs. X-rays. Run 3.					6.5 mg.
t	p	t	p	t	p
20	0.07	110	12.78	155	103.48
40	0.10	115	21.46	160	108.90
60	0.10	120	32.54	170	115.01
70	0.21	125	45.28	180	120.14
80	0.33	130	58.11	190	123.04
90	1.11	135	69.87	200	125.39
95	2.01	140	80.81	210	126.56
100	3.99	145	90.04	p_f	127.20
105	7.47	150	97.16	p_a	123.21

115°C 2 hrs. X-rays. Run 4.					6.5 mg.
t	p	t	p	t	p
20	0.05	82	12.20	110	98.72
30	0.08	84	16.29	115	108.19
40	0.10	86	21.45	120	113.64
50	0.13	88	27.59	125	118.10
60	0.32	90	34.50	130	120.93
65	0.60	92	41.51	135	123.43
70	1.34	94	48.81	140	124.94
72	2.16	96	56.30	145	126.10
74	3.16	98	63.92	150	126.68
76	4.39	100	71.59	p_f	127.20
78	6.17	102	78.31	p_a	127.70
80	8.76	105	86.77		

120°C 2 hrs. X-rays. Run 5.					6.8 mg.
t	p	t	p	t	p
10	0.04	56	19.37	75	105.89
20	0.06	58	29.72	80	114.51
30	0.09	60	41.63	85	119.97
40	0.25	62	53.69	90	122.73
45	0.90	64	64.79	95	125.06
48	2.18	66	74.87	100	126.08
50	3.90	68	83.77	105	126.63
52	7.03	70	91.73	p_f	127.20
54	11.91	72	98.56	p_a	136.17

TABLE 81 cont/.....

TABLE 81 cont.

125°C 2 hrs. X-rays. Run 6.					6.5 mg.
t	p	t	p	t	p
10	0.07	40	19.19	54	110.67
20	0.10	41	27.26	56	114.57
25	0.16	42	37.36	58	117.39
30	0.40	43	47.97	60	119.10
32	0.80	44	57.09	65	122.57
33	1.21	45	65.71	70	124.89
34	1.86	46	73.14	75	126.07
35	2.73	47	80.50	80	126.66
36	4.19	48	87.23	p_f	127.20
37	6.08	49	92.70	p_a	123.79
38	9.10	50	97.30		
39	13.49	52	105.22		

130° 2 hrs. X-rays. Run 7.					6.5 mg.
t	p	t	p	t	p
10	0.10	31	33.00	40	115.86
20	0.19	32	50.34	42	119.23
25	0.97	33	70.28	45	122.07
26	1.67	34	83.90	50	124.94
27	2.92	35	93.65	55	126.10
28	5.07	36	101.31	60	126.69
29	8.85	37	107.12	p_f	127.20
30	16.29	38	110.36	p_a	127.47

TABLE 82.

Temperature °C	Induction period min.	k_6 min.$^{-1}$	k_7 min.$^{-1}$
100°	205	6.50×10^{-3}	4.360×10^{-3}
105°	140	9.65×10^{-3}	7.050×10^{-3}
110°	87	1.513×10^{-2}	9.850×10^{-3}
115°	65	2.125×10^{-2}	1.540×10^{-2}
120°	43	4.000×10^{-2}	2.130×10^{-2}
125°	31	5.600×10^{-2}	3.260×10^{-2}
130°	23	1.008×10^{-1}	5.480×10^{-2}

(vi) Percentage/.....

(vi) Percentage decomposition.

This was calculated in terms of the equation:

$$Sr(N_3)_2 \rightarrow Sr + 3N_2$$

On irradiation with X-rays the percentage decomposition increases compared to the unirradiated salt. TABLE 83 lists a series of determinations of the percentage decomposition. For samples which had been irradiated for two hours the average percentage decomposition was 87.4% of the theoretical value.

TABLE 83.

Temperature °C	Dose.	Weight used m.g.	% decomposition.
120°	15 secs.	6.7	86.26
120°	1 min.	6.2	80.25
120°	2 "	6.5	77.25
120°	5 "	6.7	76.36
120°	15 "	6.4	80.48
120°	30 "	6.4	89.24
120°	60 "	6.6	82.63
120°	240 "	6.7	86.27
100°	120 "	6.4	80.48
105°	120 "	6.4	90.43
110°	120 "	6.5	85.88
115°	120 "	6.5	86.67
120°	120 "	6.6	93.44
125°	120 "	6.5	86.27
130°	120 "	6.5	88.63

(vii) Mathematical analysis of the results and evaluation of activation energies.

For irradiation times of up to 30 min. the power law with n = 3 fitted the acceleratory period i.e.

$$p^{1/3} = k_5 t + c_5 \quad \ldots\ldots\ldots\ldots\ldots\ldots\ldots\ldots (10)$$

With irradiation times exceeding 30 min. the above expression was no longer applicable. The Avrami-Erofeyev equation, with n = 3 gave a better analysis. The equation was used

in the form/.....

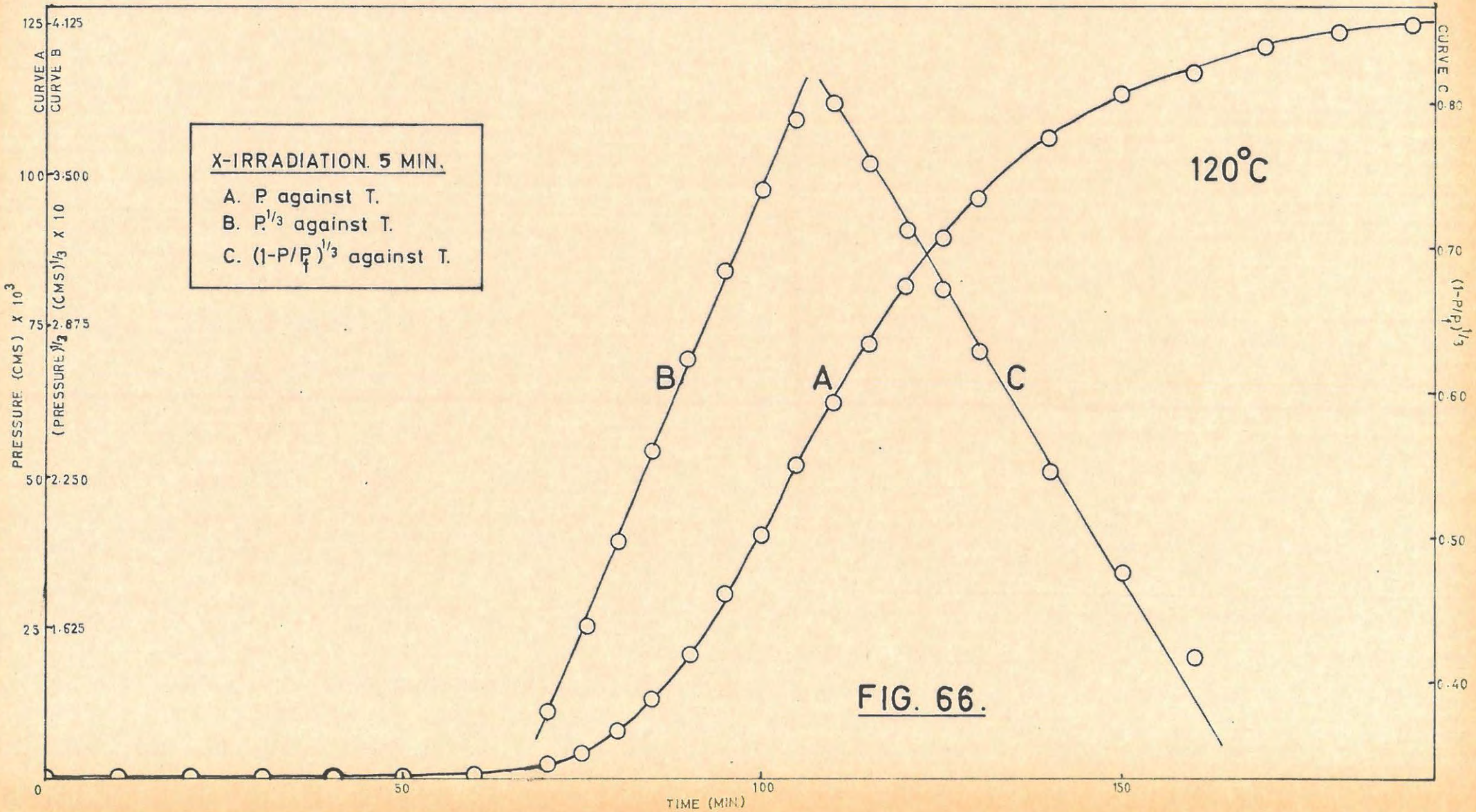
X-IRRADIATION. 5 MIN.
A. P against T.
B. $P^{1/3}$ against T.
C. $(1-P/P_f)^{1/3}$ against T.
120°C
A
B
C
PRESSURE (CMS) X 10^3
CURVE A
CURVE B
$(PRESSURE)^{1/3}$ $(CMS)^{1/3}$ X 10
CURVE C
$(1-P/P_f)^{1/3}$
TIME (MIN)
0
50
100
150
25
50
75
100
125
1.625
2.250
2.875
3.500
4.125
0.40
0.50
0.60
0.70
0.80

FIG. 66.

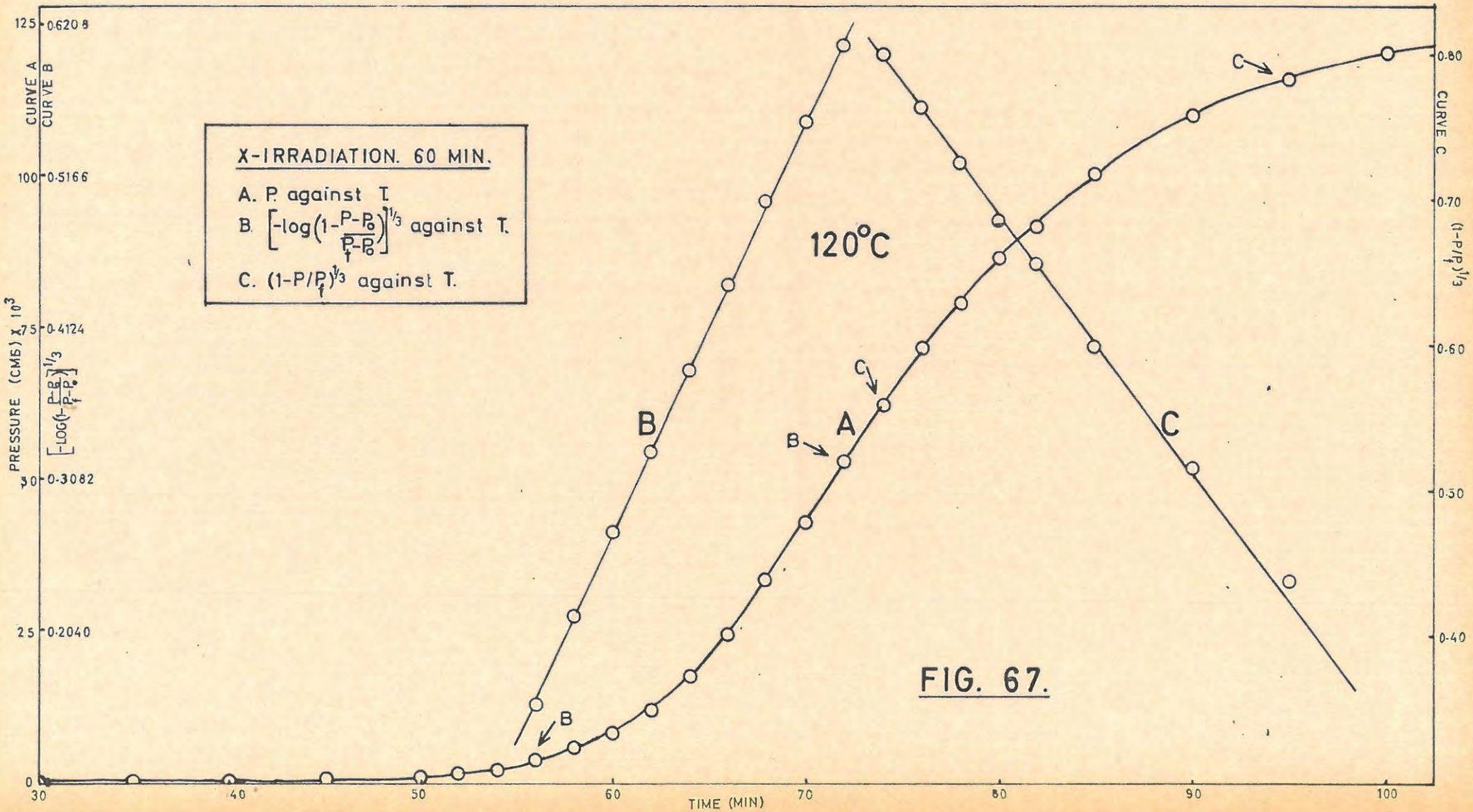
X-IRRADIATION. 60 MIN.
A. P against T.
B. $\left[-\log\left(1-\frac{P-P_0}{P_f-P_0}\right)\right]^{1/3}$ against T.
C. $(1-P/P_f)^{1/3}$ against T.
120°C
A
B
C
PRESSURE (CMS) X 10^3
CURVE A
CURVE B
CURVE C
$\left[-\log\left(1-\frac{P-P_0}{P_f-P_0}\right)\right]^{1/3}$
$(1-P/P_f)^{1/3}$
TIME (MIN)
125
100
75
50
25
0
0.6208
0.5166
0.4124
0.3082
0.2040
0.80
0.70
0.60
0.50
0.40
30
40
50
60
70
80
90
100

FIG. 67.

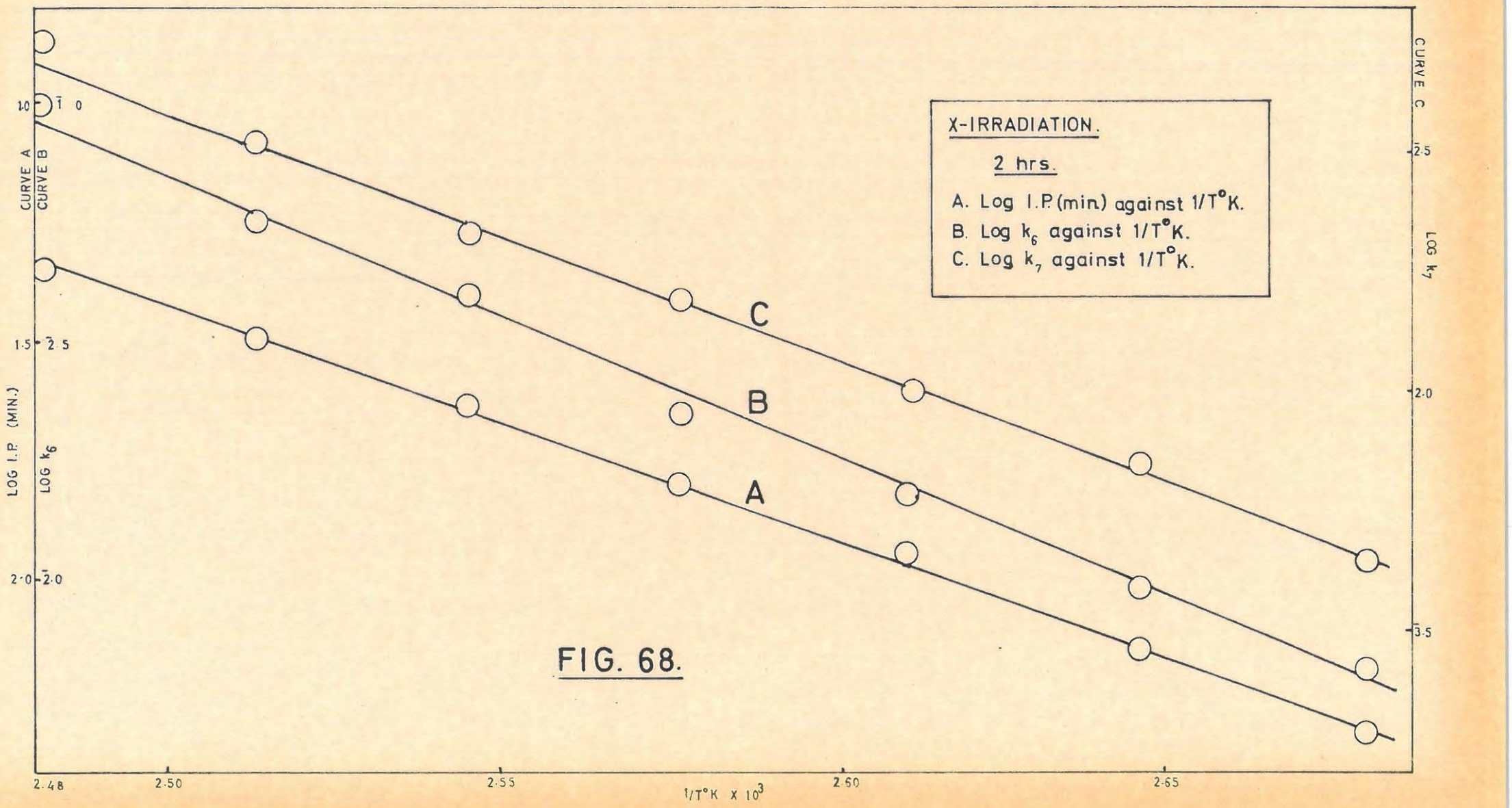
X-IRRADIATION.
2 hrs.
A. Log I.P.(min.) against 1/T°K.
B. Log k_6 against 1/T°K.
C. Log k_7 against 1/T°K.
CURVE A
CURVE B
CURVE C
LOG I.P. (MIN.)
LOG k_6
LOG k_7
1·0
$\bar{1}$·0
1·5
$\bar{2}$·5
2·0
$\bar{2}$·0
$\bar{2}$·5
2·0
$\bar{3}$·5
A
B
C
2·48
2·50
2·55
2·60
2·65
1/T°K X 10^3

FIG. 68.

in the form,

$$\left[-\log\left(1 - \frac{p - p_o}{p_f - p_o}\right)\right]^{1/3} = k_6 t + c_6 \quad \ldots\ldots\ldots\ldots (11)$$

where p_o is a small pressure (1.00×10^{-3} cm. Hg) at the end of the induction period.

The extent of fit of the power law was from $\alpha = 0.014$ to $\alpha = 0.38$ for an irradiation time of 5 min. The Avrami-Erofeyev equation held from $\alpha = 0.024$ to $\alpha = 0.40$ for an irradiation time of one hour.

The contracting sphere formula,

$$(1 - p/p_f)^{1/3} = k_7 t + c_7 \quad \ldots\ldots\ldots\ldots\ldots\ldots (2)$$

describes the decay period in all cases, the average extent of fit being $\alpha = 0.44$ to $\alpha = 0.90$.

A typical p/t plot for the decomposition of lightly irradiated (5 min.) strontium azide is shown in FIGURE 66 together with the analysis plots. FIGURE 67 gives the p/t plot and analysis for a heavily dosed (1 hr.) specimen.

When the decomposition of a heavily dosed sample is interrupted and water vapour admitted onto the salt, the subsequent acceleratory reaction is described by the power law, with n = 3, once more.

FIGURE 68 shows the Arrhenius plots of log I.P. (min.), log k_6, and log k_7, vs. $^1/_T$ °K. The activation energies obtained from these plots were:

(i) Induction period: 22.70 kcals.mole^{-1}

(ii) Acceleratory period: 26.50 kcals.mole^{-1}

(iii) Decay period: 24.00 kcals.mole^{-1}.

7.1.5. Preirradiated (γ-rays) Strontium Azide.

(i) Preliminary investigation.

The method of irradiation has been described. All ampoules were opened under argon. TABLE 84 and FIGURE 69 shows the effect of a 20 Mrad dose on the decomposition of strontium azide.

The decomposition/.....

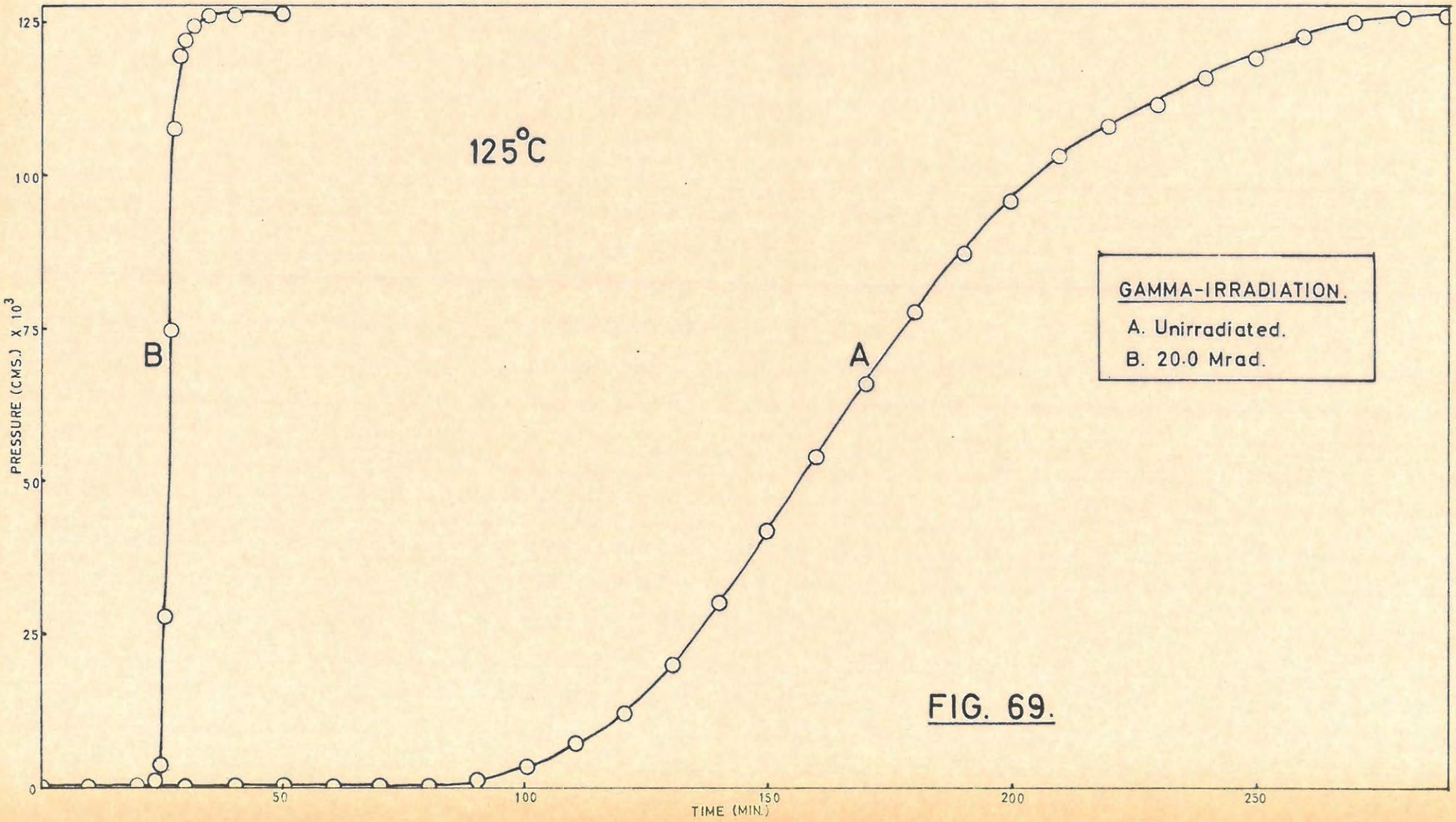
125°C
GAMMA-IRRADIATION.
A. Unirradiated.
B. 20.0 Mrad.
A
B
PRESSURE (CMS.) X 10³
TIME (MIN.)
0
25
50
75
100
125
50
100
150
200
250

FIG. 69.

The decomposition temperature was 125°C.

TABLE 84.

125°C Unirradiated blank. Run 1.					7.6 mg.
t	p	t	p	t	p
10	0.05	120	12.07	230	111.45
20	0.08	130	20.16	240	117.75
30	0.10	140	30.61	250	120.67
40	0.12	150	42.18	260	123.03
50	0.16	160	54.02	270	124.82
60	0.19	170	66.01	280	126.01
70	0.48	180	77.79	290	126.61
80	0.93	190	87.01	p_f	127.20
90	1.86	200	95.69	p_a	119.23
100	3.60	210	103.15		
110	7.00	220	108.65		

125°C 20 Mrad.		Run 2.			6.7 mg.
t	p	t	p	t	p
5	0.09	16	27.91	22	125.76
10	0.27	17	74.89	25	126.49
12	0.55	18	107.57	p_f	127.20
14	1.21	19	119.30	p_a	141.67
15	3.29	20	122.87		

(ii) Effect of varying doses of γ-rays.

The extreme sensitivity of strontium azide to γ-rays necessitated a reduction of the temperature of decomposition by 20-30°C in order to obtain a reasonably slow rate of decomposition. The decomposition temperature in this series was 100°C. The γ-ray doses ranged from 1,000 rad to 10 Mrad. All the irradiations were carried out in the Co^{60} source at Wantage. The results are tabulated in TABLE 85 and shown graphically in FIGURE 70. Reduction of the induction period and increased acceleratory and decay rates with increasing dose, are found. The acceleratory rate constants, k_5 (equation 10) for doses not exceeding 100,000 rad, and k_2 for higher doses (equation 6) together with the decay rate constants, k_7,/.....

stants, k_7, (equation 2) and the induction periods (min.), for the various preirradiation doses are given in TABLE 86. The rate constants for the decomposition of the unirradiated salt at this temperature were obtained by extrapolation of the unirradiated activation energy plots.

TABLE 85.

100°C 1,000 rad. Run 1. 6.7 mg.					
t	p	t	p	t	p
60	0.10	190	14.82	240	108.47
100	0.15	192	18.87	245	112.62
120	0.15	195	25.60	250	115.79
140	0.20	200	37.46	255	119.00
160	0.29	205	49.82	260	121.70
165	0.41	210	61.21	265	123.89
170	0.58	215	71.24	270	125.55
175	1.29	220	80.70	275	126.66
180	3.16	225	88.88	p_f	127.20
185	7.64	230	96.00	p_a	139.82
188	11.43	235	102.89		

100°C 10,000 rad. Run 2. 6.7 mg.					
t	p	t	p	t	p
20	0.03	152	4.26	180	78.41
40	0.06	154	5.87	185	91.22
60	0.06	156	8.15	190	101.09
80	0.08	158	11.61	195	108.46
100	0.13	160	15.49	200	114.54
110	0.17	162	20.35	205	120.26
120	0.28	164	26.37	210	122.91
130	0.45	166	33.17	215	124.51
140	0.68	168	40.13	220	125.58
145	1.42	170	46.77	225	126.66
148	2.28	172	53.22	p_f	127.21
150	3.07	175	63.85	p_a	147.83

TABLE 85 cont/.....

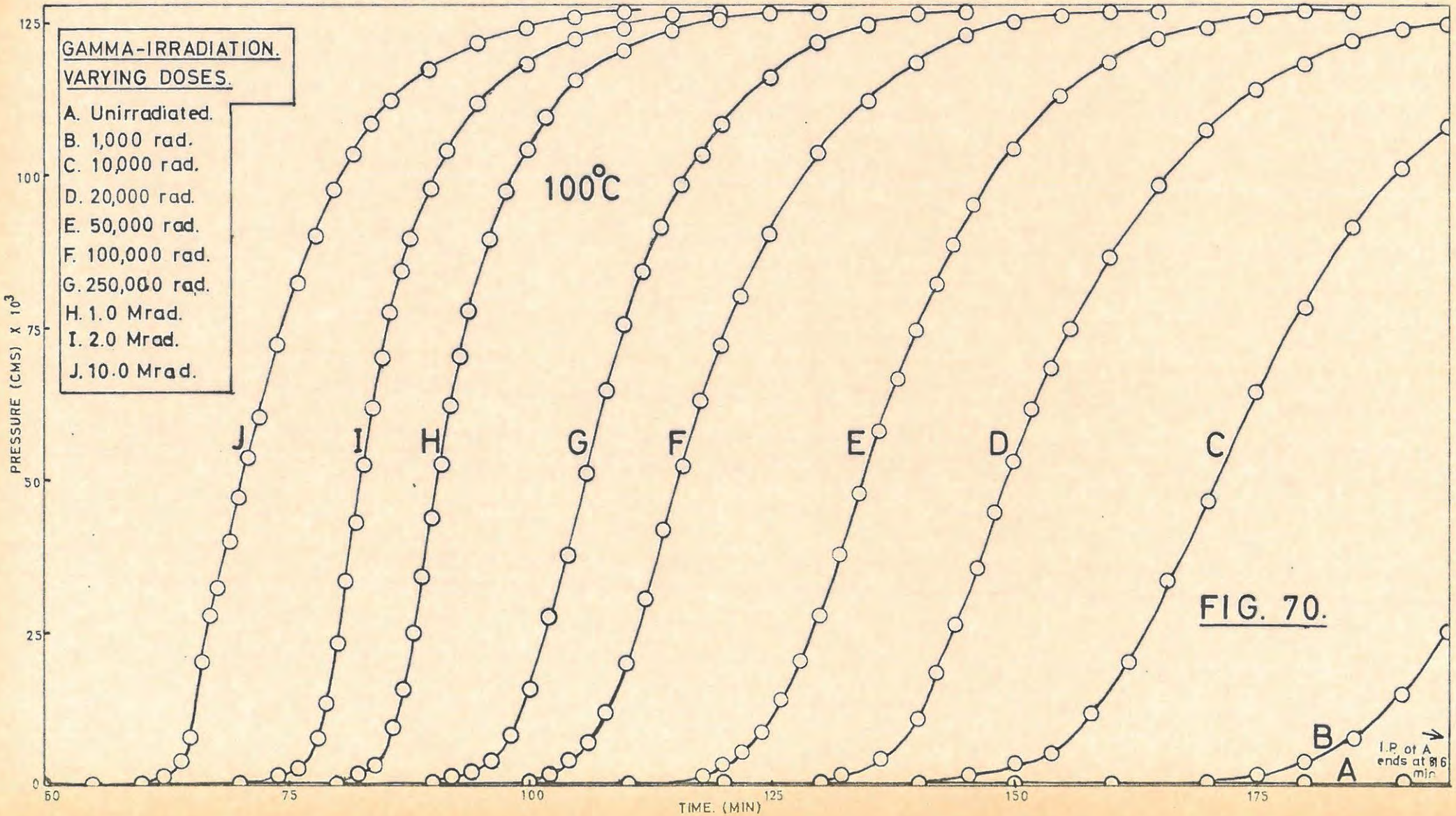
GAMMA-IRRADIATION.
VARYING DOSES.
A. Unirradiated.
B. 1,000 rad.
C. 10,000 rad.
D. 20,000 rad.
E. 50,000 rad.
F. 100,000 rad.
G. 250,000 rad.
H. 1.0 Mrad.
I. 2.0 Mrad.
J. 10.0 Mrad.
100°C
J
I
H
G
F
E
D
C
B
A
I.P. of A ends at 116 min
PRESSURE (CMS) X 10³
TIME. (MIN)
0
25
50
75
100
125
50
75
100
125
150
175

FIG. 70.

TABLE 85 cont.

100°C 20,000 rad. Run 3. 6.8 mg.					
t	p	t	p	t	p
50	0.09	140	11.61	165	98.32
80	0.12	142	18.09	170	107.38
100	0.16	144	26.21	175	114.31
120	0.22	146	35.06	180	118.36
125	0.32	148	44.85	185	121.97
130	0.64	150	53.40	190	124.05
132	1.12	152	61.59	195	125.63
134	2.05	154	68.41	200	126.68
136	3.90	156	74.77	p_f	127.20
138	7.17	160	86.56	p_a	154.25

100°C 50,000 rad Run 4. 6.8 mg.					
t	p	t	p	t	p
40	0.09	126	13.85	146	94.61
60	0.14	128	19.98	150	103.83
80	0.19	130	28.12	155	112.50
100	0.26	132	37.66	160	118.48
110	0.36	134	47.63	165	122.03
115	0.68	136	57.35	170	124.09
118	1.74	138	66.45	175	126.28
120	3.18	140	74.62	180	126.68
122	5.36	142	82.00	p_f	127.20
124	8.79	144	88.84	p_a	145.32

100°C 100,000 rad. Run 5. 6.7 mg.					
t	p	t	p	t	p
20	0.11	106	6.58	122	79.76
40	0.16	107	8.86	125	90.01
60	0.23	108	11.81	130	103.33
80	0.28	109	15.37	135	112.37
90	0.34	110	19.62	140	118.62
95	0.46	111	24.38	145	122.87
98	0.64	112	29.92	150	125.03
100	0.94	113	35.45	155	126.11
102	1.84	114	41.44	160	126.65
103	2.63	116	52.37	p_f	127.21
104	3.56	118	62.63	p_a	145.39
105	5.07	120	71.75		

TABLE 85 cont/.....

TABLE 85 cont.

100°C 250,000 rad.		Run 6.			6.7 mg.
t	p	t	p	t	p
20	0.18	100	15.98	114	91.23
40	0.25	101	21.30	116	97.95
60	0.31	102	27.37	118	103.39
70	0.38	103	32.22	120	107.96
80	0.51	104	37.46	125	116.32
90	0.67	105	43.75	130	121.16
92	1.12	106	50.83	135	124.71
94	1.84	107	57.78	140	126.10
96	3.70	108	64.73	145	126.66
97	5.40	109	70.41	p_f	127.20
98	7.64	110	75.04	p_a	139.83
99	10.94	112	83.84		

100°C 1.0 Mrad.		Run 7.			6.7 mg.
t	p	t	p	t	p
20	0.21	87	15.54	98	97.57
40	0.29	88	24.90	100	104.24
60	0.38	89	34.12	102	109.65
70	0.51	90	43.57	105	115.17
75	0.64	91	52.79	110	120.34
80	0.95	92	62.14	115	123.48
82	1.52	93	70.62	120	125.60
83	2.17	94	77.60	125	126.67
84	3.43	95	84.00	p_f	127.20
85	5.64	96	89.31	p_a	151.06
86	9.24	97	93.85		

100°C 2.0 Mrad.		Run 8.			6.7 mg.
t	p	t	p	t	p
20	0.16	79	13.03	92	103.76
30	0.23	80	23.00	95	111.14
40	0.38	81	33.29	100	118.26
50	0.45	82	42.94	105	121.91
60	0.54	83	52.10	110	124.01
70	0.61	84	61.40	115	125.60
74	1.30	85	70.25	120	126.67
75	1.77	86	77.60	p_f	127.20
76	2.76	87	84.00	p_a	151.06
77	4.57	88	89.31		
78	7.72	90	97.57		

TABLE 85 cont/.....

TABLE 85 cont.

100°C 4.0 Mrad. Run 9. 6.9 mg.					
t	p	t	p	t	p
20	0.11	80	22.09	92	112.30
30	0.17	81	33.68	94	116.32
40	0.23	82	47.08	96	119.39
50	0.30	83	60.49	100	123.01
60	0.42	84	71.16	105	125.10
65	0.63	85	80,15	110	126.16
70	1.21	86	87.46	115	126.65
75	1.79	87	93.67	p_f	127.20
78	6.44	88	98.79	p_a	154.25
79	12.09	90	106.41		

100°C 10.0 Mrad. Run 10. 6.7 mg.					
t	p	t	p	t	p
10	0.11	67	26.75	80	97.33
20	0.13	68	32.48	82	103.09
30	0.17	69	39.36	84	108.01
40	0.21	70	46.91	86	112.03
50	0.25	71	53.69	90	117.15
55	0.33	72	60.57	95	121.34
60	0.70	73	67.07	100	123.92
62	1.32	74	72.67	105	125.60
64	3.76	75	77.66	110	126.67
65	7.45	76	81.93	p_f	127.20
66	21.58	78	89.92	p_a	148.52

TABLE 86.

Dose.	Induction period (min.)	k_5 cm$^{1/3}$ min.$^{-1}$	k_7 min.$^{-1}$
0	866	6.131×10^{-4}	6.918×10^{-4}
1,000 rad	170	9.588×10^{-3}	9.050×10^{-3}
10,000 "	140	1.173×10^{-2}	1.355×10^{-2}
20,000 "	130	1.695×10^{-2}	1.505×10^{-2}
50,000 "	115	1.612×10^{-2}	1.830×10^{-2}
100,000 "	98	2.089×10^{-2}	1.845×10^{-2}
		k_2 cm. min.$^{-1}$	
250,000 "	90	1.530×10^{-1}	2.145×10^{-2}
1.0 Mrad	75	2.116×10^{-1}	3.010×10^{-2}
2.0 "	70	2.30×10^{-1}	3.150×10^{-2}
4.0 "	65	2.28×10^{-1}	3.770×10^{-2}
10.0 "	60	3.125×10^{-1}	2.350×10^{-2}

(iii) Effect of/.....

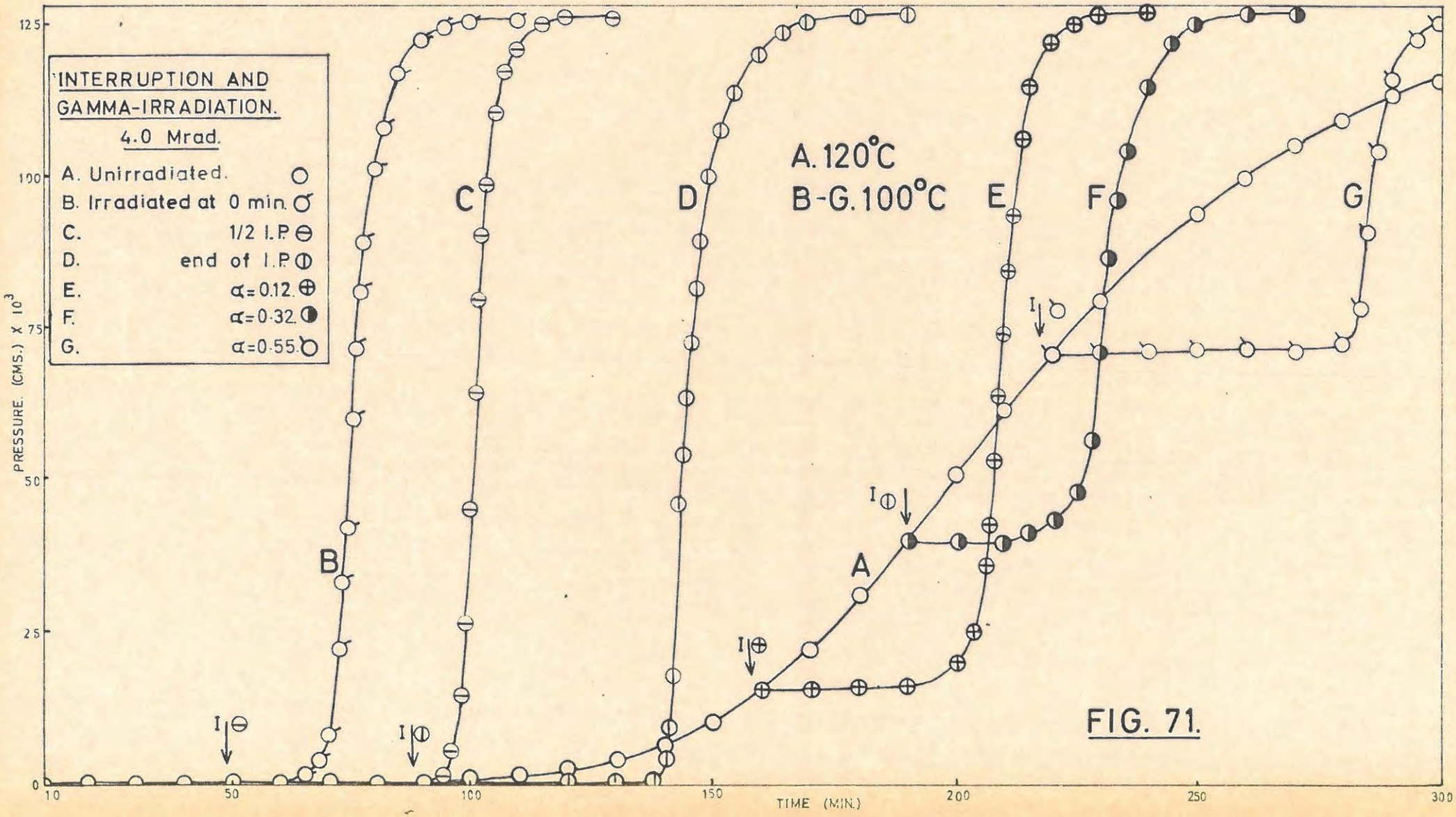
INTERRUPTION AND
GAMMA-IRRADIATION.
4.0 Mrad.
A. Unirradiated.
B. Irradiated at 0 min.
C. 1/2 I.P.
D. end of I.P.
E. α=0.12.
F. α=0·32.
G. α=0·55.
A. 120°C
B-G. 100°C
PRESSURE (CMS.) X 10³
TIME (MIN.)
0
25
50
75
100
125
10
50
100
150
200
250
300

FIG. 71.

(iii) Effect of interrupting a decomposition and irradiating the salt.

The method used to irradiate samples at various stages has been described. It was not possible to eliminate water vapour from the glass. Thus the irradiation was actually done on a mixture of strontium hydroxide and undecomposed azide. Decompositions were done at 120°C up to the point of interruption, the decomposition interrupted, irradiation performed, and the run continued at 100°C. The results appear in TABLE 87 and FIGURE 71. The irradiations were done in the spent feul facility at Harwell. In all cases there was a short induction period (due to the effect of water vapour) followed by a very rapid acceleration.

TABLE 87.

100°C 4.0 Mrad.		Run 1. Blank run			6.0 mg.
t	p	t	p	t	p
10	0.02	71	13.63	82	108.97
20	0.04	72	21.95	83	112.18
30	0.06	73	33.70	85	117.08
40	0.09	74	42.26	87	119.86
50	0.19	75	60.70	90	122.66
60	0.51	76	71.88	95	125.50
65	1.75	77	81.24	100	126.64
67	2.57	78	89.71	p_f	127.20
68	3.74	79	96.09	p_a	131.38
69	5.49	80	101.66		
70	8.42	81	105.80		

4.0 Mrad.		Run 2.			6.0 mg.
t	p	t	p	t	p
120°C		92	0.76	104	98.91
45	0.13	93	1.21	105	106.17
Irradiation		94	1.92	106	110.98
100°C		95	3.22	107	114.79
50	0.13	96	5.20	108	117.56
60	0.13	97	8.69	110	120.91

TABLE 87 cont/.....

TABLE 87 cont.

t	p	t	p	t	p
70	0.13	98	14.78	112	123.75
80	0.14	99	26.54	115	125.47
85	0.14	100	45.10	120	126.62
88	0.15	101	64.78	p_f	127.20
90	0.32	102	79.11	p_a	129.62
91	0.52	103	90.43		

4.0 Mrad.		Run 3.			6.1 mg.
t	p	t	p	t	p
120°C		137	0.88	149	95.45
30	0.15	138	1.55	150	100.16
60	0.32	139	2.78	152	107.72
90	0.68	140	4.95	154	113.28
Irradiation		141	9.43	156	116.69
100°C		142	17.94	160	120.73
100	0.69	143	46.27	165	123.66
110	0.69	144	54.96	170	125.43
120	0.71	145	63.51	175	126.63
130	0.72	146	72.68	p_f	127.20
135	0.74	147	81.51	p_a	121.50
136	0.79	148	89.34		

4.0 Mrad.		Run 4.			6.1 mg.
t	p	t	p	t	p
120°C		185	17.67	202	93.54
40	0.11	188	18.46	203	100.66
60	0.26	190	19.59	204	106.45
100	0.71	191	20.34	205	111.66
120	1.62	192	21.66	206	115.30
130	3.79	193	23.00	208	120.08
140	7.93	194	25.44	210	122.79
150	15.79	195	30.16	212	124.43
Irradiation		196	35.35	215	125.53
100°C		197	42.95	220	126.63
155	15.93	198	53.08	p_f	127.20
160	16.07	199	63.35	p_a	122.92
170	16.19	200	74.46		
180	16.69	201	84.97		

TABLE 87 cont/.....

TABLE 87 cont.

4.0 Mrad.		Run 5.			5.9 mg.
t	p	t	p	t	p
120°C		190	40.82	220	71.24
30	0.14	200	41.40	221	80.68
60	0.28	202	41.70	222	86.24
100	0.72	204	42.05	224	96.05
120	2.13	206	42.52	226	104.24
130	4.75	208	43.08	228	111.20
140	9.21	210	43.85	230	115.72
150	14.68	212	44.98	232	119.47
160	21.38	214	46.79	235	122.80
170	30.52	216	50.02	240	125.23
180	40.68	217	52.62	245	126.70
Irradiation		218	57.00	p_f	127.20
100°C		219	64.07	p_a	120.58

4.0 Mrad.		Run 6.			6.0 mg.
t	p	t	p	t	p
120°C		210	70.07	275	91.75
30	0.23	Irradiation		276	98.26
60	0.42	100°C		277	104.40
100	0.88	220	70.24	278	109.48
120	2.63	230	70.46	279	113.52
130	4.71	240	70.53	280	116.32
140	6.98	250	70.68	282	120.69
150	12.17	260	70.84	285	123.71
160	18.68	265	71.06	290	126.04
170	26.55	270	72.06	295	126.82
180	39.41	272	74.44	p_f	127.20
190	51.37	273	78.35	p_a	124.47
200	61.58	274	85.47		

(iv) Effect of admitting water vapour onto the salt in an interrupted run.

The results obtained from successive interruptions of the irradiated salt during the induction period, are rather unique and will be dealt with separately

(a) Single/.....

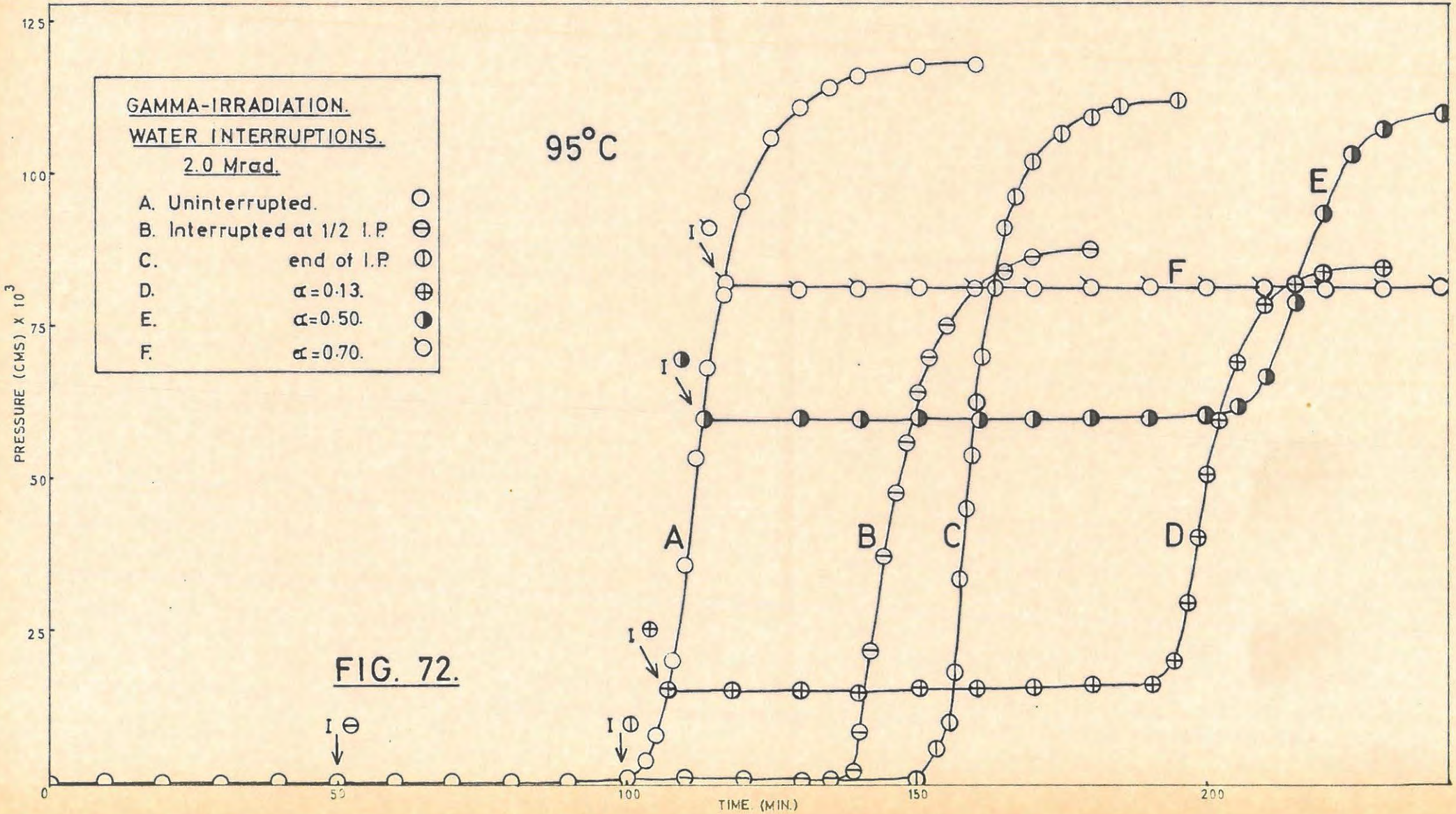
GAMMA-IRRADIATION.
WATER INTERRUPTIONS.
2.0 Mrad.
A. Uninterrupted.
B. Interrupted at 1/2 I.P.
C. end of I.P.
D. α=0·13.
E. α=0·50.
F. α=0·70.
95°C
A
B
C
D
E
F
I
PRESSURE (CMS) X 10³
TIME. (MIN.)
0
25
50
75
100
125
50
100
150
200

FIG. 72.

(a) Single interruptions.

Interruptions were done at five points on the p/t plots. The decomposition temperature was 95°C and the γ-ray dose was 2.0 Mrad in each case. The results are given in TABLE 88 and are illustrated in FIGURE 72. A new induction period and acceleratory and decay periods are again produced. "Water interruptions" in the induction period and the acceleratory period results in the subsequent acceleratory period proceeding at a faster rate than for the uninterrupted salt. The rate is slower than normal if the interruption is done at the inflexion point. In the decay period there is a flash of flame when water vapour is admitted and further reaction is destroyed. TABLE 89 shows the changes in the induction periods and acceleratory rate constants, k_2 (equation 6).

Final pressure are again lower than normal. Partial recovery of the lost pressure is possible by heating to 300°C in vacuo. Pressures are thus not normalised.

TABLE 88.

95°C 2.0 Mrad. Run 1. Uninterrupted blank, 6.0 mg.					
t	p	t	p	t	p
20	0.20	104	4.96	118	89.03
40	0.40	105	7.03	120	95.65
60	0.44	106	9.95	122	100.91
70	0.46	107	13.97	125	106.36
80	0.55	108	19.59	130	111.28
90	0.63	109	26.71	135	114.66
95	0.72	110	35.56	140	116.37
98	0.96	111	44.61	145	117.51
100	1.42	112	53.51	150	117.83
101	1.88	113	61.55	p_a	118.09
102	2.53	114	68.38		
103	3.44	116	80.73		

TABLE 88 cont/.....

TABLE 88 cont.

95°C 2.0 Mrad. Run 2. 6.0 mg.					
t	p	t	p	t	p
20	0,04	137	1,54	150	64,34
40	0,08	138	2,83	152	69,85
50	0,11	139	5,07	155	75,58
Water Interruption		140	8,55	160	81,08
80	0,12	141	13,88	165	84,37
100	0,12	142	22,18	170	86,77
120	0,14	143	31,82	175	87,73
130	0,19	144	37,29	p_a	88,22
135	0,52	146	47,73		
136	0,86	148	56,69		

95°C 2.0 Mrad. Run 3. 6.1 mg.					
t	p	t	p	t	p
30	0,11	147	2,25	157	77,39
60	0,19	148	3,87	158	82,95
70	0,32	149	6,43	160	91,16
80	0,40	150	10,80	162	96,68
90	0,49	151	18,90	165	102,35
95	0,61	152	33,00	170	107,12
Water Interruption		153	45,26	175	109,81
110	0,62	154	54,38	180	111,45
140	0,65	155	62,69	185	112,54
145	0,77	156	70,28	p_a	113,09

95°C 2.0 Mrad. Run 4. 6.0 mg.					
t	p	t	p	t	p
20	0,13	119	11,31	206	29,76
40	0,20	120	15,88	207	34,77
60	0,38	Water Interruption		208	40,05
80	0,56	130	15,88	209	45,68
90	0,64	140	15,90	210	50,99
100	0,77	150	15,90	211	55,74
105	0,97	160	15,92	212	59,75
110	1,24	180	15,94	214	66,88
112	1,48	190	15,97	216	71,79
114	2,25	200	16,40	220	78,57

TABLE 88 cont/.....

TABLE 88 cont.

t	p	t	p	t	p
115	2.92	202	16.62	225	82.31
116	4.07	203	18.62	230	84.43
117	5.67	204	20.60	235	85.29
118	8.16	205	24.13	p_a	85.73

95°C 2.0 Mrad. Run 5. 6.2 mg.					
t	p	t	p	t	p
20	0.13	101	33.29	200	67.41
40	0.24	102	45.95	202	71.48
60	0.38	103	59.45	204	77.46
80	0.52	Water Interruption		206	83.62
90	0.97	130	59.52	208	89.54
92	1.36	160	59.59	210	94.87
94	2.33	170	59.63	212	99.00
95	3.28	180	59.75	215	103.67
96	4.95	190	60.14	220	107.54
97	7.52	192	60.53	225	109.72
98	11.31	194	61.26	230	110.64
99	16.50	196	62.55	235	111.57
100	23.66	198	64.52	p_a	111.94

95°C 2.0 Mrad. Run 6. 5.9 mg.					
t	p	t	p	t	p
20	0.09	99	12.02	Water Interruption	
40	0.17	100	19.12	150	83.08
60	0.27	101	30.37	180	83.31
80	0.39	102	42.52	200	83.48
90	0.68	103	51.00	220	83.77
95	1.81	104	60.26	240	84.07
96	2.83	105	68.56	260	84.31
97	4.50	106	76.48	300	84.43
98	7.66	107	82.95	p_a	84.70

TABLE 89/.....

TABLE 89.

Point of interruption.	Induction period min.	k_2 cm. min.$^{-1}$
Uninterrupted	90	1.490×10^{-1}
½ along I.P.	85	1.875×10^{-1}
End of I.P.	50	2.310×10^{-1}
α = 0.13	80	2.400×10^{-1}
α = 0.50	87	1.025×10^{-1}
α = 0.70	No reaction	No reaction.

(b) Effect of successive interruptions.

Interruption and admission of water vapour at the end of the induction period followed by repeated interruptions and admission at the end of each new induction period resulted in a shortening of the induction period to a limiting value of approximately 30% of the original induction period after four or five interruptions. Allowing the decomposition to proceed without interruption after the sixth interruption resulted in a very fast rate of reaction culminating in an explosion at α = 0.10. The expected final pressure was obtained after the explosion. These results are shown in TABLE 90 and FIGURE 73. The temperature of decomposition was 95°C and the γ-ray dose 2.0 Mrad.

TABLE 90.

95°C 2.0 Mrad. Run 1. 6.2 mg.					
t	p	t	p	t	p
60	0.13	240	1.83	324	3.61
90	0.32	250	1.83	Water Interruption	
100	0.52	255	1.86	330	3.61
102	0.61	260	2.09	340	3.62
Water Interruption		261	2.27	345	3.62
130	0.62	262	2.41	350	3.73
140	0.62	Water Interruption		352	3.92
150	0.63	270	2.42	353	4.12
160	0.63	280	2.42	354	4.47
165	0.64	290	2.52	355	5.08
170	0.68	293	2.86	356	6.17

TABLE 90 cont/.....

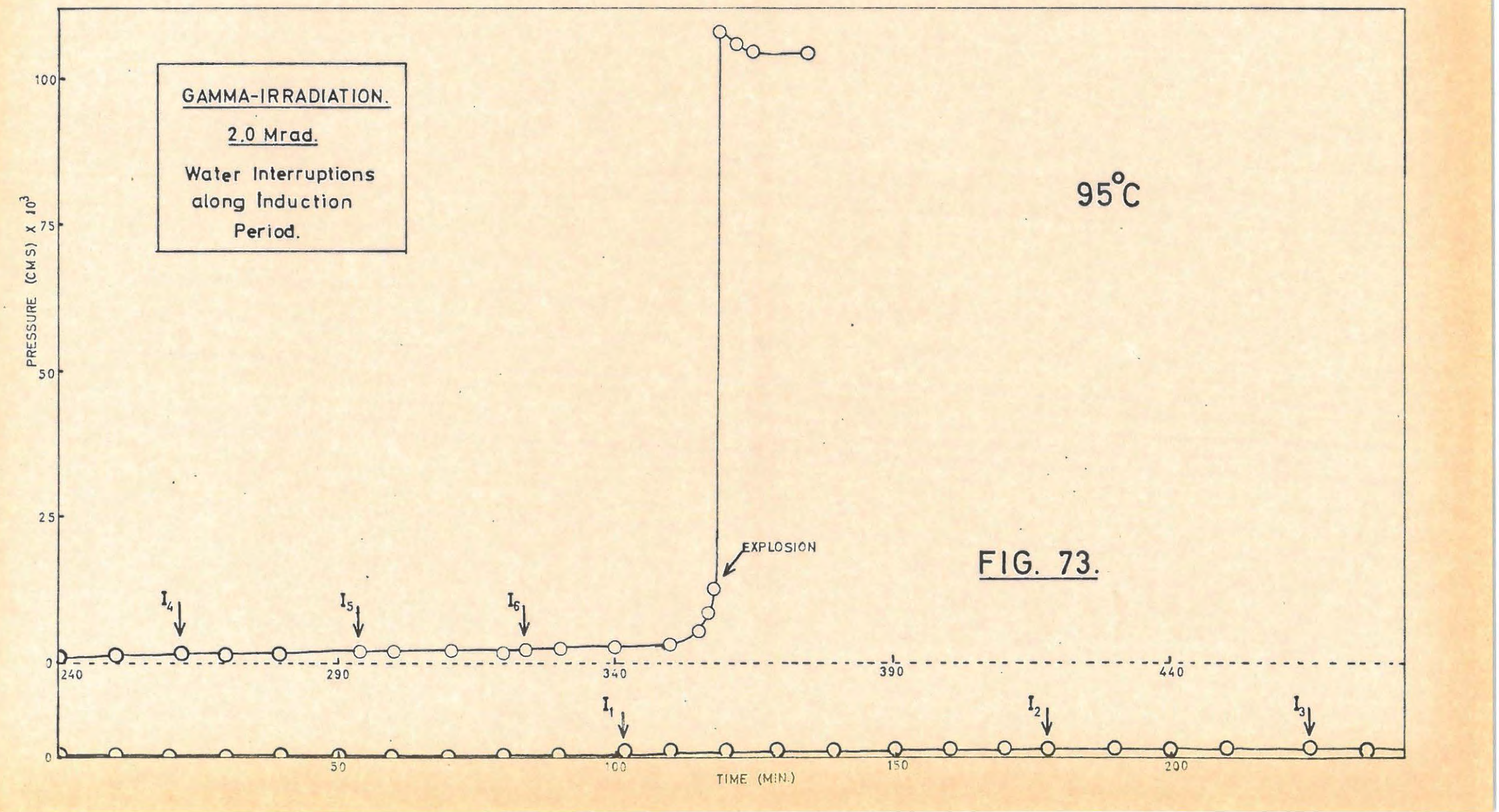
GAMMA-IRRADIATION.
2.0 Mrad.
Water Interruptions along Induction Period.
95°C
EXPLOSION
PRESSURE (CM.S) X 10³
TIME (MIN.)
100
75
50
25
0
240
290
340
390
440
50
100
150
200
I1
I2
I3
I4
I5
I6

FIG. 73.

TABLE 90 cont.

t	p	t	p	t	p
175	0.78	294	2.99	357	8.32
178	1.20	Water Interruption		358	12.61
Water Interruption		300	3.00	Explosion	
200	1.21	310	3.00	359	108.06
220	1.26	315	3.00	360	107.53
225	1.72	320	3.00	362	106.48
226	1.82	322	3.26	p_a	104.91
Water Interruption		323	3.47		

Further experiments were then performed at 95°C on a specimen preirradiated with a heavier (10 Mrad) dose. After six "water interruptions" explosion again occurred, but at a lower α value viz, $\alpha = 0.025$. The effect was highly reproducible. After three or seven interruptions no explosion resulted at 95°C.

Heating the fresh sample at 95°C in contact with water vapour for a length of time equal to the combined lengths of the induction periods produced a fast reaction but no explosion.

At 100°C explosion was obtained after two successive interruptions at $\alpha = 0.01$. No explosions were obtained at 90°C under any conditions.

Storage of the specimen for 48 hours in vacuum after the second interruption did not produce explosion when the run was allowed to proceed normally at 100°C. The normal sigmoid p/t plot was obtained.

Attemps to prepare a specimen, and then explode it in air at 110°C were unsuccessful. Failure to produce an explosion was probably due to the water vapour in the air.

The above results are all contained in TABLE 90, from run 2 onwards. Runs 2 and 3 were done under identical conditions in order to check the reproducibility.

TABLE 90 cont/.....

TABLE 90 (cont)

95°C 10.0 Mrad. Run 2. 6.2 mg.					
t	p	t	p	t	p
30	0,04	190	1.30	Water Interruption	
60	0.08	195	1,83	300	3.67
80	0.11	Water Interruption		305	3.67
85	0.17	220	1.89	310	3.75
90	0.32	225	1.92	313	4.11
93	0.63	230	2.49	314	4.52
Water Interruption		Water Interruption		315	5.47
120	0.64	250	2.51	Explosion	
140	0.65	255	2.62	316	94.31
145	0.68	258	3.07	317	91.39
150	0.76	Water Interruption		318	89.95
155	1.24	270	3.08	320	88.51
Water Interruption		275	3.08	325	87.56
180	1.25	282	3.66	p_a	87.10

~95°C 10.0 Mrad. Run 3. 6.0 mg.					
t	p	t	p	t	p
30	0.02	200	1.28	289	3.67
60	0.02	205	1.32	Water Interruption	
70	0.09	211	1.84	300	3.68
80	0.15	Water Interruption		305	3.70
90	0.27	230	1.86	310	3.84
95	0.62	235	2.11	313	4.19
Water Interruption		237	2.49	314	4.64
120	0.63	Water Interruption		315	6.00
140	0.63	250	2.50	Explosion	
150	0.64	260	2.53	316	82.89
160	0.75	266	3.08	317	81.52
165	1.26	Water Interruption		318	81.06
Water Interruption		280	3.09	320	80.61
180	1.27	285	3.19	p_a	78.70

95°C 10.0 Mrad. Run 4. 6.1 mg.					
t	p	t	p	t	p
30	0.09	180	1.25	229	18.57
60	0.17	190	1.55	230	19.87
80	0.27	192	1.86	232	22.60

TABLE 90 cont/.....

TABLE 90 cont.

t	p	t	p	t	p
90	0.38	Water Interruption		235	26.28
95	0.62	210	1.87	240	32.42
Water Interruption		220	1.96	245	40.75
120	0.63	224	2.38	250	50.67
140	0.65	225	3.34	255	58.16
150	0.72	226	9.10	260	61.31
156	1.23	227	10.86	265	62.52
Water Interruption		228	17.74	p_a	63.33

$95^{\circ}C$ 10.0 Mrad. Run 5. 6.2 mg.					
t	p	t	p	t	p
30	0.14	230	1.89	337	16.44
60	0.21	237	2.44	338	16.62
80	0.35	Water Interruption		340	16.80
90	0.52	250	2.45	345	18.12
95	0.60	255	2.55	350	19.71
Water Interruption		259	3.03	355	21.81
145	0.77	Water Interruption		360	23.59
150	0.99	270	3.04	365	24.98
152	1.20	281	3.65	370	26.66
Water Interruption		Water Interruption		375	29.96
170	1.21	300	3.75	380	34.91
180	1.22	306	4.24	385	37.24
190	1.25	Water Interruption		390	38.44
195	1.30	320	4.25	395	38.74
200	1.39	330	4.41	400	39.04
204	1.82	334	4.92	p_a	39.35
Water Interruption		335	5.92		
220	1.83	336	8.96		

In run 6 the specimen was heated at $95^{\circ}C$ in water vapour for 280 min. (the sum total of six interruptions). When the vapour was condensed in a liquid air trap the pressure in the vacuum line was only 0.97×10^{-3} cms.Hg indicating that very little decomposition had occurred. The run was then allowed to proceed normally. There was no explosion.

TABLE 90 cont/.....

TABLE 90 cont.

95°C 10.0 Mrad. Run 6. 6.2 mg.					
t	p	t	p	t	p
5	0.01	15	25.72	25	66.85
10	0.17	16	33.29	30	72.03
11	0.39	17	40.84	35	74.24
12	1.18	18	45.60	40	76.03
13	3.28	20	54.76	45	77.29
14	15.67	22	60.66	p_a	77.85

100°C 10.0 Mrad. Run 7. 6.1 mg.					
t	p	t	p	t	p
20	0.17	90	0.64	151	1.83
30	0.24	100	0.65	Explosion	
40	0.35	110	0.70	152	75.92
50	0.48	117	1.23	153	75.02
56	0.62	Water Interruption		155	74.14
Water Interruption		130	1.24	p_a	73.26
70	0.64	150	1.50		

90°C 10.0 Mrad. Run 8. 6.0 mg.					
t	p	t	p	t	p
90	0.12	Water Interruption		383	5.02
119	0.62	300	2.47	384	6.07
Water Interruption		310	2.50	385	7.53
160	0.63	315	3.06	386	10.09
180	0.63	Water Interruption		387	13.62
185	1.24	330	3.07	388	16.97
Water Interruption		346	3.66	389	19.95
210	1.25	Water Interruption		390	23.01
220	1.26	360	3.67	392	26.57
230	1.27	370	3.67	395	32.35
240	1.86	375	3.70	400	36.95
Water Interruption		380	3.98	405	39.08
260	1.87	381	4.18	410	40.32
283	2.46	382	4.53	p_a	40.63

In run 9 the decomposition temperature was 100°C. After the second interruption the specimen was kept in the vacuum line with constant pumping for 48 hours before continuing the

decomposition/.....

decomposition. The subsequent acceleration was very fast but there was no explosion.

100°C 10.0 Mrad. Run 9. 6.1 mg.					
t	p	t	p	t	p
20	0.12	100	1.23	110	55.98
46	0.60	102	1.26	111	59.88
Water Interruption		104	1.60	112	63.09
60	0.61	105	3.63	114	66.39
80	0.61	106	31.88	116	68.92
82	1.22	107	37.88	120	71.94
Water Interruption		108	45.10	125	74.13
48 hrs. pumping		109	51.48	p_a	75.01

(v) Effect of thermal annealing.

Annealing of a sample of strontium azide, preirradiated with a γ-ray dose of 1.0 Mrad, by heating at 70°C for three hours in vacuo had no effect on the subsequent decomposition at 100°C. TABLE 91 gives these results.

TABLE 91.

100°C 1.0 Mrad. Run 1. Blank run. 6.7 mg.					
t	p	t	p	t	p
20	0.21	87	15.54	98	97.57
40	0.29	88	24.90	100	104.24
60	0.38	89	34.12	102	109.65
70	0.51	90	43.57	105	115.17
75	0.64	91	52.79	110	120.34
80	0.95	92	62.14	115	123.48
82	1.52	93	70.62	120	125.60
83	2.17	94	77.60	125	126.67
84	3.43	95	84.00	p_f	127.20
85	5.64	96	89.31	p_a	151.06
86	9.24	97	93.85		

100°C 1.0 Mrad. Run 2. Annealed 3 hrs. 70°C 6.7 mg.					
t	p	t	p	t	p
20	0.05	86	11.53	98	91.56
40	0.08	87	17.46	100	98.98

TABLE 91 cont/.....

TABLE 91 cont.

t	p	t	p	t	p
60	0.11	88	26.55	102	104.73
70	0.14	89	41.40	105	111.64
75	0.18	90	48.07	110	119.30
80	0.58	91	54.53	115	123.48
81	0.99	92	60.65	120	125.60
82	1.64	93	67.11	125	126.67
83	2.76	94	72.16	p_f	127.20
84	4.67	95	78.02	p_a	151.06
85	7.33	96	82.70		

(vi) Effect of varying the temperature of decomposition.

An irradiation dose of 2.0 Mrad was selected at which the critical increment of the chemical process(es) occurring was determined. The temperature range of the decompositions was 85° - 105°C. The results are tabulated in TABLE 92. Accelera-tory and decay period rate constants, k_2 and k_7 (equation 6 and 2), and the duration of the induction periods (min.) at each temperature, are given in TABLE 93.

TABLE 92.

87.5°C 2.0 Mrad. Run 1. 6.0 mg.					
t	p	t	p	t	p
60	0.09	208	5.18	230	90.17
120	0.17	210	8.24	235	102.88
160	0.21	212	12.75	240	110.37
180	0.37	214	18.90	245	116.42
190	0.43	216	27.86	250	120.36
195	0.67	218	39.86	255	122.64
200	1.07	220	51.00	260	124.36
204	2.41	222	60.26	p_f	127.20
206	3.47	225	72.91	p_a	129.52

TABLE 92 cont/.....

TABLE 92 cont.

90°C 2.0 Mrad. Run 2. 6.1 mg.					
t	p	t	p	t	p
30	0.12	168	1.63	190	97.32
60	0.14	170	2.57	192	103.86
90	0.15	172	4.49	195	111.19
100	0.17	174	7.99	200	118.17
110	0.21	176	14.06	205	122.75
120	0.25	178	23.40	210	124.16
130	0.25	180	37.06	215	125.37
140	0.33	182	52.26	220	126.59
150	0.42	184	66.47	p_f	127.20
160	0.59	186	79.46	p_a	133.41
165	1.02	188	89.27		

92.5°C 2.0 Mrad. Run 3. 6.2 mg.					
t	p	t	p	t	p
40	0.08	156	13.27	190	115.72
80	0.19	158	27.39	200	120.11
100	0.33	160	48.16	210	123.30
120	0.45	162	65.09	220	125.24
130	0.70	164	76.77	230	126.53
140	1.08	166	84.56	p_f	127.20
150	1.77	170	95.53	p_a	129.61
152	3.01	175	104.20		
154	6.18	180	108.37		

95°C 2.0 Mrad. Run 4. 6.0 mg.					
t	p	t	p	t	p
40	0.07	105	3.83	118	97.86
60	0.14	106	6.12	120	104.97
70	0.19	107	9.43	122	110.05
80	0.24	108	14.89	125	115.24
90	0.32	109	23.66	130	120.55
95	0.46	110	35.75	135	123.55
98	0.58	111	46.16	140	125.37
100	0.72	112	56.26	145	126.59
102	1.18	113	65.59	p_f	127.20
103	1.63	114	73.75	p_a	128.44
104	2.57	116	87.91		

TABLE 92 cont/.....

TABLE 92 cont.

100°C 2.0 Mrad. Run 5. 5.9 mg.					
t	p	t	p	t	p
20	0.09	71	11.32	82	114.50
40	0.15	72	24.64	85	119.26
60	0.19	73	48.30	90	122.91
65	0.44	74	63.96	95	125.37
66	0.60	75	75.01	100	126.61
67	0.88	76	84.84	p_f	127.20
68	1.61	77	92.63	p_a	132.31
69	2.92	78	99.66		
70	5.89	80	108.67		

105°C 2.0 Mrad. Run 6. 6.0 mg.					
t	p	t	p	t	p
10	0.16	42	37.49	60	111.24
20	0.29	43	49.84	70	116.23
30	0.42	44	62.11	80	120.05
36	0.52	45	72.68	90	122.63
38	0.69	46	79.84	100	125.24
39	1.82	48	89.54	110	126.56
40	3.85	50	96.91	p_f	127.20
41	13.20	55	106.35	p_a	126.10

TABLE 93.

Temperature °C.	Induction period min.	k_2 cm min.$^{-1}$	k_7 min^{-1}
87.5°	195	9.100×10^{-2}	1.780×10^{-2}
90°	160	1.190×10^{-1}	2.680×10^{-2}
92.5°	130	1.530×10^{-1}	2.640×10^{-2}
95°	100	1.900×10^{-1}	3.160×10^{-2}
100°	66	2.850×10^{-1}	4.660×10^{-2}
105°	38	4.500×10^{-1}	3.740×10^{-2}

(vii) Percentage decomposition.

The percentage decomposition is higher after γ-ray irradiation than for the unirradiated salt. For a dose of 2.0 Mrad the average percentage decomposition is 97.63% of the theoretical value calculated from the equation:

$Sr(N_3)_2$/.....

$$Sr(N_3)_2 \rightarrow Sr + 3N_2$$

TABLE 94 lists the results of a series of determinations.

TABLE 94.

Temperature °C.	Dose.	Weight used mg.	% decomposition.
100°C	1,000 rad.	6.7	94.66
100°C	10,000 "	6.7	100.38
100°C	20,000 "	6.8	103.00
100°C	50,000 "	6.8	96.99
100°C	100,000 "	6.7	98.47
100°C	250,000 ""	6.7	94.66
100°C	1.0 Mrad.	6.7	102.29
100°C	2.0 "	6.7	102.29
100°C	4.0 "	6.9	101.11
100°C	10.0 "	6.7	100.38
87.5°	2.0 "	6.0	97.87
90°	2.0 "	6.1	99.16
92.5°	2.0 "	6.2	94.65
95°	2.0 "	6.0	97.02
100°	2.0 "	5.9	101.73
105°C	2.0 "	6.0	95.32

(viii) Mathematical analysis of the results and evaluation of activation energies.

In the acceleratory period the power law with n = 3, holds for γ-ray doses of up to 50,000 rad.

$$p^{1/3} = k_5 t + c_5 \quad \ldots\ldots\ldots\ldots\ldots\ldots\ldots\ldots (10)$$

On a dose of 20,00 rad the fit is from $\alpha = 0.016$ to $\alpha = 0.36$. However the power law is invalid with doses exceeding 50,000 rad.

The exponential law,

$$\log p = k_2 t + c_2 \quad \ldots\ldots\ldots\ldots\ldots\ldots\ldots\ldots (6)$$

describes the acceleratory period for γ-ray doses of 250,000 rad and higher. Between doses of 50,000 rads and 250,000 rads there is a period of change where neither equation fits well.

The decay reaction is described by the contracting sphere

formula over/.....

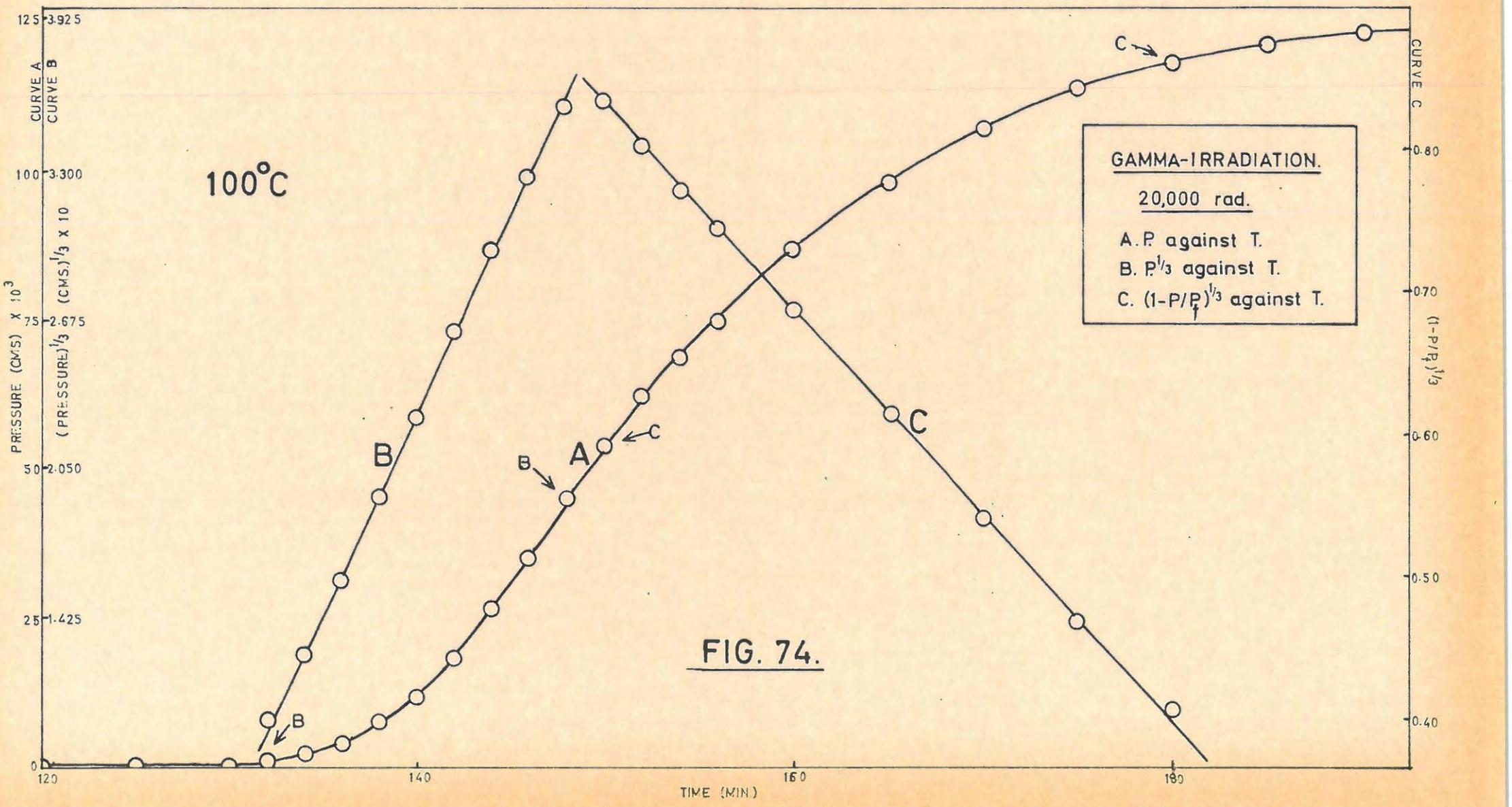
100°C
GAMMA-IRRADIATION.
20,000 rad.
A. P against T.
B. $P^{1/3}$ against T.
C. $(1-P/P_f)^{1/3}$ against T.
PRESSURE (CMS) X 10^3
CURVE A
CURVE B
$(PRESSURE)^{1/3}$ $(CMS.)^{1/3}$ X 10
CURVE C
$(1-P/P_f)^{1/3}$
TIME (MIN)
125
100
75
50
25
0
3.925
3.300
2.675
2.050
1.425
0.80
0.70
0.60
0.50
0.40
120
140
160
180
A
B
C

FIG. 74.

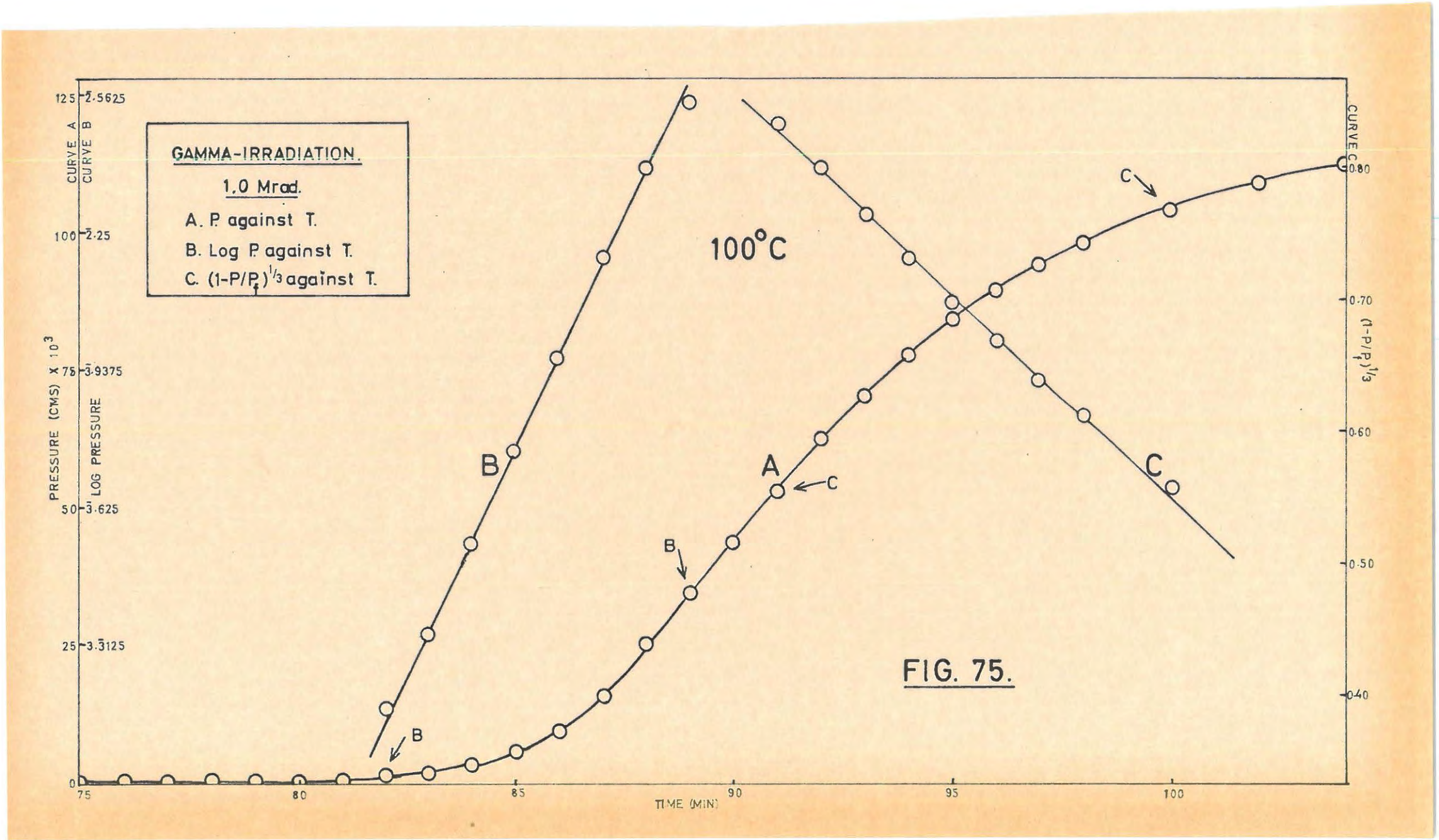
GAMMA-IRRADIATION.
1.0 Mrad.
A. P against T.
B. Log P against T.
C. $(1-P/P_f)^{1/3}$ against T.
100°C
A
B
C
PRESSURE (CMS) X 10^3
LOG PRESSURE
CURVE A
CURVE B
CURVE C
$(1-P/P_f)^{1/3}$
TIME (MIN)
0
25
50
75
100
125
3·3125
3·625
3·9375
2·25
2·5625
0·40
0·50
0·60
0·70
0·80
75
80
85
90
95
100

FIG. 75.

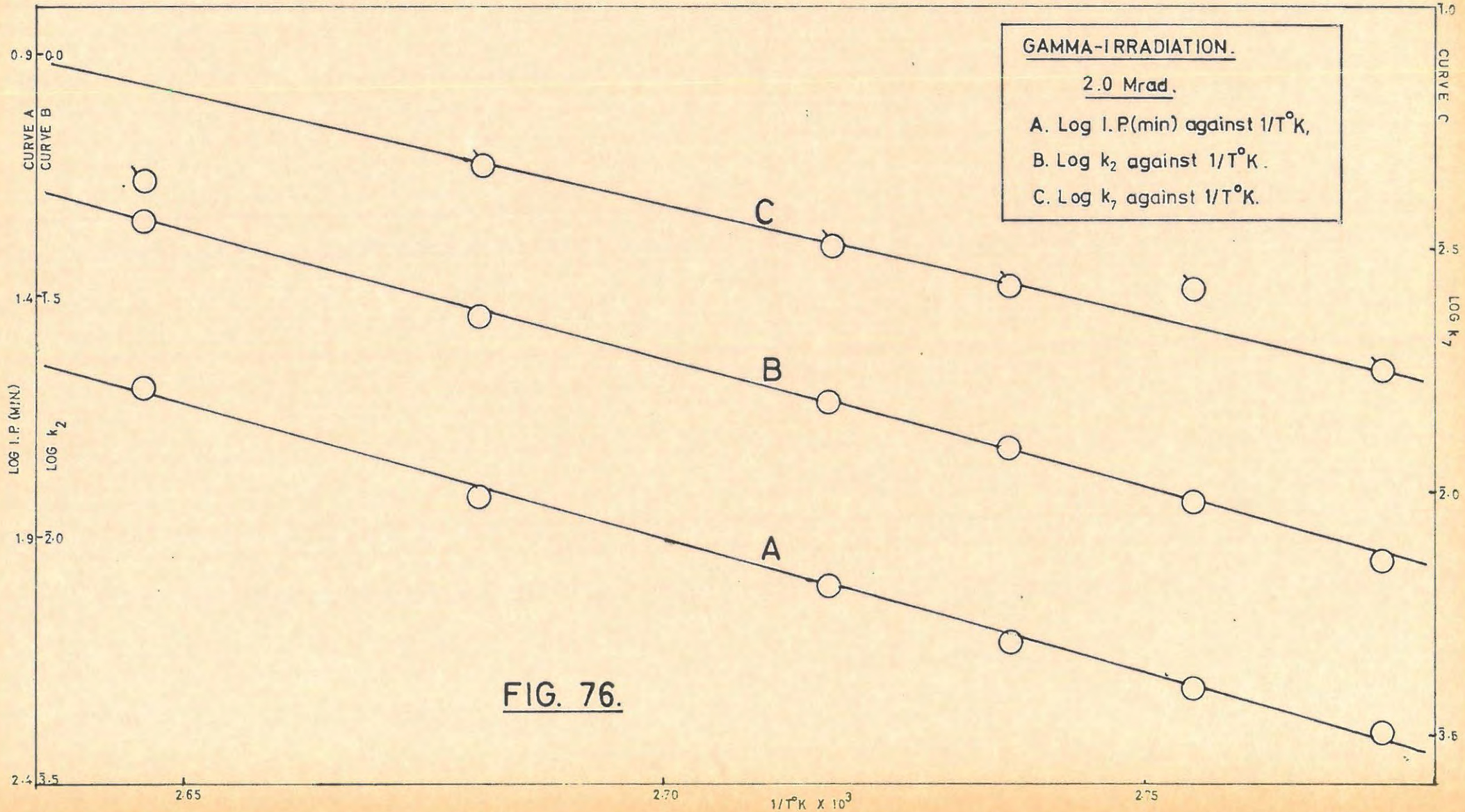
GAMMA-IRRADIATION.
2.0 Mrad.
A. Log I.P.(min) against 1/T°K,
B. Log k2 against 1/T°K.
C. Log k7 against 1/T°K.
CURVE A
CURVE B
CURVE C
LOG I.P (MIN.)
LOG k2
LOG k7
0·9
0·0
1·4
1·5
1·9
2·0
2·4
3·5
2·5
3·0
3·5
1·0
2·65
2·70
2·75
1/T°K X 10³
A
B
C

FIG. 76.

formula over the whole range of γ-ray irradiations.

$$(1 - {}^{p}/_{p_f})^{1/3} = k_7 t + c_7 \quad \ldots\ldots\ldots\ldots\ldots\ldots (2)$$

For heavily dosed specimens the exponential law holds to an α value of approximately 0.30. The decay equation holds from α = 0.50. Between these two values the decomposition proceeds at an almost linear rate.

FIGURE 74 shows the p/t plot for the decomposition of a specimen irradiated with a low dose (20,000 rad) with the corresponding analysis. FIGURE 75 shows the same plots for a high dose (1.0 Mrad).

Activation energies were calculated from the plots of log I.P., log k_2, and log k_7, vs. ${}^{1}/_{T}$ °K, respectively, for specimens preirradiated with a dose of 2.0 Mrad. The following values were obtained:

(i) Induction period: 24.70 kcals.mole^{-1}

(ii) Acceleratory period: 24.00 kcals. mole^{-1}

(iii) Decay period: 20.10 kcals.mole^{-1}.

The activation energy plots are shown in FIGURE 76.

7.1.6. Superimposed Irradiations.

(i) Superimposed ultra-violet light and x-ray irradiations.

Decompositions were performed on specimens irradiated prior to decomposition firstly with X-rays, and then ultra-violet light, and vice versa. Two series were done with irradiation times chosen so that (i) the induction period for the ultra-violet light irradiated specimen was shorter than that for the x-ray irradiated specimen and (ii) vice versa. All decompositions were done at 110°C. TABLE 95 and FIGURE 77 show the results for decompositions of type (i) and TABLE 96 and FIGURE 78 the results for type (ii).

In all the above cases the acceleratory and decay periods of the p/t plots have the same characteristics as the

decomposition of/.....

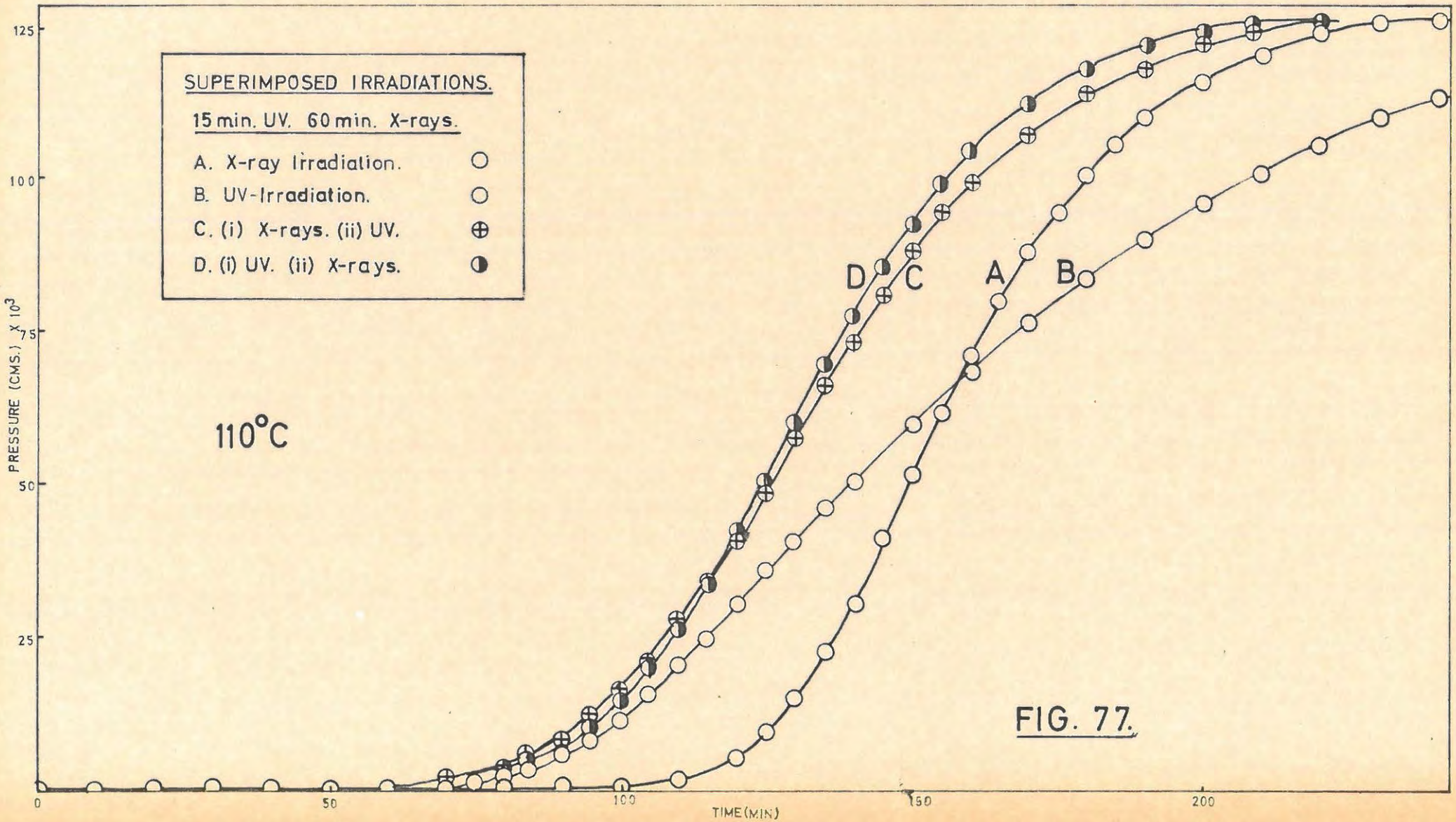
SUPERIMPOSED IRRADIATIONS.
15 min. UV. 60 min. X-rays.
A. X-ray Irradiation.
B. UV-Irradiation.
C. (i) X-rays. (ii) UV.
D. (i) UV. (ii) X-rays.
110°C
PRESSURE (CMS.) X 10³
TIME (MIN)
125
100
75
50
25
0
50
100
150
200
A
B
C
D

FIG. 77.

decomposition of a specimen preirradiated with X-rays only. The induction period always corresponds to the shorter induction period.

TABLE 95.

110°C 15 min U.V. Run 1. U.V. blank 6.4 mg.					
t	p	t	p	t	p
30	0.04	120	30.09	220	105.52
60	0.22	125	35.42	230	109.81
70	0.52	130	40.49	240	113.64
75	1.01	135	45.61	250	117.54
80	1.88	140	50.63	260	120.93
85	3.37	150	59.85	270	123.21
90	5.30	160	68.56	280	124.94
95	7.95	170	76.45	290	126.10
100	11.31	180	83.43	300	126.69
105	15.26	190	89.68	p_f	127.20
110	19.81	200	95.66	p_a	127.27
115	24.68	210	100.79		

110°C 60 min X-rays Run 2 X-ray blank 6.5 mg.					
t	p	t	p	t	p
40	0.13	130	14.80	180	100.13
60	0.17	135	22.13	185	105.40
80	0.22	140	30.94	190	109.71
90	0.33	145	41.21	200	115.78
100	0.61	150	51.46	210	120.92
105	1.03	155	61.20	220	123.75
110	1.83	160	70.91	230	125.49
115	3.03	165	79.94	240	126.65
120	5.32	170	87.44	p_f	127.20
125	9.09	175	93.88	p_a	126.10

110°C (i) 15 min. U.V. Run 3. (ii) 60 min. X-rays. 6.6 mg.					
t	p	t	p	t	p
20	0.07	105	19.73	160	104.40
40	0.12	110	26.10	165	108.99
60	0.24	115	33.35	170	112.63
65	0.35	120	41.81	175	115.79

TABLE 95 cont/.....

TABLE 95 cont.

t	p	t	p	t	p
70	0.63	125	50.87	180	117.92
75	1.18	130	60.06	190	121.16
80	2.19	135	69.02	200	123.89
85	3.90	140	77.20	210	125.55
90	6.46	145	85.20	220	126.66
95	9.98	150	92.65	p_f	127.20
100	14.45	155	98.93	p_a	139.82

110°C (i) 60 min X-rays Run 4. (ii) 15 min U.V. 6.5 mg.					
t	p	t	p	t	p
20	0.05	105	21.24	160	99.09
40	0.09	110	27.02	165	103.53
60	0.29	115	33.48	170	107.56
65	0.54	120	40.59	180	113.75
70	1.06	125	48.49	190	117.44
75	1.95	130	56.93	220	125.52
80	3.38	135	65.46	230	126.65
85	5.43	140	72.80	p_f	127.20
90	8.23	145	80.52	p_a	138.00
95	11.95	150	87.72		
100	16.17	155	94.27		

TABLE 96.

110°C 1 min. U.V. Run 1. U.V. blank 6.3 mg.					
t	p	t	p	t	p
40	0.05	160	16.12	270	81.60
60	0.08	170	20.63	280	87.42
70	0.13	180	25.72	300	97.58
80	0.22	190	31.35	320	106.65
90	0.47	200	37.22	340	113.86
100	0.91	210	42.91	360	118.99
110	1.74	220	48.62	380	123.06
120	3.23	230	54.70	400	125.42
130	5.40	240	61.12	420	126.60
140	8.29	250	67.91	p_f	127.20
150	11.79	260	75.05	p_a	122.07

TABLE 96 cont/.....

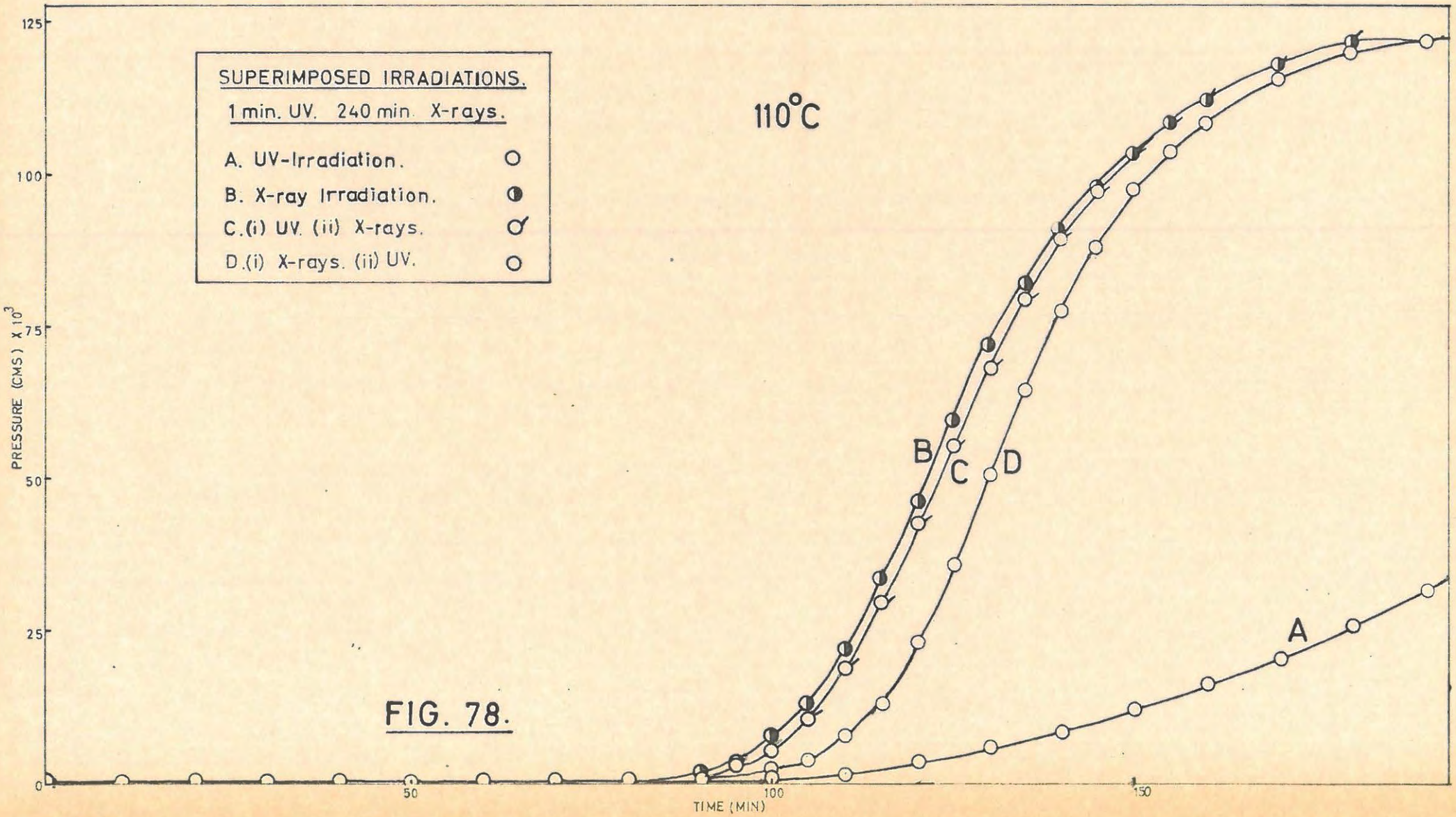
SUPERIMPOSED IRRADIATIONS.
1 min. UV. 240 min. X-rays.
A. UV-Irradiation.
B. X-ray Irradiation.
C.(i) UV. (ii) X-rays.
D.(i) X-rays. (ii) UV.
110°C
PRESSURE (CMS) X 10³
TIME (MIN)
0
25
50
75
100
125
50
100
150
A
B
C
D

FIG. 78.

TABLE 96 cont.

110°C 240 min. X-rays Run 2. X-ray blank 6.4 mg.					
t	p	t	p	t	p
40	0.17	115	33.61	160	112.33
60	0.17	120	46.52	170	117.39
70	0.27	125	59.49	180	120.84
80	0.54	130	71.36	190	123.15
90	1.94	135	81.92	200	124.93
95	3.77	140	91.19	210	126.07
100	7.16	145	98.34	220	126.66
105	13.11	150	104.14	p_f	127.20
110	22.05	155	108.47	p_a	123.79

110°C (i) 1 min. U.V. Run 3. (ii) 240 min. X-rays 6.4 mg.					
t	p	t	p	t	p
40	0.06	115	29.51	160	111.90
60	0.10	120	42.56	170	118.03
70	0.17	125	55.64	180	122.02
80	0.49	130	68.31	190	124.90
90	1.75	135	79.48	200	126.07
95	3.12	140	89.01	210	126.65
100	5.84	145	97.03	p_f	127.20
105	10.73	150	103.27	p_a	126.10
110	18.84	155	108.68		

110°C (i) 240 min. X-rays Run 4. (ii) 1 min. U.V. 6.3 mg.					
t	p	t	p	t	p
40	0.18	115	13.34	160	108.70
60	0.23	120	23.04	170	116.05
70	0.28	125	35.68	180	120.10
80	0.41	130	50.69	190	122.45
90	0.67	135	64.85	200	124.23
95	1.08	140	77.43	210	125.42
100	2.00	145	88.09	220	126.62
105	3.79	150	97.34	p_f	127.21
110	7.25	155	103.75	p_a	119.79

(ii) Mathematical/.....

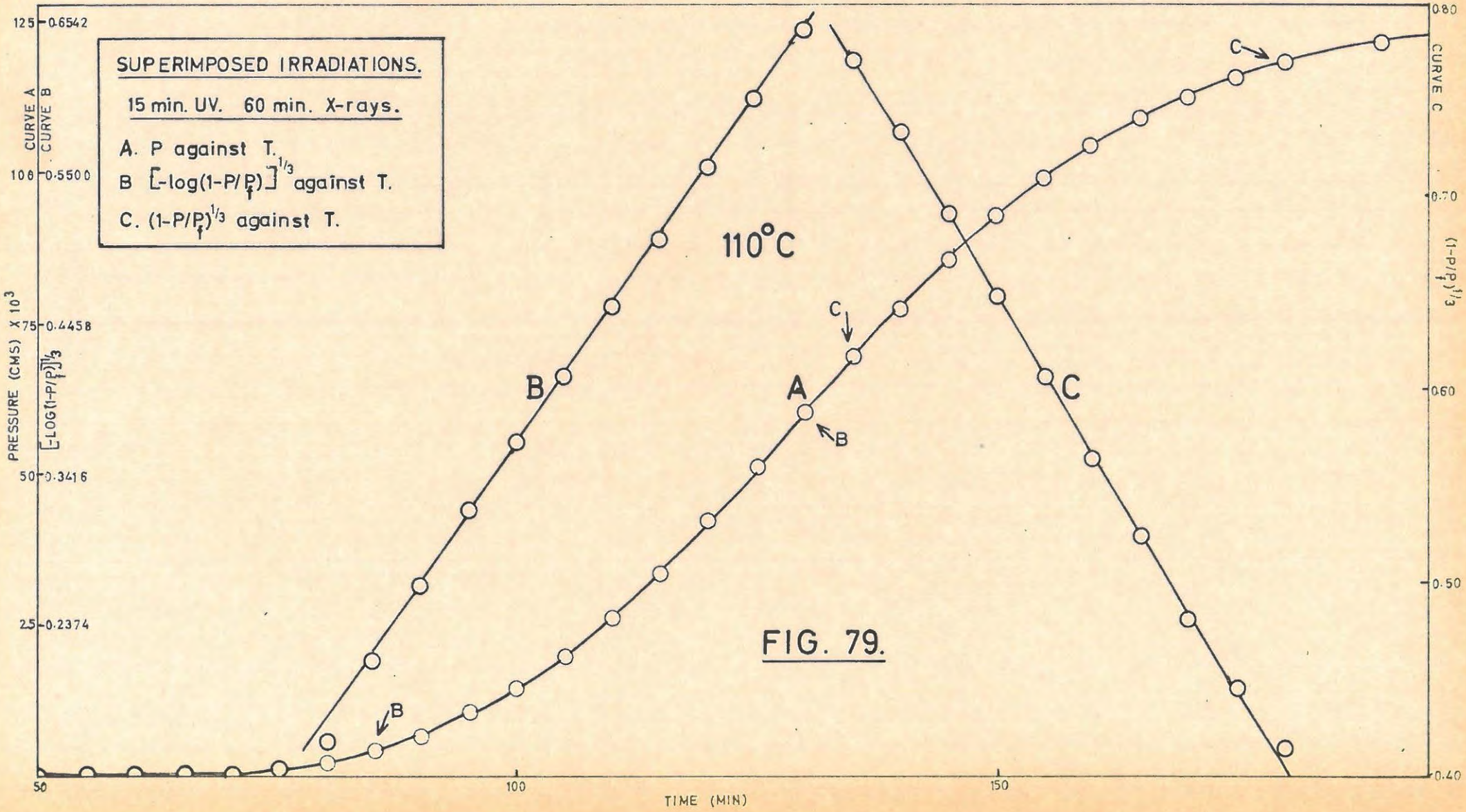
SUPERIMPOSED IRRADIATIONS.
15 min. UV. 60 min. X-rays.
A. P against T.
B $[-\log(1-P/P_f)]^{1/3}$ against T.
C. $(1-P/P_f)^{1/3}$ against T.
110°C
A
B
C
PRESSURE (CMS) X 10^3
CURVE A
CURVE B
CURVE C
$[-\log(1-P/P_f)]^{1/3}$
$(1-P/P_f)^{1/3}$
TIME (MIN)
125
100
75
50
25
0.6542
0.5500
0.4458
0.3416
0.2374
0.80
0.70
0.60
0.50
0.40
50
100
150

FIG. 79.

(ii) Mathematical analysis of the results.

The Avrami-Erofeyev equation in the form

$$\left[- \log \left(1 - \frac{p - p_o}{p_f - p_o}\right)\right]^{1/3} = k_6 t + c_6 \ldots\ldots\ldots (11)$$

when $p_o = 1.0 \times 10^{-3}$ cm.Hg fitted the acceleratory period.

The decay period was described by the contracting sphere formula

$$(1 - p/p_f)^{1/3} = k_7 t + c_7 \ldots\ldots\ldots\ldots\ldots\ldots (2)$$

FIGURE 79 shows a typical p/t plot with its analysis.

7.2. DISCUSSION.

7.2.1. Unirradiated Strontium Azide.

The reproducibility of the results for the thermal decomposition of ground strontium azide was very good. No ageing effect was found. The pressure-time plots for the isothermal decomposition show that there is a true induction period during which time there is no measurable evolution of gas. This is followed by an acceleratory decomposition where the pressure-time plots obey the simple power law with the exponent n = 3. The expression fits the whole of the acceleratory period showing that there is no significant overlap or ingestion of nuclei before the decay reaction commences. Such changes would have necessitated the use of the more sophisticated Avrami-Erofeyev equation, as for barium azide. The decay reaction is described by the contracting sphere formula. The activation energies for all three phases of decomposition are approximately the same. (cf CaN_6 later).

It is considered that the geometric form of the nuclei during the acceleratory period is that of a steadily expanding 2-dimensional reaction centre; the radial rate of growth being constant. These nuclei increase in number linearly with time. The value of n = 3 in the power law is consistent with such a picture of nucleation and growth. However it must be appreciated that the following two possibilities would also yield a power of three. These are,

(i) three-dimensional growth of nuclei from a fixed number of centres, or

(ii) one-dimensional nuclei increasing in number as the square of the time.

The experiments involving the destruction of the metal nuclei by water vapour discount possibility (i) since after destruction the complete course of reaction is repeated. Possibility (ii) is not likely since the decay reaction commences at

$\alpha \approx 0.40$ and/.....

$\alpha \approx 0.40$ and such a mechanism would not account for this relatively high fractional decomposition.

The nuclei are considered to be surface ones and when they touch the surface of the spherical particle will be covered by reaction product. Reaction then proceeds by the inward progression of the interface. This type of mechanism explains the applicability of the contracting sphere expression for the decay reaction.

It can be assumed that no nuclei are initially present since any metal atoms or specks would have been destroyed by contact with water vapour or oxygen present in the air, during the preparation or subsequent handling of the salt. It is considered that a slow surface decomposition occurs at localities on the surface of the particle where disorganisation or mechanical damage has taken place. In such places, there will be a higher thermodynamical instability occasioned by strains and unsaturation of the cohesive forces. Such regions could be formed during grinding, by the aggregation and collapse of vacancies. Accordingly, it is suggested, as for barium azide, that the reaction $N_3^- + N_3^- \rightarrow 3N_2$ occurs on the surface of the particle during the induction period with the formation of strontium atoms. These crystallize to the metal at the end of the induction period and reaction then takes place at an expanding metal nucleus. The experiments with water vapour indicate that strontium is formed during the induction period. Destruction of the metal by water vapour returns the reaction, in effect, to zero time and a new induction period takes place.

The mechanism suggested for barium azide for the growth of nuclei during the acceleratory period and the inward movement of the reaction interface during the decay period appears to be equally applicable here. However, it is possible that an alternative mechanism may apply during the decay period and this will be discussed in the general discussion. The activa-

tion energies for the slow surface decomposition, the nuclear growth process, and the interface reaction during decay, are 23.3, 25.0 and 21.7 kcal.mole^{-1} respectively.

Interruptions with water vapour during the induction period result in the subsequent acceleratory period having virtually the same rate constant as the acceleratory period for an uninterrupted decomposition. This is valid even after five successive interruptions. Therefore it is concluded that there must be a very large number of potential nuclear forming sites and the same number of new nuclei must be formed after each interruption. Interruptions in the acceleratory and decay periods results in lower rate constants in the new acceleratory period. This must be due to considerable ingestion of the potential nuclear forming sites by the growing nuclei. At the end of the new induction period there will then be fewer nuclei present than at the end of the original induction period and consequently the rate of gas evolution will be less. (TABLE 61).

The chemical equation for the decomposition is considered to be

$$Sr(N_3)_2 \rightarrow Sr + 3N_2$$

The volume of gas evolved in a decomposition is only 71.2% of the theoretical value. It is considered that the remaining strontium azide is undecomposed at the end of the reaction. This view is supported by the fact that after preirradiation with γ-rays there is virtually 100% decomposition but the activation energies obtained are the same within experimental error indicating that the same process(es) are occurring in both instances.

7.2.2. Preirradiated (γ-rays) Strontium Azide.

Preirradiation produces no colour change in the salt. The subsequent thermal decomposition is characterised by a shorter induction period and increased values for the rate constants as compared to the unirradiated salt. The same

kinetic expressions/.....

kinetic expressions are obeyed up to a dose of 100,000 rad, but for doses greater than 250,000 rad the acceleratory period is described by the exponential law. However, the activation energies are practically unchanged. No ageing of the irradiation effect was detectable and annealing the salt in vacuo at 70°C for 3 hours produced no diminution in the radiation effect. Admission of water vapour at various points in the decomposition up to $\alpha = 0.5$ causes the reaction to begin afresh with a shorter induction period. The rate constants in the acceleratory period are slightly increased for interruptions at α values of up to $\alpha = 0.13$ but decreased at $\alpha = 0.50$.

The results for the decomposition of preirradiated strontium azide differ from those for preirradiated barium azide in that there is no change in the activation energies as compared to those for the corresponding unirradiated salt, in particular the energy for the induction period is unchanged. Consequently it can be assumed that the same rate determining process is occurring over the induction period for the decomposition of both irradiated and unirradiated strontium azide. It is suggested, therefore, that irradiation produces a high concentration of vacancies in the salt. The primary act of irradiation is to strip electrons from the azide ions i.e.

$$N_3^- \rightarrow N_3 + e^-$$

or to raise the electron to an excited state in the ion. The following reactions could then produce vacancies:

$$N_3 + N_3^{-\ddagger} \rightarrow 3N_2 + \boxed{A} + F$$

$$N_3 + F \rightarrow N_3^- + \boxed{A}$$

$$N_3 + \boxed{C} + N_3 \rightarrow 3N_2 + \boxed{C} + 2\boxed{A}$$

where $\boxed{A}$, $\boxed{C}$, F and $N_3^{-\ddagger}$ are as given in barium azide. In addition, vacancies could be "boiled off" from jogs in dislocations by the method proposed by Seitz.[93]

It is then postulated that during the induction period

the vacancies/.....

the vacancies aggregate and collapse to produce regions of high strain at which decomposition proceeds. This decomposition reaction will be the same as the slow surface decomposition postulated for unirradiated strontium azide during the induction period. The rate determining step during the induction period will be this slow decomposition. The strontium atoms produced will crystallize at the end of the induction period to form metallic nuclei and thereafter reaction will proceed as for the unirradiated salt, except that it will be much faster because of the greater number of nuclei. The induction period will be shorter because of the more rapid production of strontium atoms. The increase in the decay rate constant on pre-irradiation suggests that the two-dimensional nuclei are formed at internal surfaces as well as on the surface of the particle. This will probably occur in the sub-grain boundaries. The decay stage for the irradiated salt will therefore consist of a large number of "contracting envelope" reaction interfaces in a single particle. Consequently the rate will be higher than for the unirradiated salt. The results for the series of runs where the decomposition was interrupted, the salt irradiated, and the decomposition continued (FIGURE 71), support the suggestion that nuclei are formed internally since the irradiation effect is found to be to the same marked degree when interruption is performed in the acceleratory or decay period. Interruption in the decay period means that the salt particles are covered with the decomposition product, and yet the irradiation effect is found.

The change in the mathematical equation describing the acceleratory period from the power law (n = 3) to the exponential law at high γ-ray doses, must be interpreted as being due to the onset of a branching chain (material chains) mechanism. This can be visualized as being due to heavy radiation damage along dislocations. Reaction commences and proceeds along such line defects and branches on reaching an intersection of

dislocation/.....

dislocations. A similar type of mechanism has been suggested to explain the applicability of the exponential law in the decomposition of silver oxalate.[27] There is a transition region in the p/t plot for the decomposition of a heavily irradiated specimen where neither the exponential law nor the contracting sphere formula fit (FIGURE 75). This part of the plot is linear. It is assumed that at this stage in the decomposition the rapid branching reaction is over and reaction consists of the plate-like one-dimensional growth of nuclei in sub-grain boundaries from the dislocations along which the branching reaction took place. The exponential law fits over only 30% of the decomposition which would be expected if reaction was confined to a dislocation network.

The admission of water vapour during the acceleratory period will destroy the metal nuclei. On recommencing the reaction, the centres of product of the reaction between water and strontium will act as vacancy traps, and thus the nuclei will form earlier than before interruption. Consequently the induction period will become shorter. When interruptions are done near the inflexion point ($\alpha \sim 0.50$) the subsequent acceleratory rate constant is decreased. This is a result of a decrease in the number of available vacancies i.e. a depletion of the "vacancy reservoir" will have occurred during the decomposition before interruption. Interruptions at low α values, however, (e.g. $\alpha = 0.13$) result in increased rate constants for the acceleratory period. At this stage there is still a large "reservoir" of vacancies. Each vacancy trap can act as a centre where several nuclei are formed. There will thus be an increase in the number of nuclei and consequently an increase in the rate constant. This idea is further enlarged below.

The runs involving the successive interruption and admission of water vapour without allowing the pressure to rise above the value usually taken as marking the end of the induction period are of great interest, and produced results totally

different from/.....

different from the other alkaline earth azides. It is assumed that the concentration of vacancies is very high indeed after a dose of 10 Mrad. This assumption is supported by the fact that strontium azide is very much more sensitive to preirradiation than either calcium or barium azides (see general discussion later). With repeated interruptions the number of vacancy traps (product of Sr and H_2C reaction) will increase and if the reaction is allowed to proceed (at a certain stage viz. 6th interruption) the concentration of nuclei around a trap is so high that a vigorous reaction develops and self-heating causes explosion. After seven interruptions the number of available vacancies has begun to fall and when reaction is allowed to proceed self-heating is not great enough to initiate explosion. The duration of the induction period decreases with repeated interruptions because nuclei form sooner around a trap.

7.2.3. Preirradiated (X-rays) Strontium Azide.

The effects of preirradiation by X-rays are similar to those found with strontium azide which has been preirradiated by γ-rays. One marked difference is found however in that with a heavy X-ray dose the acceleratory period is described by the Avrami-Erofeyev equation with $n = 3$. This indicates that the overlap and ingestion of the nuclei becomes more significant as the number of nuclei increase with increasing dose. Evidently the irradiation effect is never so great as to cause the rapid chain branching reaction that one finds with heavy doses of γ-rays. The irradiation effects can be explained by the same reasoning as for the effects of γ-rays on strontium azide.

7.2.4. Preirradiated (Ultra-Violet Light) Strontium Azide.

The salt is not darkened by preirradiation with ultra-violet light. The subsequent thermal decomposition differs from that of unirradiated strontium azide in that the

induction period/.....

induction period is reduced and the velocity constant for the acceleratory period is increased. The increase in the rate constant is not very great, certainly not as great as with γ-ray or X-ray irradiated strontium azide. The most signicant features of the study are (i) the steady fall in the inflexion point of the p/t plot (FIGURE 56) and (ii) the change in the exponent, n, in the power law from 3 to 2 as the ultraviolet dose is increased. Except for this change, the kinetic expressions are the same as for the decomposition of unirradiated strontium azide. There is a slight fall in the activation energies but the change is not significant. It is suggested that the effects of irradiation are similar to those of preirradiation by γ-rays and X-rays except that the effect is largely confined to the surface of the azide particle. This view is supported by the fact that there is not a drastic change in the rate constant for the decay reaction after irradiation. Also irradiation after interruption of the decomposition of unirradiated salt is effective only when the expected time of acceleration due to the U.V. effect is less than the time at which the decay reaction commences (FIGURE 57). This too indicates that the nuclei are primarily surface ones. Two-dimensional nuclei are considered to grow and increase in number linearly with time during the acceleratory period of the lightly dosed specimens, i.e. when the exponent in the power law is 3. However, during the same period for the decomposition of heavily irradiated strontium azide the value of n decreases to 2 signifying that the number of surface nuclei is so great at the end of the induction period that any further increase in number with time is virtually "swamped". The fall in the inflexion point as the U.V. dose is increased is probably due to the fact that photolysis occurs at high doses so that the surface is partly covered with strontium carbonate or strontium hydroxide. Thus when the nuclei cease growing over

the surface a smaller fraction of the salt will have been decomposed than with the unirradiated salt.

The change to a value of n = 3 for the new acceleratory period after interruption(s), admission of water vapour, and recommencement of heating, is due to a fall in the number of vacancies with partial decomposition (or repeated interruptions), so that the salt after interruption resembles a lightly irradiated specimen.

8. THE THERMAL DECOMPOSITION OF CALCIUM AZIDE.

8.1 RESULTS.

8.1.1. Preparation.

Two specimens of calcium azide were used;

(a) that prepared by Brown[115], by a method similar to that used for the preparation of strontium azide. This specimen had been finely ground and stored over P_2O_5 in a vacuum desiccator for one year;

(b) a freshly prepared sample which was not ground.

8.1.2. Unirradiated Calcium Azide.

(i) Effect of varying the temperature of decomposition.

The critical increment of the process(es) occurring was determined by two methods, viz. (1) individual runs and (2) split run methods.

(1) Individual runs.

Approximately 4.5 mg. of specimen (a) which had been annealed for 24 hours at 60°C in vacuum was used in each run. These runs were done in the normal manner where the temperature remained fixed for the duration of the whole run. Rate constants were determined over the temperature range 105° - 125°C. The results are given in TABLE 97. Acceleratory and decay rate constants, k_5 and k_7 (equations 10 and 2), and the duration of the induction period (min.), are given in TABLE 98.

TABLE 97.

105°C		Run 1.			4.5 mg.
t	p	t	p	t	p
50	0.09	220	5.71	350	60.21
100	0.21	230	7.28	360	66.75
110	0.27	240	9.19	380	78.11
120	0.38	250	11.68	400	88.42
130	0.52	260	14.65	420	97.83

TABLE 97 cont/.....

TABLE 97 cont.

t	p	t	p	t	p
140	0.63	270	17.75	440	106.67
150	0.85	280	21.62	460	113.68
160	1.16	290	26.14	480	119.22
170	1.52	300	31.08	500	123.18
180	2.00	310	36.14	520	125.48
190	2.62	320	41.92	540	126.63
200	3.52	330	47.76	p_f	127.20
210	4.44	340	53.99	p_a	129.03

110°C	Run 2.			4.5 mg.	
t	p	t	p	t	p
40	0.06	160	13.76	270	105.09
60	0.16	170	19.24	280	109.76
70	0.25	180	26.14	290	114.00
80	0.42	190	34.40	300	117.78
90	0.72	200	44.45	310	120.52
100	1.11	210	54.30	320	123.28
110	1.76	220	64.33	330	124.96
120	2.82	230	73.91	340	126.08
130	4.33	240	83.23	p_f	127.20
140	6.41	250	91.67	p_a	135.57
150	9.66	260	99.51		

115°C	Run 3.			4.5 mg.	
t	p	t	p	t	p
20	0.01	105	15.71	165	92.47
40	0.11	110	20.49	170	96.55
50	0.29	115	26.16	180	105.18
60	0.67	120	32.24	190	111.57
65	0.99	125	38.94	200	116.48
70	1.51	130	45.93	210	120.38
75	2.20	135	53.13	220	123.20
80	3.02	140	60.05	230	124.91
85	4.40	145	66.98	240	126.06
90	6.15	150	73.85	250	126.63
95	8.50	155	80.16	p_f	127.20
100	11.75	160	86.67	p_a	130.20

TABLE 97 cont/.....

TABLE 97 cont.

120°C		Run 4.			4.6 mg.
t	p	t	p	t	p
20	0.03	75	25.98	125	113.23
30	0.15	80	35.50	130	116.38
35	0.29	85	47.80	135	118.79
40	0.63	90	59.27	140	121.19
45	1.27	95	70.72	150	123.91
50	2.24	100	80.97	160	125.55
55	4.04	105	90.03	170	126.65
60	6.75	110	97.63	p_f	127.20
65	11.12	115	104.02	p_a	130.33
70	16.97	120	109.09		

125°C		Run 5.			4.6 mg.
t	p	t	p	t	p
20	0.06	50	15.48	75	97.96
25	0.15	52	21.33	80	106.87
30	0.40	54	28.64	85	113.54
35	1.16	56	37.03	90	118.27
38	1.94	58	45.83	95	121.40
40	2.84	60	53.75	100	124.19
42	3.92	62	61.16	105	125.83
44	5.62	64	68.23	110	126.93
46	7.90	67	77.40	p_f	127.20
48	11.05	70	85.79	p_a	131.18

TABLE 98

Temperature °C.	Induction period min.	k_5 $cm^{1/3}$ $min.^{-1}$	k_7 $min.^{-1}$
105°	140	1.70×10^{-3}	3.10×10^{-3}
110°	85	2.80×10^{-3}	4.70×10^{-3}
115°	60	4.50×10^{-3}	6.50×10^{-3}
120°	40	6.85×10^{-3}	9.55×10^{-3}
125°	32	1.32×10^{-2}	1.437×10^{-2}

(2) Split runs.

The activation energy of the acceleratory period only was determined by this method . The decomposition was allowed to proceed at a particular fixed temperature for sufficient

time for cont/.....

time for the rate constant to be determined. The sample was then raised out of the decomposition chamber and allowed to cool while the temperature was adjusted to a new value. The decomposition was then continued until the new rate constant was obtained. In this manner several rate constants for the acceleratory period were determined from a single decomposition.

Split run decompositions were performed on specimens (a) and (b) above. The results appear in TABLE 99. The acceleratory rate constants obtained, k_5 (equation 10), are listed in TABLE 100. Pressures are not normalised.

A decomposition of freshly prepared unground calcium azide (specimen b) where the decomposition was taken to completion at a fixed temperature (110°C) was also performed to check the applicability of the mathematical analysis. This run is shown in TABLE 101.

TABLE 99.

Specimen (a)		Run 1.			4.9 mg.
t	p	t	p	t	p
110°C		205	5.30	240	15.67
100	0.60	208	5.79	242	17.57
105°C		211	6.43	244	19.81
120	1.07	214	7.24	246	22.18
130	1.24	217	8.10	248	24.94
140	1.42	220	9.07	125°C	
150	1.67	115°C		250	25.20
160	2.02	224	9.16	252	25.98
170	2.41	226	9.64	254	29.24
180	3.00	228	10.63	255	31.24
185	3.37	230	11.67	256	33.29
190	3.87	232	12.82	257	35.72
195	4.41	234	13.96	258	38.24
200	5.07	236	15.26	259	40.84
110°C		120°C		260	43.19

TABLE 99 cont/.....

TABLE 99 cont.

Specimen (b)		Run 2.			4.9 mg.
t	p	t	p	t	p
115°C		162	7.10	196	18.01
90	1.61	165	7.81	198	19.35
105°C		168	8.55	200	21.21
100	1.81	171	9.32	202	23.16
110	2.41	115°C		204	25.20
120	2.83	175	9.48	206	27.58
130	3.47	178	10.13	125°C	
135	3.87	180	10.97	210	28.68
140	4.28	182	11.84	211	29.80
145	4.84	184	12.75	212	31.49
110°C		186	13.81	213	33.00
150	5.07	188	14.86	214	34.81
153	5.42	190	16.08	215	36.66
156	5.92	120°C		216	38.22
159	6.43	194	16.45		

Specimen (b)		Run 3.			4.9 mg.
t	p	t	p	t	p
120°C		161	6.43	192	16.08
80	1.67	164	7.10	120°C	
105°C		167	7.81	196	16.29
90	2.17	170	8.64	198	17.14
100	2.41	173	9.48	200	18.67
110	2.74	115°C		202	20.04
120	3.19	176	9.64	204	21.69
130	3.47	178	9.96	206	23.16
140	4.18	180	10.46	208	24.69
145	4.72	182	11.14	210	26.78
150	5.30	184	12.02	212	28.97
110°C		186	12.93	214	31.24
155	5.67	188	13.88	216	33.29
158	5.90	190	14.86		

TABLE 100/.....

TABLE 100

Temperature °C.	k_5 $cm^{1/3}min.^{-1}$ Run 1.	k_5 $cm^{1/3}min.^{-1}$ Run 2.	k_5 $cm^{1/3}min.^{-1}$ Run 3.
105°	1.402×10^{-3}	1.173×10^{-3}	1.290×10^{-3}
110°	2.514×10^{-3}	2.063×10^{-3}	2.127×10^{-3}
115°	3.545×10^{-3}	3.225×10^{-3}	2.965×10^{-3}
120°	5.415×10^{-3}	4.515×10^{-3}	3.870×10^{-3}
125°	7.670×10^{-3}	6.085×10^{-3}	

TABLE 101

110°C Specimen (b) Run 1.					4.7 mg.
t	p	t	p	t	p
40	0.22	140	12.28	210	89.80
50	0.29	145	15.79	220	99.46
60	0.35	150	19.73	230	106.92
70	0.41	155	24.60	240	113.13
80	0.55	160	29.74	250	117.36
90	0.75	165	35.08	260	120.60
100	1.18	170	41.17	270	122.77
105	1.52	175	47.07	280	124.42
110	2.05	180	53.36	290	125.52
115	2.82	185	59.66	300	126.63
120	3.71	190	65.92	p_f	127.20
125	5.04	195	72.07	p_a	139.82
130	6.97	200	78.05		
135	9.21	205	84.28		

(ii) Mathematical analysis of the results and evaluation of activation energies.

The mathematical analysis given by Brown[115] was confirmed for ground calcium azide (specimen a). The accelera-tory period was described by the power law with n = 3 i.e.

$$p^{1/3} = k_5 t + c_5 \quad \ldots\ldots\ldots\ldots\ldots\ldots\ldots\ldots (10)$$

The extent of fit was $\alpha = 0.04$ to $\alpha = 0.39$.

The contracting sphere formula,

$$(1 - p/p_f)^{1/3} = k_7 t + c_7 \quad \ldots\ldots\ldots\ldots\ldots\ldots (2)$$

described the/.....

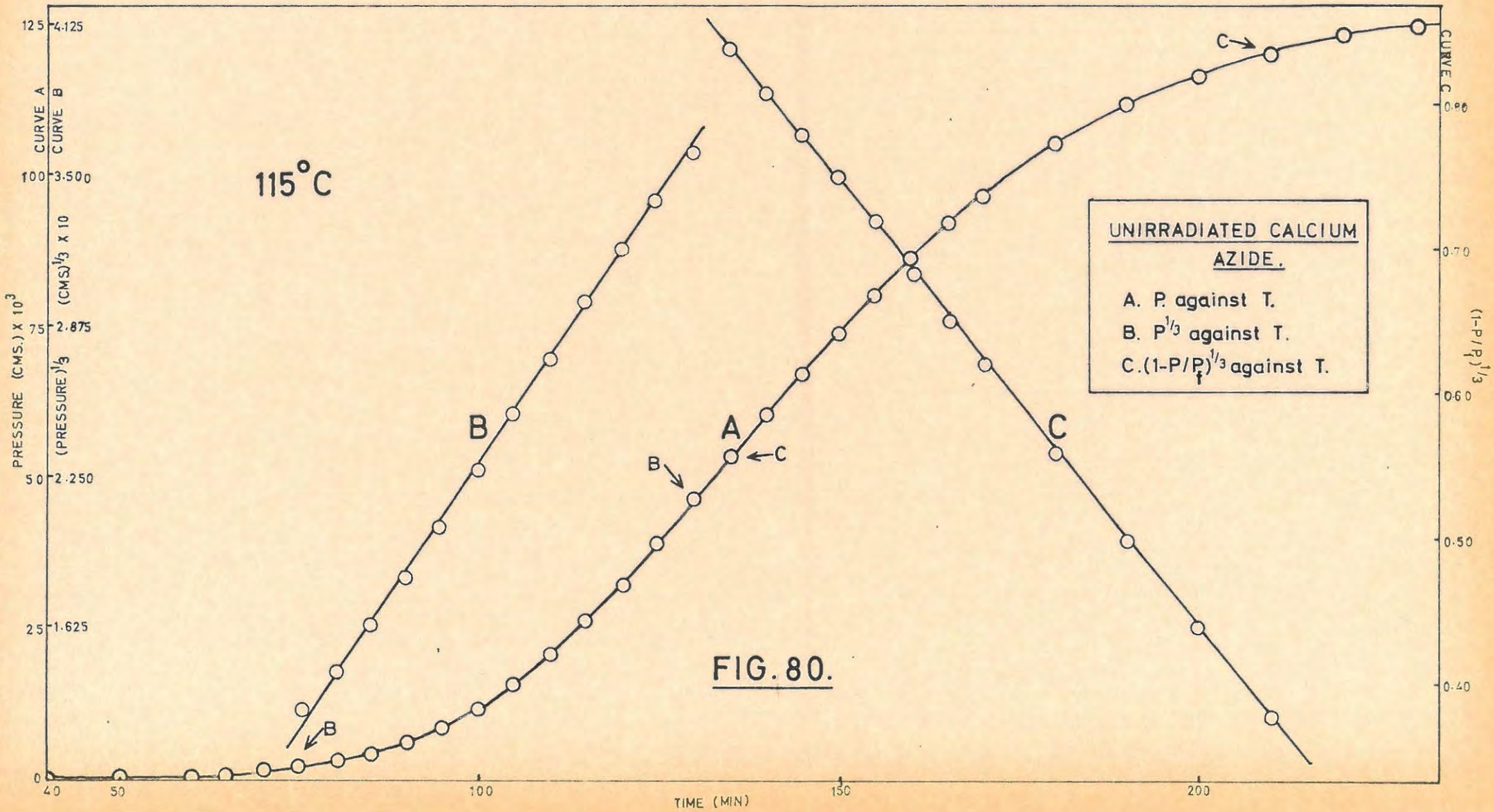
115°C
UNIRRADIATED CALCIUM AZIDE.
A. P against T.
B. $P^{1/3}$ against T.
C. $(1-P/P_f)^{1/3}$ against T.
PRESSURE (CMS.) X 10^3
CURVE A
CURVE B
$(PRESSURE)^{1/3}$ $(CMS)^{1/3}$ X 10
CURVE C
$(1-P/P_f)^{1/3}$
TIME (MIN)
A
B
C

FIG. 80.

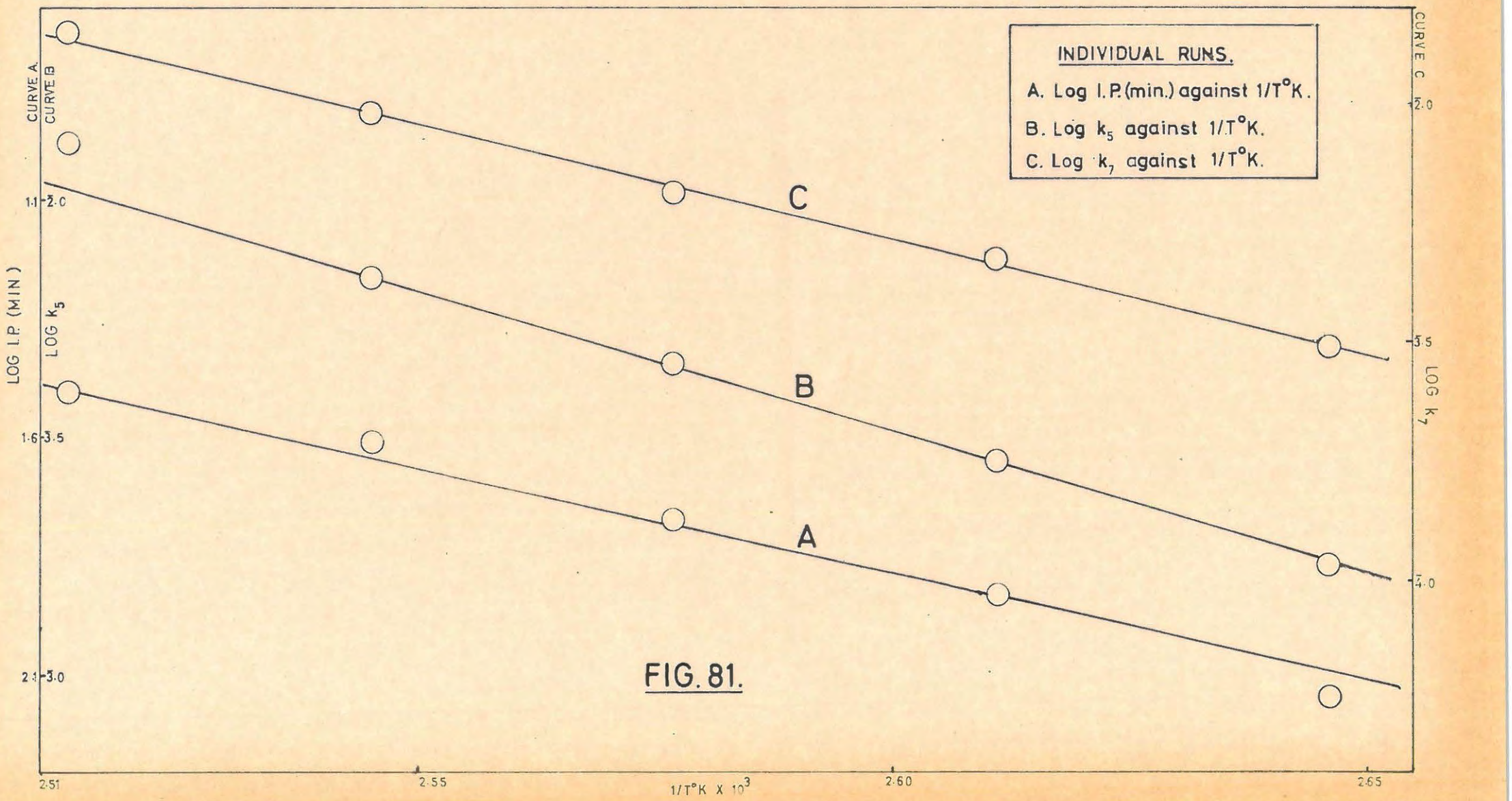
INDIVIDUAL RUNS.
A. Log I.P.(min.) against 1/T°K.
B. Log k_5 against 1/T°K.
C. Log k_7 against 1/T°K.
C
B
A
CURVE A
CURVE B
CURVE C
LOG I.P. (MIN)
LOG k_5
LOG k_7
1·1
2·0
1·6
3·5
2·1
3·0
3·5
3·0
2·51
2·55
2·60
2·65
1/T°K X 10^3

FIG. 81.

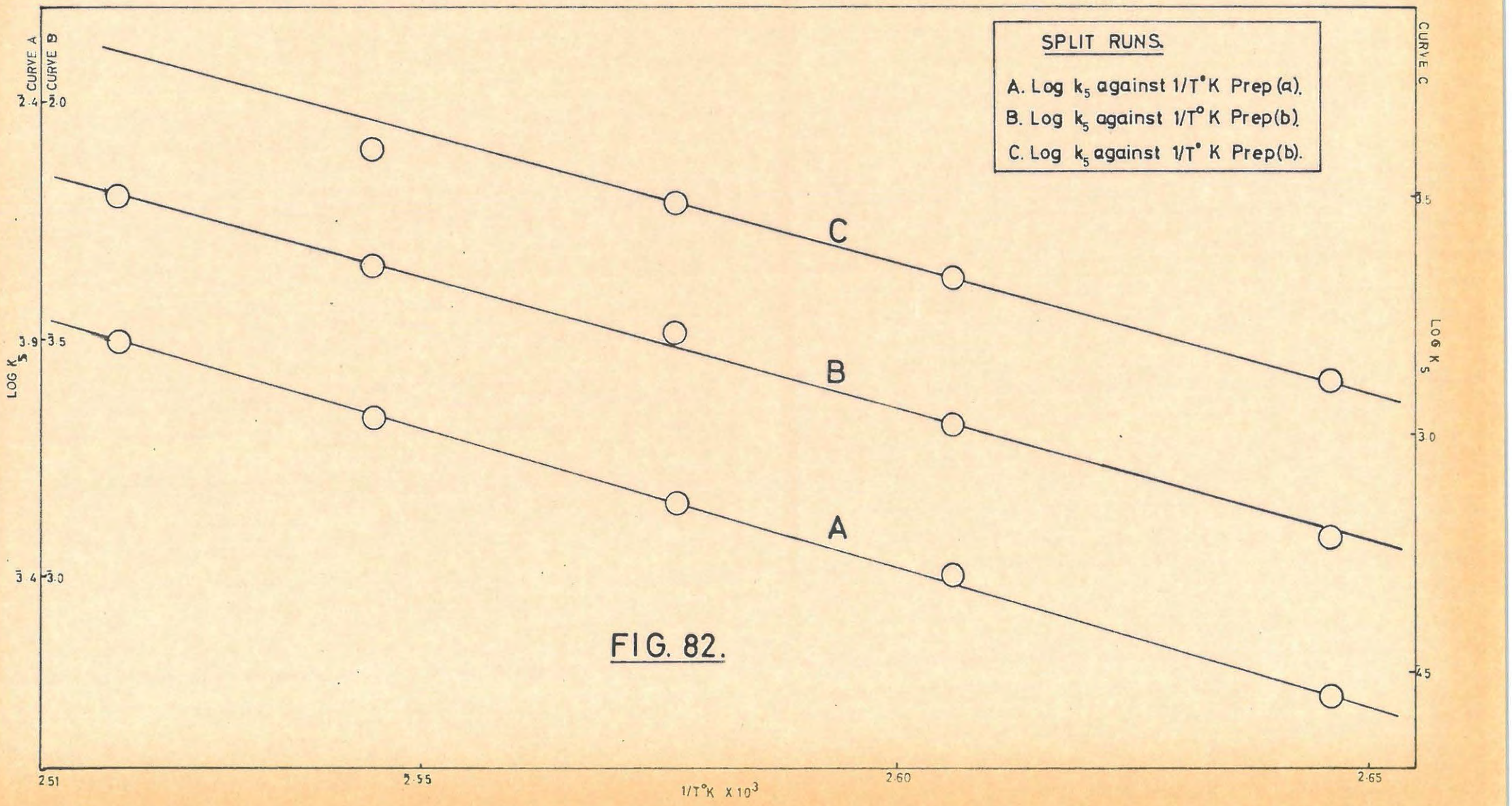
SPLIT RUNS.
A. Log k_5 against 1/T°K Prep (a).
B. Log k_5 against 1/T° K Prep(b).
C. Log k_5 against 1/T° K Prep(b).
CURVE A
CURVE B
CURVE C
LOG K_5
2·4
2·0
3·9
3·5
3·4
3·0
3·5
3·0
4·5
C
B
A
2·51
2·55
2·60
2·65
1/T°K X 10^3

FIG. 82.

described the decay period from $\alpha = 0.42$ to $\alpha = 0.90$ FIGURE 80 shows a typical p/t plot with the corresponding analysis plots.

The above equations also apply to the freshly prepared samples (b), but the extent of fit of the power law decreases to a range of $\alpha = 0.04$ to $\alpha = 0.31$.

Activation energy values obtained from the plots of log I.P. (min), log k_5, and log k_7, vs $^1/T$, are listed in TABLE 102. The Arrhenius plots are shown in FIGURES 81 and 82.

TABLE 102.

Type of run and specimen.	Activation energies kcals. mole^{-1}		
	Induction period.	Acceleratory period.	Decay period.
Individual (a)	20.60	26.90	21.00
Split (a)		26.46	
Split (b)		24.30	
Split (b)		26.10	

8.1.3 Preirradiated (Ultra-Violet Light) Calcium Azide.

(i) Effect of varying doses of ultra-violet light.

The apparatus and techniques used have been described previously. All irradiations were done at a distance of 80 cm. from the lamp. The effect of a steadily increasing dose on the subsequent thermal decomposition is shown in FIGURE 83. The results are tabulated in TABLE 103. The decomposition temperature was 110°C in each case, and doses ranged from 2 seconds to 30 minutes. Progressive shortening of the induction period, an increase in the acceleratory rate constants, and a fall in the inflexion point of the p/t plot with increasing dose, are the main features. The acceleratory rate constants, k_5 (equation 10) for irradiation times of up to 1 minute, and k_1 (equation 1), for heavier doses are listed in TABLE 104 together with the induction period and inflexion point values (α_i).

The above/.....

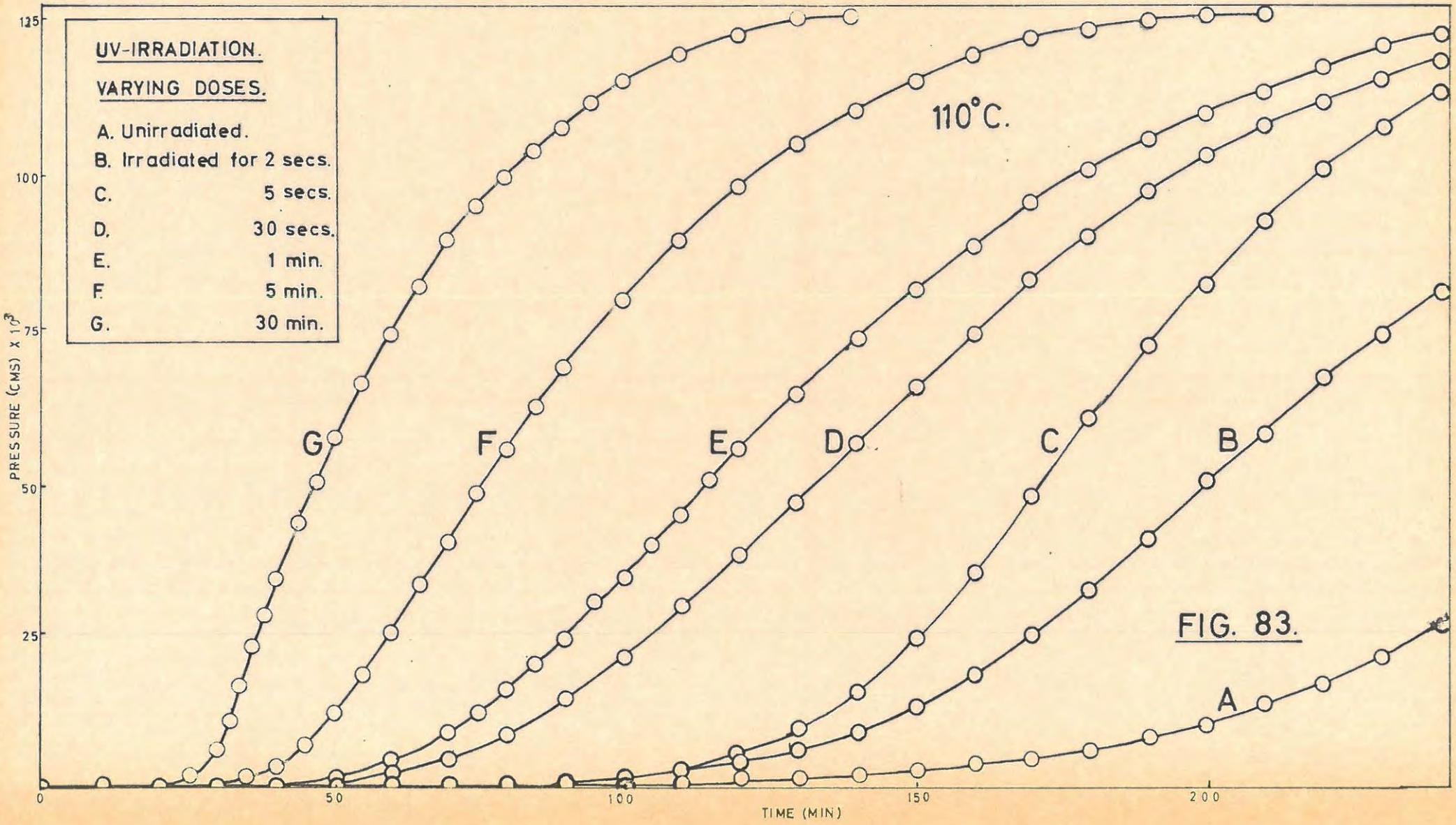
UV-IRRADIATION.
VARYING DOSES.
A. Unirradiated.
B. Irradiated for 2 secs.
C. 5 secs.
D. 30 secs.
E. 1 min.
F. 5 min.
G. 30 min.
110°C.
G
F
E
D
C
B
A
PRESSURE (CMS) X 10³
TIME (MIN)
0
50
100
150
200
25
50
75
100
125

FIG. 83.

The above experiments were all performed using specimen (a).

TABLE 103.

110°C Unirradiated blank. Run 1.					4.9 mg.
t	p	t	p	t	p
30	0.04	180	5.75	310	80.67
60	0.18	190	7.73	320	88.65
70	0.26	200	10.17	330	96.01
80	0.37	210	13.13	340	102.62
90	0.51	220	16.67	350	107.85
100	0.67	230	21.09	360	112.67
110	0.84	240	26.87	370	116.50
120	1.09	250	33.42	380	120.39
130	1.44	260	39.72	390	123.20
140	1.90	270	47.49	400	125.48
150	2.50	280	55.90	410	126.62
160	3.37	290	64.19	p_f	127.20
170	4.38	300	72.63	p_a	130.80

110°C 2 secs. U.V. Run 2.					4.5 mg.
t	p	t	p	t	p
20	0.01	150	12.69	260	95.72
40	0.03	160	17.98	270	100.82
60	0.12	170	24.66	280	105.60
70	0.22	180	31.96	290	109.26
80	0.42	190	40.45	300	112.36
90	0.73	200	49.52	320	118.05
100	1.25	210	57.71	340	122.08
110	2.25	220	67.01	380	126.52
120	3.78	230	74.43	p_f	127.20
130	5.83	240	81.71	p_a	123.79
140	8.67	250	88.78		

110°C 5 secs. U.V. Run 3.					4.5 mg.
t	p	t	p	t	p
20	0.02	140	15.31	240	114.21
40	0.04	150	24.00	250	117.75
60	0.11	160	35.03	260	120.62
70	0.24	170	47.68	270	123.53

TABLE 103 cont/.....

TABLE 103 cont.

t	p	t	p	t	p
80	0.43	180	60.22	280	125.67
90	0.85	190	71.97	290	126.21
100	1.64	200	82.36	p_f	127.20
110	3.04	210	92.82	p_a	118.10
120	5.15	220	101.24		
130	9.15	230	108.65		

110°C 15 secs. U.V. Run 4.					4.4 mg.
t	p	t	p	t	p
20	0.07	120	41.84	220	112.54
30	0.13	130	51.74	230	115.86
40	0.27	140	61.87	240	118.66
50	0.73	150	71.15	250	120.93
60	1.81	160	79.23	260	122.64
70	4.28	170	87.25	280	125.52
80	8.10	180	94.15	300	126.68
90	14.47	190	100.27	p_f	127.20
100	22.42	200	104.99	p_a	127.27
110	31.53	210	109.27		

110°C 30 secs. U.V. Run 5.					4.5 mg.
t	p	t	p	t	p
10	0.01	110	29.15	210	108.59
20	0.01	120	37.59	220	112.83
30	0.06	130	46.76	230	116.08
40	0.23	140	56.15	240	119.36
50	0.82	150	65.19	250	121.58
60	2.14	160	74.02	260	123.81
70	4.49	170	82.96	270	125.50
80	8.71	180	90.48	280	126.63
90	14.13	190	97.33	p_f	127.20
100	20.86	200	103.39	p_a	133.77

110°C 1 min. U.V. Run 6.					4.9 mg.
t	p	t	p	t	p
10	0.04	85	19.91	170	95.70
20	0.09	90	24.29	180	101.05
30	0.15	95	29.36	190	106.36

TABLE 103 cont/.....

TABLE 103 cont.

t	p	t	p	t	p
35	0.29	100	34.34	200	110.63
40	0.54	105	39.21	210	114.80
45	0.96	110	44.48	220	118.51
50	1.63	115	49.86	230	121.73
55	2.70	120	54.83	240	123.91
60	4.14	125	59.37	250	125.55
65	6.25	130	64.29	260	126.65
70	8.80	140	73.22	p_f	127.20
75	11.95	150	81.41	p_a	141.67
80	15.78	160	88.64		

110°C 5 min. U.V. Run 7.					4.5 mg.
t	p	t	p	t	p
10	0.01	65	33.29	140	110.96
20	0.05	70	40.52	150	115.86
25	0.17	75	48.09	160	120.36
30	0.60	80	55.15	170	122.64
35	1.54	85	61.87	180	124.38
40	3.47	90	68.13	190	125.52
45	6.97	100	79.69	200	126.10
50	12.02	110	89.68	210	126.69
55	18.23	120	98.21	p_f	127.20
60	25.46	130	105.52	p_a	127.71

110°C 10 min. U.V. Run 8.					4.6 mg.
t	p	t	p	t	p
10	0.02	55	31.38	150	100.36
20	0.13	60	37.90	160	105.46
25	0.37	65	43.70	170	110.70
30	1.47	70	48.85	180	115.01
35	4.07	75	53.91	190	118.26
38	7.02	80	58.45	200	122.13
40	9.47	90	66.01	210	124.94
42	12.30	100	72.73	220	126.63
44	15.29	110	77.99	p_f	127.20
46	18.40	120	84.35	p_a	133.77
48	21.09	130	89.53		
50	23.96	140	94.85		

TABLE 103 cont/.....

TABLE 103 cont.

110°C 30 min. U.V. Run 9.					4.5 mg.
t	p	t	p	t	p
10	0.05	42	38.87	85	104.33
20	0.25	44	43.43	90	108.51
22	0.54	46	47.87	95	112.24
24	1.03	48	52.18	100	115.49
26	1.94	50	56.66	105	117.67
28	3.61	52	60.54	110	119.88
30	6.30	55	66.19	115	122.11
32	11.02	60	74.26	120	123.80
34	16.86	65	81.87	125	125.50
36	23.19	70	89.85	130	126.64
38	28.33	75	94.72	p_f	127.20
40	33.98	80	99.71	p_a	132.58

TABLE 104.

Dose	Induction period min.	k_5 $cm^{1/3}$ $min.^{-1}$	Inflexion point α_i.
0	100	2.140×10^{-3}	0.50
2 secs.	88	2.740×10^{-3}	0.50
5 "	85	3.850×10^{-3}	0.47
15 "	48	3.890×10^{-3}	0.47
30 "	45	3.85×10^{-3}	0.44
1 min.	42	4.48×10^{-3}	0.39
		k_1 $cm^{1/2}$ $min.^{-1}$	
5 min.	30	4.928×10^{-3}	0.35
10 "	27	6.392×10^{-3}	0.28
30 "	23	1.193×10^{-2}	0.26

(ii) Effect of admitting water vapour onto the salt in an interrupted run.

The procedure adopted in "water interruptions" has been given earlier. Interruptions were performed at five points in the decomposition. The decomposition temperature was 110°C and the time of irradiation was 10 minutes.

The effect of the "water interruptions" is to regenerate a new induction period after each interruption. The rate constant for the subsequent acceleratory period decreases as

the α value/.....

the α value of each interruption increases.

A series of successive interruptions at the end of each regenerated induction period was performed before allowing the decomposition to proceed to completion. The accelera-tory rate was again lower than normal.

The p/t values for these runs are shown in TABLE 105 while FIGURE 84 illustrates them graphically. TABLE 106 gives the acceleratory rate constants, k_5 (equation 10), and the length of the induction periods (min). Run 8 in TABLE 103 was irradiated under identical conditions and serves as a blank, uninterrupted, run for the series.

Final pressures were lower than normal on all these runs. Partial recovery of the lost pressure was obtained by heating the salt to 300°C in vacuo. Pressures are thus not normalised in the following table.

TABLE 105.

110°C 10 min. U.V. Run 1.					4.5. mg.
t	p	t	p	t	p
15	0.13	65	17.35	140	59.45
Water Interruption		70	21.93	150	61.87
30	0.16	75	26.51	160	63.51
35	0.19	80	30.66	190	68.13
40	0.29	90	37.92	210	69.42
45	1.12	100	43.88	240	70.72
50	3.00	110	48.81	260	71.59
55	6.83	120	53.24	p_a	72.03
60	12.38	130	56.36		

110°C 10 min. U.V. Run 2.					4.6 mg.
t	p	t	p	t	p
10	0.07	75	16.08	150	71.15
20	0.17	80	22.18	160	74.69
28	0.60	85	27.86	170	77.85
Water Interruption		90	33.29	180	80.15
40	0.62	95	38.24	190	82.48
50	0.81	100	42.52	200	84.37

TABLE 105 cont/.....

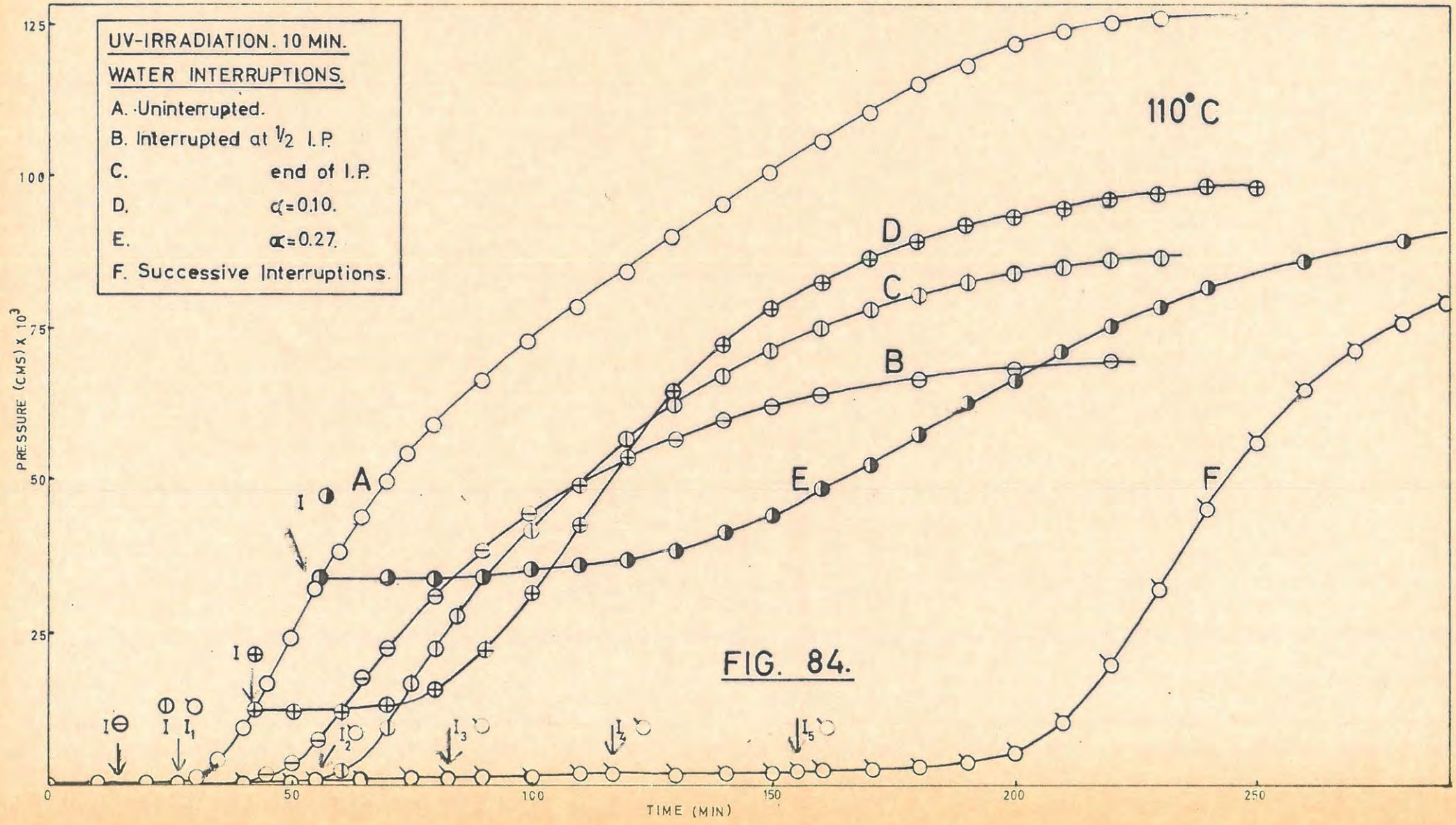
UV-IRRADIATION. 10 MIN.
WATER INTERRUPTIONS.
A. Uninterrupted.
B. Interrupted at 1/2 I.P.
C. end of I.P.
D. α=0.10.
E. α=0.27.
F. Successive Interruptions.
110°C
A
B
C
D
E
F
I
I1
I2
I3
I4
I5
PRESSURE (CMS) X 10³
TIME (MIN)
0
50
100
150
200
250
25
50
75
100
125

FIG. 84.

TABLE 105 cont.

t	p	t	p	t	p
55	1.02	110	50.26	210	85.33
60	2.10	120	56.69	220	86.29
65	4.84	130	62.28	p_a	86.77
70	9.96	140	66.85		

110°C 10 min. U.V. Run 3.					4.5 mg.
t	p	t	p	t	p
10	0.13	80	16.03	150	77.69
20	0.27	85	18.36	160	82.35
30	2.02	90	21.79	170	85.84
35	6.30	95	26.24	180	88.97
38	12.93	100	31.38	190	91.24
Water Interruption 105			36.85	200	93.08
50	12.94	110	42.46	210	94.95
55	12.97	115	47.74	220	96.36
60	13.07	120	53.45	230	97.31
65	13.23	125	58.89	240	97.78
70	13.71	130	63.57	p_a	98.26
75	14.61	140	71.59		

110°C 10 min. U.V. Run 4.					4.0mg.
t	p	t	p	t	p
20	0.39	80	34.09	210	71.18
25	0.52	90	34.32	220	75.07
30	0.97	100	34.81	230	78.73
35	2.17	110	35.83	240	81.62
40	5.79	120	36.72	260	86.76
45	14.47	130	38.62	280	90.20
48	21.21	140	41.13	300	92.95
50	26.25	150	44.35	320	94.95
52	31.24	160	48.56	340	96.99
53	33.89	170	52.79	360	97.50
Water Interruption 180			57.36	p_a	98.23
60	33.92	190	62.03		
70	33.97	200	66.59		

TABLE 105 cont/.....

TABLE 105 cont.

110°C 10 min. U.V. Run 5.					4.5 mg.
t	p	t	p	t	p
20	0.39	Water Interruption		200	71.88
30	2.41	70	63.99	220	73.25
35	7.72	100	64.25	240	74.72
40	20.74	120	65.60	260	75.95
45	36.66	140	67.02	p_a	77.54
50	51.00	160	68.43		
55	63.92	180	70.09		

110°C 10 min. U.V. Run 6.					4.8 mg.
t	p	t	p	t	p
10	0.04	115	2.23	230	32.25
20	0.17	117	2.41	235	39.05
25	0.50	Water Interruption		240	45.19
26	0.62	140	2.43	245	51.10
Water Interruption 150			2.65	250	56.25
35	0.63	155	3.01	260	64.88
45	0.65	Water Interruption		270	71.14
50	0.77	170	3.02	280	75.48
55	1.22	180	3.11	290	79.04
Water Interruption 185			3.28	300	82.24
70	1.24	190	3.61	310	84.09
75	1.30	200	5.42	320	85.96
80	1.52	205	7.29	330	86.91
83	1.81	210	10.25	340	87.86
Water Interruption 215			14.15	350	88.82
100	1.82	220	19.30	360	89.30
110	1.94	225.	25.43	p_a	89.78

TABLE 106.

Point of Interruption.	k_5 $cm^{1/3}$ $min.^{-1}$	Induction period min.	Number of Interruption.	Induction period, minutes.
Uninterrupted	9.65×10^{-3}	28	0	26
1/2 along I.P.	8.30×10^{-3}	28	1	29
End of I.P.	8.25×10^{-3}	27	2	28
$\alpha = 0.10$	5.90×10^{-3}	30	3	34
$\alpha = 0.27$	2.52×10^{-3}	42	4	38
$\alpha = 0.50$	1.30×10^{-3}	50	5	35
5 consecutive	5.80×10^{-3}	35		

(iii) Mathematical analysis of the results.

The acceleratory period is described by the power law with n = 3 for low irradiation doses i.e.

$$p^{1/3} = k_5 t + c_5 \quad \ldots\ldots\ldots\ldots\ldots\ldots\ldots\ldots\ldots\ldots (10)$$

This equation is valid for irradiation times of up to one minute.

The value of n decreases from 3 to 2 with heavier doses (5 min. and more). The equation thus becomes,

$$p^{1/2} = k_1 t + c_1 \quad \ldots\ldots\ldots\ldots\ldots\ldots\ldots\ldots\ldots\ldots (1)$$

The contracting sphere formula is applicable to the decay period irrespective of the dose.

$$(1 - p/p_f)^{1/3} = k_7 t + c_7 \quad \ldots\ldots\ldots\ldots\ldots\ldots\ldots\ldots (2)$$

FIGURE 85 shows the p/t plot for the thermal decomposition after a low dose of ultra-violet light together with the analysis. FIGURE 86 gives the same results for a heavy dose.

Analysis of the acceleratory period produced after a "water interruption" shows that for all points of interruption the integer n charges back to 3 from 2 as a result of this procedure.

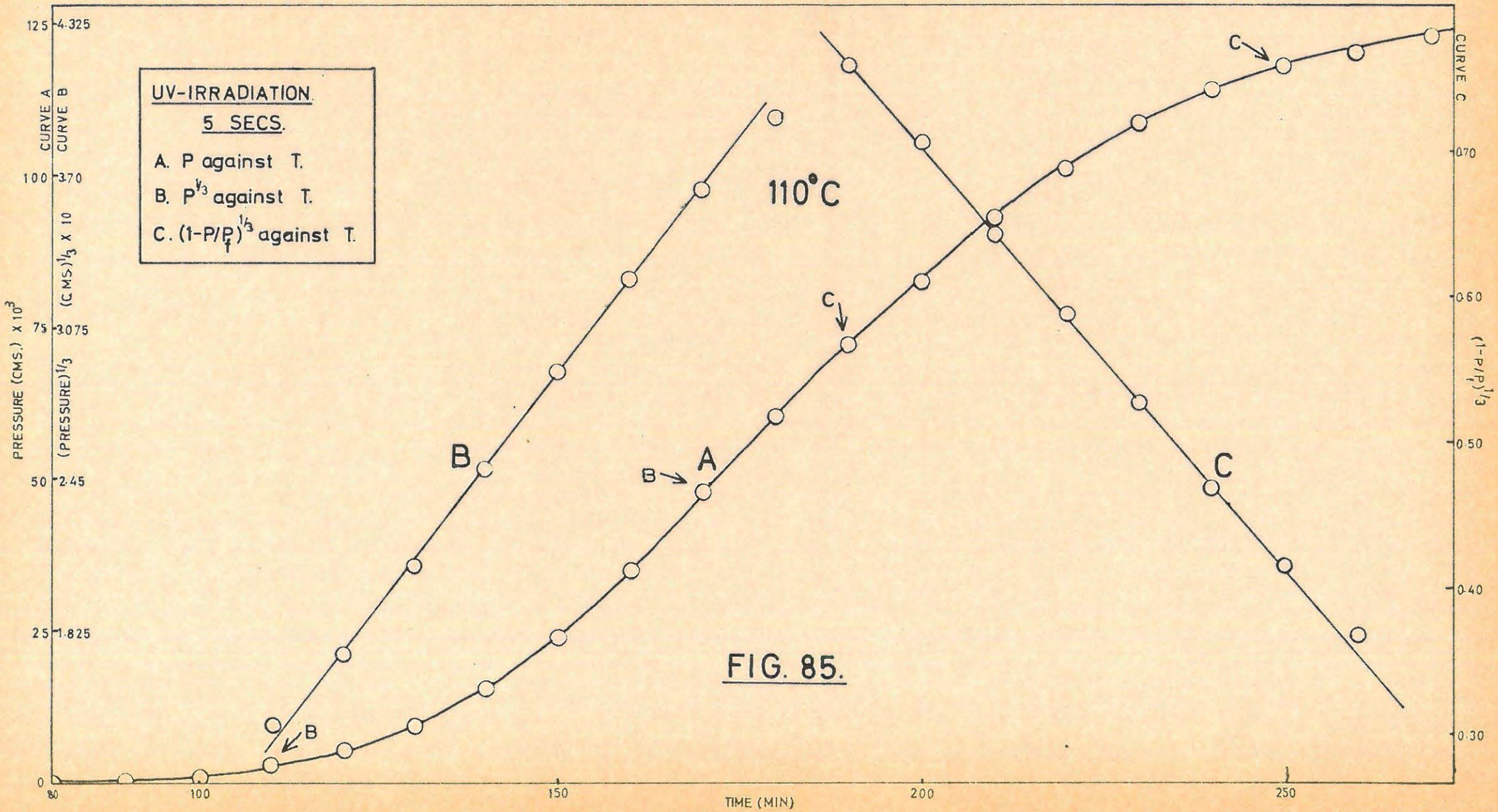
UV-IRRADIATION.
5 SECS.
A. P against T.
B. P^1/3 against T.
C. (1-P/P_f)^1/3 against T.
110°C
A
B
C
PRESSURE (CMS.) X 10^3
CURVE A
CURVE B
(PRESSURE)^1/3
(C MS)^1/3 X 10
CURVE C
(1-P/P_f)^1/3
TIME (MIN)
125
100
75
50
25
0
4.325
3.70
3.075
2.45
1.825
0.70
0.60
0.50
0.40
0.30
80
100
150
200
250

FIG. 85.

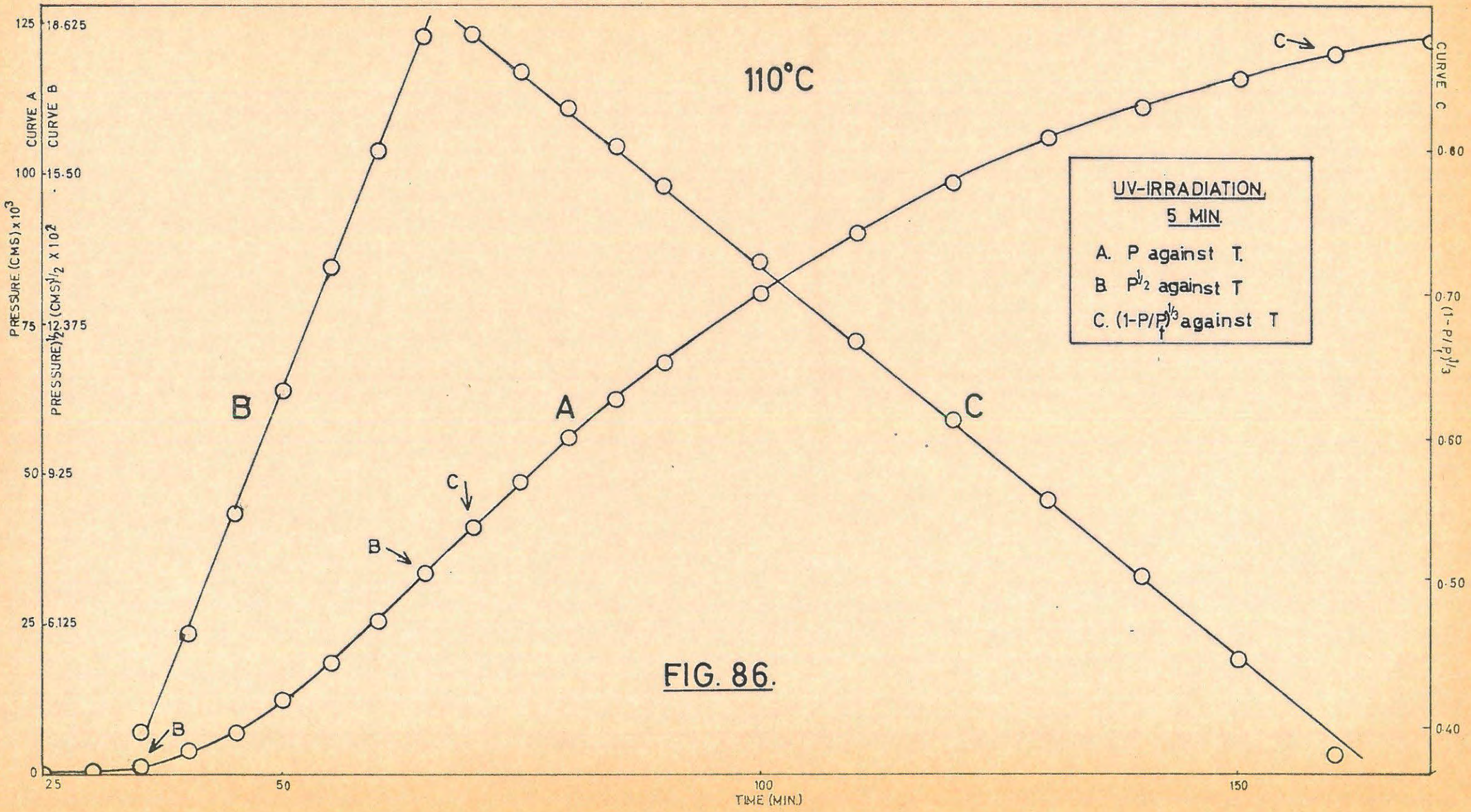
110°C
UV-IRRADIATION,
5 MIN.
A. P against T.
B $P^{1/2}$ against T
C. $(1-P/P_i)^{1/3}$ against T
PRESSURE (CMS) x 10^3
CURVE A
CURVE B
$(PRESSURE)^{1/2}$ X 10^2
CURVE C
$(1-P/P_i)^{1/3}$
TIME (MIN.)
125
100
75
50
25
0
18.625
15.50
12.375
9.25
6.125
0.60
0.70
0.60
0.50
0.40
25
50
100
150
A
B
C

FIG. 86.

8.2. DISCUSSION.

8.2.1. Unirradiated Calcium Azide.

The activation energies for the thermal decomposition of calcium azide which had been annealed after storage for one year in vacuo were, within experimental error, the same as those for the freshly prepared salt[116] - in particular there was no reduction in the value for the acceleratory period as found by Tompkins and Young.[176] It was not possible to remove the discrepancy between the activation energies for the induction period (or decay period) and the acceleratory period. This applied to split runs and individual runs. In addition split runs with freshly prepared salt still did not reduce the energy for the acceleratory period to 18 kcal.mole^{-1}. Tompkins and Young report that with the calcium azide used by them such experimental procedures gave only one value for the activation energy for the acceleratory period, namely 18 kcal.mole^{-1}. It can only be suggested that the reason for the "ageing" phenomen is connected with their method of preparation in that the salt was precipitated from a saturated aqueous solution by the addition of absolute alcohol followed by cooling to -10^{o}C, whereas the specimens used in this work were crystallized from conductance water at 25^{o}C. Work is in progress to determine the effect of different modes of preparation on the kinetics of decomposition.

Thomas and Young[176] also state that the absolute value of the acceleratory rate constant in a split run is dependent upon the initial temperature at which the run is commenced. The higher the initial temperature the greater the rate constant (FIGURE 5 paper). The work done here indicates that with unground material the values obtained for the rate constants are not reproducible enough to substantiate this statement.

8.2.2. Preirradiated/.....

8.2.2. Preirradiated (Ultra-Violet Light) Calcium Azide.

The additional work carried out on the effect of preirradiation by ultra-violet light on the subsequent thermal decomposition showed that calcium azide behaves in an analogous manner to strontium azide, which is to be expected since the two salts resemble each other in most of the effects which have been studied. The same interpretation of the results can thus be applied (Cf. strontium azide discussion).

9. COMPARISON TABLE OF AZIDE RESULTS.

TABLE 107.

UNIRRADIATED AZIDES.			
	Calcium Azide A.W. Ca 40.08.	Strontium Azide A.W. Sr 87.6	Barium Azide A.W. Ba 137.4
Kinetic equations	Acceleratory period; power law, $p^{1/3} = k_5 t + c_5$ Decay period; contracting sphere, $(1-p/p_f)^{1/3} = k_7 t + c_7$	Acceleratory period; power law $p^{1/3} = k_5 t + c_5$ Decay period; contracting sphere, $(1-p/p_f)^{1/3} = k_7 t + c_7$	Acceleratory period; Avrami-Erofeyev equation, $\left[-\log(1-\frac{p-p_o}{p_f-p_o})\right]^{1/4} = k_3 t + c_3$ Decay period; contracting sphere, $(1-p/p_f)^{1/3} = k_7 t + c_7$
Activation energies kcal.mole^{-1}	Induction period: 18.2 Acceleratory period: 27.1 Decay period:18.8	Induction period: 23.3 Acceleratory period: 25.0 Decay period: 21.7	Induction period: 26.5 Acceleratory period: 26.8 Decay period: 26.1
Type of nuclei	2-dimensional increasing in number linearly with time. Supported by "water interruptions".	2-dimensional increasing in number linearly with time. Supported by "water interruptions".	3-dimensional increasing in number linearly with time. Marked overlap and ingestion of nuclei.

TABLE 107/.....

TABLE 107 cont.

	Calcium Azide	Strontium Azide	Barium Azide.
"Water interruptions" (i) Various stages.	Induction period repeated. k_5 constant but lower than k_5 uninterrupted. Initial decomposition of favoured centres.	Induction period repeated. k_5 approximately the same along I.P. then a gradual decrease with increasing α.	Induction period repeated. k_3 decreases as α increases.
(ii) Successive	Induction period $\sim t_i$ k_5 lower than normal.	Induction period repeated and $\sim t_i$. k_5 only slightly lower normal.	Induction period $\sim t_i$. k_3 lower than normal.
Mechanism (i) Nuclear formation.	Slow surface decomposition to give Ca atoms. Nuclei formed by crystallization at end of induction period. Activation energy that for $N_3^- + N_3^- \rightarrow 3N_2 + 2e^-$. Slow evolution of nitrogen over induction period.	As for Calcium Azide.	As for Calcium Azide.
		True induction period.	True induction period.
(ii) Nuclear growth over acceleratory period.	N_3^- + metal $\rightarrow N_3$ (electron in condution band of metal) $N_3 + N_3^-$ (strained) $\rightarrow 3N_2 + F + \square$	As for Calcium Azide.	As for Calcium Azide.

TABLE 107 cont/.....

TABLE 107 cont.

	Calcium Azide	Strontium Azide	Barium Azide.
(ii) Nuclear growth over acceleratory period.	$F + F \rightarrow \square\square + 2e^-$ $2e^- + Ca^{++} \rightarrow Ca$ The Ca adds on to interface	As for calcium azide	As for calcium azide.
(iii) Reaction in decay.	$N_3^- + N_3^-$ (strained) $\rightarrow 3N_2$ Due to compressive action of metal or to pressure of trapped N_2. Activation energy same as that for induction period.	As for calcium azide, or could be as for barium azide but not likely as nuclei are 2-dimensional and there is no inward growth during the acceleratory period.	Could be as for calcium azide or a continuation of (ii). Likely to be latter because of <u>inward</u> growth of 3-dimensional nuclei.
Decomposition reaction.	$CaN_6 \rightarrow Ca + 3N_2$	$SrN_6 \rightarrow Sr + 3N_2$	$BaN_6 \rightarrow Ba + 3N_2$
Inflexion point α_i	0.42	0.40	0.62
% Decomposition	93.4%	71.2%	93.0%
Ageing	No ageing effect after 1 year.	As for calcium azide.	As for calcium azide.
IRRADIATED (γ-RAYS) AZIDES.			
Characteristics	No colour change at 8 Mrad. No F-centres? Probably vacancies.	No colour change at 10 Mrad. No F-centres? Probably vacancies.	Buff colour at 10 Mrad. Probably F-centres formed.

TABLE 107 cont/.....

TABLE 107 cont.

	Calcium Azide	Strontium Azide	Barium Azide.
Varying dose.	Induction period decreases. Acceleratory and decay period rate constants, k_5 and k_7, increase but constant after 40,000 rad. No change in α_i.	Induction period decreases. Acceleratory period rate constants, k_5 and k_2, and decay rate constant, k_7 increase. No change in α_i.	Induction period decreases. Acceleratory and decay period rate constants, k_3 and k_7, increase. α_i decreases.
Kinetic equations.	Acceleratory period; power law, $p^{1/3} = k_5 t + c_5$ Decay period; contracting sphere, $(1-{}^{p}/_{p_f})^{1/3} = k_7 t + c_7$	Acceleratory period; power law up to 50,000 rad, $p^{1/3} = k_5 t + c_5$ Exponential law from 250,000 rad. $\log p = k_2 t + c_2$ Decay period; contracting sphere, $(1-{}^{p}/_{p_f})^{1/3} = k_7 t + c_7$	Acceleratory period; Avrami-Erofeyev equation, $\left[-\log(1-\frac{p-p_o}{p_f-p_o})\right]^{1/4} = k_3 t + c_3$ Decay period; contracting sphere, $(1-{}^{p}/_{p_f})^{1/3} = k_7 t + c_7$
Activation energies kcal.mole^{-1}	8.0 Mrad. Induction period: 19.8. Acceleratory period: 28.1 Decay period: 22.5 i.e. no change from unirradiated.	2.0 Mrad (log p plots). Induction period: 24.7 Acceleratory period: 24.0 Decay period: 20.1 i.e. no change from unirradiated.	0.5 Mrad. Induction period: 21.9 Acceleratory period: 27.0 Decay period: 28.4 4.0 Mrad. Induction period: 20.6 Acceleratory period: 26.8 Decay period: 27.5 Slight decrease in induction period value.

TABLE 107 cont/....

TABLE 107 cont.

	Calcium Azide	Strontium Azide	Barium Azide
Type of nuclei	Internal and external 2-dimensional nuclei increasing linearly with time. This supported by "water interruptions".	Up to 50,000 rad, as for calcium azide. Above 250,000 rad plate-like nuclei growing over grain boundaries after branching along dislocations.	External 3-dimensional nuclei increasing linearly with time. Overlap and ingestion marked.
Nuclear formation	Vacancies aggregating at internal and external surfaces to give strained N_3^- ions which decompose as in unirradiated material. Support from unchanged activation energy.	As for calcium azide.	Aggregation of F-centres which collapse to give Ba atoms. Ba atoms migrate to the surface to form nuclei. Activation energy is that for migration.
Nuclear growth in acceleratory and decay periods.	As for unirradiated.	As for unirradiated.	As for unirradiated.
"Water interruptions" (i) Various stages	Induction period decreases and k_5 decreases slightly. Large reservoir of vacancies and formation of traps.	Induction period decreases, k_2 increases at low α values, then decreases. Large reservoir and traps also.	Induction period increases, k_3 decreases.

TABLE 107 cont/.....

TABLE 107

	Calcium Azide	Strontium Azide	Barium Azide
"Water interruptions". (ii) Successive.	Induction period steadily reduced and k_5 slightly less than normal. p_a 30% of normal p_f. 44% of normal on strong heating (nitride formation).	Steady decrease in induction period and explosion after 6th interruption (10 Mrad, 95°C). Destroyed nuclei act as vacancy traps, self heating gives explosion. No explosion after 7 interruptions due to depletion of vacancy reservoir. At 100°C explosion after 2 interruptions.	Induction period markedly longer and k_3 reduced. p_a 53% of normal p_f but recovery on strong heating. Gradual depletion of F-centres.
Annealing	50°C, 1 hr. No effect.	70°C, 3 hrs. No effect.	70°C, 2 hrs. No effect.
Ageing	Nil	Nil	Nil
Interruption and irradiation.	Irradiation effect found throughout, including decay, despite water vapour reacting on salt.	As for calcium azide.	As for calcium Azide.
% Decomposition	93.4%	97.6%	93.0%
IRRADIATED (X-RAYS) AZIDES.			
Varying dose	Induction period decreases. Acceleratory and decay rate constants increase.	As for calcium azide.	

TABLE 107 cont/.....

TABLE 107

	Calcium Azide	Strontium Azide	Barium Azide.
Kinetic equations	Acceleratory period; power law, $p^{1/3} = k_5 t + c_5$ Decay period; contracting sphere $(1-{}^{p}/_{p_f})^{1/3} = k_7 t + c_7$	Acceleratory period; power law up to 30 min. $p^{1/3} = k_5 t + c_5$ Above 30 min. Avrami-Erofeyev equation $\left[-\log(1-\frac{p-p_o}{p_f-p_o})\right]^{1/3} = k_6 t + c_6$ Decay period; contracting sphere, $(1-{}^{p}/_{p_f})^{1/3} = k_7 t + c_7$	
Activation energies kcal.mole^{-1}	Induction period: 19.2 Acceleratory period: 27.1 Decay period: 21.9	Induction period: 22.7 Acceleratory period: 26.5 Decay period: 24.0	
Type of nuclei	2-dimensional increasing linearly with time. Internal and external as shown by increase in k_7.	As for calcium azide but with considerable overlap and ingestion at high doses.	
Reaction mechanism	As for γ-rays.	As for γ-rays.	
α_i	No change with increasing dose.	No change with increasing dose.	

TABLE 107

	Calcium Azide	Strontium Azide	Barium Azide.
Water interruptions (i) At various stages.	Small decrease in induction period at small α values. k_5 lower than normal.	As for calcium azide. Kinetic equation reverts back to power law.	
(ii) Successive	As for (i) above. Final k_5 value lower than normal.	As for calcium azide.	
Interruption and irradiation		Effect obtained at all stages, including decay. Indicitive of internal nuclei.	
% Decomposition	93.4%	87.4%	
IRRADIATED (ULTRA-VIOLET LIGHT) AZIDES.			
Varying dose.	Decrease in induction period, and increase in acceleratory rate constants as dose increases. α_1 decreases markedly with increasing dose.	As for calcium azide.	As for calcium azide.
Kinetic equations.	Acceleratory period; power law. Low doses, up to 1 min $n = 3$ i.e. $p^{1/3} = k_5 t + c_5$	Acceleratory period; power law Low doses, up to 10 secs. $n = 3$ i.e. $p^{1/3} = k_5 t + c_5$	Acceleratory period; Avrami-Erofeyev equation with $n = 6$ $\left[-\log(1-\frac{p-p_o}{p_f-p_o})\right]^{1/6} = k_4 t + c_4$

TABLE 107 cont/.....

TABLE 107

	Calcium Azide	Strontium Azide	Barium Azide
Kinetic equations	High doses n = 2 i.e. $p^{1/2} = k_1 t + c_1$ Decay period; contracting sphere, $(1-{}^{p}/_{p_f})^{1/3} = k_7 t + c_7$	High doses n = 2 i.e. $p^{1/2} = k_1 t + c_1$ Decay period, contracting sphere, $(1-{}^{p}/_{p_f})^{1/3} = k_7 t + c_7$	Decay period; contracting sphere, $(1-{}^{p}/_{p_f})^{1/3} = k_7 t + c_7$
Activation energies, kcal.mole^{-1}.	From $p^{1/2}$ vs. t Induction period; 16.2 Acceleratory period; 27.4 Decay period; 25.7	From $p^{1/2}$ vs. t Induction period; 19.5 Acceleratory period; 23.0 Decay period; 25.7	Induction period 23.1 Acceleratory period; 27.7 Decay period; 25.0
Type of nuclei	Surface 2-dimensional nuclei increasing linearly with time, but as dose increases 2-dimensional from a fixed number of centres.	As for calcium azide.	Surface nuclei growing 3-dimensionally and increasing as the third power of time.
"Water interruptions". (i) At various stages.	Induction period approximately constant. Gradual decrease in acceleratory period rate constant. Equation changes from n = 2 to n = 3 for interruptions beyond end of induction period.	As for calcium azide.	Increase in duration of induction period and decrease in acceleratory rate constant. Equation changes from n = 6 to n = 4.

TABLE 107 cont/.....

TABLE 107.

	Calcium Azide	Strontium Azide	Barium Azide
"Water interruptions". (ii) Successive.	Slight increase in induction period and decrease in accelerator rate constant. Equation changes as in (i).	As for calcium azide.	Marked increase in induction period. Decrease in accelerator rate constant. Change of equation as in (i)
Mechanism	With a heavy dose get a large number of nuclei at end of induction period and growth swamps formation. Hence $p^{1/2}$. Mechanism as for γ-rays. On repeated "water interruption" anion vacancy reservoir depleted and $p^{1/3}$ holds.	As for calcium azide.	As for γ-rays.
Interruption and irradiation.		Irradiation only effective at low α values where effect can be felt before complete surface coverage occurs.	As for strontium azide.
Ageing	Nil	Nil	Nil
% Decomposition	93.4%	87.3%	93.0%

10. GENERAL DISCUSSION/.....

10. GENERAL DISCUSSION OF THE DECOMPOSITION OF THE ALKALINE EARTH AZIDES.

The most significant results and conclusions for the decomposition of the azides have been collected together in TABLE 107. Some of these are discussed below.

10.1. Unirradiated Azides.

The azides resemble each other in that the general form of the p/t plots for the isothermal decomposition are the same. The postulated processes occurring during the induction period are similar and are concerned with a slow surface decomposition at favoured sites on the surface of the solid. During the acceleratory period in the decomposition of calcium and strontium azides the nuclei grow two-dimensionally, whereas with barium azide the growth is three-dimensional. In all cases the nuclei increase in number linearly with time. The same mechanism for growth has been postulated for all the azides and this is supported by the fact that the activation energies during the acceleratory period are similar, calcium azide 27.1 kcal.mole^{-1}, strontium azide, 25.0 kcal.mole^{-1}, and barium azide, 26.8 kcal. mole^{-1}.

The decay mechanism for calcium azide is considered to be different from that for barium azide because the activation energy for this period is different from that for the corresponding acceleratory period. In the case of barium azide the same mechanism is considered to apply to both the acceleratory and decay periods. For calcium azide it is considered that in the decay the metal sheath around the azide particle will exert compressive stresses on the lattice. Distortion of adjacent azide ions at the reactant/product interface will be at a maximum and the azide ions would interact in this region of stress. The reaction would thus be the same one as occurs in the induction period in agreement with the activation energies. Alternatively stress could also be produced at the interface by

pockets of/.....

pockets of trapped nitrogen at high pressure.

It is possible that a mechanism similar to that postulated for calcium azide may apply to the decay reaction for strontium azide where, although the activation energy for the decay reaction is not very different from that for the acceleratory period, the nuclei grow two-dimensionally over the acceleratory period. The two-dimensional growth, of course, means that during this spreading surface reaction there is no tendency for reaction to penetrate inwards from the interface and consequently when the decay stage commences a different mechanism may operate as with calcium azide. The surface nuclei in the decomposition of barium azide grow three-dimensionally during the acceleratory period so that it is reasonable to propose the same reaction mechanism in the decay stage as in the acceleratory stage.

The three azides also resemble one another in that there is no age effect.

10.2. Irradiation by γ-rays.

The relative sensitivity of the azides to preirradiation by γ-rays is indicated in the following table which expresses the percentage change in the rate constants and induction periods for irradiated salt as compared to the corresponding values for unirradiated salt i.e. the percentages are obtained from the formula

$$\% \text{ Charge} = \frac{\text{Irradiated value}}{\text{Unirradiated value}} \times \frac{100}{1}$$

Azide	Percentage change.		
	Induction period	Acceleratory period	Decay period
Strontium	8.07	3153.0	3678.0
Calcium	15.2	1750.0	379.0
Barium	28.0	455.0	586.0

The γ-ray/.....

The γ-ray dose was 0.25 Mrad in all cases. Strontium azide is quite obviously the most sensitive with barium azide the least sensitive. The effects on the subsequent thermal decomposition are very similar for all the azides and any differences are explicable, either on the type of nucleus (2 or 3 dimensional) or on the sensitivity to γ-rays, e.g. the explosive runs with strontium azide after treatment with water vapour. The nucleation process during the decomposition of irradiated barium azide is considered to be different from the same process with irradiated strontium and calcium azides in that the concept of F-centres, which aggregate and collapse internally, is invoked for the former. With the latter two substances the migration of vacancies is considered to be an essential step in the nucleation process.

The greater sensitivity of strontium to γ-rays is shown by the fact that the nature of the course of decomposition is altered with doses greater than 250,000 rad in that the exponential law describes the p/t plot for the acceleratory period. In addition, in the runs with water vapour, it is possible, under suitable conditions to bring about an explosive reaction.

No measurable evolution of gas occurred during preirradiation of all the azides and the irradiation effect was permanent for at least one year.

10.3. Irradiation by X-rays.

The effects of preirradiation by X-rays were very similar for the two azides studied. X-ray effects were not studied for barium azide but work is in progress to make a detailed study of these effects which, from the work of Erofeyev and Sviridov[114] are complex.

10.4. Irradiation by Ultra-Violet Light.

Barium azide is far less sensitive to preirradiation by ultra-violet light than either calcium or strontium azide.

This relative/.....

This relative insensitivity was also found for preirradiation by γ-rays. The irradiation effect appears to be confined to the surface of the particle for all three azides and the effects are similar for all three except that the type of nuclei differ. Three-dimensional nuclei are present in the decomposition of barium azide whereas with calcium and strontium azides the nuclei grow two-dimensionally. The increase in number of nuclei with time alters with heavy doses for calcium and strontium azides - reaction appears to proceed from a fixed number of centres. The normal linear increase in the number of nuclei with time is, however, restored after treatment with water vapour. In the case of barium azide the rate of increase of number of nuclei is different from that for the decomposition of unirradiated salt for all doses with ultra-violet light. The number of nuclei increases as the cube of the time for the irradiated specimen, which is the value found previously by Wischin[3] for the decomposition of unirradiated "single" crystals. The linear rate is again restored on treatment with water vapour.

11. SUMMARY/.....

11. SUMMARY.

The rate of thermal decomposition of mercuric oxalate is increased by irradiation with γ-rays. The effects of the irradiation are similar to those for nickel oxalate in that an unstable intermediate is produced which decomposes faster than the parent substance on heating. This initial decomposition affects the subsequent reaction. Thus, although nickel oxalate is insensitive to ultra-violet light, and mercuric oxalate is sensitive, both react similarly to γ-rays.

The alkaline earth azides, however, are affected by pre-irradiation by γ-rays in a different manner, namely the acceleration of the reaction occurs as a result of point defects created in the solid by the radiation. The three alkaline earth azides behave in an essentially similar manner when pre-irradiated by ultra-violet light, X-rays or γ-rays. Mercuric oxalate, however, is affected differently by X-rays than by ultra-violet light or γ-rays.

12. BIBLIOGRAPHY/.....

12. BIBLIOGRAPHY.

(1) Harvey, Trans. Faraday Soc., 29, 653 (1933).

(2) Garner and Hailes, Proc. Roy.Soc., A 139, 576 (1933).

(3) Wischin, Proc. Roy. Soc., A 172, 314 (1939).

(4) Bright and Garner, J.C.S., 1872 (1934).

(5) Garner and Tanner, J.C.S., 47 (1930).

(6) Garner and Maggs, Proc. Roy. Soc., A 172, 299 (1939).

(7) Boldyrev and Skorik, Fiz. Shchelochnogaliodnykh Kristallov, Riga, 527 (1961).

(8) Prout, J. Inorg. Nucl. Chem., 7, 368 (1958).

(9) Groocock and Tompkins, Proc. Roy. Soc., A 223, 267 (1954).

(10) Jach, Trans. Faraday Soc., 59, 947 (1963).

(11) Herley, Ph.D. Thesis, Rhodes Univ. (1961).

(12) Prout and Tompkins, Trans. Faraday Soc., 43, 148 (1947).

(13) Hailes, Trans. Faraday Soc., 29, 544 (1933).

(14) Garner and Gomm, J.C.S., 2123 (1931).

(15) Garner and Marke, J.C.S., 657 (1936).

(16) Garner and Haycock, Proc. Roy. Soc., A 211, 335 (1952).

(17) Mott and Gurney, Proc. Roy. Soc., A 164, 151 (1938).

(18) Cooper and Garner, Trans. Faraday Soc., 32, 1739 (1936).

(19) Bagdassarian, Acta. phys.-chim. U.R.R.S., 20, 441 (1945).

(20) Garner and Southam, J.C.S., 1705 (1935).

(21) Jacobs and Tompkins, Chemistry of the Solid State, Ed. Garner, 185 (Butterworths 1955).

(22) Tompkins and Young, Unpublished work.

(23) Bartlett and Tompkins, Unpublished work.

(24) Fischbeck and Spengler, Z. Anorg. Chem., 241, 209 (1939).

(25) Garner and Hailes, Proc. Roy. Soc., A 139, 576 (1933).

(26) McDonald, J.C.S. 839 (1936).

(27) Finch, Jacobs and Tompkins, J.C.S. 2053 (1954).

(28) Prout and Tompkins, Trans. Faraday Soc., 40, 488 (1944).

(29) Bircumshaw and Harris, J.C.S. 1898 (1948).

(30) Bircumshaw and Edwards, J.C.S., 1800 (1950).

(31) Glasner and Steinberg, J. Inorg. Nucl. Chem., 16, 279 (1961).

(32)/.....

(32) Prout and Tompkins, Trans. Faraday Soc., 42, 482 (1946).

(33) McDonald, Trans. Faraday Soc., 34, 977 (1938).

(34) Hill, Trans. Faraday Soc., 54, 685 (1958).

(35) Avrami, J. Chem. Phys., 7, 1103 (1939);
8, 212 (1940); 9, 177 (1941).

(36) Erofeyev, C.R. Acad. Sci. U.R.S.S., 52, 511 (1946).

(37) Fergusson, Phys. Rev., 66, 220 (1944).

(38) Mott. Trans. Faraday Soc., 34, 500 (1938).

(39) Frenkel, Phys. Rev., 37, 17, 276 (1931).

(40) Seitz, Rev. Mod. Phys., 18, 384 (1946); 26, 17 (1954).

(41) Pohl, Proc. Phys. Soc. Lond., 49, (1937), extra part 3.

(42) De Boer, Rec. Trav. Chim. Pays-Bas., 56, 301 (1937).

(43) Mollwo, Ann. Phys. Lpz., 29, 394 (1937).

(44) Hilsch and Pohl, Z. Physik, 64, 606 (1930).

(45) Lehfeldt, Gottinger Nachr., 1, 170 (1935).

(46) Sheppard, Photo. J., 65, 380 (1925).

(47) Sheppard and Hudson, J. Amer. Chem. Soc., 49, 1814 (1927).

(48) Anastasevich and Frenkel, J. Expr. and Theor. Phys. U.S.S.R., 11, 127 (1941).

(49) Mitchell, Phil. Mag., 40, 249 (1949).

(50) Stasiw and Teltow, Gottinger Nachr., 93, 100, 110 (1941).

(51) Stasiw and Teltow, Ann. d. Physik., (5) 40, 181 (1941).

(52) Stasiw and Teltow, Gottinger Nachr., 155 (1947)

(53) Stasiw and Teltow, Ann. d. Physik., (6) 1, 261 (1947).

(54) Stasiw and Teltow, Z. Anorg. Chem., 257, 103, 109 (1948).

(55) Mitchell, Chemistry of the Solid State, Ed. Garner, 231 (Butterworths 1955).

(56) Grimly and Mott, Disc. Faraday Soc., 1, 183 (1947).

(57) Mott, Proc. Roy. Soc., A 172, 325 (1939).

(58) Thomas and Tompkins, Proc. Roy. Soc., A 209, 550 (1951).

(59) Thomas and Tompkins, J. Chem. Phys., 20, 662 (1952).

(60) Thomas and Tompkins, Proc. Roy. Soc., A 210, 111 (1951).

(61) Jacobs and Tompkins, Proc. Roy. Soc., A 215, 254 (1952).

(62) Jacobs and Tompkins, Proc. Roy Soc., A 215, 265 (1952).

(63)/.....

(63) Jacobs, Tompkins and Young, Disc. Faraday Soc., 28, 234 (1959).

(64) Jacobs, Tompkins and Verneker, J.Phys. Chem., 66, 1113 (1962).

(65) Dodds, J. Chem. Phys., 35, 1815 (1961).

(66) Garner and Reeves, Trans. Faraday Soc., 51, 694 (1955).

(67) Meiler and Noyes, J.Amer. Chem. Soc., 52, 527 (1930).

(68) Miller and Brous, J. Chem. Phys. 1, 482 (1933).

(69) Jacobs, J. Appl. Phys., 17, 596 (1946).

(70) Jacobs and Dobischek, Phys. Rev., 81, 1019 (1951).

(71) Seitz and Koehler, J. Proc. Intern. Conf. on Peaceful Uses of Atomic Energy, 7, 615 (1955).

(72) Eggen, Unpublished work.

(73) Eggen and Laubenstein, Phys. Rev., 91, 238 (1955).

(74) Huntington, Phys. Rev., 93, 1414 (1954).

(75) Kohn, Phys. Rev., 91, 1092 (1953).

(76) Kinchin and Pease, Rept. Prog. in Phys., 18, 1 (1959).

(77) Snyder and Neufeld, Phys. Rev., 97, 1636 (1955); 99, 1326 (1955); 103, 862 (1956).

(78) Harrison and Seitz, Phys. Rev., 98, 1530 (1955) A.

(79) Sampson, Hurwitz and Clancy, Phys. Rev., 99, 1657 (1955)A.

(80) Bruch, McHugh and Hochenberg, J. Metals, 8, 1362 (1956).

(81) Seitz, Solid State Physics (Acad.Press), 2, 307 (1956).

(82) Brinkman, J. Appl. Phys., 25, 961 (1954).

(83) Brinkman, Amer. J. Phys., 24, 246 (1956).

(84) Keating, Phys. Rev., 97, 832 (1955).

(85) Lambert and Guinier, Action des Rayonnements de Grande Energie sur les Solides, (ed Cauchios), Gauthier-Villars Paris (1956).

(86) Gibson, Goland, Milgram and Vineyard, Phys. Rev., 120, 1229 (1960).

(87) Vineyard, Disc. Faraday Soc., 31, 7 (1961).

(88)/.....

(88) Vineyard, Radiation Damage in Solids, Ed. Billington, 291 (Acad. Press 1962).

(89) Dienes, Reactivity of Solids, Ed. De Boer, 416 (Elsevier 1960).

(90) Erginsoy, A.S.T.M. Spec. Tech. Publ. No. 359, 79 (1963).

(91) Dugdale, Proc. Bristol Conf. Phys. Soc. London, 246 (1955).

(92) Cleland, Crawford and Holmes, Phys. Rev. 102, 722 (1956).

(93) Seitz, Rev. Mod. Phys. 26, 1 (1954).

(94) Varley, Nature, 174, 886 (1954).

(95) Varley, J. Nucl. Energy, 1, 130 (1954).

(96) Varley, Prog. in Nucl. Energy, 1, Chapter 8, (Pergamon Press 1956).

(97) Mitchell, Wiegand and Smoluchowski, Phys. Rev., 122, 1406 (1961).

(98) Howard, Vosko and Smoluchowski, Phys. Rev., 117, 442 (1960).

(99) Smoluchowski and Wiegand, Disc. Faraday Soc., 31, 151 (1961).

(100) Durup and Platzman, Disc. Faraday Soc., 31, 156 (1961).

(101) Bethe and Ashkin, Expt. Nucl. Phys., Ed Segrè, 1, 166 (Wiley 1953).

(102) Burhop, The Auger Effect, (C.U.P. 1952).

(103) Garner and Moon, J.C.S., 1398 (1933).

(104) Muraour, Chim. et Ind., 30, 39 (1933).

(105) Maggs. Trans. Faraday Soc., 35, 433 (1939).

(106) Bowden and Singh, Proc. Roy. Soc., A 227, 22 (1954).

(107) Flanagan, J. Phys. Chem., 66, 416 (1962).

(108) Flanagan, Trans. Faraday Soc. 57, 797 (1961).

(109) Groocock, Proc. Roy. Soc., A 246, 225 (1958).

(110) Hall and Walton, J. Inorg. Nucl. Chem., 6, 288 (1958).

(111) Cunningham, J. Phys. Chem., 65, 628 (1961).

(112) Johnson, J. Amer. Chem. Soc., 80, 4460 (1958).

(113) Cunningham and Heal, Trans. Faraday Soc., 54, 1355 (1958).

(114)/.....

(114) Erofeyev and Sviridov, Institut Khimi A.N. BSSR. Sbnorik nauch rabot no. 5(i), 113 (1956).

(115) Prout and Brown, Nature, 205, 1314 (1965).

(116) Prout and Brown, Unpublished work.

(117) Freeman and Anderson, J. Phys. Chem., 63, 1344 (1959).

(118) Freeman, Anderson and Campisi, J. Phys. Chem., 64, 1727 (1960).

(119) Freeman and Anderson, J. Phys. Chem., 65, 1662 (1961).

(120) Zirkind and Freeman, Nature, 199, 1280 (1963).

(121) Hyde and Freeman, J. Phys. Chem. 65, 1636 (1961).

(122) Cole, J. Chem. Phys., 35, 1169 (1961).

(123) Cassel and Liebman, J. Chem. Phys., 34, 343 (1961).

(124) Anderson and Freeman, A.S.T.M. Spec. Tech. Publ. No. 359, 58 (1963).

(125) Prout and Brown, A.S.T.M. Spec. Tech. Publ. No. 359, 38 (1963).

(126) Jach, J. Phys. Chem., 68, 731 (1964).

(127) Herley and Prout, Nature, 184, 445 (1959).

(128) Haynes and Young, Disc. Faraday Soc., 31, 229 (1961).

(129) Boldyrev, Zakharov, Eroshkin and Sokolova, Dokl. Akad. Nauk. S.S.R., 129, 365 (1959).

(130) Boldyrev, Izd. Akad. Nauk. S.S.R., 42 (1962).

(131) Young, J.C.S., 4533 (1960).

(132) Jach, Reactivity of Solids, Ed. De Boer, 334 (Elsevier 1961).

(133) Cobble and Boyd, J. Phys. Chem., 63, 919 (1959).

(134) Bowen, Eggleston and Kropschot, J. Appl. Phys., 23, 630 (1952).

(135) Prout and Herley, J. Phys. Chem., 66, 961 (1962).

(136) Herley and Prout, J. Inorg. Nucl. Chem., 16, 16 (1960).

(137) Prout and Sole, J. Inorg. Nucl. Chem., 9, 232 (1959).

(138) Herley and Prout, J. Phys. Chem., 65, 208 (1961).

(139) Dienes and Vineyard, Radiation Effects in Solids, (Interscience Publ. New York 1957).

(140)/.....

(140) Boldyrev and Oblivantsev, Kinetika i Kataliz, 3, 887 (1962).

(141) Boldyrev, Izd. Akad. Nauk S.S.R., 42 (1962).

(142) Boldyrev and Bystrykh, Russian Chem. Rev., 32, 426 (1963).

(143) Huang, Proc. Roy. Soc., A 190, 102 (1947).

(144) Senio and Tucker, Phys. Rev., 99, 1777 (1955).

(145) Prout and Woods, A.S.T.M. Spec. Tech. Publ. No. 359, 50 (1963).

(146) Prout and Brown, Nature, 203, 398 (1965).

(147) Prout and Brown, Unpublished work.

(148) Konazaki, J. Phys. and Chem. Solids, 2, 107 (1957).

(149) Ozaroff, Crystallography and Crystal Perfection (Acad. Press London 1963).

(150) Blaunshtein and Starodubtsev, Tr. Tashkentsk Konf. po Mirnomu Ispol's At. Energii Akad. Nauk. Uz. S.S.R., 1, 163 (1961).

(151) Prout, Paper read at A.S.T.M. Conf. in Seattle 1965 (in the press).

(152) Herley and Prout, J. Amer. Chem. Soc., 82, 1540 (1960).

(153) Prout, Nature, 183, 884 (1959).

(154) Brown, Unpublished work.

(155) Simpson, Taylor and Andersom, J.C.S., 2378 (1958).

(156) Heal, Trans. Faraday Soc., 53, 210 (1957).

(157) Boldyrev, Oblivantsev and Lykhin, Dokl. Akad. Nauk. S.S.R., 159, 1113 (1964).

(158) Johnson, A.S.T.M. Spec. Tech. Publ. No. 359, 71 (1963).

(159) Allen and Ghormley, J. Chem. Phys., 15, 208 (1947).

(160) Doigan and Davis, J. Phys. Chem., 56, 764 (1952).

(161) Hennig, Lees and Matheson, J. Chem. Phys., 21, 644 (1953).

(162) Hochanadel and Davis, J. Chem. Phys. 27, 333 (1957).

(163) Johnson and Forten, Disc. Faraday Soc., 31, 238 (1961).

(164) Chen and Johnson, J. Phys. Chem., 66, 2248 (1962).

(165) Prince, Thesis Stevens Inst. of Tech. Hoboken N.J.

(166)/.....

(166) Boyd, Graham and Larsen, J. Phys. Chem., 66, 300 (1962).

(167) Heal, Canad. J. Chem., 31, 91 (1953).

(168) Logan and Moore, J. Phys. Chem., 67, 1042 (1963).

(169) Garner, Gomm and Hailes, J.C.S., 1393 (1933).

(170) Bartlett, Tompkins and Young, Nature, 179, 365 (1957).

(171) Osinovik, Kand. dissertatsia, Minsk (1955).

(172) Sviridov, Dokl Akad. Nauk. Belorus S.S.R., 2, 291 (1958).

(173) Andreev, Physik. Z. Sowjet Union, 6, 121 (1934).

(174) Marke, Trans. Faraday Soc., 33, 770 (1937).

(175) Tompkins and Young, Disc. Faraday Soc., 23, 202 (1957).

(176) Tompkins and Young, Trans. Faraday Soc., 61, 1470 (1965).

(177) Herley, M.Sc. Thesis, Rhodes Univ. (1959).

(178) Prout and Herley, J. Chem. Educ. 37, 643 (1960).

(179) Hume and Topley, Proc. Roy. Soc., A 120, 211 (1928).

(180) Seitz, Phys. Rev. 80, 241 (1950).

(181) Mott and Gurney, Electronic Processes in Ionic Crystals, 12 (O.U.P. London 1940).

(182) Vaughan and Phillips, J.C.S. 2736 (1949).

(183) Singh, Trans. Faraday Soc., 52, 1623 (1956).

(184) Dreyfus and Levy, Proc. Roy. Soc. A 246, 233 (1958).

(185) Llewellyn and Whitmore, J.S.C., 881 (1947).

(186) Heal, Trans. Faraday Soc., 53, 210 (1957).

(187) Kaufman, Proc. Roy. Soc., A 246, 219 (1958).

(188) Gray, Quart. Rev., 17, 463 (1963).

(189) Scott, Smith and Thompson, J. Phys. Chem., 57, 757 (1953).

(190) Inorganic Synthesis, Ed. Booth, 1, 73 (McGraw-Hill 1939).